

Durham E-Theses

Mapping intertidal vegetation in the wash estuary using remote sensing techniques

Thomas, D.C. Reid

How to cite:

Thomas, D.C. Reid (1993) *Mapping intertidal vegetation in the wash estuary using remote sensing techniques*, Durham theses, Durham University. Available at Durham E-Theses Online:
<http://etheses.dur.ac.uk/5759/>

Use policy

The full-text may be used and/or reproduced, and given to third parties in any format or medium, without prior permission or charge, for personal research or study, educational, or not-for-profit purposes provided that:

- a full bibliographic reference is made to the original source
- a [link](#) is made to the metadata record in Durham E-Theses
- the full-text is not changed in any way

The full-text must not be sold in any format or medium without the formal permission of the copyright holders.

Please consult the [full Durham E-Theses policy](#) for further details.

Mapping Intertidal Vegetation in the Wash Estuary Using Remote Sensing Techniques.

D. C. Reid Thomas

The copyright of this thesis rests with the author.
No quotation from it should be published without
his prior written consent and information derived
from it should be acknowledged.

Thesis submitted for the degree of Master of Science.
University of Durham, Department of Geography.

October, 1993.



15 JUN 1994

Declaration

This thesis is the result of my own work. Data from other authors which are referred to in the thesis are acknowledged at the appropriate point in the text.

Statement of Copyright

The copyright of this thesis rests with the author. No quotation from it should be published without prior written consent and information derived from it should be acknowledged.

Abstract

Reid Thomas, D.C. (1993)

Mapping Intertidal Vegetation in the Wash Estuary Using Remote Sensing Techniques.

The mapping and monitoring of the intertidal zone of the East Coast of England is of considerable interest to conservationists and coastal managers. Intertidal vegetation offers natural protection against coastal erosion and considerably reduces the cost of man made sea defences. Monitoring of intertidal vegetation may also be of value in providing an early warning of sea-level change. This thesis considers the most effective way of classifying and monitoring the intertidal zone using remote sensing techniques and incorporating the results into a coastal monitoring Geographic Information System (GIS). The coastal monitoring GIS is used to model the advantages and disadvantages of different classification strategies. The Wash Estuary forms the principal study area.

This study uses multi-temporal data which requires atmospheric and radiometric correction. All Landsat 5 TM images used in the present study were referenced to a common image, based on the techniques of F.G.Hall of NASA, to allow meaningful comparisons to be made. The data sets were geometrically corrected to allow incorporation into the coastal monitoring GIS. Two strategies were used to classify the intertidal zone: a conventional maximum likelihood classifier and a fully constrained mixture model using the least squares technique. The results of the classifications were incorporated into the coastal monitoring GIS along with information acquired from previous ground based surveys. Statistical analysis of the classifications was carried out by cross tabulation with the ground based surveys in order to determine the accuracy of the methods. Detailed, reliable information arrived at cheaply, objectively and at regular intervals would provide a valuable resource for the management and monitoring of the coastal environment.

Acknowledgements

Many people have helped in the completion of this thesis. I would like to thank Professor Tooley and the Durham Geography Graduates Association and Friends of the Department for providing the tuition fees for this research. I would also like to thank my second supervisor, Dr I. Shennan for arranging the research assistant contract which provided my maintenance.

I am also very grateful to I. Sproxton and Dr C. Zong for making available many of the techniques and much of the data on which this thesis is based. I would also like to thank all of the technical and computing staff, especially Chris Mullaney and Mark Scott, for their advice and support throughout the year.

My greatest thanks go to my supervisor Dr Donoghue for introducing me to the subject and arranging the place for the Master's research. I would also like to acknowledge his constant help and support throughout the year.

Finally, I wish to thank my family for their support throughout my time in Durham.

LIST OF CONTENTS

Chapter 1 Saltmarshes and Their Importance	1
The Wash Estuary	1
The recognition of saltmarsh providing coastal protection and flood protection	7
Conservational concerns	7
Reclamation issues	9
Rising sea level	10
Previous surveys of the Wash Estuary	11
Chapter 2 Remote Sensing of Saltmarsh Vegetation	14
Leaf structure	14
Pigment absorption in the visible wavelengths of the electromagnetic spectrum	16
High reflectance in the Near Infrared (NIR) wavelengths of the electromagnetic spectrum	18
The "red edge"	18
The NIR plateau	18
Phenology	19
The vegetation canopy	21
Inventory	22
Biomass estimation	23
Classification	23
Landsat 5 TM data	25
Chapter 3 Analysis of Wash Estuary Vegetation Spectra	28
Method	30
Discussion	36
Distinguishing between vegetation and other cover types	36
Green Peak	36
Red Position	36
Red width	37
Red depth	37
Red asymmetry	38
Red edge	38
The gradient of the red edge	38
H/h ratio	39
Comparison with spectra taken from Landsat 5 TM	40

Chapter 4 Atmospheric and Radiometric Correction	44
Radiometric calibration	44
Irradiance	45
Atmospheric correction	46
Radiometric rectification	49
Radiometric control set selection	51
Calculation of the rectification transform	52
Chapter 5 The Wash Geographical Information System	62
Comparison of the digitised and N.C.C. maps	66
Comparison between the two ground survey dates	67
Integration of satellite sensor data into the Wash coastal monitoring GIS	70
Transfer of data from the Terra-Mar image processor to the pcArc/Info GIS	72
Filtering	72
Geometric correction	74
Masking	79
Method of comparison of surveys within the GIS	80
Chapter 6 Maximum Likelihood Classifier	83
Multispectral classification	84
Training area selection	85
Results of the maximum likelihood classification (MLC)	91
Comparison between the 1982/4 N.C.C. survey and the MLC classifications of the May 1984 Landsat 5 TM image	101
Comparison between the 1982/4 N.C.C. survey and the MLC classifications of the September 1991 Landsat 5 TM image	103
Comparison between the 1984 M.L.C. classification and the 1991 MLC classification	106
Comparison of the two independent classifications	106
Conclusions from the maximum likelihood classifications	108
Problems with the maximum likelihood classifier	111
Chapter 7 Mixture Modelling	115
Linear mixture modelling	119
Application of the mixture model to Landsat 5 TM data of the Wash Estuary	122
Endmember selection	122
Transect comparison	156
Results of the mixture model analysis	161

Comparison between the vegetation proportion map of the May 1984 Landsat 5 TM image and the N.C.C. 1982/4 vegetation survey	164
Comparison between the vegetation proportion map of the September 1991 Landsat 5 TM image and the N.C.C. 1982/4 vegetation survey	167
Comparison between the vegetation proportion map of the May 1984 Landsat 5 TM image and the vegetation proportion map of the September 1991 Landsat 5 TM image	169
Conclusions from the mixture model surveys	171
Problems with the mixture model	172
 Chapter 8 Discussion and Conclusions	 180
Comparison between the vegetation proportion map of the 1984 Landsat 5 TM image and the MLC classifications of the May 1984 Landsat 5 TM image	183
Comparison between the 1991 maximum likelihood surveys and the 1991 mixture model survey	185
Conclusions from the comparison of the two survey methods	188
Conclusions from the classification strategies	188
 References	 194
 Appendix I The Rectification Transformation	 201
Appendix II The Vegetation Parameter Algorithm	205
 List of Tables	
Table 2.1 Characteristics of Landsat 5 TM data	26
Table 2.2 TM band applications	26
Table 3.1 Features of Wash Estuary vegetation spectra	32
Table 4.1 Radiometric control sets for Landsat TM image (14/5/84) and Landsat TM image (7/9/91)	54
Table 4.2 Comparison of rectified and unrectified spectrally invariant pixels	59
Table 5.1 Areas in hectares of vegetation zones of the Wash saltmarshes	67
Table 6.1 Cross tabulation of the 1982/4 N.C.C. survey with the 1984 MLC - operator 1	97
Table 6.2 Cross tabulation of the 1982/4 N.C.C. survey with the 1984 MLC - operator 2	97
Table 6.3 Cross tabulation of the 1982/4 N.C.C. survey with the 1991 MLC - operator 1	98

Table 6.4	Cross tabulation of the 1982/4 N.C.C. survey with the 1991 MLC - operator 2	98
Table 6.5	Cross tabulation of operator 1 1984 MLC and operator 2 1984 MLC	99
Table 6.6	Cross tabulation of operator 1 1991 MLC and operator 2 1991 MLC	99
Table 6.7	Cross tabulation of the 1984 and 1991 MLCs	100
Table 6.8	Areas of the saltmarsh zones	100
Table 7.1	Mixture model estimates of % vegetation cover in May 1984 and September 1991 Landsat 5 TM images of the Wash	153
Table 7.2	Transects from Butterwick and Leverton saltmarshes	157
Table 7.3	Summary of mixture model and 1984 N.C.C. saltmarsh surveys	161
Table 7.4	Cross tabulation of the 1984 mixture model and the 1982/4 N.C.C. survey	162
Table 7.5	Cross tabulation of the 1991 mixture model and the 1982/4 N.C.C. survey	162
Table 7.6	Cross tabulation of the 1984 mixture model and the 1991 mixture model	162
Table 7.7	Cross tabulation of the 1984 mixture model total saltmarsh estimate with the N.C.C. 1982/4 survey total saltmarsh estimate	163
Table 7.8	Cross tabulation of the 1991 mixture model total saltmarsh estimate with the N.C.C. 1982/4 survey total saltmarsh estimate	163
Table 7.9	Cross tabulation of the 1984 mixture model total saltmarsh estimate with the 1991 mixture model total saltmarsh estimate	163
Table 7.10	Cross tabulation of the total saltmarsh estimate of the N.C.C. 1982/4 survey and that of the map produced from the combination of the 1991 vegetation and pioneer proportion maps	175
Table 8.1	Wash Estuary surveys	180
Table 8.2	Cross tabulation of the 1984 mixture model with the 1984 MLC (operator 1)	181
Table 8.3	Cross tabulation of the 1984 mixture model with the 1984 MLC (operator 2)	181
Table 8.4	Cross tabulation of the 1991 mixture model with the 1991 MLC (operator 1)	181
Table 8.5	Cross tabulation of the 1991 mixture model with the 1991 MLC (operator 2)	181
Table 8.6	Cross tabulation of the 1984 mixture model with the 1984 MLC (operator 1)	182
Table 8.7	Cross tabulation of the 1984 mixture model with the 1984 MLC (operator 2)	182
Table 8.8	Cross tabulation of the 1991 mixture model with the 1991 MLC (operator 1)	182
Table 8.9	Cross tabulation of the 1991 mixture model with the 1991 MLC (operator 2)	182
Table 8.10	Summary of Wash Estuary saltmarsh surveys	189

List of Figures

Fig. 1.1a	Location map of the study area	2
Fig. 1.1b	Wash Estuary location map	3
Fig. 1.2	Generalised saltmarsh vegetation zones	5
Fig. 1.3	Effectiveness of saltings in coastal defence	8
Fig. 2.1	Diagram of a leaf cross section	15
Fig. 2.2	Vegetation reflectance and absorption features	17
Fig. 3.1	Hypothetical vegetation spectrum	29
Fig. 3.2	Intertidal mud	33
Fig. 3.3	Bare agricultural field	33
Fig. 3.4	Grass growing on the seabank	33
Fig. 3.5	Agropyron 1	33
Fig. 3.6	Agropyron 2	34
Fig. 3.7	Puccinellia East	34
Fig. 3.8	Puccinellia from the Upper marsh	34
Fig. 3.9	Puccinellia from the Middle marsh	34
Fig. 3.10	Halimione from the Upper marsh	35
Fig. 3.11	Halimione from the Middle marsh	35
Fig. 3.12	Puccinellia East ground and TM spectra	41
Fig. 3.13	Agropyron 2 ground and TM spectra	41
Fig. 3.14	Middle marsh Puccinellia ground and TM spectra	41
Fig. 3.15	Middle marsh Halimione ground and TM spectra	41
Fig. 4.1	Atmospheric absorption	47
Fig. 4.2	Dark and bright radiometric control sets from Landsat 5 TM (14/5/84 and 7/9/91).	55
Fig. 4.3	Flowchart of atmospheric and radiometric rectification	56
Fig. 5.1	Procedure for the assessment of classification strategies	63
Fig. 5.2	Diagrammatic representation of the contents of the Wash coastal monitoring GIS	64
Fig. 5.3	The Freiston shore	69
Fig. 5.4	The Freiston shore	69
Fig. 5.5	Procedures for integrating classified Landsat 5 TM imagery into pc Arc/Info	71
Fig. 5.6	Unfiltered classified extract of the Wash Estuary	73
Fig. 5.7	Filtered classified extract of the Wash Estuary	73
Fig. 5.8	Terra-Mar zoom images used for locating ground control points	75
Fig. 5.9	Geometric correction by cubic convolution	78
Fig. 6.1	Three-dimensional cluster diagram of training sets used in a classification	86
Fig. 6.2	High-low graphs summarising the spectral characteristics of the 1991 training sets	87

Fig. 6.3	Location of training areas on the September 1991 Landsat 5 TM image	89
Fig. 6.4	Extracted area of the September Landsat 5 TM image of the Wash Estuary	92
Fig. 6.5	Application of the maximum likelihood classifier to an extract of the September Landsat 5 TM image of the Wash Estuary	93
Fig. 6.6	The result of operator 1 applying the maximum likelihood classifier to the September 1991 Landsat 5 TM image	94
Fig. 6.7	Generalised vegetation cover of the Wash Estuary (maximum likelihood classification of 14/5/84 Landsat 5 TM image)	95
Fig. 6.8	Generalised vegetation cover of the Wash Estuary (maximum likelihood classification of 7/9/91 Landsat 5 TM image)	96
Fig. 6.9	Comparison of the 1982/4 N.C.C. survey and the 1984 maximum likelihood classification (operator 1)	102
Fig. 6.10	Comparison of the 1982/4 N.C.C. survey and the 1991 maximum likelihood classification (operator 1)	104
Fig. 6.11	Comparison of the 1991 maximum likelihood classification and the 1984 maximum likelihood classification (operator 1)	105
Fig. 6.12	Summary of the maximum likelihood classifications	109
Fig. 7.1	Linear and non-linear mixing	117
Fig. 7.2	Euclidean space of Principal Components 1 and 2 illustrating the scatter of pixels around a single mixing plane	120
Fig. 7.3	Scatter plot of the entire Wash Estuary	123
Fig. 7.4	Principal Component Analysis of a small extract of the intertidal zone of the Wash Estuary	124
Fig. 7.5	Friedman and Turkey Pursuit Algorithm	125
Fig. 7.6	Principal Component Analysis of extract 1	127
Fig. 7.7a	Location in feature space of the spectra taken from the water/sediment mixing line	128
Fig. 7.7b	Water mixing line	129
Fig. 7.8a	Location in feature space of the spectra taken from the intertidal mixing line	130
Fig. 7.8b	Intertidal mixing line	131
Fig. 7.9a	Location in feature space of the spectra taken from the vegetation mixing line	132
Fig. 7.9b	Vegetation mixing line	133
Fig. 7.10	September 1991 endmembers	134
Fig. 7.11a	Extract 1, PC1 against PC3	135
Fig. 7.12a	Extract 1, PC2 against PC3	135
Fig. 7.11b	September 1991 Endmembers (PC1 against PC3)	136
Fig. 7.12b	September 1991 Endmembers (PC2 against PC3)	136
Fig. 7.13	May 1984 Endmembers	137
Fig. 7.14	Principal Component Analysis of Extract 2	139
Fig. 7.15	Principal Component Analysis of Extract 3	140
Fig. 7.14b	September 1991 Endmembers (Extract 2)	141
Fig. 7.15b	September 1991 Endmembers (Extract 3)	141
Fig. 7.16	Extract 2, PC1 against PC3	142
Fig. 7.17	Extract 2, PC2 against PC3	142

Fig. 7.18	Extract 3, PC1 against PC3	143
Fig. 7.19	Extract 3, PC2 against PC3	143
Fig. 7.20	Generalised linear spectral mixing within the intertidal zone	144
Fig. 7.21	1991 water endmember in SPAM and TM formats	145
Fig. 7.22	1991 intertidal endmembers in SPAM and TM formats	145
Fig. 7.23	1991 pioneer endmember in SPAM and TM formats	145
Fig. 7.24	1991 vegetation endmember in SPAM and TM formats	145
Fig. 7.25	September 1991 proportion map of the water endmember	146
Fig. 7.26	September 1991 proportion map of the first intertidal sand/mudflat endmember	147
Fig. 7.27	September 1991 proportion map of the second intertidal sand/mudflat	148
Fig. 7.28	September 1991 proportion map of the pioneer endmember	149
Fig. 7.29	September 1991 proportion map of the saltmarsh vegetation endmember	150
Fig. 7.30	% Saltmarsh vegetation cover of the Wash Estuary. Proportion image from the 14/5/84 Landsat 5 TM image	151
Fig. 7.31	% Saltmarsh vegetation cover of the Wash Estuary. Proportion image from the 7/9/91 Landsat 5 TM image	152
Fig. 7.32	Histograms of the data contained in the vegetation proportion maps of the 1984 and 1991 Landsat 5 TM images	155
Fig. 7.33	Butterwick transect	158
Fig. 7.34	Butterwick transect	158
Fig. 7.35	Leverton transect	159
Fig. 7.36	Leverton transect	159
Fig. 7.37	Comparison of the 1982/4 N.C.C. survey and the 1984 vegetation proportion map	165
Fig. 7.38	Comparison of the 1982/4 N.C.C. survey and the 1991 vegetation proportion map	168
Fig. 7.39	Comparison of the 1984 vegetation proportion map and the 1991 proportion map	170
Fig. 7.40	Comparison of the 1982/4 N.C.C. survey and the combined 1991 vegetation and pioneer proportion maps	176
Fig. 7.41	Wash Estuary saltmarsh surveys	177
Fig. 8.1	Comparison of the 1984 mixture model survey and the 1984 maximum likelihood classification	184
Fig. 8.2	Comparison of the 1991 mixture model survey and the 1991 maximum likelihood classification (operator 1)	187
Fig. 8.3	Wash Estuary saltmarsh surveys	190

CHAPTER 1

SALTMARSHES AND THEIR IMPORTANCE

This thesis is concerned with the mapping of the vegetation of the intertidal zone using remote sensing techniques. The thesis starts by looking at the need for monitoring the intertidal zone and goes on to look at the specific problems posed by the remote sensing of vegetation in general and the remote sensing of saltmarsh vegetation in particular. The thesis assesses the most diagnostic characteristics of vegetation spectra in an attempt to aid classification procedures before applying and comparing two different surveying strategies, a maximum likelihood classifier and mixture modelling. Before these strategies could be carried out the Landsat 5 TM data had to be radiometrically and atmospherically corrected. The results of the classifications were geometrically corrected and imported into a Geographic Information System for further comparison.

THE WASH ESTUARY

The choice of the Wash Estuary (Figs. 1.1a, 1.1b) as a study area partly reflects the availability of data but is also in recognition of the fact that the Wash Estuary and the surrounding Fenlands is one of the most significant areas of coastal lowlands in the United Kingdom. The Wash Estuary is one of the United Kingdom's major areas of saltmarsh, with over 4,000 hectares (Doody, 1992), and is of international importance in conservation terms. The saltmarshes and intertidal flats represent an integral part of the continuous system of sea embankments which protect the economically valuable low lying areas of the Fenland from tidal and storm surge inundation. In common with many other estuaries, the saltmarshes around the Wash Estuary face a number of natural and human pressures. The human pressures include the introduction of pollutants to the estuarine environment and the legacy of past reclamations and improvements to sea embankments. Of the natural pressures perhaps the most important is the potential for an acceleration in the rate of sea-level rise. The area



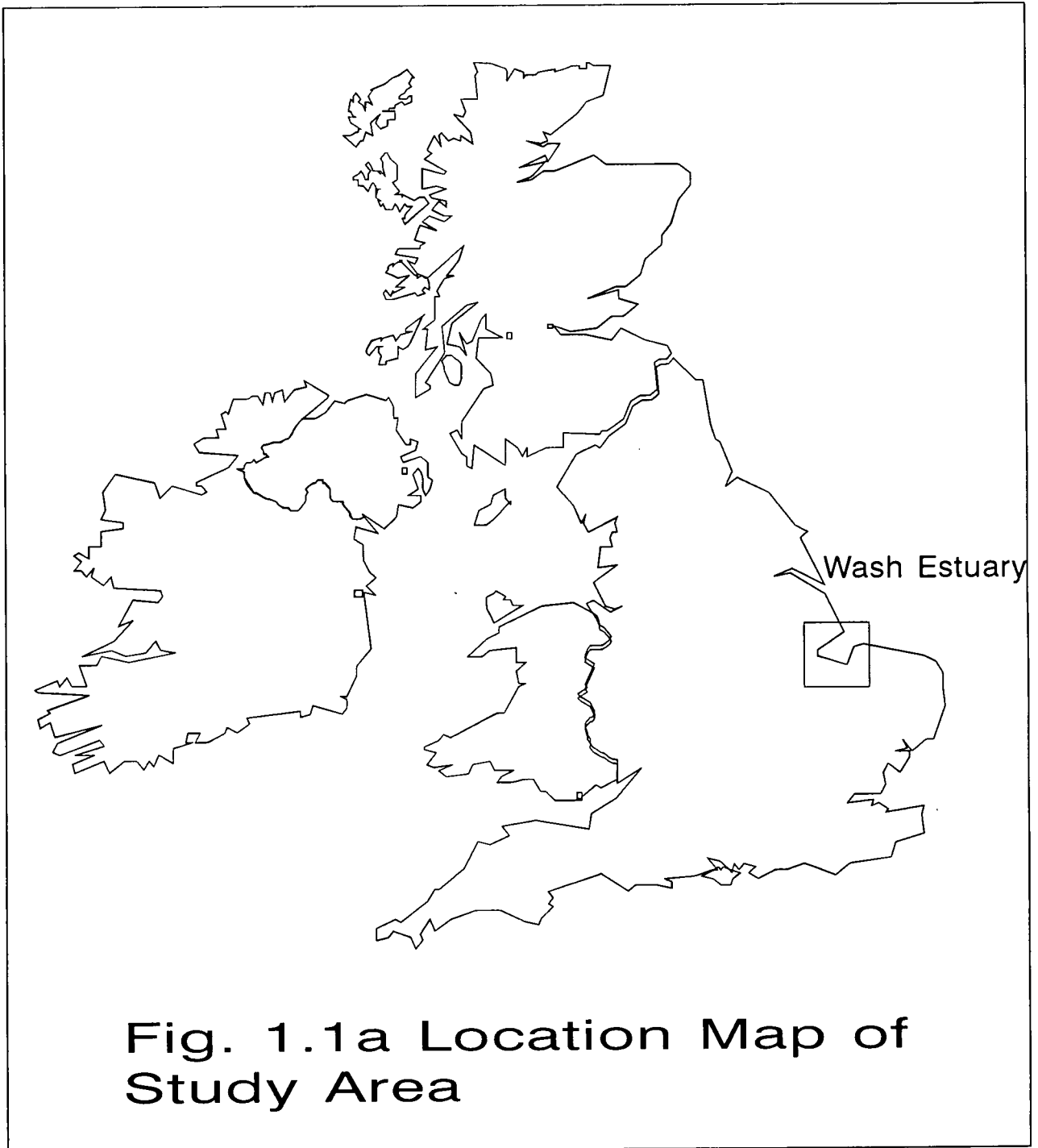
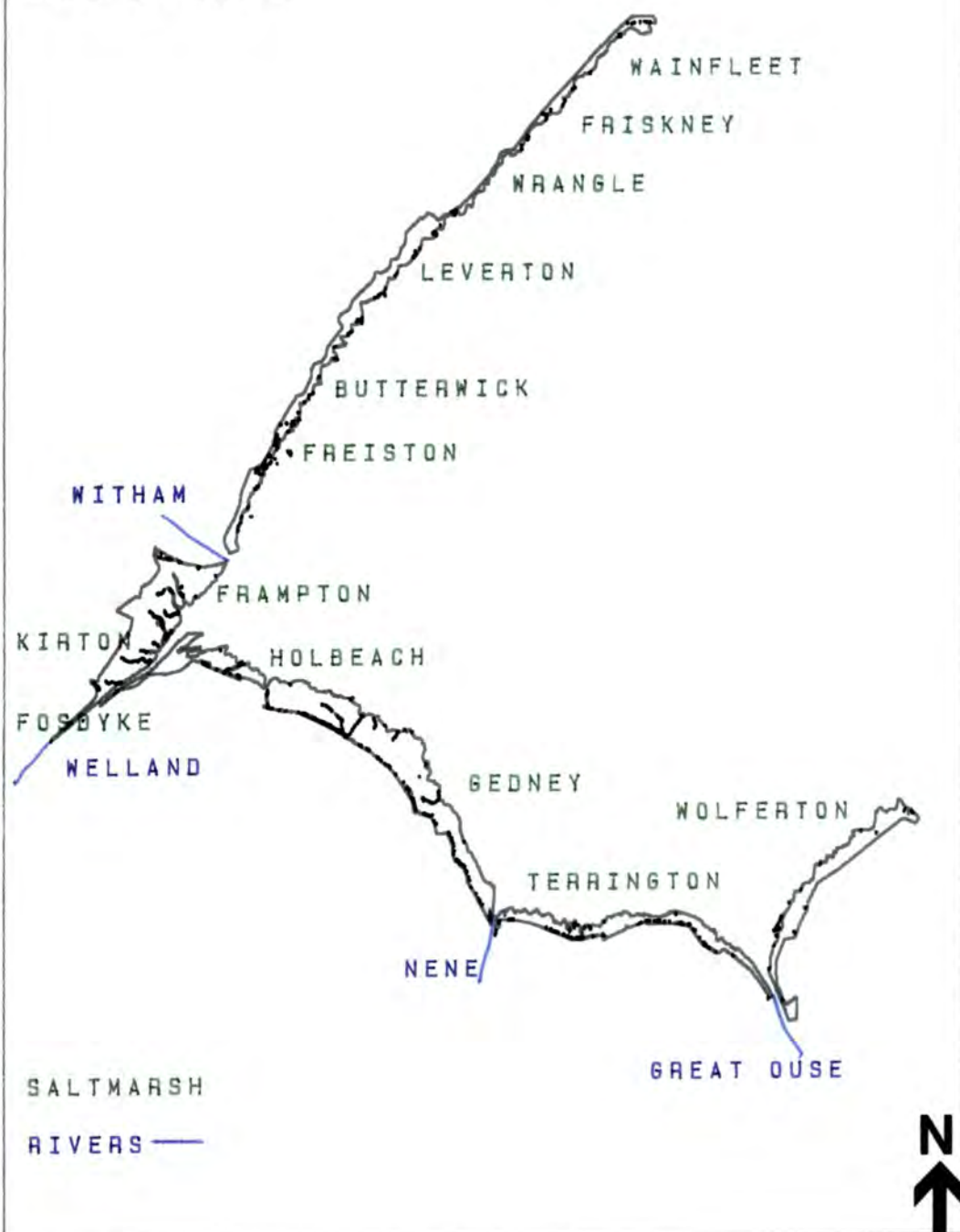


Fig. 1.1b WASH ESTUARY LOCATION MAP

SCALE 1 : 236,000



surrounding the Wash Estuary potentially at risk has been estimated as high as 4700 km² (Shennan and Sproxton, 1992(a)).

In order to assess the potential of remote sensing in its ability to monitor saltmarsh it is necessary to understand the physical and biological structure of saltmarshes and the special problems that these cause for remote sensing. Saltmarshes form environments high in the intertidal zone and are widely developed on low energy coasts in temperate and high latitudes. They are created by the deposition of fine silts and sands in sheltered locations and subsequent colonisation by halophytic plants. The plants act as a buffer to tidal currents and waves, encouraging more silts to settle. These environments grade seawards into mud-flats or sand-flats, to which they are genetically related, and from which they are often separated by either a ramp or a cliff. Landwards saltmarshes may grade upwards and landwards into freshwater marshes and coastal vegetation communities (Allen and Pye, 1992).

Saltmarshes frequently display a strong spatial structure, usually in the form of parallel zones of vegetation, the communities changing with increasing surface elevation. The lower levels of the saltmarsh are more frequently inundated with saltwater and support Pioneer communities of *Salicornia europaea*, *Suaeda maritima*, *Aster tripolium* and *Spartina anglica* individually or in combinations. The Pioneer zone of the Wash Estuary is typically characterised by the presence of *Salicornia europaea* and smaller amounts of *Spartina anglica*. As the frequency of tidal inundation decreases additional species appear. The communities which develop above the Pioneer zone in the Wash Estuary are usually characterised by the presence of *Puccinellia maritima* and *Halimione portulacoides*. At the back of the more mature Wash saltmarshes, such as Leverton and Frampton (Fig. 1.1b), *Festuca rubra* and *Agropyron pungens* are found (Gray, 1992) (Fig. 1.2).

At the higher elevations there is an increase in competition and niche overlap. This is a major reason why it is difficult to quantify the niche of a vegetation species across a range of saltmarshes as there may be considerable variations in floristic structure. This is especially relevant at higher elevations where more species occur, and hence more combinations of biological interactions are possible. These facts are of significance in the

Generalised Saltmarsh Vegetation Zones of the Wash Estuary

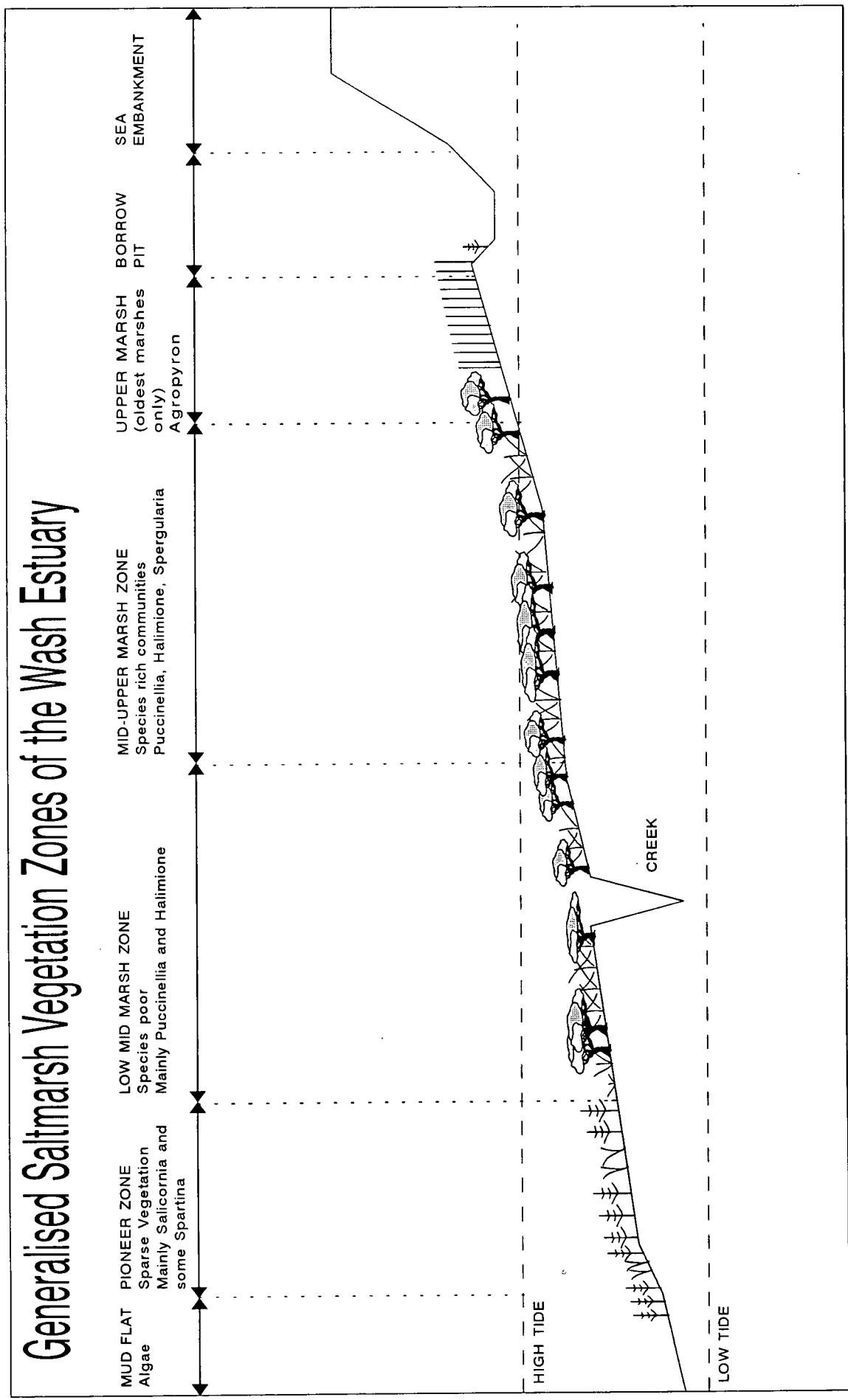


Fig.1.2 Generalised Saltmarsh Vegetation Zones

remote sensing of saltmarshes as the diversity of species in the upper reaches make classification particularly difficult. Greater precision in determining species is obtained with species such as *Salicornia europaea* and *Spartina anglica* which occupy the lower parts of the intertidal zone where species are limited more by physical than biological factors and hence there is less species diversity. This has frequently been borne out by the findings of remote sensing studies of saltmarshes (chapter 3). There are, however, other difficulties in the lower regions of saltmarshes because the vegetation becomes increasingly mixed with areas of mud.

Although the saltmarsh of the Wash forms only a narrow band around the estuary the pattern of vegetation is often complex resulting from a combination of natural vegetation succession, grazing and reclamation. Grazing tends to increase species diversity whereas reclamation retards the process towards saltmarsh maturity. The older and more mature saltmarshes of the estuary such as Frampton and Holbeach (Fig. 1.1b), which have the most diverse Upper marsh communities, represent the sites of greatest conservation value (Hill, 1988).

Saltmarshes are considered intrinsically interesting environments by scientists on account of their variability and the rapidity with which physical, chemical and biological processes operate. Similarly saltmarshes are valued by ecologists, conservationists and ornithologists as important wildlife habitats. In contrast to the views of conservationists, industrialists and local planning authorities have traditionally regarded saltmarshes as areas of low economic value suitable only for waste-dumping and industrial development and have sought to make such areas more productive through land reclamation and dredging to facilitate navigation. As a result saltmarshes have been subjected to extreme pressure. A good example of this is the rapid destruction of the saltmarshes of the eastern seaboard of the United States. Similarly over 29,000 hectares of Wash saltmarsh have been reclaimed since the seventeenth century (Doody, 1992). In recent years such attitudes have begun to change. Recent studies of the coast of the United Kingdom, such as the N.C.C.'s estuaries review (Davidson, 1991) and the Anglican Sea Defence study (N.R.A., Anglican Region, 1992), have indicated a real need for increased monitoring. This requirement may be categorised under four headings:

1. THE RECOGNITION OF SALTMARSH PROVIDING COASTAL PROTECTION AND FLOOD PROTECTION

All low lying parts of the East coast, including the area surrounding the Wash Estuary, are prone to flooding during severe storm surges. This was demonstrated by the great floods of 1953. Although the seawalls surrounding the reclaimed marshes were not directly overtopped, several were breached leading to flooding of valuable agricultural land behind the sea walls. The floods led to a review of coastal protection strategies. One of the findings of the review has been the recognition of the value of saltmarshes in coastal protection. With a healthy salting fronting a sea wall the costs of building and maintaining an effective defence are comparatively low. If the saltmarsh is eroded and lost, the cost dramatically increases (N.R.A., 1992) (Fig. 1.3).

Areas of saltmarsh act as a dissipator to storm wave action, absorbing tide and wave energy, and provide a substantial weight to the seaward toe of a seawall to give increased stability against water pushing against it. Reduction in the width or height of saltmarshes reduces the effectiveness in dampening waves and increases the risk of overtopping, breaching or even complete failure under storm conditions. In Essex alone, of the 440 km of sea walls maintained by the N.R.A. 300 km rely on a salting as a "first line" of defence against the tide (N.R.A., 1992). If the saltings were lost the additional cost for sea defences would be many hundreds of millions of pounds (N.R.A., 1992; Brampton, 1992).

2. CONSERVATIONAL CONCERNS

Saltmarshes provide a vital link in the chain of marine energy flow through their efficient transfer of solar energy into forms which are usable by a wide variety of estuarine organisms. The total area covered by active saltmarsh in Great Britain is in the region of 44,000 hectares (Brampton, 1992), concentrated largely in eastern and southeastern England, northwest England and the Bristol Channel. The richness of flora and fauna in these areas has resulted in over 80% of British saltmarshes being designated as Sites of Special Scientific Interest (S.S.S.I.) (Brampton, 1992). The salt marshes of the East coast are part of the Eastern Atlantic Flyway, a migration route for millions of birds. The fertile areas of

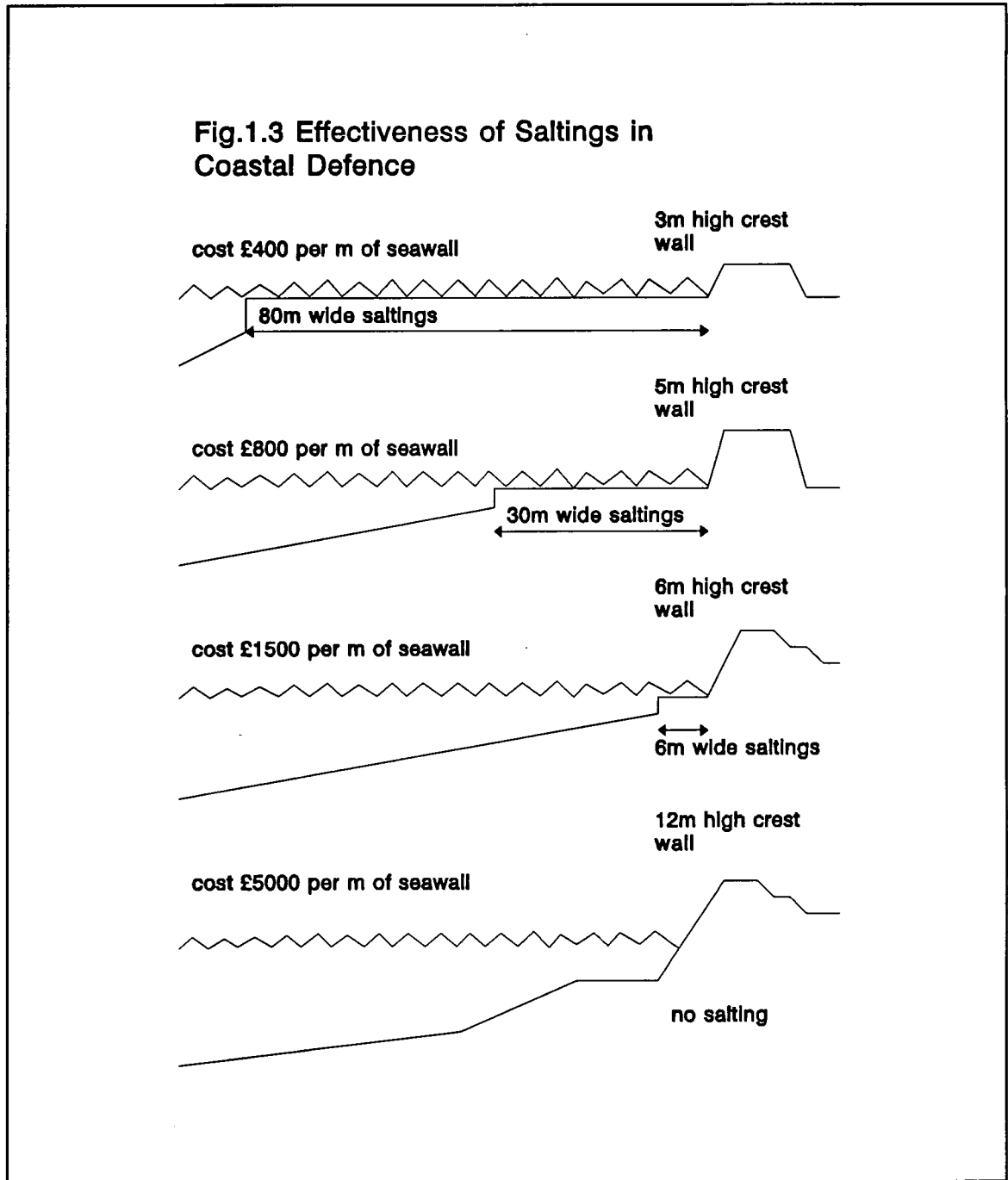


Fig. 1.3 Figures taken from N.R.A. 1992

saltmarsh are the main feeding grounds in the winter that enable survival between breeding seasons. Any loss of mudflat and saltmarsh has a direct and instant impact on bird numbers (N.R.A., 1992). The importance of these areas in the United Kingdom has risen in direct proportion to the loss of similar habitats in countries such as the Netherlands. It is therefore essential that these habitats are closely monitored in order to identify loss or changes in their character in response to changing external pressures.

3. RECLAMATION ISSUES

The existing coastline of the Wash Estuary is the result of a process of gradual reclamation which began in Roman times, and from the 16th century to the present produced in the region of 32,000 hectares of agricultural land (Dalby, 1957). The repeated phases of reclamation were made possible by enhanced sediment accretion and colonisation by saltmarsh vegetation in front of the new embankments. Recent research has questioned the assumption that continued accretion will sustain the latest rates of reclamation (Hill, 1988).

The process of reclamation adopted around the Wash Estuary of first building a cradge bank followed by a larger sea embankment using material excavated from borrow pits at the top of the saltmarshes (Fig. 1.2) has the immediate effect of destroying or seriously disturbing the saltmarsh communities within the upper 70 m of the marsh. These, being at the back of the saltmarshes, are generally the most mature portions of a saltmarsh. As a result many of the saltmarshes are maintained in a relatively immature state and are prevented from reaching sedimentary equilibrium. Relatively rapid accretion will take place until equilibrium is once more approached (Pethick, 1981). Rates of accretion are not only affected by the age of the saltmarsh but also by the sediment supply. The advance of the saltmarsh is also governed by the angle and width of the intertidal zone. It is these considerations that have supported a view that there may be a practical limit to continued reclamation (Shennan and Sproxton, 1992(a)). Some problems have already begun to occur. At Freiston Shore (Fig. 1.1b) and North East of the Horseshoe the earth embankments have been eroded because of inadequate protection afforded by narrow and depleted saltmarshes. At both these locations the fronting saltmarshes are dominated by Lower and Pioneer marsh communities such as *Salicornia*.

As a result of these considerations the N.C.C. has adopted a policy of objection to all reclamation in the Wash Estuary S.S.S.I.. Similarly the Lincolnshire and Norfolk County Councils have imposed a moratorium on all reclamation since the early 1980s. A joint working party on reclamation and conservation in the Wash Estuary was formed to "examine, in detail, the current vegetation, rates of accretion and likely future development of identified saltmarsh areas in relation to the dates of their last reclamation and past management" (Hill,

1988). The 1982/4 N.C.C. survey of the Wash Estuary was an integral part of this study. Since the early 1980s, mainly as a result of a decline in the demand for agricultural land, no new reclamation has taken place in the estuary. This does not however rule out the possibility of future reclamation. The response of a saltmarsh to such reclamations is of great importance and therefore needs to be closely monitored if environmental impacts are to be kept to a minimum.

4. RISING SEA LEVEL

The increase in the rate of global sea level rise forecasted to occur during the next century will enhance the upward sea level trend in southern England where most British saltmarshes are located. The mean sea level of the North Norfolk coast is presently rising by 1.5 mm/year (Shennan, 1989), a rate which may increase by a factor of two or more during the next century if warnings about global warming and thermal expansion of the oceans prove to be correct. The physical and ecological response of saltmarshes to such an increase is of widespread concern. Any threat to the survival of saltmarshes posed by sea level rise will be compounded by the presence of sea walls which prevent the natural landward marsh migration. Saltmarshes face the threat of being "squeezed" out of existence between a fixed sea wall and a rising sea level (N.R.A., 1992). Similarly the natural progression from mudflats to low marsh to high marsh has been prevented due to the construction of earth embankments from areas of mature saltmarsh, replacing mature marsh with borrow pits. As a result, there are now very few areas of "high" marsh still existing in the Wash Estuary. Many saltmarshes in Essex, Kent and parts of the south coast are already experiencing serious erosion and there is concern that the marshes may deteriorate further and in some areas disappear altogether.

It must, however, be noted that it is by no means certain that increased marsh erosion in S.E. England is associated with changing sea level; the role of changes in inshore wave energy, sediment supply and the effect of human activities, including dredging and channel modifications, have not yet been fully evaluated. Accretion of sediment in the Wash and North Norfolk has largely been fed by erosion of coastal cliffs in Lincolnshire, Humberside and Northeast Norfolk in the past. Extensive coastal protection works have been undertaken

in these sediment source areas, especially since the 1953 floods, causing a reduction in sediment supply. There is already considerable evidence that the low water mark is moving landwards on many parts of the East Anglian coast (Pye, 1992). This is a trend which can only be enhanced by the reduction in sediment supply. It therefore seems probable that shoreline retreat will spread and possibly accelerate as the effects of reduced sediment supply become more apparent and as sea level starts to rise at a more rapid rate. Careful monitoring of saltmarshes is necessary to establish the effects of such changes.

It has even been hypothesised that close monitoring of changes in saltmarsh vegetation could provide an early warning of stress to the system induced by sea level rise or other environmental changes (Allen and Pye, 1992). The critical relationship between tidal levels, accretion rates and distribution of saltmarsh flora suggests that saltmarshes and intertidal flats are susceptible to any changes in the local wave climate, tidal regime or sediment supply resulting from acceleration in the rate of sea level rise. It is possible that changes in the distribution of saltmarsh flora and intertidal sediments may provide the earliest evidence of accelerated sea level rise. The identification of any acceleration in the rate of sea level rise through routine monitoring is of obvious importance in the context of coastal management. Remote sensing is ideally suited to the monitoring of such changes and may also help in the estimation of the current rates of vertical and lateral accretion/erosion on British saltmarshes.

The result of these concerns has been a review of coastal management strategies. Policies of land abandonment and set back of sea walls on a large scale are now being actively considered and there is renewed interest in the development of "soft-engineering" options for saltmarsh creation and restoration (Brampton, 1992). This growth of interest has revealed that many of the basic physical and biological processes governing the formation of dynamics of saltmarshes remain poorly understood and require study.

PREVIOUS SURVEYS OF THE WASH ESTUARY

Following the recommendations of a joint working party on reclamation and conservation in the Wash Estuary, two surveys of the Wash saltmarshes were carried out in the 1970s and 1980s. The first, in connection with the Water Storage Scheme Feasibility

Study, was conducted between 1971 and 1974 and was based on a combination of ground survey and aerial photographs obtained in 1971 (N.E.R.C., 1976). The second survey, employing the same techniques, was conducted by the N.C.C., between 1982 and 1985, using aerial photographs obtained in March 1982 and June 1984 (Hill, 1988). The 1982/4 survey classified the saltmarsh vegetation into twelve communities using the National Vegetation Classification, whereas the 1971/4 study identified eight communities on the basis of dominant and sub-dominant species. Both the 1971/4 and 1982/4 surveys produced a quantified measure of the extent of the Wash saltmarshes and their constituent floral communities. In addition to mapping the saltmarsh vegetation both the surveys included measurements of the width of the saltmarsh at 46 points around the Wash together with surface altitudes and sediment accretion rates along a series of 12 (11 in 1982/4) transects.

It has been seen that there is a pressing need for the monitoring of saltmarsh environments. Saltmarsh surface levels and widths need to be closely monitored as they are of considerable importance in coastal protection and management and provide valuable wildlife habitats. Saltmarsh management requires:

- the inventorying of saltmarsh size
- information on the boundaries, extent and condition of the wetland areas
- classification
- monitoring of the resource

Such information is often difficult to collect through ground studies. Past coastal inventory programmes have relied primarily on aerial photography as the basic data source but there is clearly a potential for the integration of satellite surveys into coastal surveying and management programmes.

Allen, J.R.L and Pye, K. 1992: Coastal saltmarshes: their nature and importance. **Saltmarshes. Morphodynamics, Conservation and Engineering Significance**. Cambridge University Press, Cambridge: 1-18.

Brampton, A.H. 1992: Engineering significance of British saltmarshes. In J.R.L. Allen and K. Pye (eds) **Saltmarshes. Morphodynamics, Conservation and Engineering Significance**. Cambridge University Press, Cambridge: 115-122.

Dalby, R. 1957: **Problems of Land Reclamation**, 5. Salt marsh in the Wash Agricultural Review. vol. 2: 31-37.

Davidson, N.C. 1991: **Estuaries, Wildlife and Man. A Summary of Nature Conservation and Estuaries in Great Britain**. Peterborough, Nature Conservancy Council.

Doody, J.P. 1992: The conservation of British saltmarshes. In J.R.L. Allen and K. Pye (eds) **Saltmarshes. Morphodynamics, Conservation and Engineering Significance**. Cambridge University Press, Cambridge: 80-114.

Gray, A.J. 1992: Saltmarsh plant ecology: zonation and succession revisited. In J.R.L. Allen and K. Pye (eds) **Saltmarshes. Morphodynamics, Conservation and Engineering Significance**. Cambridge University Press, Cambridge: 63-79.

Hill, M.I. 1988: **Saltmarsh Vegetation of the Wash. An Assessment of Change From 1971 to 1985**. N.C.C. Publications, Peterborough.

National Environment Research Council, 1976: **The Wash Water Storage Scheme Feasibility Study. A Report on the Ecological Studies**. N.E.R.C. Publications Series C, No.15.

National Rivers Authority, Anglian Region, 1992: **East Anglian Salt Marshes**. N.R.A. Publications, Peterborough.

Pethick, J.S. 1981: Long Term Accretion Rates on tidal saltmarshes. **Journal of Sedimentary Petrology**. vol. 51: 571-577.

Pye, K. 1992: Saltmarshes on the Barrier Coastline of North Norfolk, Eastern England. In J.R.L. Allen and K. Pye (eds) **Saltmarshes. Morphodynamics, Conservation and Engineering Significance**. Cambridge University Press, Cambridge: 148-178.

Shennan, I.S and Sproxton, J. 1992(a): **Monitoring Coastal Environmental Change Using Satellite Imagery Within A Geographical Information System**. Unpublished work.

Shennan, I. 1989: Holocene crustal movements and sea level changes in Great Britain. **Journal of Quaternary Science**. vol. 4: 77-89.

CHAPTER 2

REMOTE SENSING OF SALTMARSH VEGETATION

The study of spectra for the identification of minerals has become well established as a means of survey in geology. Considerable detail has been revealed even through the relatively coarse spectral resolution of satellite sensor data such as that from Landsat TM. Different clay minerals typically exhibit spectra with troughs and peaks at significantly different wavelengths. The presence or absence of troughs at these specified wavelengths defines the presence or absence of the mineral. It has been hoped that similar techniques could be used to differentiate between vegetation types. But whereas different types of minerals show clear diagnostic features in their spectra the same cannot be said for vegetation.

The fundamental differences between the spectra of green plants in the visible and very-near infrared portions of the electromagnetic spectrum and those of all other natural materials mean that vegetation is the most easily analysed part of the terrestrial surface using remote sensing techniques. Having said this the spectra of widely different types of vegetation can have extremely similar spectral responses. In the context of saltmarshes *Puccinellia maritima* and *Halimione portulacoides* were found to have very similar spectral responses. Many applications of remote sensing to vegetation patterns depend on a knowledge of spectral properties of individual leaves and plants. These properties are best understood by examining the physical and chemical structure of leaves.

LEAF STRUCTURE (Fig. 2.1)

The uppermost layer, the *upper epidermis*, consists of specialised cells that fit closely together without openings or gaps between them. The *upper epidermis* is covered by a translucent waxy layer, the *cuticle*. This layer prevents moisture loss from the interior of the leaf. The underside of the leaf is protected by the *lower epidermis*, similar to the upper

Leaf Structure

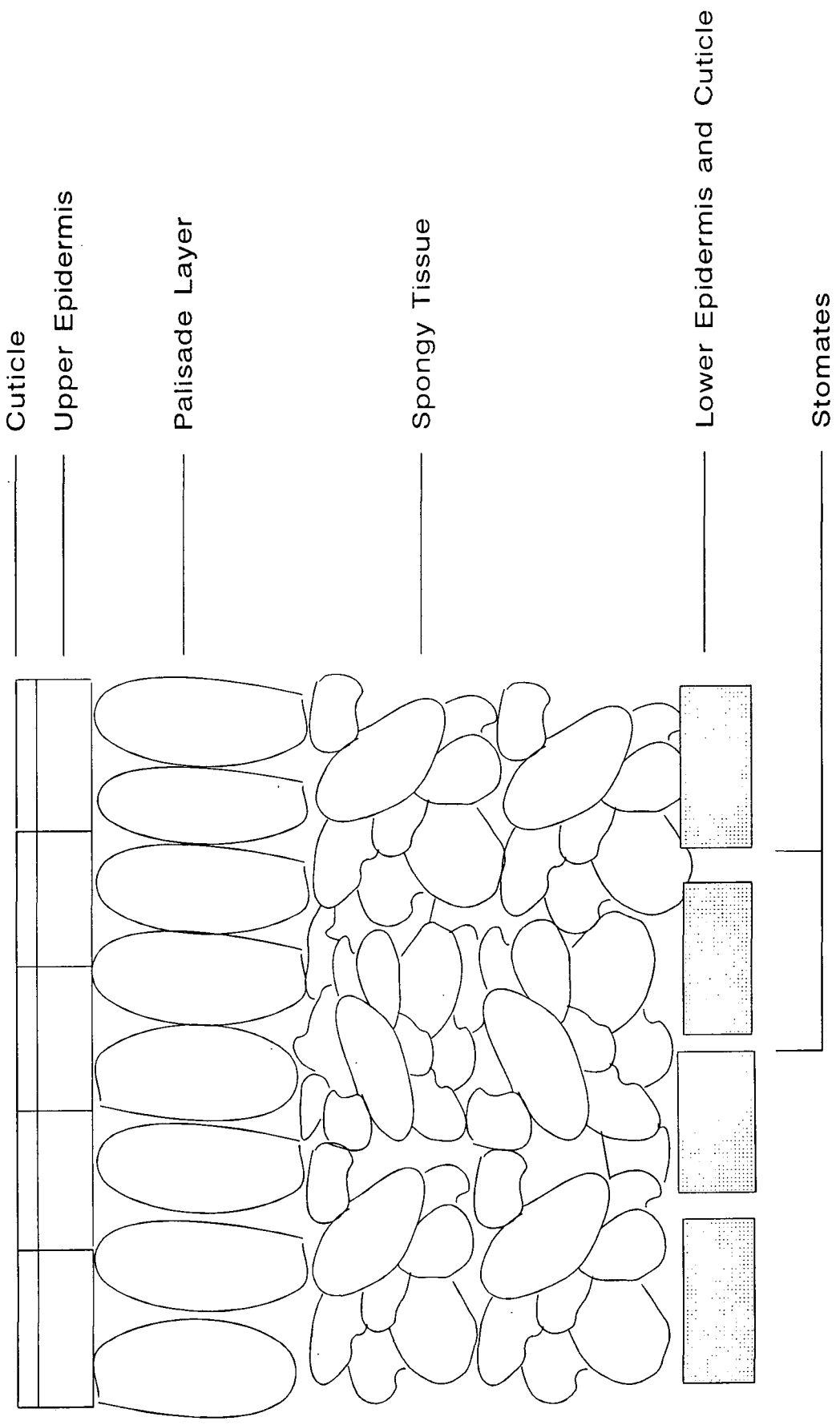


Fig. 2.1 Diagram of a leaf cross section

epidermis except that it includes openings called *stomates*. The stomates allow CO₂ to enter the leaf for the process of photosynthesis to take place. On the upperside of the leaf, just below the epidermis, is the *palisade tissue* consisting of vertically elongated cells arranged in parallel. Palisade cells contain *chlorophyll* and other pigments active in photosynthesis. Below the palisade tissue is the *spongy mesophyll* tissue which consists of irregularly shaped cells separated by interconnected air spaces. The surface of the mesophyll has a large surface area and forms the site of oxygen and carbon dioxide exchange necessary for photosynthesis and respiration. Although leaf structure is by no means identical for all plants this description outlines the major components common to most higher vegetation, and the components that are important in their spectral behaviour. The wavelength and reflectance peaks of vegetation are defined by the spectral characteristics common to all types of green vegetation (Fig. 2.2). These may be summarised as follows:

Pigment absorption in the visible wavelengths of the electromagnetic spectrum

In the visible portion of the spectrum, chlorophyll dominates the spectral response of the living leaf. Higher plants contain four primary pigments: chlorophyll a; chlorophyll b; beta carotene; and xanthophyll. Chlorophyll enables a plant to absorb sunlight. Light that passes through the upper tissue of the leaf is received by pigment molecules in the palisade layer. Chlorophyll a and b are dominant when looking at the visible wavelength portion of vegetation spectra. Chlorophyll a and b both absorb at wavelengths 0.43-0.6 μm and 0.5-0.65 μm (Fig. 2.2). This essentially results in the preferential absorption of blue and red light. Chlorophyll pigment may absorb as much as 70-90% of incident light in these regions (Campbell, 1987). The area between the two troughs of the chlorophyll absorption features is marked by a reflectance peak in green light. This gives all vegetation its characteristic green colour. As all higher plants contain chlorophyll a and b, every detailed spectrum of vegetation, no matter what the species, will show the same absorption features and the green reflectance peak at visible wavelengths.

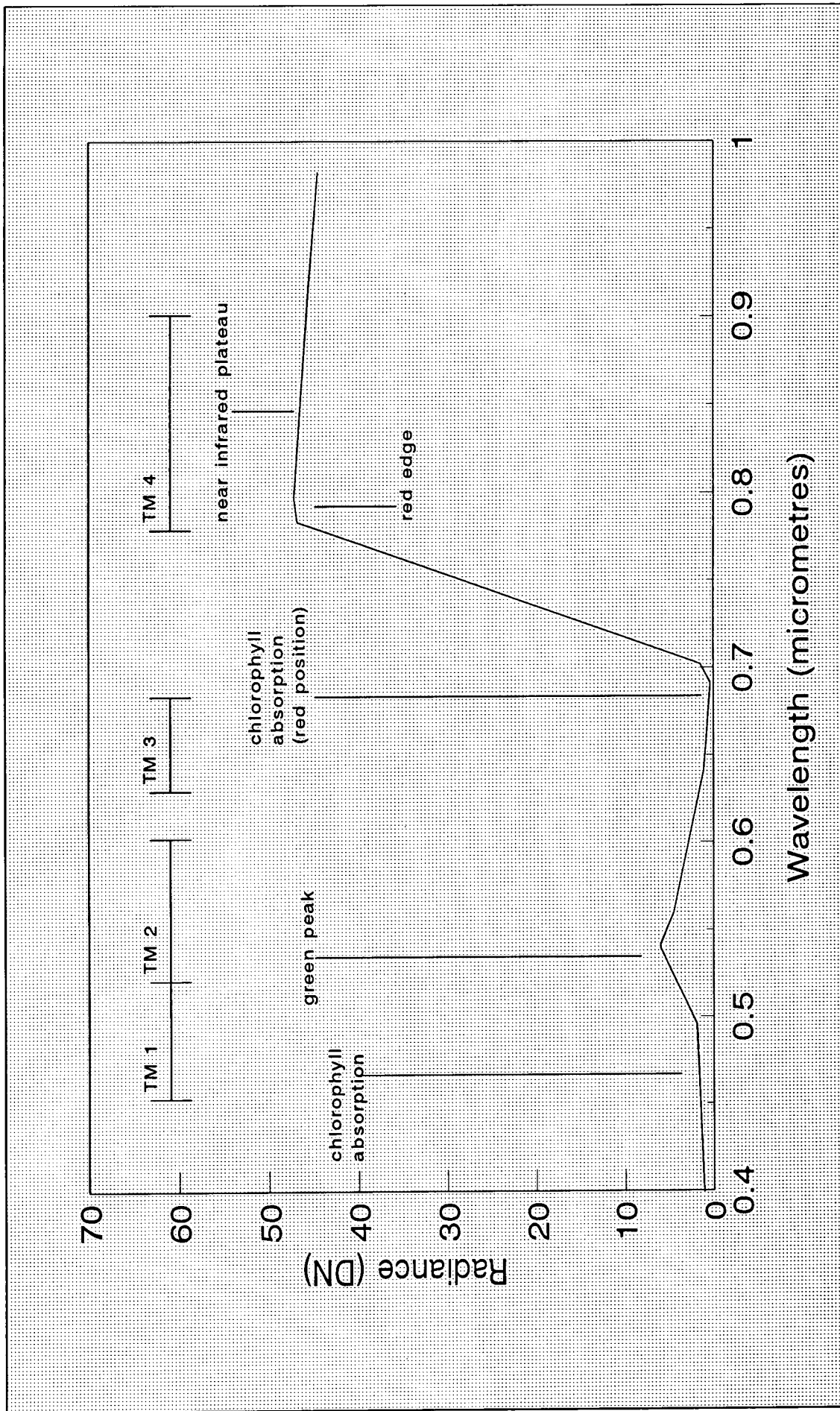


Fig 2.2 Vegetation reflectance and absorption features. Landsat 5 TM bands are illustrated.

High reflectance in the Near Infrared (NIR) wavelengths of the electromagnetic spectrum

Plant cells are very efficient at preventing NIR electromagnetic energy entering their structure. The high reflectance in the infrared is associated with the spongy mesophyll tissue of higher plants. The cuticle and epidermis are almost completely transparent to infrared radiation with the result that very little infrared radiation is reflected from the outer portion of the leaf. Radiation passing through the upper epidermis is strongly scattered by mesophyll and cavities within the leaf. The boundaries between cell walls and air spaces strongly reflect radiation at NIR wavelengths. The result is that very little NIR energy is absorbed internally by the leaf. Approximately 60% is scattered upward (reflected) or downward (transmitted) (Campbell, 1987). Some studies also suggest that the palisade tissue may also be important in infrared reflectance. Stomates, nuclei and cytoplasm also contribute to NIR light scattering (Woolley, 1971). It is the internal structure of the leaf that is responsible for the bright NIR reflectance of living vegetation.

The 'Red Edge'

At the edge of the visible spectrum, as the absorption of red light by chlorophyll pigments begins to decline, reflectance rises sharply. The 'red edge', the slope between the area of low visible reflectance and higher NIR reflectance, is a major feature of vegetation spectra. This behaviour explains the usefulness of the NIR spectrum for vegetation studies using remote sensing techniques and facilitates the separation of vegetated from non-vegetated surfaces as non-vegetated surfaces are usually much darker in the NIR. Furthermore differences in the reflectance characteristics of different plant species are markedly more pronounced in the NIR than in the visible. As a result discrimination of vegetation species is often possible using NIR reflectance. This fact was verified in the present study (chapters 3, 6).

The NIR Plateau

The NIR plateau, located between 0.8 and 1.3 μm , is a characteristic of the leaf

tissue. The plateau is not uniform and contains potentially diagnostic features that may be related to both cellular arrangement within the leaf and hydration state. As water is lost from a fully turgid leaf the reflectance increases but the different patterns in this increase change with plant species (Woolley, 1971). Cellular arrangement within a leaf is genetically controlled and is therefore potentially a characteristic that may be used for separating or identifying vegetation types, though this area of the spectrum is not examined in detail in the present study. In the longer wavelengths, beyond 1.3 μm , leaf water content appears to control the spectral properties of the leaf.

The result of these similar features is that there is far less variation in the spectra of different vegetation types than there are amongst the spectra of different types of minerals. This is a major problem when looking to distinguish between vegetation types on the basis of their spectral characteristics. The identification of vegetation types from their spectra is further complicated by the fact that the shape of the spectral curve is dynamic. The shape of the curve changes as a result of phenology, senescence and stress.

PHENOLOGY

This is the relationship between vegetative growth and environment and is often dominated by seasonal changes in vegetation growth and decline. Many phenological changes can be monitored by means of remote sensing as plants change in appearance and structure during the growing cycle. Of special significance are spectral and physiological changes that occur as a plant matures. On the East coast of the United States, Drake (1976) monitored red and infrared reflectance of three saltmarshes at intervals of two weeks between February and August 1974. There was found to be an abrupt decline in red reflectance at the onset of greening in the Spring and was correlated with an increase in green biomass. Through the seasons plants experience chemical, physical and biological changes known as senescence, that result in a progressive deterioration of leaves, stems, fruits and flowers. This process has a marked impact on the reflectance properties of vegetation.

Changes in the chlorophyll content with maturity produces a "shift" in the red absorption area of vegetation. Collins (1978) studied changes in the spectral response of

vegetation as maturity approached and in particular the shift in position of the red chlorophyll absorption edge towards longer wavelengths. As vegetation approaches maturity, chlorophyll increases in abundance. Increased concentrations change the molecular form in a manner that adds absorption bands to the edge of the chlorophyll absorption region, thereby producing the red shift. The magnitude of the shift was found to vary between vegetation species.

During the onset of senescence deterioration of cell walls in the mesophyll tissue produces a distinctive decline in infrared reflectance. Reflectance in the near-infrared region is apparently controlled by the nature of the complex cavities within the leaf and the internal reflection and re-reflection of infrared radiation within these cavities. Some workers suggest that moisture stress or natural maturity of a leaf causes these cavities to collapse as a plant wilts but others maintain that it is more likely that decreases in NIR reflection are caused by the deterioration of cell walls rather than the physical changes in the cavities themselves (Campbell, 1987). Changes in the infrared reflectance can reveal changes in vegetative vigour and infrared images have been valuable in detecting and mapping the presence, distribution and spread of crop diseases and phenology. An accompanying increase in visible reflectance may be the result of a decline in the abundance and effectiveness of chlorophyll as an absorber of visible radiation. The reduction in chlorophyll absorption resulting from senescence is often accompanied by the release of other pigments that produce new absorption bands in the visible part of the spectrum.

The phenology of a specific plant defines its seasonal pattern of growth, flowering, senescence and dormancy. Phenology patterns differ between species and this can be used to the advantage of remotely sensed vegetation surveys. Bartlett and Klemas (1980) illustrated the potential of seasonality for the spectral discrimination of one saltmarsh plant community from another. The discrimination of *Spartina alterniflora* from *Spartina patens* and *Distichlis spicata* proved to be almost entirely dependent on season. Carter and Schubert (1973) conducted a similar study of several wetland vegetation types during May through October in Virginia and arrived at similar conclusions.

Multi-temporal imagery of saltmarsh has been shown to be useful in the process of classification by Hobbs and Shennan (1986) in the present study area. Hobbs and Shennan

(1986) suggest that separation of vegetated from non-vegetated marsh will be most effective using imagery acquired in late summer (September), when the Pioneer zone contains mature *Salicornia*. By September the *Salicornia* zone is indistinguishable in spectral terms from the mid-marsh, whereas in July the *Salicornia* zone is often classified as mud. Sites of 5-35% *Salicornia* coverage recorded in July showed 99-100% coverage in September. Thus comparison of July and September images are required to assess the extent of the *Salicornia* zone, or Pioneer marsh, through a process of subtraction. In this case the acquisition of ground reflectance data in July and September improves discrimination among saltmarsh surfaces by exploitation of the seasonality exhibited by various vegetation groups. The next chapter of this present work concerns itself with the spectral characteristics of Wash saltmarsh vegetation.

THE VEGETATION CANOPY

A final problem with regard to the remote sensing of vegetation is the fact that the reflectance characteristics of a leaf are insufficient to describe the remotely sensed reflectance of a vegetation canopy. Knowledge of the spectral behaviour of individual leaves is important for understanding the spectral characteristics of vegetation canopies but cannot in itself completely explain reflectance from areas of complete vegetation cover. A vegetation canopy is not a large leaf but is composed of: a mosaic of leaves that may vary in size, orientation, shape and coverage of the ground surface; other plant structures such as branches; detrital material; background and shadow (Curran, 1985). Such problems were clearly illustrated by Budd and Milton (1982) who were unable to observe any significant correlation between spectral data and canopy parameters of *Spartina anglica*. The poor correlations could be attributed to muddy leaves, different moisture contents of the substrate, the quantity of dead vegetation in the canopy, or of differing amounts of shadow in the vegetation canopy. The amount of shadow depends in on the angle of illumination, and the shapes and orientation of leaves. Shadowing has a tendency to decrease canopy reflectance below the values normally observed in the laboratory for individual leaves. As a result the reflectance of a vegetation canopy tends to be lower than values measured for individual leaves. The relative decrease is much lower in the NIR than in the visible (Campbell, 1987). This makes the taking of field measurements essential if practical applications are to be developed. Likewise

attempts should always be made, when looking to compare vegetation spectra, to take the measurements under similar conditions. This is often unfeasible in practice and therefore requires some form of atmospheric rectification or normalisation technique (chapter 4).

Bartlett and Klemas (1980) showed that the spectral reflectance of *Spartina alterniflora* depended strongly on the characteristics of its canopy. Canopy reflectance characteristics are also affected by changing seasons. Over a period of six months (October to March) red canopy reflectance is not particularly useful in monitoring canopy parameters. The relatively small amounts of green plant material present at the bottom of the canopy during this period produce widespread homogeneity in the visible reflectance for a number of species.

The spectral signature of vegetation canopies changes through both space and time. Such factors have made it very difficult to differentiate between vegetation types, solely on the basis of remotely sensed spectra, on anything more detailed than broad vegetation groups in previously unmapped areas.

Previous work on the remote sensing of saltmarshes can be placed into three categories:

INVENTORY

The earliest studies tended to concentrate on the delineation of saltmarshes in an attempt to inventory the amounts of saltmarsh. The most common remote sensing method used in such studies has been qualitative interpretation of aerial photographs. Black and white panchromatic, black and white infrared and colour-infrared aerial photographs have been used to yield qualitative information (Hubbard and Grimes, 1974) about saltmarshes and are frequently used by land resource managers. The two comprehensive surveys of the Wash Estuary carried out in the 1970s (N.E.R.C., 1976) and 1980s (Hill, 1988) relied on aerial photographs. These methods have the disadvantages of being spatially restrictive, time consuming and costly as they require the use of highly skilled personnel. As the production of satellite sensor data has grown satellite multispectral images have been used for delineation

of the wetland boundary, plant community mapping and in monitoring the impact of man on saltmarshes. Satellite imagery has the advantage of being synoptic, rapid and can be used to provide a temporal perspective by identifying and quantifying any changes between surveys. A good example of a satellite based study is Hong and IIsaka's (1982) study of landuse change and reclamation in Tokyo Bay using multi-temporal Landsat images. A more complex study is that of Browder *et al.* (1989) in their modelling trends of wetland losses using Landsat TM satellite imagery.

BIOMASS ESTIMATION

More recently effort has been directed towards the interpretation of remotely sensed data for the estimation of saltmarsh biomass and primary productivity using techniques that have been successfully applied to other forms of vegetation such as band ratioing. There have been numerous published reports on the relationship between canopy properties and spectral data of saltmarsh vegetation using hand-held radiometers and spectrometers. Bartlett and Klemas (1979, 1980) illustrated that because visible reflectance is inversely related to the % of green vegetation, while infrared reflectance is positively correlated with the amount of vegetation present, the infrared/red canopy reflectance ratio is proportional to green biomass of the *Spartina alterniflora* canopy during the period April through September. Similarly Budd and Milton (1982) found high positive correlations between reflectance and the biomass of *Zostera marina* and *Fucus vesiculosus* in Britain. Likewise Gross *et al.* (1986) reported that the above ground live biomass of *Spartina anglica* in French marshes could be accurately predicted from spectral data collected using hand held radiometers. A further study conducted by Gross *et al.* (1988) developed equations, based on spectral measurements of marsh canopy in one saltmarsh, to accurately predict biomass of Brittany saltmarshes from spectral data. Early in the growing season accurate estimates were calculated for the biomass of *Puccinellia maritima*, *Halimione portulacoides* and *Spartina alterniflora*.

CLASSIFICATION

Hobbs and Shennan (1986) looked at the ability of remote sensing methods to distinguish between saltmarsh vegetated and non-vegetated surfaces in the Wash Estuary,

using ground measurements in the first four TM bands at 1 m spatial resolution. At least seven surface types were clearly identified in the intertidal zone. This implied that Landsat TM satellite imagery could be of considerable use in the delineation, classification and monitoring of saltmarshes. It must however be noted that the ground resolution of Landsat TM imagery is in the order of 30 m. The imbalance between the spatial resolution of satellite sensors and ground sampling is a severe limitation in the use of satellite sensor data in an operational mode. This is especially true of the remote sensing of saltmarshes as the diversity of species in the upper reaches of saltmarshes and the mixture of mud and vegetation in the lower reaches makes classification particularly difficult. The use of SPOT HRV Panchromatic imagery, with a spatial resolution of 10 m, or aerial photography may reduce such problems but it is still likely that some form of mixture modelling will be essential in the accurate evaluation of saltmarshes using remote sensing techniques (chapter 7). It is not only the great mixture of vegetation species that makes remote sensing of saltmarshes particularly challenging: the state of the tide is also of great importance when examining the spectral characteristics of saltmarshes (Donoghue and Zong, 1992). It may well be that the successful interpretation of saltmarsh imagery may only result from images taken at low tide.

Donoghue and Shennan (1987) assessed the feasibility of using Landsat TM data for saltmarsh species classification having gained training information from ground studies. The study highlighted many of the problems that have to be overcome in moving from ground based to satellite based studies. One of the limitations they found was that spectral vectors, as obtained by Landsat TM, may not characterise relevant botanical features with sufficient precision. Landsat TM operates in broad bands because of the small signal obtained as a result of the short residence of the detector in each instantaneous field of view. The result is that only very coarse spectral detail can be resolved. This is clearly a problem when trying to classify spectrally very similar types of vegetation in a saltmarsh and illustrates one of the many special problems that the remote sensing of saltmarshes presents.

The shape of the spectral curve for any type of vegetation is dynamic: the shape of the curve changes as a result of senescence, phenology and stress. This was clearly illustrated by Gross *et al.* (1988). The equations that were calculated to estimate the biomass of Brittany saltmarshes were found to be specific only to the saltmarshes of the coast of Brittany. An

attempt to apply the same equations to saltmarsh in Delaware met with poor levels of accuracy in biomass estimation. In order to distinguish vegetation types it is sometimes necessary to have reference to phenological spectral curves. Ungar and Collins (1977) compiled an atlas of high resolution spectra of selected crops with details of soil type and crop development stage. Further work of this type may prove to be of significant value for ecological and land use mapping. The difference in the phenology of different species of saltmarsh vegetation may be used to the advantage of species classification using remote sensing methods (Donoghue and Shennan, 1987). A further point mentioned in this study was the fact that most of the spectral signatures of intertidal vegetation exhibit seasonal hysteresis and as a result ground survey and image acquisition should be contemporary. Accurate training data is of the utmost importance in the successful interpretation of remotely sensed images of saltmarshes. Where the saltmarsh consists of vegetation communities for which adequate training data have been obtained, the classified image correlates in great detail with field observations. This implies that with accurate training data satellite imagery will provide accurate spectral and spatial characteristics. Chapter 3 goes on to look at the spectral signatures of the training areas used in the present study.

LANDSAT 5 TM DATA

The data used in the present study are predominantly Landsat 5 Thematic Mapper data. Data from the Landsat series of satellites have been available since 1972 and the temporal range represents a valuable resource for environmental mapping. The Landsat Thematic Mapper (TM) carried on Landsat 4 and Landsat 5 was designed with the intention of mapping vegetation and therefore provides an appropriate data source for the present study. The choice of the spectral bands sensed by TM is directly related to the spectral response of vegetation. Fig. 2.2 illustrates the location of the first four Landsat TM bands in relation to the spectral response of vegetation. Landsat TM has 7 bands of which only six are normally used for mapping vegetation. TM bands 1 and 3 correspond to the chlorophyll absorption bands and TM band 2 corresponds with the green peak. TM band 4 senses the part of the vegetation spectrum where reflectance is dominated by the physical structure of green leaves and by the mesophyll layer in particular. TM band 5 lies between two deep water absorption bands and is sensitive to vegetation moisture. TM band 7 has a similar

response for vegetation as band 5 and its choice was governed more by geological mapping considerations rather than vegetation mapping considerations (N.E.R.C. 1983). TM band 6 corresponds with part of the thermal infrared region of the electromagnetic spectrum, sensing the emitted longwave radiation of the Earth's surface. The characteristics of Landsat 5 TM data are outlined in Table 2.1 and their potential uses are listed in Table 2.2.

Table 2.1 CHARACTERISTICS OF LANDSAT 5 TM DATA

Quantization levels	256
Field of view	186 km
Spatial resolution	30 m
Altitude of satellite	705 km
Return period	16 days

Table 2.2 TM BAND APPLICATIONS

TM BANDS	WAVELENGTH (μm)	APPLICATIONS
1	0.45 - 0.52 (blue-green)	Separation of coniferous and deciduous woodlands. Studies of sediment laden water: longshore drift, estuarine plumes, suspended sediment in lakes and rivers. Identification of sediment source areas. Bathymetry. Surface properties of snow and ice. Soil organic matter
2	0.52 - 0.60 (green)	Indicator of green vegetation through chlorophyll reflection. Biogeomorphic indicators-soil erosion. Pedological studies, soil toxicity and disturbed ground. Ratio 2/4 limonitic rock mapping and for redness of desert sand.
3	0.63 - 0.69 (red)	Indicator of green vegetation through chlorophyll absorption. Vegetation cover mapping and identification of cropping practices for erosion studies. Ratio 3/4 geobotanical relationships. Lithological separation (iron rich rocks) and structural studies.
4	0.79 - 0.90 (near-IR)	Vegetation survey through reflection by mesophyll layer. Water body delineation, spring lines and drainage network morphometry. Reconnaissance mapping and geobotanical studies.
5	1.55 - 1.75 (mid-IR)	Leaf moisture. Lithological mapping, bedrock/drift separation. Soil moisture mapping. Ratio 4/5 separates hydrous and iron rich rocks, ratio 5/7 for clay mineral differentiation.
6	10.4 - 12.5 (thermal)	Plant heat stress, evapotranspiration. Lithological mapping, geological reconnaissance studies, thermal mapping of sediments. Ground water studies, topographic mapping and extraction of sub-surface anomalies. bathymetry of lakes and discrimination of silicious rich rock.
7	2.08 - 2.35 (mid-IR)	Lithological discrimination, metamorphic rocks, hydrous minerals and carbonates separation. Hydrothermal alteration.

Table 2.2 Landsat TM band applications (taken from N.E.R.C. 1983)

Bartlett, D.S. and Klemas, V. 1979: Assessment of tidal wetland habitat and productivity. **Proceedings of the 13th Symposium on Remote Sensing of Environment**. Ann Arbor, Michigan: 1241-1260.

Bartlett, D.S. and Klemas, V. 1980: Quantitative assessment of tidal wetlands using remote sensing. **Environmental Management**. vol. 4: 337-345.

Browder, J.A., Nelson May, L., Rosenthal, A., Gosselink, J.G. and Baumann, R.H. 1989: Modelling future trends in wetland loss and brown shrimp production in Louisiana using Thematic Mapper Imagery. **Remote Sensing of Environment**. vol. 28: 45-59.

Budd, J.T.C. and Milton, E.J. 1982: Remote sensing of saltmarsh in the first four proposed thematic bands. **International Journal of Remote Sensing**. vol. 3: 147-161.

Campbell, J.B. 1987: Remote sensing applications in the plant sciences. **Introduction to Remote Sensing**. Guildford Press, London: 366-403.

Carter, V. and Schubert, J. 1973: Coastal wetlands analysis from ERTS MSS digital data and field spectral measurements. **Proceedings of the Ninth International Symposium on Remote Sensing of the Environment**. Ann Arbor Michigan, USA: 1241-1260.

Collins, W. 1978: Remote sensing of crop type and maturity. **Photogrammetric Engineering and Remote Sensing**. vol. 44: 43-55.

Curran, P.J. 1985: **Principles of Remote Sensing**. Longman, New York.

Donoghue, D.N.M. and Shennan, I. 1987: A preliminary assessment of Landsat TM imagery for mapping vegetation and sediment distribution in the Wash Estuary. **International Journal of Remote Sensing**. vol. 8: 1101-1108.

Donoghue, D.N.M., and Zong, Y. 1992: **Coastal Sediment Mapping in the Tees Estuary**. Department of Geography, University of Durham. Unpublished work.

Drake, B.G. 1976: Seasonal changes in reflectance and standing crop biomass in three salt marsh communities. **Plant Physiology**. vol. 58: 696-699.

Gross, M.F., Klemas, V. and Levasseur, J.E. 1986: Remote sensing of *Spartina anglica* in Five French Salt Marshes. **International Journal of Remote Sensing**. vol. 7: 657-664.

Gross, M.F., Klemas, V. and Levasseur, J.E. 1988: **Remote sensing of saltmarsh vegetation in France**. **International Journal of Remote Sensing**. vol. 9: 397-408.

Hill, M.I. 1988: **Saltmarsh Vegetation of the Wash. An Assessment of Change From 1971 to 1985**. N.C.C. Publications, Peterborough.

Hobbs, A.J and Shennan, I. 1986: Remote sensing of saltmarsh reclamation in the Wash, England. **Journal of Coastal Research**. vol. 2: 181-198.

Hong, J.K and Iisaka, J. 1982: Coastal environmental change analysis by Landsat MSS data. **Remote Sensing of Environment**. vol. 12: 107-116.

Hubbard, J.C.E. and Grimes, B.H. 1974: Coastal vegetation surveys. In Barrett, E.C and Curtis L.F. (eds) **Environmental Remote Sensing**. London, Edward Arnold: 129-141.

National Environment Research Council, 1976: **The Wash Water Storage Scheme Feasibility Study. A Report on the Ecological Studies**. N.E.R.C. Publications Series C, No.15.

National Environment Research Council, 1983: **Thematic Mapper Data: Characteristics and Use**. Landsat-4, February 4, 1983. Reading, Berkshire.

Ungar, S.G. and Collins, 1977: **Atlas of Selected Crop Spectra, Imperial Valley California**. NASA Institute for Space Studies, GSFC Tech, Mem., TM-9473, June 1977.

Woolley, J.T. 1971: Reflectance and Transmittance of Light by Leaves. **Plant Physiology**. vol. 47: 656-662.

CHAPTER 3

ANALYSIS OF WASH ESTUARY VEGETATION SPECTRA

It has often been hypothesised that imaging spectrometry is a key to material identification in remote sensing as it allows continuous spectral sampling at an interval sufficiently narrow to resolve diagnostic spectral features (Goetz, 1984; 1992). In the case of vegetation spectra, diagnostic features may include details of:

- the red edge
- red depth
- chlorophyll a and b absorption features
- the character of the green peak (Fig. 3.1).

The major differences that there are in leaf reflectance of different vegetation species are mainly dependent on leaf thickness (Curran, 1985). This affects both the pigment content (visible reflectance) and physiological structure (Near Infrared reflectance). Past applications, concerned with remotely sensed vegetation classification and monitoring, have concentrated on the different intensity of NIR reflectance and chlorophyll absorption (Tucker, 1979; Bauer, 1986). In the case of the remote sensing of saltmarshes this may be illustrated by the study of Bartlett and Klemas (1980) who took canopy reflectance measurements during the period April through to October in the visible spectral region and showed that these values were inversely related to the percentage of green vegetation within the canopy. This chapter looks at high spectral resolution saltmarsh vegetation spectra taken with the Geophysical Environmental Research SIRIS Spectrometer in an attempt to identify and quantify diagnostic spectral features for different saltmarsh species. The chapter goes on to compare the ground measurement spectra with spectra produced by analysis of satellite borne sensors. This was done to establish if any of the broad characteristics of an individual vegetation spectrum, taken from detailed ground measurements could also be identifiable from the air and space. The ability of being able to classify vegetation in some degree of detail from space has considerable application in the field of environmental management inventory, classification and monitoring and is the basis of the maximum likelihood classifier used in chapter 6 of the present study.

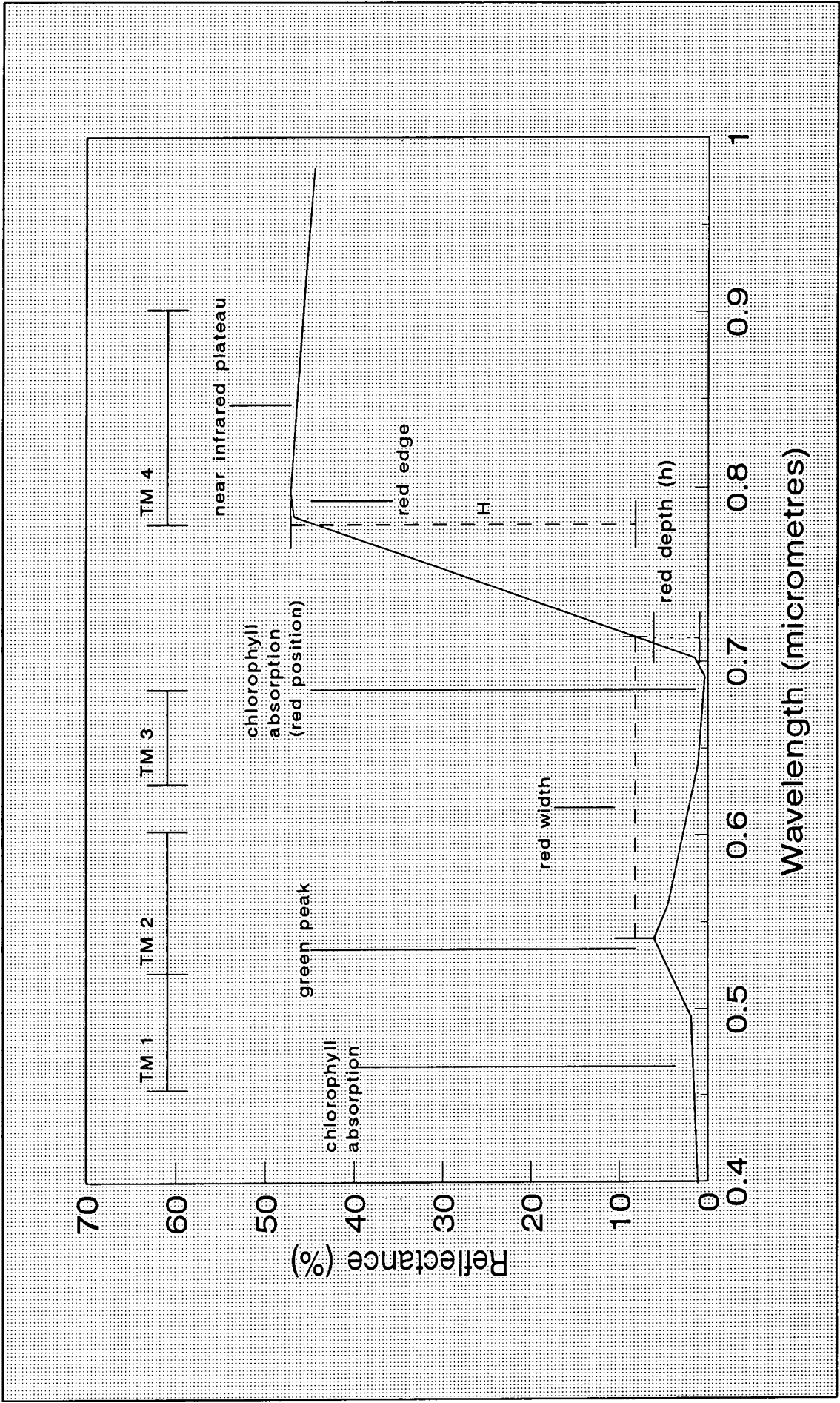


Fig 3.1 Hypothetical vegetation spectrum. TM bands and features calculated by the vegetation algorithms are illustrated.

It is clear from looking at the spectral curves of different vegetation species that their spectra do vary (Figs. 3.2-3.11). What is often lacking is a way of adequately describing the shape of the spectra, via objective means, that allows for comparison and hence potential differentiation of vegetation species. In this study simple mathematical algorithms, written by Dr. Donoghue of the University of Durham were applied to describe accurately and objectively several of the features of the vegetation spectra (Appendix II). This description allows an accurate, objective comparison of different vegetation species and provide data about the most useful spectral features for discriminating between vegetation classes.

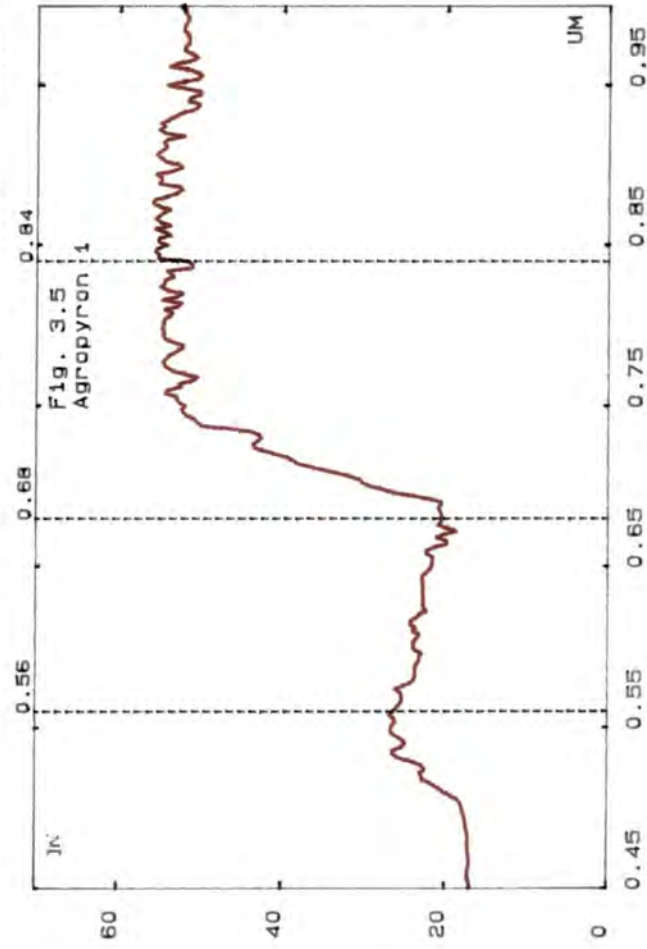
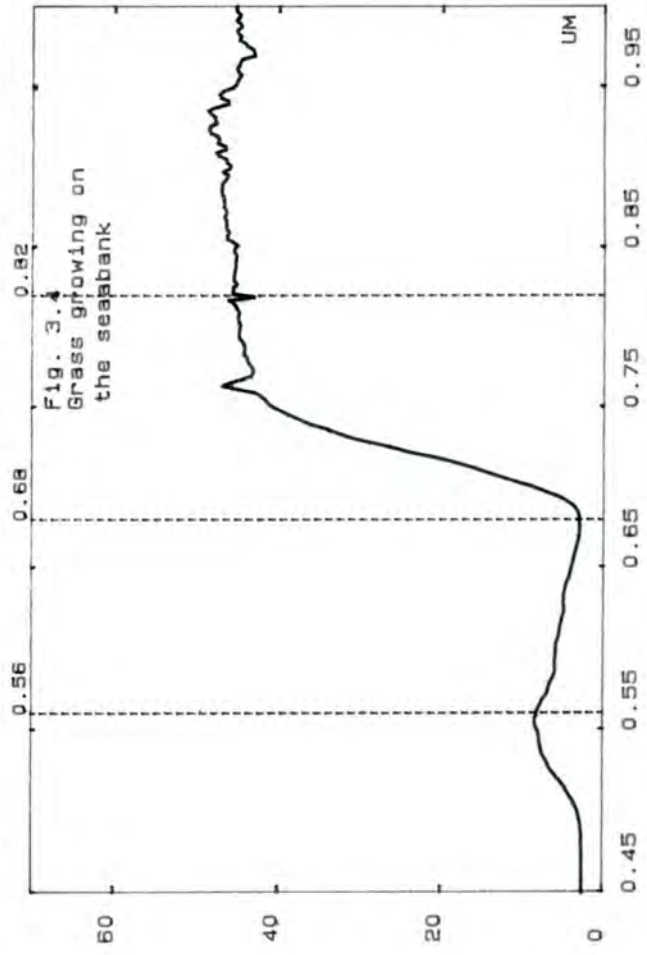
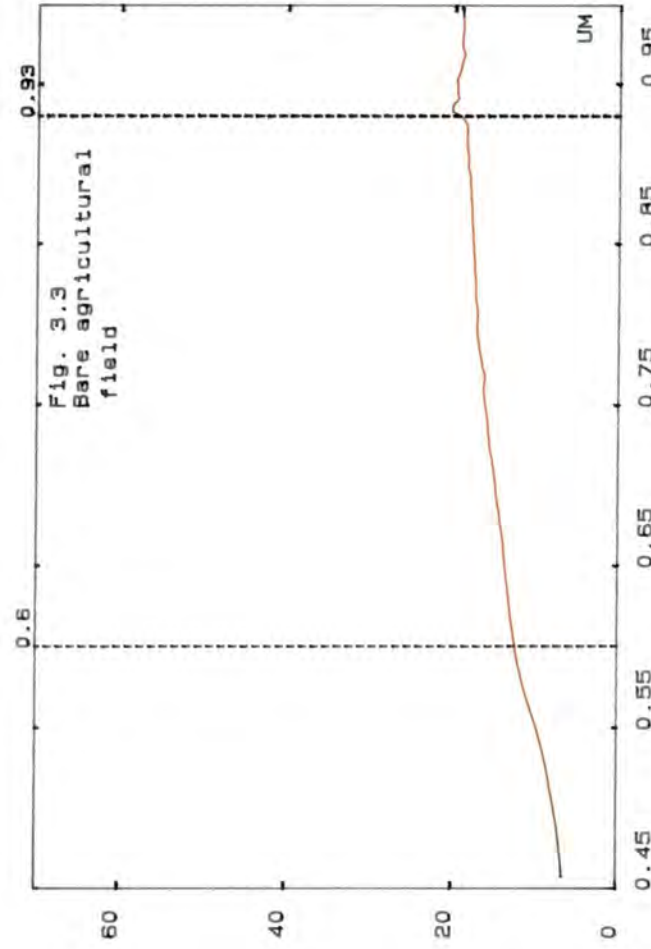
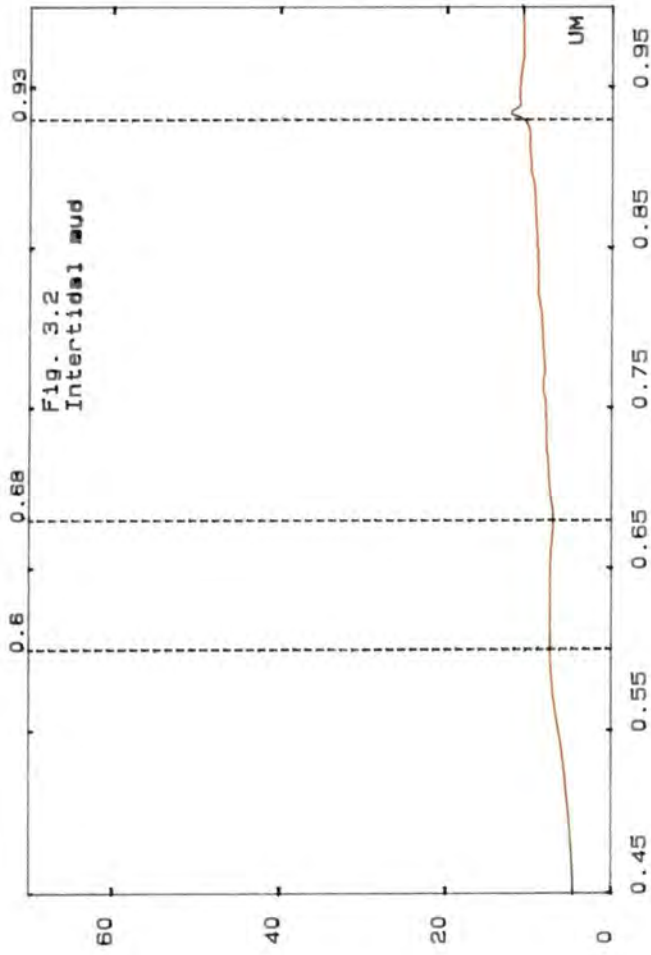
METHOD

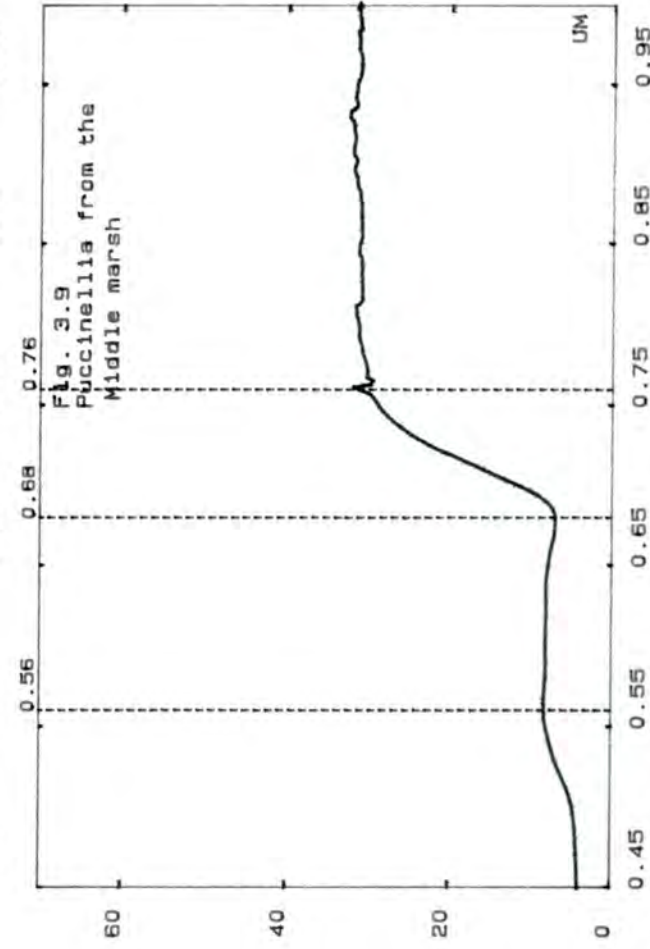
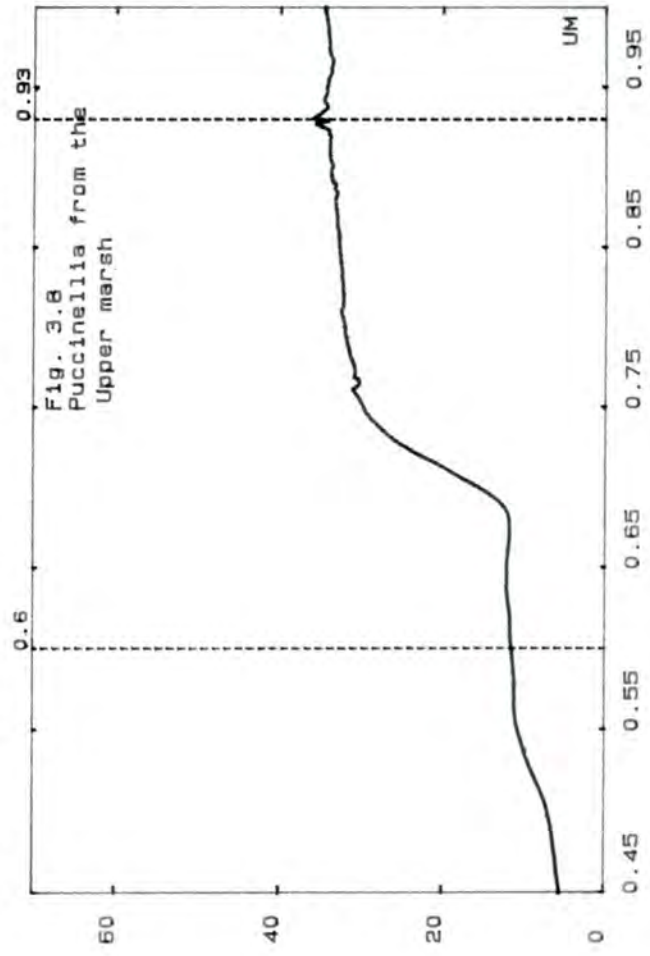
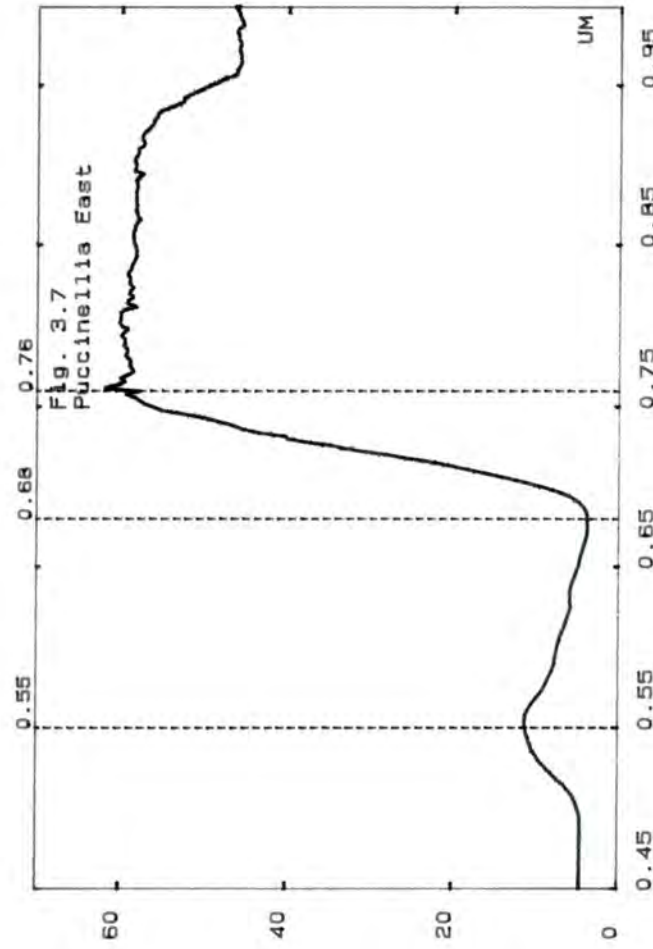
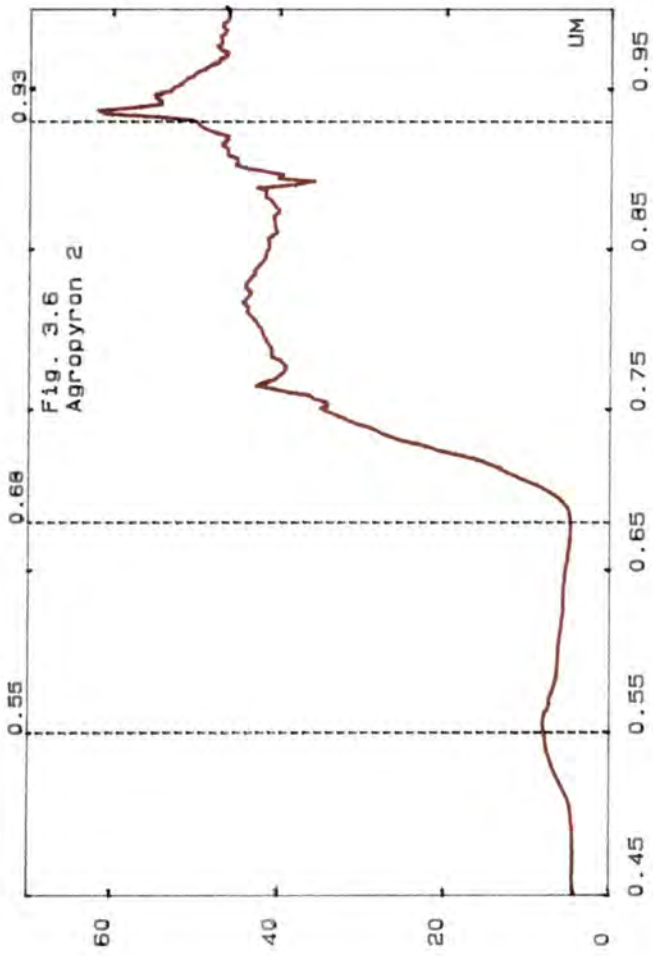
Ground measurements were taken during late May/June 1991 using a SIRIS field spectrometer. Early summer was chosen as this ensured that all vegetation would be photosynthetically active and hence allow a degree of comparison. This time period also allowed comparison with the May 1984 Landsat 5 TM image of the Wash Estuary, taken at a similar stage in the growing cycle. Ideally measurements should be taken throughout the growing cycle in order to identify the times of the year that offer the best chance of discrimination. Hobbs and Shennan(1986) illustrated that such knowledge is often essential for discriminating the Pioneer zone from the rest of the marsh. Temporal measurements were not possible in the timescale of an MSc but this issue should be addressed if the study is expanded. Raw spectra also include atmospheric transmission, path radiance, insolation and instrumental features. Measurements of target and a reference surface (fibrofax) were taken in the field. The two readings were referenced against each other to remove the effects of differing illumination conditions, atmospheric interference and instrument effects. Five readings were taken for each surface type and the results averaged. The spectra recorded from the Wash are illustrated in Figs. 3.2-3.11 (processed and produced on T-Spectra (T-Spectra, 1991)).

The second step involved running a C-program which calculated several characteristics of a vegetation spectrum in order to allow objective description and comparison (Appendix II). The characteristics calculated were: green peak; position of the chlorophyll absorption feature in the red part of the spectrum; the depth of the red

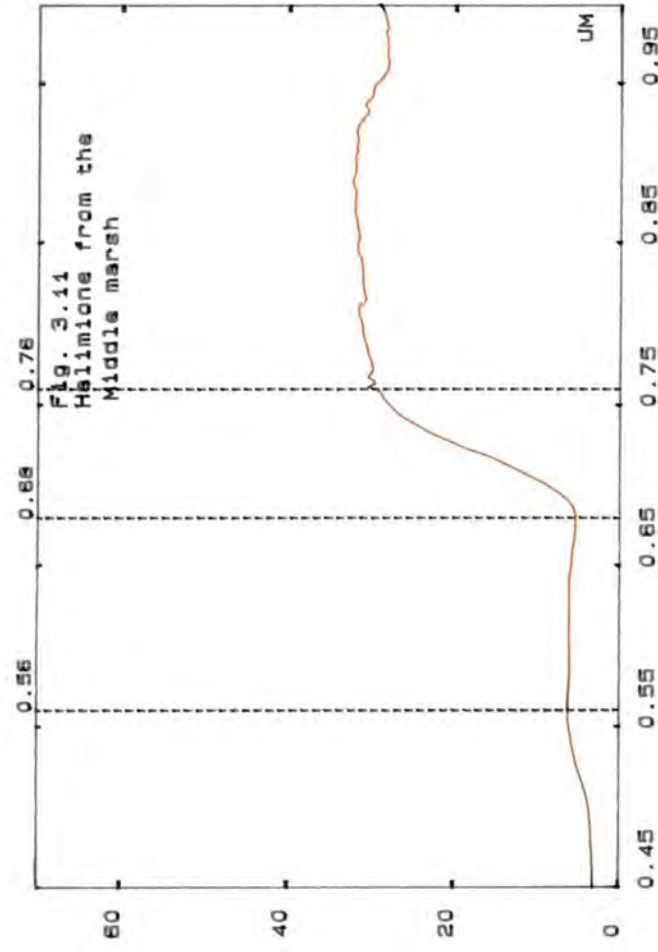
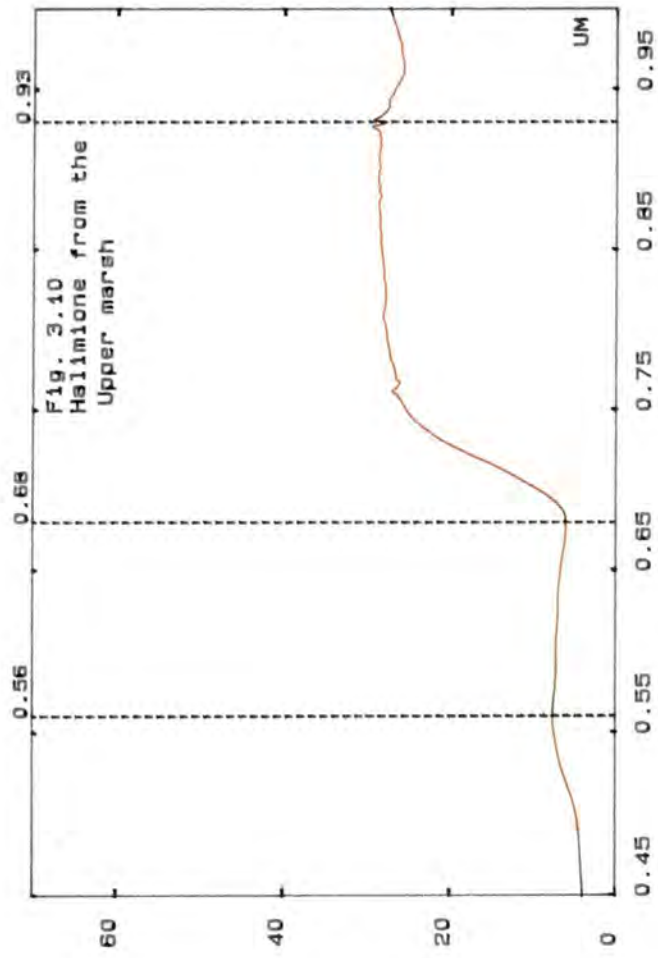
chlorophyll absorption feature; red width (delimiting the photosynthetically active part of vegetation); red asymmetry; H/h ratio (combining information of green and NIR reflectance); the position of the red edge; and the gradient of the red edge (Fig. 3.1). The results were then compared to see if any of the characteristics proved to be particularly helpful in discriminating between vegetation species (Table 3.1).

The final stage of this analysis compared the spectra taken by the field spectrometer with the spectra obtained from the processing of satellite sensor data. All the spectra used were taken at similar times of year in an attempt to minimise differences resulting from senescence. The corresponding spectra were stacked and plotted on the same graph to allow easy comparison (Figs. 3.12-3.15). This was done to establish if any of the broader characteristics seen in the spectra taken from the ground measurements were also visible in the Landsat 5 TM data.





(all units are relative reflectance)



(all units are relative reflectance)

DISCUSSION

DISTINGUISHING BETWEEN VEGETATION AND OTHER COVER TYPES

By comparing Figs. 3.2 and 3.3 with the plots of the vegetation spectra (Figs. 3.4-3.11) it becomes immediately apparent that it is very easy to distinguish between vegetation cover and other ground cover types. This fact also holds true for the parameters given in Table 3.1: vegetation ground cover may be easily distinguished from other ground covers (bare field, soil and mud) by looking at the red depth, red width, red asymmetry and H/h ratio. This is much as would be expected due to vegetation's very distinctive spectral features.

GREEN PEAK

The position of the green peak proves to be very consistent throughout the vegetation spectra, both in the plots and in Table 3.1 with the green peak consistently being calculated between $0.554 \mu\text{m}$ and $0.6 \mu\text{m}$. This is again to be expected. All species of higher vegetation contain chlorophyll a and b which absorb in the same region of the electromagnetic spectrum, no matter what the species. The area between the chlorophyll absorption features gives the green peak, a position which varies very little between plant species. It is therefore unlikely that the position of this feature will be of much use in discriminating and identifying different species of vegetation on the basis of their spectral characteristics.

RED POSITION

The red position is constant between different species of vegetation. This is again what would be expected as it marks the region of strongest absorption of red light by chlorophyll a and b. Due to the fact that all green vegetation contains these pigments this point is constant between vegetation types. The algorithm calculated the red position of Seabank grass, Middle marsh *Puccinellia*, Upper marsh *Halimione* and Middle marsh *Halimione* all at $0.678 \mu\text{m}$. This implies that this feature will be unlikely to be of much use in discriminating and identifying different species of vegetation.

RED WIDTH

As there is little difference in the position of the green peak between vegetation species and likewise the position of the red edge there is unlikely to be a great deal of variation in the size of the red width between different types of vegetation. This is confirmed both by the plots and the figures in Table 3.1. Very little variation is apparent among the different plant species. Again this implies that this characteristic is unlikely to be of much assistance in discriminating between vegetation species.

RED DEPTH

Considerable variation can be seen in the size of the red depth both on the plots and in the figures in Table 3.1. A good example is a comparison of seabank grass (Fig. 3.4), *Puccinellia* East (Fig. 3.7) and *Puccinellia* (Figs. 3.8 and 3.9). At first this may seem to indicate a potential in distinguishing between different types of vegetation but it must be noted that the size of the red depth is very much subject to the influence of the health of the plant, phenological changes and senescence. The red depth for the spectrum of a given vegetation type changes both through space and time. This fact was illustrated even over the relatively small area of the Wash. Different spectral recordings would occur for the same vegetation type, the only difference being that one area had been grazed whereas the other had not. A good illustration of this is the difference in the spectral response of *Puccinellia* growing on the East coast of the Wash (Fig. 3.7) which is frequently grazed and *Puccinellia* growing elsewhere in the Wash Estuary (Figs 3.8 and 3.9). This would imply that unless the changes that occur in spectra as a result of the aforementioned factors are taken into account the size of the red depth is of limited use in identifying different species of vegetation. If these factors are accounted for then this characteristic does have a diagnostic potential. This is in keeping with the findings of other studies of vegetation spectra (Tucker *et al.*, 1986) and indeed the vegetative index worked out from both TM data and A.V.H.R.R. data make use of a feature very similar to this (Quarmby *et al.*, 1992; Tucker *et al.*, 1986).

RED ASYMMETRY

This parameter is a measure of the degree of symmetry in the area of red absorption. The parameter may be useful in detecting subtle red edge shifts within a species as a result of stress (Banninger, 1990) but both the plots and Table 3.1 imply that this feature is of little help in distinguishing between vegetation species. This is to be expected as the position of the green peak, red position and red edge does not to vary to any great extent between vegetation species.

RED EDGE

If the position of the red edge is studied in Table 3.1 considerable variation can be seen. This is more likely to be due to the nature of the algorithm rather than actual variation in the position of the red edge between plant species. The algorithm was designed for looking at pure vegetation spectra and not for spectra which also contained mixtures of mud and detrital material. Where the position of the red edge was calculated correctly (Figs. 3.7, 3.9, 3.11) the position does not appear to vary to any great extent. The lack of variation is much as would be expected as all vascular plants strongly reflect near-infrared light due to the presence of mesophyll which produces discontinuities in the refractive indices within a leaf. The height of this edge may vary considerably among plant species and seasons. It should be noted that the red edge often appears as a featureless slope because the output of many spectrometers is greatly smoothed to "improve" the signal to noise ratio, and has therefore seldom been subjected to much study. Greater study of this feature might prove rewarding (Horler, 1983) but it is beyond the scope of the present study.

THE GRADIENT OF THE RED EDGE

Until the algorithm for calculating the position of the red edge is made more rigorous it is only sensible at this stage to look at the vegetation spectra where the position of the red edge has been calculated with a reasonable degree of accuracy (*Puccinellia* East, Middle marsh *Puccinellia*, and Middle marsh *Halimione*). In the cases where accurate figures for the position of the red edge were calculated, and also through visual interpretation of the plots,

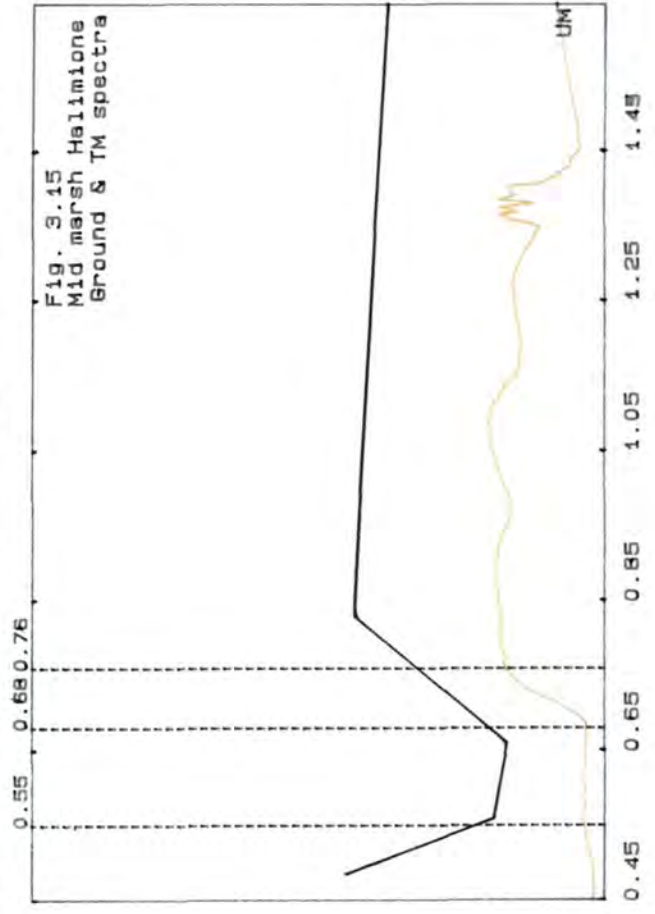
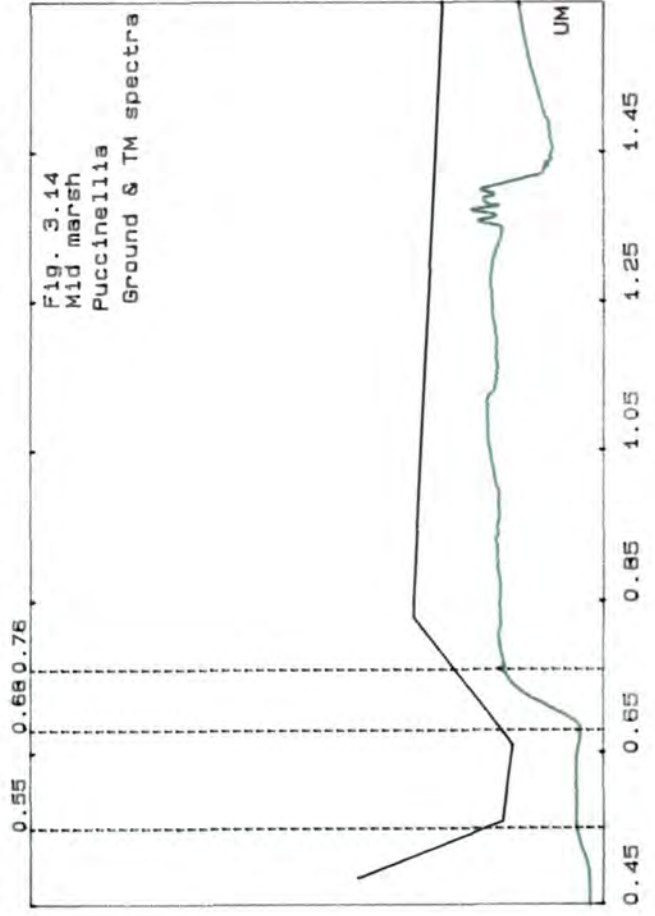
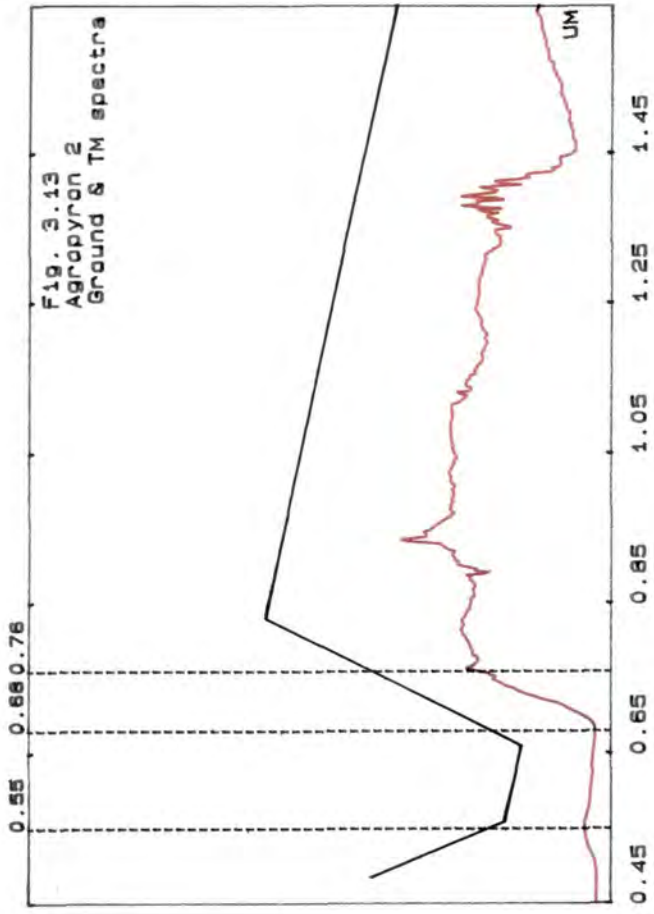
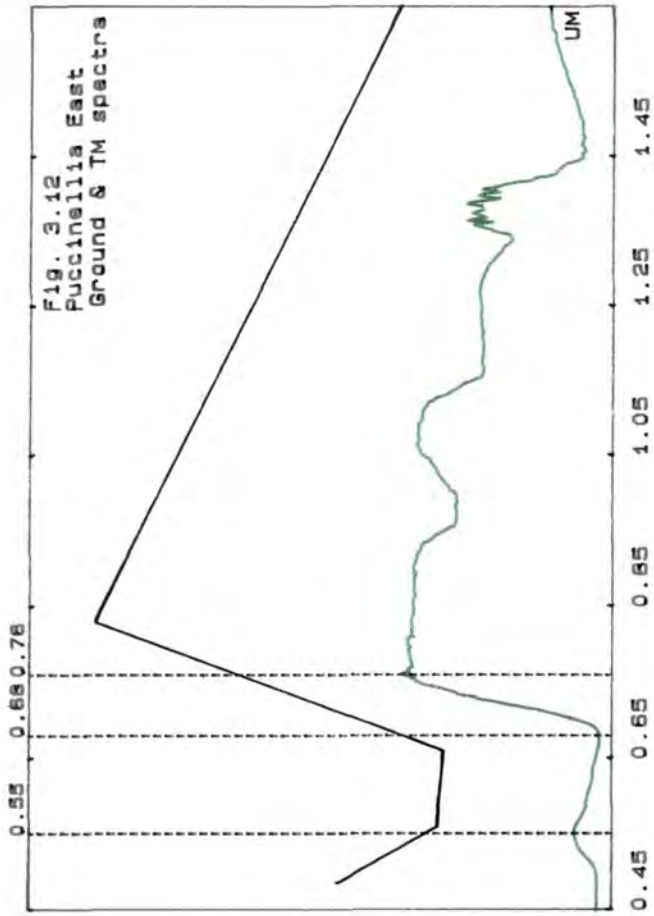
there appears to be considerable variation between plant species in terms of the red gradient. This is what would be expected as most remote sensing applications concerned with the identification of different vegetation covers have taken advantage of the large differences that there are in plants' abilities in reflecting very near infrared radiation and also in their concentrations of chlorophyll. The gradient of the red edge is very sensitive to the very NIR reflectance ability of a plant and its chlorophyll absorption. A good example of this is seen by comparing the plots and table figures for the spectra of *Puccinellia* (Fig 3.7) and Middle marsh *Halimione* (Fig. 3.11). This suggests that this characteristic could have considerable potential in discriminating between vegetation species. Again the factors mentioned in the discussion of the red depth must be taken into account as these will have a considerable affect on the gradient of the red edge.

H/h RATIO

This parameter is essentially a form of vegetation index, taking account of both the concentrations of chlorophyll and the plants ability to reflect energy at NIR wavelengths. This feature appears to have considerable potential in discriminating between plant species. For example the figure for *Agropyron* is 38.02 whilst that for Upper marsh *Puccinellia* is 22.18. Various forms of vegetation index have been widely used for the mapping of broad vegetation types and in the field of crop estimation (Quarmby, 1992). A vegetation index is so useful because it takes account of both a plant's ability to reflect NIR energy and also chlorophyll content. Again it must be borne in mind that a vegetation index changes markedly as a result of phenology, senescence and stress. These factors must be taken into account when any comparisons of vegetation spectra are carried out.

COMPARISON WITH SPECTRA TAKEN FROM LANDSAT 5 TM (14/5/84)

Landsat 5 TM bands (Table 3.1) are much broader than the SIRIS spectrometer bands. The bands on a satellite have to be much broader because of the small signal obtained as a result of the short residence time of the sensor in each instantaneous field of view. This means that only very coarse spectral detail can be resolved. Similarly because of the relatively coarse spatial resolution of Landsat 5 TM data (30 m) compared with the intricate nature of the saltmarsh the spectral response of a Landsat pixel does not illustrate the characteristics of an individual leaf but of the vegetation canopy as a whole and with it the whole range of added difficulties that were mentioned in the preceding chapter. It is therefore quite surprising and encouraging that the general shapes of the spectra taken from the ground measurements and those taken from the satellite fit remarkably well. The positioning of the Landsat TM bands 2, 3 and 4 means that the important diagnostic features, the green peak, the red absorption area and the red edge and Near infrared plateau, are all picked out. In a visual comparison of the respective spectra (Figs. 3.12-3.15) it can be seen that the gradient of the red edge, the position of the green peak and the red absorption area are all very well matched. This is only a very crude comparison. A more accurate study would compare ground spectra taken at the same time as the area is sensed by the satellite, but it does show that satellite sensor data is capable of distinguishing between different saltmarsh vegetation classes. This is very encouraging in the light of the aims of this present study which looks to survey and classify intertidal vegetation using Landsat 5 TM data. The discrimination of saltmarsh vegetation species from satellite altitudes is examined in more detail in chapter 6.



The most helpful features in distinguishing between plant species, through looking at their spectra, are the absorption and reflectance characteristics in the red visible and near-infrared characteristics of a plant. These differences are most clearly shown in parameters such as the edge gradient and the H/h ratio. This is in keeping with the findings of past studies. The application of the algorithms provide an objective means of describing and comparing different vegetation spectra. It must always be remembered that the spectra of vegetation are dynamic, changing both through space and time. Such factors have made it very difficult to differentiate between vegetation types, solely on the basis of single date remotely sensed spectra. It is often necessary to use multi-temporal and multi-sensor data sets, which make use of the temporal characteristics of the vegetation spectra, for the monitoring and classification of diverse vegetation systems, especially in spatially complex regions such as saltmarshes.

The results of the present analysis show that there may be considerable difficulty in distinguishing between the spectral response of *Puccinellia* and *Halimione* as both their shape and figures calculated by the algorithm proved to be very similar. If the study is to be expanded it is recommended that detailed spectral readings are taken throughout the growing season in order to establish the phenological characteristics of individual saltmarsh species. This may help to locate the optimum time of the year for species discrimination.

Banninger, C. 1990: Fluorescence Line Imager Measured "Red Edge" Shifts. **Proceedings In Imaging Spectroscopy of the Terrestrial Environment**. vol. 1298

Bartlett, D.S. and Klemas, V. 1980: Quantitative assessment of tidal wetlands using remote sensing. **Environmental Management**. vol. 4: 337-345.

Bauer, M.E. 1986: Field spectroscopy of agricultural crops. **Transactions on Geoscience and Remote Sensing**. vol. 24: 65-75.

Curran, P.J. 1985: **Principles of Remote Sensing**. Longman, New York.

Goetz, A.F.H. 1984: High spectral resolution of the land. **Proceedings In the Society for Optical Engineering**. vol. 47.

Goetz, A.F.H. 1992: Imaging spectrometry for earth remote sensing. In Toselli, F. and Bodechtal, J. (eds) **Imaging Spectroscopy: Fundamentals and Prospective Applications**. Kluwer Academic Publishers, London: 1-20.

Hobbs, A.J. and Shennan, I. 1986: Remote Sensing of saltmarsh reclamation in the Wash, England. **Journal of Coastal Research**. vol. 2: 181-198.

Horler, D.N. 1983: Red Edge Measurements For Remote Sensing Plant Chlorophyll Content. **Space Research Symposium on Remote Sensing and Mineral Exploration**. Ottawa.

Quarmby, N.A., 1992: Towards Continental Scale Crop Estimation. **International Journal of Remote Sensing**. vol. 13: 981-989.

Quarmby, N.A., Townshend, J.R.G., Settle, J.J. and White, K.H. 1992: Linear mixture modelling applied to A.V.H.R.R. data for crop area estimation. **International Journal of Remote Sensing**. vol. 13: 415-425.

T-Spectra 1991: **User's Guide to T-spectra Software**. Terra-Mar Resource Information Services, Inc. Mountain View, California.

Tucker, C.J 1979: Red and photographic infrared linear combinations for monitoring vegetation. **Remote Sensing of Environment**. vol. 8: 127-150.

Tucker, C.J., Fung, I.Y., Keeling, C.D. and Gammon, R.H. 1986: Relationship Between Atmospheric CO₂ Variations and a Satellite Derived Vegetation Index. **Nature**. vol. 319: 195-199.

CHAPTER 4

ATMOSPHERIC AND RADIOMETRIC CORRECTION

Chapters 2 and 3 illustrated that single date satellite imagery rarely permits the accurate classification of a wide range of vegetation cover types due to the spectral ambiguity at given physiological stages. It is therefore often essential to use multi-temporal data sets for the classification and monitoring of vegetation systems which are complex both in terms of space and in species diversity. Monitoring change of vegetation systems by its very definition relies on the use of multi-temporal imagery. Similarly the construction of a mixture model often relies on the use of multi-temporal and/or multi-sensor data.

In quantitative studies the use of multi-temporal and multi-sensor data presents a number of specific problems which must be accounted for if objective, comparable results are to be generated. The radiance of a surface received by a sensor may vary over several orders of magnitude depending upon the atmospheric conditions and viewing geometry. The sensor response will also be affected by solar irradiance and instrumental factors. It is necessary either to normalise radiance values to a standard set of conditions, or to retrieve the surface reflectance characteristics by applying suitable radiometric and atmospheric corrections.

RADIOMETRIC CALIBRATION

Before launch a sensor has to be calibrated in laboratory conditions in order to calculate the sensitivity of the instrument in converting the signal (spectral radiance) into quantised digital numbers (DN). This gives an equation (Richter, 1992):

$$SR(i) = c_0(i) + c_1(i) * DN(i)$$

Where $c_0(i)$ and $c_1(i)$ are offset and slope of the linear calibration function in band (i) and $SR(i)$ is the spectral radiance as received by the sensor.

In flight calibration must also be carried out in order to monitor the changes in the radiometric sensitivity of the instrument that occur during its operation. This is especially important in the case of long-term space missions. This may be illustrated by the case of the Coastal Zone Scanner where a sensitivity decay was found to occur during the course of the mission. Similarly the results of in flight calibration for Landsat and SPOT sensors have been shown to differ from pre-flight values (Slater *et al.*, 1987). Fortunately TM data comes ready radiometrically calibrated (United States Geological Survey, 1984). This fact, combined with the method of image referencing used in this study, discussed later in the chapter, means that the problems of radiometric calibration are greatly reduced in the present study.

IRRADIANCE

Irradiance is the intensity of electromagnetic energy striking a unit area on the surface of the Earth. On a bright, clear day in summer the amount of radiant energy penetrating the Earth's atmosphere, interacting with the Earth's surface and being reflected or emitted back through the atmosphere to be retrieved by a satellite sensor, will be much greater than on a dark, cloudy day in winter. As a result of these different irradiance conditions the radiance readings from a summer's day will be much higher than those from a winter's day. The shape of the spectral curve for a spectrally invariant target will not change except for the fact that DN values will be much higher for days with stronger solar irradiance conditions. In order to carry out accurate and objective comparisons of multi-temporal imagery it is necessary to normalise the irradiance conditions of the different images. If this is not done there will be no way of discovering whether differences in the intensity of DN values of a surface target are the result of changes in the spectral nature of the target or simply the result of differences in solar irradiance levels.

ATMOSPHERIC CORRECTION

As electromagnetic radiation passes through the atmosphere its frequency, intensity, spectral distribution and direction are all altered as a result of atmospheric **scattering**, **refraction** and **absorption** (Curran, 1985). The effects are most severe in visible and infrared wavelengths and are thus of a key concern in the present study.

Atmospheric scattering is most severe at visible wavelengths. It affects the direction of visible radiation. Atmospheric scattering can also alter the spectral distribution of visible and near visible wavelengths (Curran, 1985). Scattering may include Rayleigh, mie, non-selective and Raman scattering depending on the size of particles causing the scattering. For example Rayleigh scattering is associated with gas molecules whereas non-selective scattering results from water droplets and dust. The most important form of scattering is the Rayleigh scatter which affects short visible wavelengths and results in haze (Curran, 1985). This may be seen in band 1 of the vegetation spectra taken from the May 1984 Landsat5 TM image (chapter 3, Figs. 3.12-3.15)

Atmospheric refraction occurs as electromagnetic radiation passes through a stratified atmosphere. This is seldom a problem when the atmosphere is stable but when it is turbulent it can result in the bending of electromagnetic waves and the geometric correction of the remotely sensed data becomes highly problematical (Curran, 1985). Fortunately Landsat has near nadir viewing and therefore atmospheric depth is constant between Landsat TM images.

Atmospheric absorption affects electromagnetic radiation at wavelengths both shorter and longer than visible light. Absorption results when an atmospheric atom or molecule is excited by the absorption of electromagnetic energy (Curran, 1985). The radiation is not re-emitted at the wavelength at which it was absorbed, as occurs during scatter. The energy is used in heat motion and released at much longer wavelengths. Water vapour, ozone and carbon dioxide, the primary absorbers of electromagnetic energy in the atmosphere, interact with electromagnetic radiation by vibrational and rotational transitions, the net effect being absorption in specific wavebands (Fig. 4.1). At short wavelengths these bands are narrow

Atmospheric Absorption

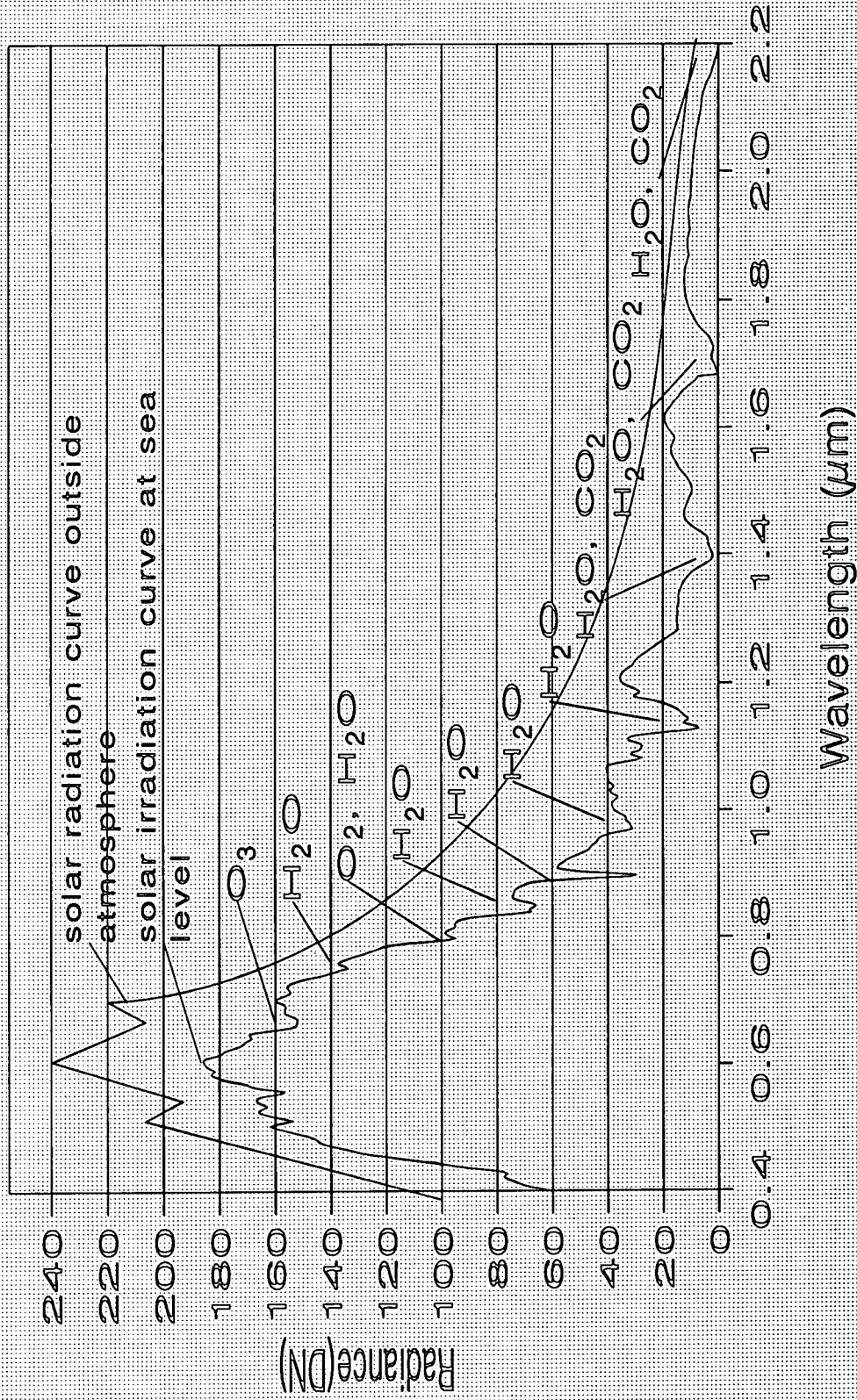


Fig. 4.1 Atmospheric Absorption

but their width increases in the infrared region. The regions of the electromagnetic spectrum in which atmospheric absorption is low are commonly termed atmospheric windows. Atmospheric windows are not totally free from atmospheric absorption. Gases and suspended particles in the atmosphere absorb radiation reflected and emitted from the Earth's surface. This results in a decrease in the radiation signal at the sensor. The gases and particles also emit radiation of their own, adding to the radiation signal at the sensor (Curran, 1985). The effects are variable in space and time and necessitate the atmospheric correction of remotely sensed data in multi-temporal studies.

If atmospheric correction and radiometric calibration are not carried out supposed differences in the reflectance characteristics of a target may be attributed to differences in atmosphere or irradiance conditions, or differences in the radiometric sensitivity of the instrument. For example, if the reflectance in the red and near-infrared part of the spectrum are used to estimate the quantity and vigour of green vegetation on the ground, only adequate atmospheric and radiometric corrections can ensure that any temporal or spatial changes observed within scene data are real differences and not artifacts introduced by the radiometric calibration of the sensor, or by atmospheric and irradiance differences. In cases where absolute radiance values are to be evaluated, such as in the comparison of ground measurements and satellite measurements, the atmospheric correction is of vital importance.

Some atmospheric correction packages such as Lowtran require information of the prevailing weather conditions at the time of sensing. Such information about the atmospheric conditions at the time and place of observation is not readily available and obtaining this will add to the total cost of the remotely sensed survey.

Tucker (1979) reviewed a number a number of methods for minimising the effects of unwanted atmospheric and radiometric contributions in the remote sensing of vegetation. Most of these methods included the use of some form of combination of radiation measurements in two, or more, spectral bands. Some of these combinations are expressed in terms of radiances in two spectral bands such as: the ratio (Jordan, 1969); vegetation index (Kauth and Thomas, 1976), and the transformed vegetation index (Rouse *et al.*, 1973). Some other combinations such as the soil brightness index, and the green vegetation index (Kauth

and Thomas, 1976) make use of radiance measurements in more than two spectral bands. A particular combination may be found to minimise the effects of unwanted contributions from various factors in a limited range. However as Dave (1980) discusses in his paper, there is no reason to assume that this is the case at all wavelengths under all conditions of observation. Another disadvantage of these methods are that they only give relative values, not absolute radiance or reflectance values.

RADIOMETRIC RECTIFICATION

The present study makes use of both multi-temporal and multi-sensor imagery and it is therefore necessary to have some form of atmospheric normalisation, so that radiance values are normalised to a standard set of irradiance and atmospheric conditions, or to apply an atmospheric correction model to allow the retrieval of absolute target reflectance values (Hill and Sturm, 1991; Sturm, 1992). Due to the fact that data from several different sensors, including Landsat TM, Spot HRV and Daedalus ATM, may be used in a future study of the area it is also necessary to have some kind of radiometric correction or normalisation.

The method of correction chosen in the present study is based on the methods of Hall *et al.* (1991) which allows the use of both multi-temporal and multi-sensor data. The Radiometric rectification technique has the advantage of not requiring sensor calibration or the use of atmospheric turbidity data. The method corrects images for a common scene in a relative, rather than an absolute sense. Images are rectified relative to a selected reference image. It is important to take care in selecting the reference image as the atmospheric, irradiance and radiometric conditions of this image forms the conditions which all other images are normalised to. The reference image should therefore be the image with the clearest atmospheric conditions. The digital count values from all images rectified using the technique should appear to have been acquired with the reference image sensor, under the same atmospheric and irradiance conditions as the reference image (Hall *et al.*, 1991). The technique has the advantage that all images may be corrected to absolute surface reflectance values. This may be achieved by using the radiometric rectification technique along with an atmospheric correction algorithm with atmospheric turbidity data acquired for the reference image. In this way atmospheric turbidity data acquired concurrent with any satellite image

may be used to infer absolute reflectance values from any other, historic or future satellite image rectified to it (Hall *et al.*, 1991). This means that only one set of atmospheric conditions has to be corrected for rather than applying a different correction to each individual image. The retrieval of absolute surface reflectance values is important as it allows qualitative and quantitative comparisons to be made of spectral target signatures between images. The technique ensures that any temporal or spatial changes observed within the image are real differences in the spectral nature of the target and not radiometric or atmospheric differences.

Hall *et al.* (1991) made use of radiometric control sets to calculate a series of affine transformations to reference a series of images. These radiometric control sets were taken from the extremes of a Kauth-Thomas (1976) greenness-brightness tasseled cap scattergram. The Tasseled Cap Transformation (TCT) of Kauth and Thomas (1976) is a linear transformation that projects soil and vegetation information into a single plane in multispectral data space. In this plane the major components of a vegetation scene are displayed in two dimensions (Campbell, 1987). The concept was originally applied to MSS data but Crist and Cicone (1984) extended the technique to the six non-thermal bands of TM data to produce a new set of variables. The first two bands of the TCT contain almost all the information of a vegetational scene, often 95% or more (Campbell, 1987). TCT 1, a band that conveys information concerning abundance and vigour of vegetation, approximates to "greenness". TCT 2 is known as "brightness" and approximates to soil brightness (Campbell, 1987).

The underlying assumption of the Hall *et al.* approach (1991) is that an image always contains at least some pixels that have the same average surface reflectance between images. This implies that the only changes in their spectral signature between images will be linear, resulting from differences in atmospheric, solar irradiance and radiometric conditions. Normalising the images will account for these differences. This will only hold true if the differences in sensor calibration, irradiance and atmospheric conditions between images introduces only linear differences in the radiance values. Such differences will only stretch, shrink or rotate the Kauth-Thomas greenness-brightness scattergram. Hall *et al.* (1991) argue that the extremes of the scattergram will always correspond to surface elements with the

same spectral reflectance between images. By using a series of "dark" and "bright" radiometric control sets, selected from the extremes of the Kauth-Thomas scattergram, Hall *et al.* (1991) were able to construct a simple rectification algorithm involving linear equations which allowed a series of images to be referenced against each other. The result of the transformation is that all the images appear as if they were taken under the same atmospheric and irradiance conditions, by a sensor with the same radiometric sensitivity. All the images in the present study were rectified in this way but for the purposes of illustration the radiometric rectification of only one pair of images, Landsat 5 TM (14/5/84) and Landsat 5 TM (7/9/91), is described here in detail. The May 1984 Landsat TM image has the clearest atmospheric conditions and hence formed the reference image to which all the other images in the study were normalised. The radiometric rectification algorithm of Hall *et al.* (1991) consists of two major components:

1. RADIOMETRIC CONTROL SET SELECTION

The first component requires the selection of radiometric control sets in both the reference image and in the image that is to be radiometrically rectified. In this illustration the 1991 image is the image which is to be rectified. The control sets contain pixels that have little or no variation in their mean surface reflectance between images. Unlike geometric control points used in spatial image rectification (chapter 5) the members of these control sets are not necessarily the same pixels in each image. Hall *et al.* (1991) argue strongly against using a fixed pixel approach. A fixed pixel approach would introduce several problems such as image mis-registration. The use of fixed pixels would also require the manual selection of a sufficient number of image-to-image pairs of suitable pixels. This would be very labour intensive, particularly when several images from a number of years are being referenced, and would add to the overall cost of processing. Perhaps most importantly, in regard to the future work on the Wash Estuary, a fixed pixel approach would not allow for the integration of data-sets with different spatial resolutions such as Daedalus and Spot HRV imagery.

2. CALCULATION OF THE RECTIFICATION TRANSFORM:

The second component involved in the technique radiometrically rectifies the images using a linear transformation with coefficients calculated to equate the individual band means (in raw digital counts) of the radiometric control sets in each image (Hall *et al.*, 1991). The band by band average DN values of the radiometric control sets are used to compute the coefficients of linear transformations relating all DN values band by band between the images. This is illustrated by the examples in Fig.4.2 and Table 4.1. This empirical transformation is theoretically the product of linear transformations, accounting separately for sensor, irradiance and atmospheric effects, and is consequently linear itself. For a sensor with n bands, a set of linear transformations called the **rectification transforms** are created (all equations taken from Hall *et al.* 1991):

$$y_i = m_i x_i + c_i$$

Where y is the average DN value of the pixels in the radiometric control sets in the reference image (May 1984 Landsat 5 TM image, bright and dark control sets) and x is the average DN value of the pixels in the radiometric control sets in the image which is to be rectified (September 1991 Landsat 5 TM image) (Fig. 4.2). For the i th band, the radiometrically rectified values, x'_i , are given by:

$$x'_i = y_i$$

The coefficients \mathbf{m}_i and \mathbf{c}_i are defined by equating the transformed means of the radiometric control sets in the subject image (September 1991) to those of the reference image (May 1984) (Table 4.1, Fig. 4.2):

$$\mathbf{D}'_{si} = \mathbf{m}_i \mathbf{D}_{si} + \mathbf{c}_i = \mathbf{D}_{ri}$$

and:

$$\mathbf{B}'_{si} = \mathbf{m}_i \mathbf{B}_{si} + \mathbf{c}_i = \mathbf{B}_{ri}$$

Where \mathbf{D}_{si} , \mathbf{D}_{ri} , \mathbf{B}_{si} and \mathbf{B}_{ri} are respectively the means of the dark (**D**) and bright (**B**) radiometric control sets in the **ith** band of the untransformed subject image (**s**) (September 1991) and the reference image (**r**) (May, 1984). Solving the equations simultaneously results in:

$$\mathbf{m}_i = (\mathbf{B}_{ri} - \mathbf{D}_{ri}) / (\mathbf{B}_{si} - \mathbf{D}_{si})$$

$$\mathbf{c}_i = (\mathbf{D}_{ri} \mathbf{B}_{si} - \mathbf{D}_{si} \mathbf{B}_{ri}) / (\mathbf{B}_{si} - \mathbf{D}_{si})$$

This results in the affine transformation:

$$\mathbf{x}'_i = \mathbf{m}_i \mathbf{x}_i + \mathbf{c}_i$$

This equation is then applied to every pixel in the subject image. The method is summarised in Fig. 4.3.

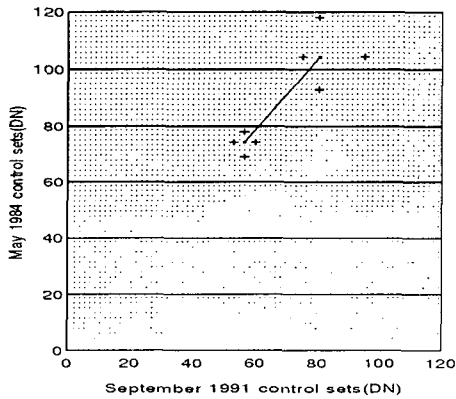
IMAGE	LANDSAT 5 TM BANDS					
BRIGHT: Landsat 5 TM (14/5/84)	BAND 1	BAND 2	BAND 3	BAND 4	BAND 5	BAND 7
min (DN)	93	38	40	41	58	34
max (DN)	118	57	71	70	109	66
mean (DN)	104.4	45.64	52.88	52.68	79.76	48.56
BRIGHT: Landsat 5 TM (7/9/91)	BAND 1	BAND 2	BAND 3	BAND 4	BAND 5	BAND 7
min	75	29	29	26	45	28
max	95	50	61	57	85	51
mean	80.41	36.94	42.94	40.24	62	37.76
DARK: Landsat 5 TM (14/5/84)	BAND 1	BAND 2	BAND 3	BAND 4	BAND 5	BAND 7
min	69	23	17	8	3	1
max	78	27	21	11	9	7
mean	74.27	25.26	19.02	9.67	6.06	4.09
DARK: Landsat 5 TM (7/9/91)	BAND 1	BAND 2	BAND 3	BAND 4	BAND 5	BAND 7
min	53	19	13	5	0	1
max	60	22	16	8	6	6
mean	56.42	20.2	14	6.96	3.99	2.99

Table 4.1 Radiometric Control Sets For Landsat TM Image (14/5/84) And Landsat TM Image (7/9/91).

Rectification Transforms

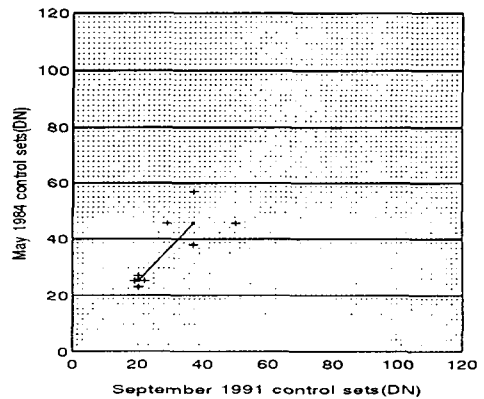
Band 1 Rectification Transform

$$x' = 1.26x + 3.41$$



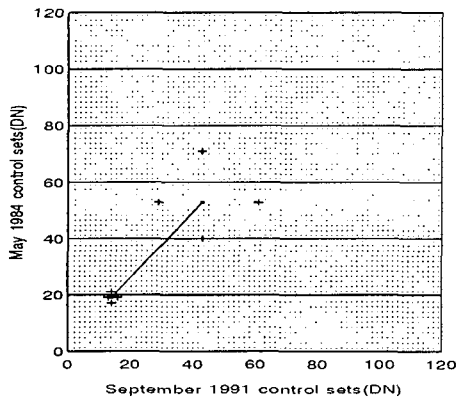
Band 2 Rectification Transform

$$x' = 1.22 + 0.67$$



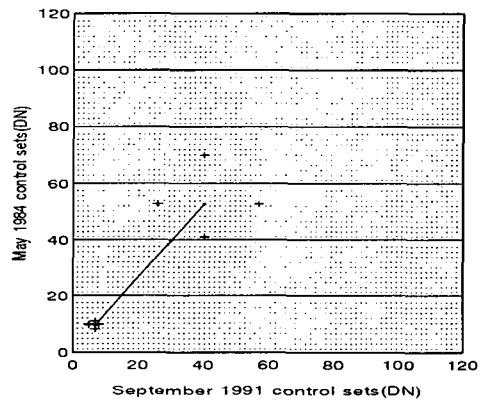
Band 3 Rectification Transform

$$x' = 1.17x + 2.64$$



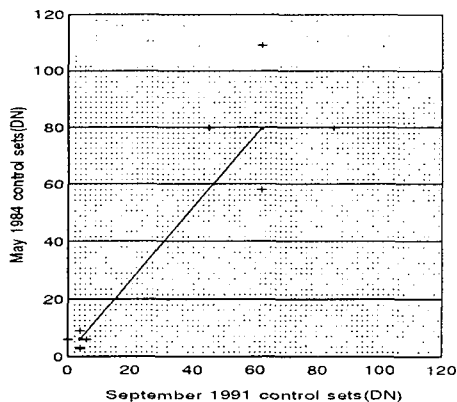
Band 4 Rectification Transform

$$x' = 1.29x + 0.67$$



Band 5 Rectification Transform

$$x' = 1.27x + 0.99$$



Band 7 Rectification Transform

$$x' = 1.28x + 0.27$$

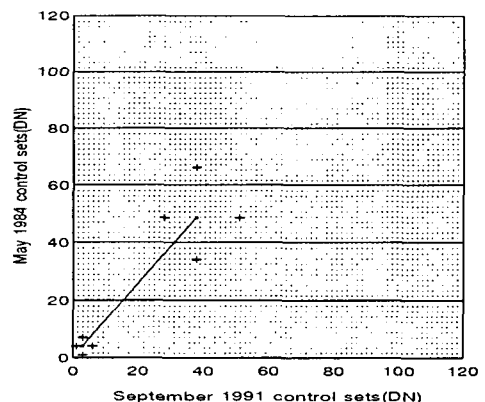


Fig. 4.2 Dark and bright radiometric control sets from Landsat5 TM (14/5/84 and 7/9/91). Confidence limits are illustrated (min and max of control sets).

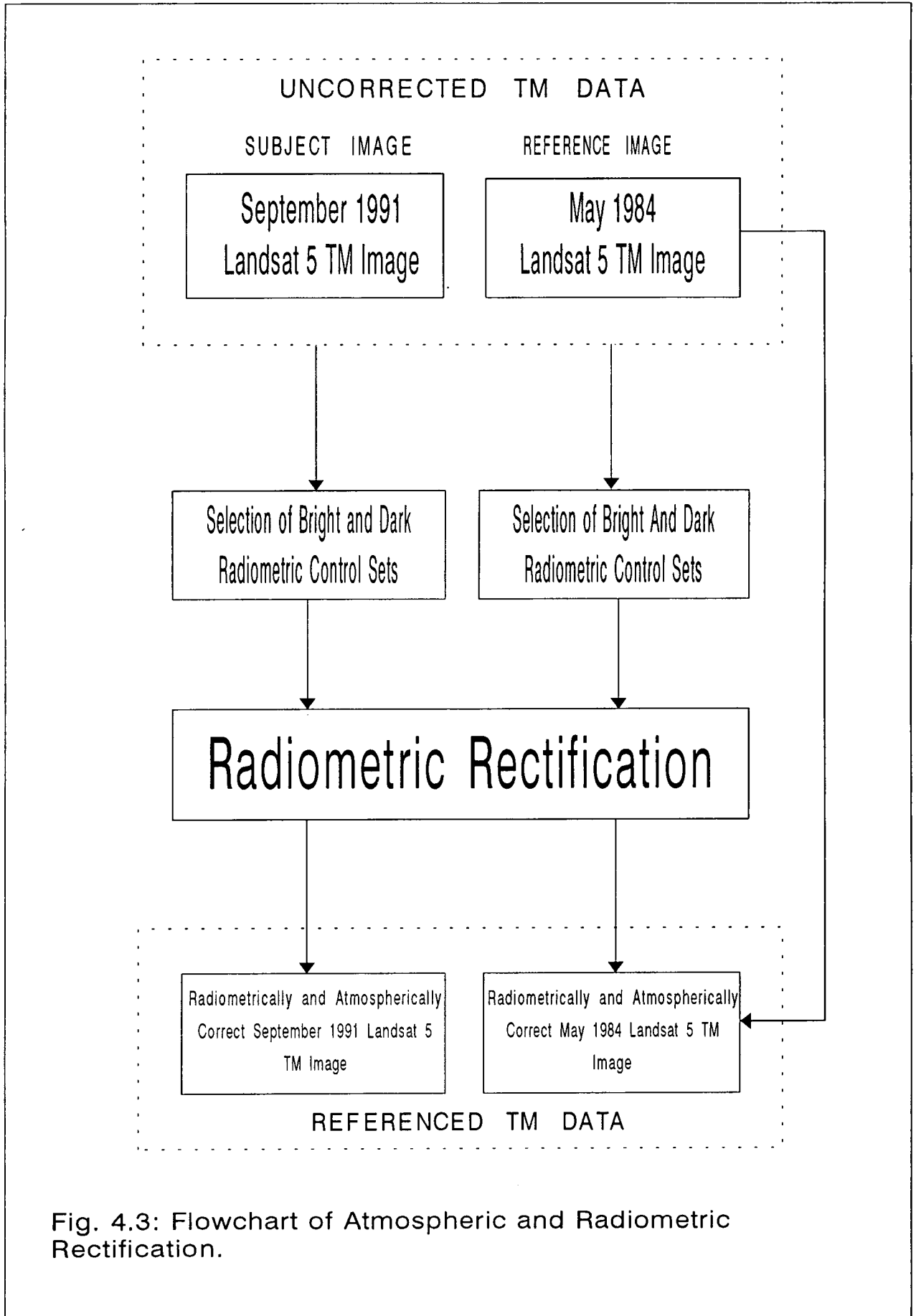


Fig. 4.3: Flowchart of Atmospheric and Radiometric Rectification.

Hall *et al.* (1991) suggest that the control sets should be selected from the non-vegetated extremes of the Kauth-Thomas (KT) greenness-brightness scattergram as these should correspond with the spectrally invariant pixels in the data set such as rock outcrops, car parks, urban areas and deep water.

The methodology of Hall *et al.* (1991) implies that in the reference image dark radiometric control sets are defined by selecting the pixels from the darkest area of the KT scattergram both in terms of brightness and greenness. This is designed to exclude water pixels contaminated by sun glint or sediment and the greenness threshold would eliminate water-edge pixels and water containing algal blooms or high sediment concentrations. In the bright control sets the KT brightness and greenness values are applied in reverse order. The thresholds are chosen to exclude vegetated pixels and to leave enough pixels for an accurate estimate of the set's mean digital count value (Hall *et al.*, 1991).

In the subject image (September 1991), the reference image threshold values do not apply. Atmospheric and sensor differences translate, rotate and scale the KT histogram. This implies that the threshold values for the non-reference images must be re-calculated. The thresholds are chosen to maintain a fraction of radiometric control pixels to total image pixels equal to that of the reference image (Hall *et al.*, 1991).

In the present study the methodology had to be considerably modified as the use of the KT extremes proved to be highly problematical in the Wash area due to the absence of suitable bright control sets. Hall *et al.* (1991) emphasised in their paper that control pixels should be taken only from the extremes of the Kauth-Thomas scattergram to reduce the likelihood of including pixels with changing reflectance characteristics. The Radiometric rectification assumes that the scene contains populations of elements whose mean reflectance do not change with time. By choosing pixels at the extremes, Hall *et al.* (1991) argued that error in the affine transformation would be minimised by separating the mean values as much as possible (increasing $(\mathbf{B}_{si} - \mathbf{D}_{si})$). The extremes of the Kauth-Thomas scattergram in the Landsat 5 TM images of the Wash Estuary proved to be water, vegetation and bare soil. Vegetation and bare soil are not suitable as bright control points as their spectral signatures are variable over time. The agricultural area surrounding the Wash Estuary is some of the

best in Britain and the crop spectral signatures proved to be considerably brighter than any spectrally invariable pixels such as urban areas. Even the application of a greenness threshold was unable to mask out these "bright control point" pixels.

It was therefore decided to select "bright" control sets from slightly darker regions of the KT brightness-greenness scattergram. With the aid of the Kauth-Thomas scattergram, a brightness, greenness, wetness image and a 2,4, 5 false colour composite image "bright" control sets were chosen from areas corresponding to urban areas of the Wash Estuary region such as the town of Boston. The selection of pixels proved problematical as there are very few urban areas near the Wash Estuary and those that do exist are frequently mixed with arable land and gardens. Even the inclusion of a very small number of vegetation pixels, or urban and vegetation "mixels", in the bright control sets greatly effected the accuracy of the rectification as non linear changes are introduced into the equation. This was clearly illustrated in the first attempt of defining bright radiometric control sets. Spurious results were generated as a direct result of including a number of vegetation pixels and mixels in the bright radiometric control sets.

The careful selection of the control sets is of the utmost importance to the accuracy of the rectification and should be conducted with extreme care. The second attempt at defining bright control sets was carried out with much greater care and aided by the use of the T-Spectra software that allowed the detailed examination of individual spectrum of pixels. In this way individual pixels in the bright radiometric control sets were examined and pixels which looked, from the reference spectrum, to have any vegetation element within them were excluded. This ensured that only spectrally constant pixels were included in the radiometric control sets. A much more satisfactory rectification was achieved using this method.

IMAGE	LANDSAT 5 TM BANDS					
	BAND 1	BAND 2	BAND 3	BAND 4	BAND 5	BAND 7
Unrectified Landsat 5 TM (7/9/91)	76.79	35.9	41.31	42.24	57.14	34.69
Rectified Landsat 5 TM (7/9/91)	101.04	44.86	51.61	53.11	71.25	43.96
Reference Landsat 5 TM (14/5/84)	104.6	46.8	53.1	51.6	69.6	42.5

Table 4.2 Comparison Of Rectified And Unrectified Spectrally Invariant Pixels.

The selection of the dark control sets proved to be a much simpler task with the selection of dark pixels corresponding to the deep water of the sea adjacent to the Wash. It must be noted that nearshore waters could not be used as these were contaminated with sediments and would therefore have spectrally variable signatures.

After selection of the radiometric control sets Hall *et al.* (1991) recommended that it is prudent to ascertain to what degree the radiance values in the radiometric control sets are corrected by linear transformations. This is necessary to satisfy the assumptions underlying the radiometric rectification approach. Use of meteorological data may be used to identify possible non-linear distortions of the KT greenness-brightness histogram. For example episodic events such as recent rainstorms would modify the bright extreme of KT greenness-brightness histogram, creating non-linear transformations between the images. Radiance plots of the scene elements common to both radiometric control sets should produce a linear relationship, unless the relationship has been destroyed by atmospheric heterogeneity within the image, or non-linear calibration effects (Table 4.2).

A C-program (Appendix 1) was written to calculate the affine rectification transformations for each band in the set of images (Fig. 4.2). The program first runs through the data set finding the sum and the means of the bright and dark control sets in each image. The program then calculates the rectification transforms and applies the transformations to every pixel in the subject image. The data is rounded to rid the data sets of decimals (pixels must have values which are whole numbers in Terra-Mar) and writes the results into an output file. The success of the rectification was evaluated by comparing a number of pixel

pairs in the images that were not included in the radiometric control sets (Table 4.2). There is a very good correlation between the two rectified images implying a satisfactory transformation. Even better results were achieved when comparing dark pixels. The method was then applied to all the data sets being used in the present study resulting in a series of images that appear to have been taken at the same time thus having the same atmospheric and irradiance conditions and taken by sensors that have all been radiometrically calibrated to the same degree of sensitivity. This is an absolutely essential first step in any objective comparison of multi-temporal and multi-sensor images.

Some form of atmospheric and radiometric correction or normalisation is an essential prerequisite to any meaningful and objective comparison of multi-temporal and multi-sensor data. The radiometric rectification technique of Hall *et al.* (1991) is a satisfactory method of carrying out the normalisation. It should be noted that the technique needed considerable modification before it could be satisfactorily applied to the present study area in the Wash Estuary. The absence of suitable control pixels at the bright extremes of the Kauth-Thomas brightness-greenness scattergram proved to be the biggest problem. The importance of the careful selection of the radiometric control sets cannot be overemphasised. Even the inclusion of only a few vegetation pixels and mixels in a bright radiometric control set greatly affected the accuracy of the rectification transformation as the inclusion results in non-linear changes being included in the equations. The method of Hall *et al.* (1991) only allows for linear transformations. The affine nature of the transformation linking the images may be destroyed by heterogeneity in the atmospheric properties across the scene. Fortunately this is unlikely to be of great importance in the present study due to the relatively small size of the study area. Similarly the affine nature of the affine transformation may be destroyed by non-linearity in calibration differences between sensors and non-linear distortions in KT greenness-brightness histogram such as the occurrence of heavy rainfall preceding one of the image acquisition dates. The prevailing weather conditions at the date of the taking of the image should therefore be briefly looked at to avoid such problems. Care is therefore needed in the application of this atmospheric and radiometric normalisation technique.

Campbell, J.B. 1987: Remote Sensing Applications in the Plant Sciences. **Introduction to Remote Sensing**. Guildford Press, London: 366-403.

Curran, P.J. 1985: **Principles of Remote Sensing**. 53-54, Longman, New York.

Crist, E.P. and Cicone R.C. 1984: A physically-based transformation of Thematic Mapper data - The TM Tassled Cap, **I.E.E.E. Transactions in Geoscience and Remote Sensing**. vol. 10: 1127-1134.

Dave, J.V. 1980: Effect of atmospheric conditions on remote sensing of vegetation parameters. **Remote Sensing of Environment**. vol. 10: 87-99.

Hall, F.G. Strebel, D.E., Nickeson, J.E. and Goetz, S.J. 1991: Radiometric rectification: toward a common radiometric response among multirate, multisensor images. **Remote Sensing of Environment**. vol. 35: 11-27.

Hill, J. and Sturm, B. 1991: Radiometric correction of multitemporal Thematic Mapper data for use in agricultural land-cover classification and vegetation monitoring. **International Journal Of Remote Sensing**. vol. 12: 1471-1491.

Jordan, C.F. 1969: Derivation of Leaf Area Index from quality of light on the forest floor. **Ecology**. vol. 50: 663-666.

Kauth, R.J. and Thomas, G.S. 1976: The Tassled Cap - A graphic description of the spectral development of agricultural crops as seen by Landsat. **Proceedings of the Symposium Machine Processing of Remote Sensing Data**. LARS, Purdue.

Richter, R. 1992: Atmospheric correction of imaging spectrometer data. In Toselli, F. and Bodechtel, J. (eds) **Imaging Spectroscopy: Fundamentals and Prospective Applications**. Kluwer Academic Publishers, London: 259-266.

Rouse, J.W., Hass, R.H., Schell, J.A. and Deering, D.W. 1973: Monitoring vegetation systems in the great plains with ERTS. **Third ERTS Symposium**. NASA SP-351 I: 309-317.

Slater, P.N., Biggar, S.F., Holm, R.G., Jackson, R.D., Mao, Y., Moran, M.S., Palmer, J.M. and Yuan, B. 1987: Reflectance- and radiance-based methods for the inflight calibration of multispectral sensors. **Remote Sensing of Environment**. vol. 22: 11-37.

Sturm, B. 1992: Atmospheric and Radiometric corrections for imaging spectroscopy. In F.Toselli and J.Bodechtel **Imaging Spectroscopy: Fundamentals and Prospective Applications**. Kluwer Academic Publishers, London: 47-60.

Tucker, C.J. 1979: Red and photographic infrared linear combinations for monitoring vegetation. **Remote Sensing of Environment**. vol. 8: 127-150.

United States Geological Survey and National Oceanic and Atmospheric Administration, 1984: **Landsat 4 Data Users Handbook**.

CHAPTER 5

THE WASH GEOGRAPHICAL INFORMATION SYSTEM

The remainder of the thesis is devoted to examining two different strategies for classifying Landsat 5 TM satellite images of saltmarsh. The strategies used are maximum likelihood classification and mixture modelling. The results of the classifications are compared against each other and also with the 1982/4 N.C.C. survey in an attempt to identify the most useful strategy for the mapping and monitoring of coastal vegetation. The comparison of different surveys were all carried out using the Wash coastal monitoring geographic information system (GIS) (Fig. 5.1). Analysis of satellite imagery represents a practical, consistent, quick and economic technique of obtaining accurate data for large areas, at regular intervals. By integrating data derived from satellite imagery with information from ground surveys into a digitised form within a GIS, the spatial data processing functions of the system can be used to provide a temporal perspective by identifying and quantifying changes between images and surveys. The integration of remotely sensed data into a GIS is no easy task. The potential of remotely sensed data has not been fully exploited by GIS users due to: the variable accuracy of thematic maps derived from remotely sensed images; the awkward geographic referencing; the complex tape formatting systems used for satellite sensor images; and the huge task of handling the large amount of data associated with multispectral sensors (Davis *et al.*, 1991; Jackson, 1992). These issues are addressed in the present chapter.

The inclusion of satellite classifications in the Wash coastal monitoring GIS allows objective, quantifiable comparisons and estimates of vegetation cover to be made and provides a methodology which can be easily repeated. A key concern was the ease of use as this would be crucial in an operational mode where the operator may often be a non-specialist. The first of the classification strategies, the maximum likelihood classifier, was carried out by two independent operators to establish the objectivity of the methods used. Consistency between operators would again be essential in an operational mode.

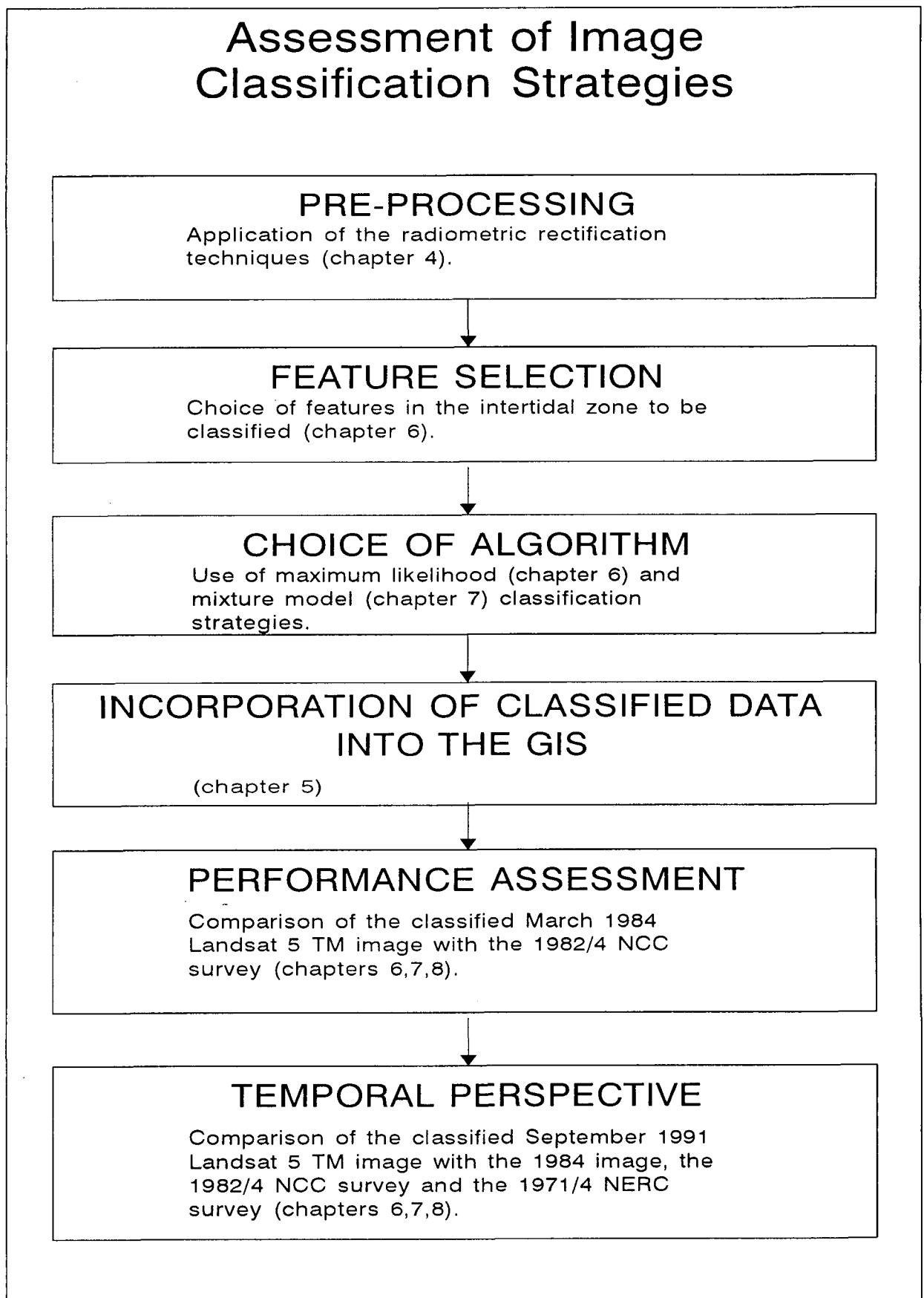


Fig 5.1 Procedure for the assessment of classification strategies.

The Wash Coastal Monitoring GIS

Mixture model
proportion maps of
the September 1991
Landsat 5 TM image

Mixture model
proportion maps of
the March 1984
Landsat 5 TM image

Maximum likelihood
classification of the
September 1991
Landsat 5 TM image

Maximum likelihood
classification of the
March 1984 Landsat
5 TM image

Past reclamations

Sea embankments

Mean high and low
water marks of the
Estuary

0, 5 and 10m
contours

Digitised version of
the 1982/4 NCC
survey

Digitised version of
the 1971/4 NERC
survey

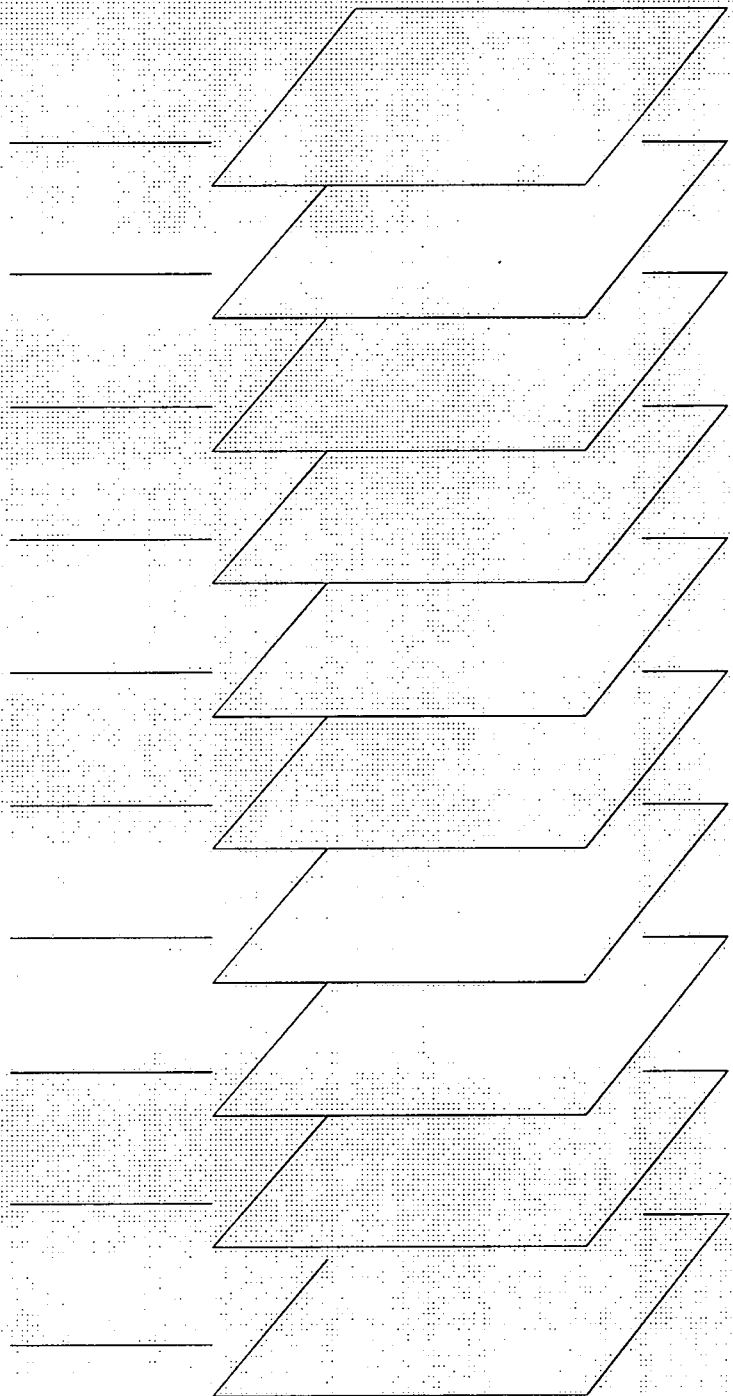


Fig 5.2 Diagrammatic representation of the contents of the Wash coastal monitoring GIS.

The Wash coastal monitoring GIS was set up in order to examine the possibilities of using classified Landsat TM imagery, within a geographic information system, for the routine monitoring of coastal change. Previous research undertaken at the University of Durham has sought to integrate data derived from satellite and airborne imagery with information from ground based surveys using a GIS (Shennan and Sproxtton, 1992(b)). The spatial data processing functions of the system were used by Sproxtton to establish a monitoring capability, objectively quantifying spatial and temporal changes between surveys and images. This chapter outlines the features and capabilities of the Wash coastal monitoring GIS and reviews the work carried out by Sproxtton. The chapter goes on to look at a method of integrating the results of the classification strategies into the GIS.

THE WASH GEOGRAPHICAL INFORMATION SYSTEM

The essential features of a coastal monitoring GIS are the abilities to store a range of geographically referenced variables in digital form and overlay digital maps from different sources in order to identify and quantify change through time. In this study the sixteen vegetation maps from the 1971/4 (N.E.R.C., 1976) and 1982/4 (Hill, 1988) N.C.C. surveys, digitised by Sproxtton using pcArc/Info (version 3.4d), were used to form the first layers of the GIS. The individual digitised maps were transformed to national grid coordinates and were combined using the Arc/Info command MAPJOIN. With the information in a digital form within the GIS Sproxtton was able to produce single maps of the vegetation surveys. In a digital format surveys can be easily manipulated within GIS to produce vegetation maps of comparison and change. The digitised N.E.R.C. and N.C.C. surveys formed the main input into the GIS and were accompanied by: digitised data of the sea embankments; the Mean High Water and Mean Low Water marks of the Estuary; and the 0, 5 and 10 m O.D. contours (Fig 5.2). The digitised maps of the N.E.R.C. and N.C.C. surveys, produced by Sproxtton, provides a considerable resource for the academic community.

COMPARISON OF THE DIGITISED MAPS AND THE N.C.C. MAPS

Although the N.E.R.C. and N.C.C. surveys are broadly comparable, both having used air-photo interpretation, different classification schemes were used. Hill (1988) divided the saltmarsh vegetation into 12 communities using the National Vegetation Classification, whereas Randerson (1975) identified eight communities on the basis of dominant and sub-dominant species. The lack of consistency in this respect reduces the potential for direct comparison at a detailed level for some communities, particularly Middle and Lower marsh communities, but more general comparisons can be carried out by the aggregation of vegetation species in the GIS. The saltmarsh zones were aggregated by Sproxton into the following categories:

UPPER MARSH *Agropyron*, Upper Marsh, *Puccinellia* and *Spergularia*.

MIDDLE MARSH *Puccinellia*, *Puccinellia* and *Halimione* and *Halimione*.

LOWER MARSH Transitional lower marsh, *Aster*, *Aster* and *Salicornia*.

PIONEER MARSH *Salicornia*, *Spartina*, *Salicornia* and *Spartina*, *Salicornia* and *Suaeda* and *Suaeda maritima*.

Some discrepancies between the areas calculated from the GIS coverages and those published by Hill (1988) are to be expected because of the different methods of calculation. The areas of the different saltmarsh vegetation and ground cover types in the digitised maps were obtained by Sproxton from the coverage polygon attribute tables (PAT) for different shoreline sections and the Wash Estuary as a whole. The figures given by Hill (1988) were manually calculated using the "dot grid" method. A comparison of the areas derived from the previous surveys (Hill, 1988) and those calculated for their equivalent coverages revealed closer agreement for the 1982/4 survey than the 1971/4 survey (Table 5.1).

In the case of the 1982/4 survey the discrepancies reported by Sproxton between the N.C.C. figures and the computed areas for the total saltmarsh coverage of the Wash Estuary were minor (0.09-0.96%). Larger differences were recorded for individual communities such as *Agropyron* and *Puccinellia/Halimione*. These differences were found to occur mainly on sections with extensive inter-digitation of species and probably resulted from mapping errors

at the time of the original N.C.C. area calculations. The accuracy of the digital maps in all cases was verified by Sproxton using hard-copy graphical output from the GIS.

Saltmarsh Zone	1971/4 Digitised Coverage	N.E.R.C. Survey 1971/4	11982/4 Digitised Coverage	N.C.C. SURVEY 1982/4
Upper Marsh	625.53	605.40	748.67	732.10
Middle Marsh	1913.33	1654.40	2366.16	2412.40
Lower Marsh	997.43	1127.00	807.72	811.80
Others	110.43	0.00	231.54	210.40
Total	3646.72	3386.80	4154.08	4157.70

Table 5.1 Areas in hectares of vegetation zones of the Wash Saltmarshes (Sproxton 1992)

In contrast to the 1982/4 survey, an examination by Sproxton of the 1971/4 N.E.R.C. survey (Table 5.1) and its digitised equivalent revealed a discrepancy of over 250 hectares even after accounting for post-1973 reclamation. The accuracy of the digital maps were again verified, suggesting that the "dot grid" method used to calculate the areas from the 1971/4 survey was not sufficiently accurate (Sproxton, personal communication).

COMPARISON BETWEEN THE TWO GROUND SURVEY DATES

With the digital map data in the GIS, the information can be overlain or combined to identify any significant changes and trends using the Arc/Info OVERLAY commands. The overlaying of the two N.E.R.C. and N.C.C. saltmarsh surveys within the GIS represents an improvement over the simple comparison of saltmarsh areas by providing the potential to create maps of the spatial patterns of different vegetation communities. At the broadest level of generalisation Sproxton merged all the vegetation classes, by removing the internal boundaries, to form a single saltmarsh class for each survey. In order to identify areas of saltmarsh expansion and contraction between the two surveys the gross saltmarsh coverage for the 1971/4 survey was overlaid on the equivalent 1982/4 gross saltmarsh coverage. The results of overlaying the two surveys demonstrated that expansion of the saltmarsh occurred between the two survey dates. Appreciable variation in the amount of saltmarsh growth is

apparent for different shoreline sections. The greatest areas of expansion are evident on the west shore seaward of the 1970s reclamations on the Wainfleet marsh. Large areas of expansion also occurred in front of older reclamations (1949-50) on the Fosdyke marsh on the south shore. Other areas of expansion were recorded by Sproxton along the west shore near Leverton where the pattern of growth is suggestive of sediment accretion associated with levee development between the larger tidal creeks (Kestner, 1975). Modest expansion also took place near Gedney and along the east shore (Shennan and Sproxton, 1992(b)). Although the areas of greater expansion were associated with the more recent reclamations, expansion was generally recorded by Sproxton around all the shores of the Wash. Using the GIS the maximum widths of selected areas of saltmarsh expansion could also be recorded (Shennan and Sproxton, 1992(b)):

Wainfleet	480 m
Fosdyke/Holbeach	580 m
Leverton	562 m
Gedney	324 m

The result of overlaying the coverages reveals that the area of contraction is considerably less than expansion. Contraction was identified by Sproxton in a number of discrete areas, namely Frampton, Holbeach and Gedney. At Horsehoe and at Freiston the usual trend of saltmarsh in front of a recent reclamation has been reversed. The extent of the Home Office reclamation and the excavation of large areas of borrow pits on the Freiston Shore has resulted in extensive deterioration in the quality of the remaining Lower marsh (Fig 5.3 and Fig 5.4). The degradation of the saltmarsh is such that during winter, at the time of greatest wave action, the natural protection provided by the remaining lower marsh species is at a minimum. Sproxton reports that at Freiston Shore the length of exposed earth bank is 1.69 km and the marsh has been reduced in width to less than 200 m. Similarly the length of the exposed bank north of the Horseshoe is 566 m and the width of the fronting marsh has been reduced to 20 m. The vulnerability of sea embankments at Freiston and the Horseshoe to wave action has necessitated the reinforcement of the earth banks with artificial protection (Shennan and Sproxton, 1992(b)). The Wash coastal monitoring GIS is able to identify specific areas of saltmarsh expansion and contraction, the effects of saltmarsh

reclamation and areas of weak natural coastal protection.



Fig. 5.3 The Freiston Shore



Fig. 5.4 The Freiston Shore

In addition to revealing changes at the saltmarsh front the GIS can be used to identify changes in the zonal pattern of the broad aggregated vegetation communities within the saltmarsh. By overlaying the Middle marsh areas from the 1982/4 survey with the Lower marsh areas from the earlier survey Sproxton was able to measure the degree of maturation of the Wash saltmarshes. Generally the greatest expansion of Middle marsh was identified on saltmarshes fronting the more recent reclamations such as Butterwick and Wainfleet. On the more mature marshes, such as Frampton and Holbeach, where the expansion of the Middle marsh over the Lower marsh was more modest, expansion tended to be restricted to the Upper marsh zone. Sproxton suggested that these contrasting patterns of expansion in the Upper and Middle marsh areas may reflect the fact that the less mature saltmarshes are still approaching sedimentary and ecological equilibrium after successive phases of reclamation.

INTEGRATION OF SATELLITE SENSOR DATA INTO THE WASH COASTAL MONITORING GIS

The two Landsat 5 TM images, 14/5/84 and 7/9/91, radiometrically and atmospherically referenced to a standard set of conditions (chapter 4), formed the data sets on which the classification strategies were carried out (chapters 6 and 7). In an operational mode the resulting classification of such images would form the basic input for the identification and quantification of areas of change. By classifying the image the size of the dataset is dramatically reduced and therefore becomes much more manageable. This helps to overcome the major problem of dataset size in incorporating satellite sensor data into a GIS. The remainder of this chapter is devoted to the processes that were carried out on the classified images in order to integrate them into the GIS (Fig 5.5). Once in the GIS areas of change can be identified and monitored, and the relative benefits of different classification strategies evaluated.

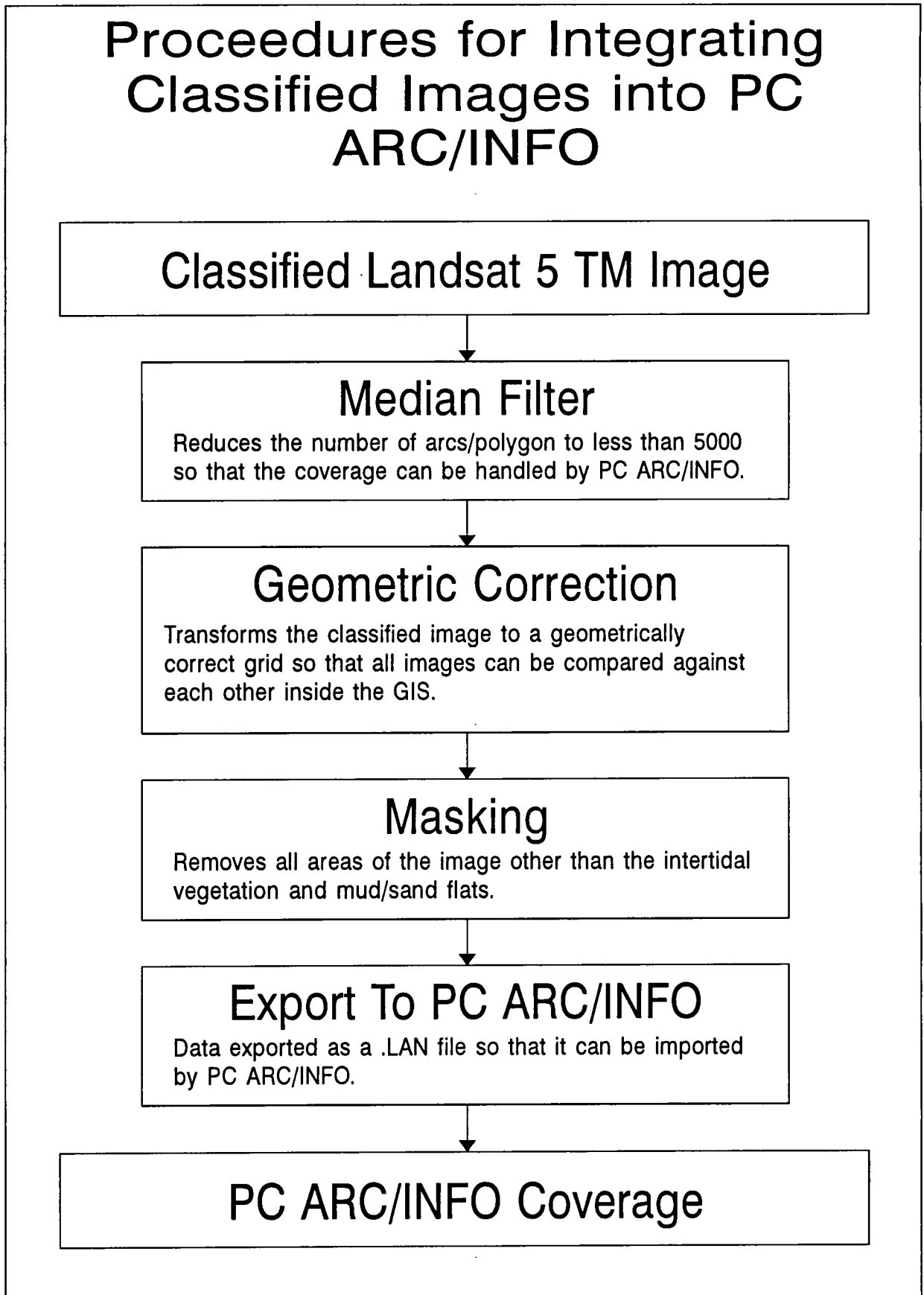


Fig 5.5 Procedures for integrating classified Landsat 5 TM imagery into PC ARC/INFO.

TRANSFER OF DATA FROM THE TERRA-MAR IMAGE PROCESSOR (Terra-Mar 1991) TO THE PCARC/INFO GIS

Once classification has been performed (chapter 6 and 7) the next issue to be addressed is how best to arrange the data into a form where it can be imported and manipulated by the pcArc/Info GIS system. This involves a wide range of problems which are related to the capabilities of the image processing and GIS software packages. In an operational mode it would be best to write a C-program that takes care of the operations described in the following paragraphs.

FILTERING

The first problem is a purely technical one related to the computing capabilities of pcArc/Info. This system limits the number of arcs per polygon to 5,000 (pcArc/Info 3.4D). With isolated classified pixels within the classification of the mosaic-like saltmarsh this limit is exceeded unless the image is filtered. The use of a median [3,3] filter is one method of getting around this technical limitation. The median filter uses a kernel as a sampling unit. The [3,3] kernel defines a matrix of nine pixels; the median spectral value of the kernel is calculated and the centre pixel is substituted with the result of the calculation (Terra-Mar 4.0, 1991). It must be noted that the application of a spatial filter reduces the accuracy of the overall classification. A median filter has the effect of decreasing spatial differentiation. The disadvantages of using a spatial filter are especially relevant in the case of saltmarsh where areas of pure *Halimione* or *Puccinellia* often only occur in areas of two or three pixels. By applying a median filter these areas would be smoothed out (Fig 5.6 and 5.7). In Figures 5.6 and 5.7 red represents the upper marsh, blue areas of mixed *Puccinellia* and *Halimione*, purple areas of pure *Puccinellia* and orange areas of pure *Halimione*. The application of the filter removes many of the pure areas of *Halimione* and considerably smoothes the output of the other classes. Although Fig. 5.7 produces a more tidy appearance it is further removed from reality than the unfiltered Fig. 5.6.

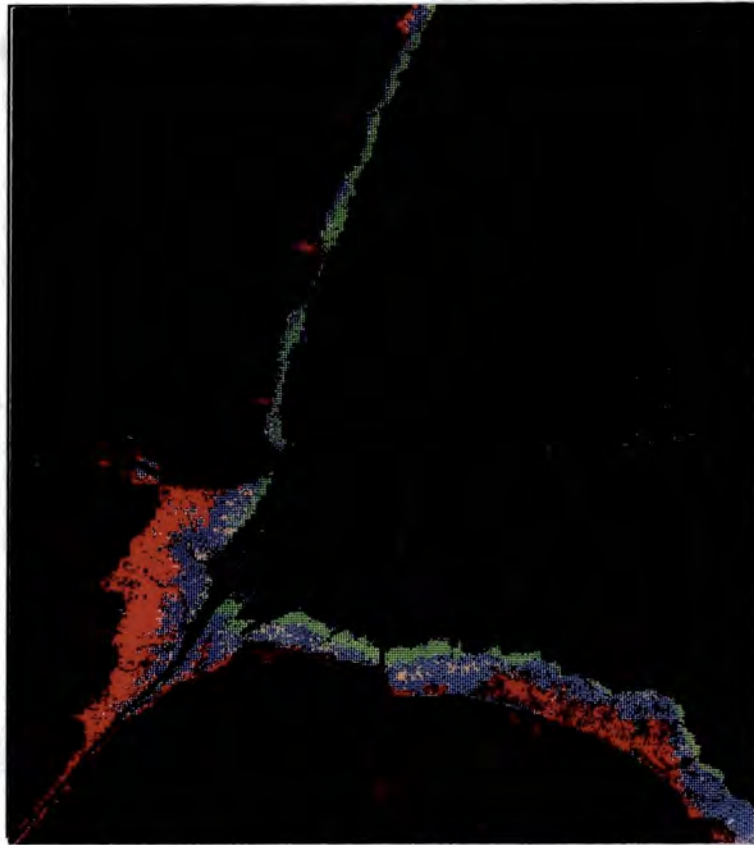


Fig. 5.6 Unfiltered classified extract of the Wash Estuary (Landsat5 TM 7/9/91)

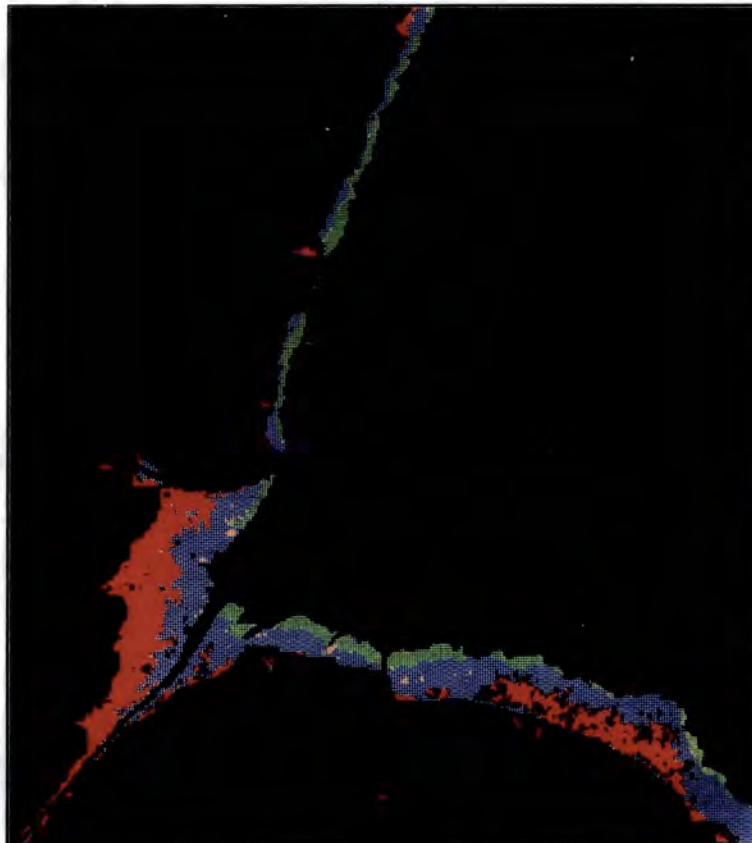


Fig. 5.7 Filtered classified extract of the Wash Estuary (Landsat5 TM 7/9/91)

The problem of the limited number of arcs could be overcome by using a different Arc/Info package, such as the Arc/Info package that runs on Sun Workstations, which allows a greater number of arcs per polygon to be used, or by using a raster based GIS such as the GRID option in Arc/Info. The second classification strategy, mixture modelling, was carried out using GRID. This bypasses the need for applying a filter to the classified satellite sensor data and therefore more closely approximates reality.

GEOMETRIC CORRECTION

The filtered classified images then have to be geometrically corrected as a precursor to incorporation and manipulation within the GIS. The most difficult but most rigorous approach to image registration is to apply knowledge of sensor geometry and motion to derive accurate co-ordinates for each pixel in a scene (Campbell, 1987). In the present study no attempt was made to apply knowledge of the system geometry. The correction method applied was performed using a geometrically correct coverage file imported from the GIS system. The classified satellite image was treated as an array of values that must be manipulated to create another array with the desired geometry. The input image, the classified satellite image, is represented by the dashed grid in Fig. 5.9. Superimposed over the classified image is a second array, symbolised by the hard line grid (Fig 5.9), which represents the pixels in the transformed output image with the desired geometric properties. The location of the output pixels are derived from locational information provided by Ground Control Points (GCPs). GCPs are points on the image that can be located with precision on the image and on the planometrically correct map (in this case a geometrically correct coverage file of the sea embankment of the Wash Estuary imported from pcArc/Info) (Fig. 5.8). In the present study the filtered classified images were geometrically corrected by reference to a series of identifiable features on the seabank. The location of the GCPs establishes the mathematical relationship between the output and input images.

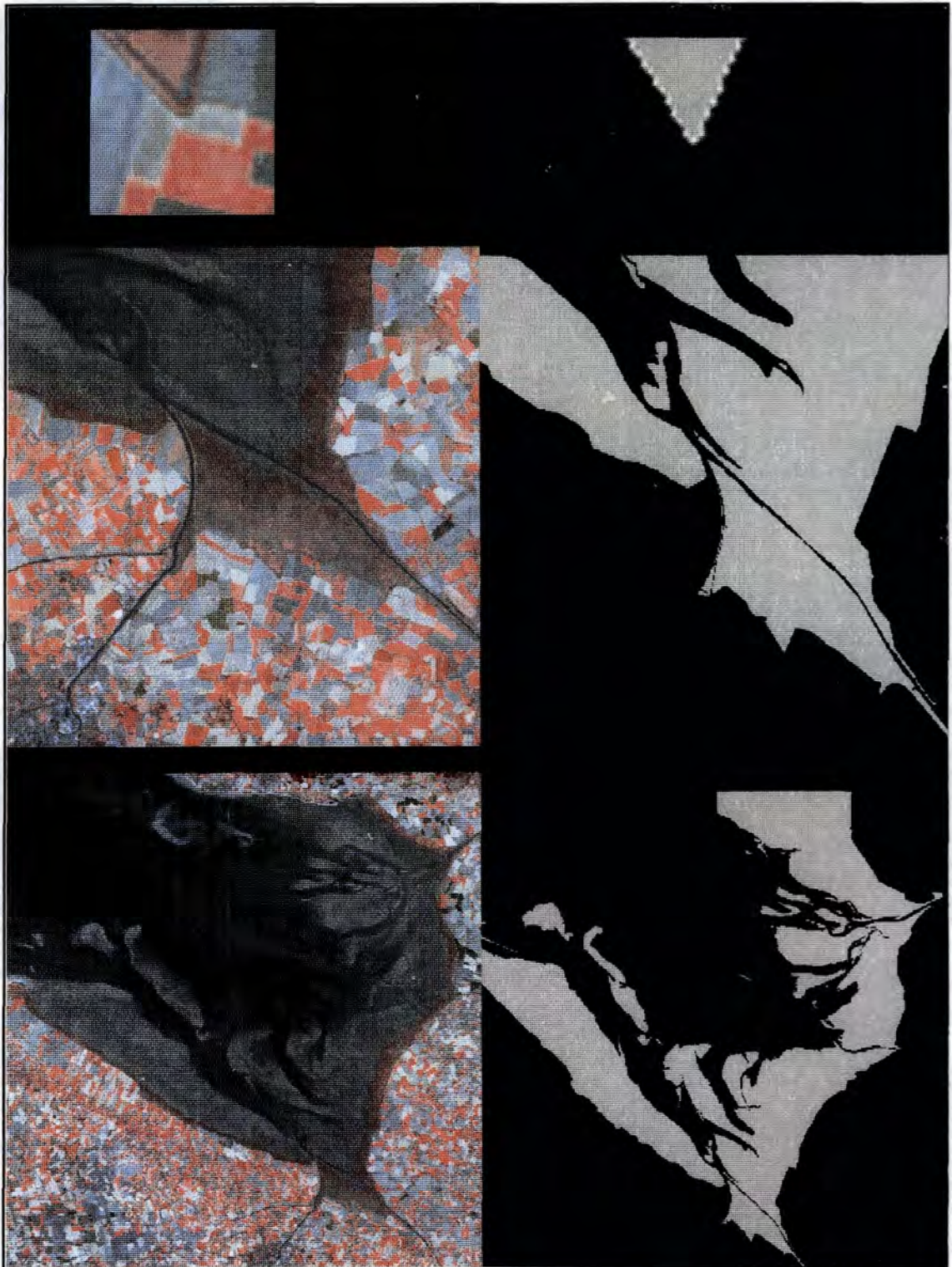


Fig. 5.8 Terra-Mar zoom images used for locating Ground Control Points.

A practical problem of the image registration procedure is the selection of the GCPs. Ideally GCPs should be as small as one pixel if it can be easily identified against its background such as the R.A.F. bombing sites in the middle of the saltmarsh. In practice such GCPs are rare and are more often formed by spectrally distinct areas of pixels such as a sharp corner of the sea embankment. Matching GCPs between the coverage and the image proved to be an arduous and highly subjective exercise, even with the magnifying capabilities of the Terra-Mar image processing system. Identifiable features, such as sharp bends in the embankment, often occupy several pixels (Fig. 5.8). Fourteen GCPs were selected to define the relationship between the uncorrected image and the geometrically correct output image. No matter how accurately this process is done no two operators would achieve the same results as the selection of GCPs is highly selective. In the present study GCP selection was carried out by two independent operators to produce rectified images where the spatial distortion is less than 15 m on the ground. Even this small error can lead to considerable difficulties when overlaying classifications produced by different operators

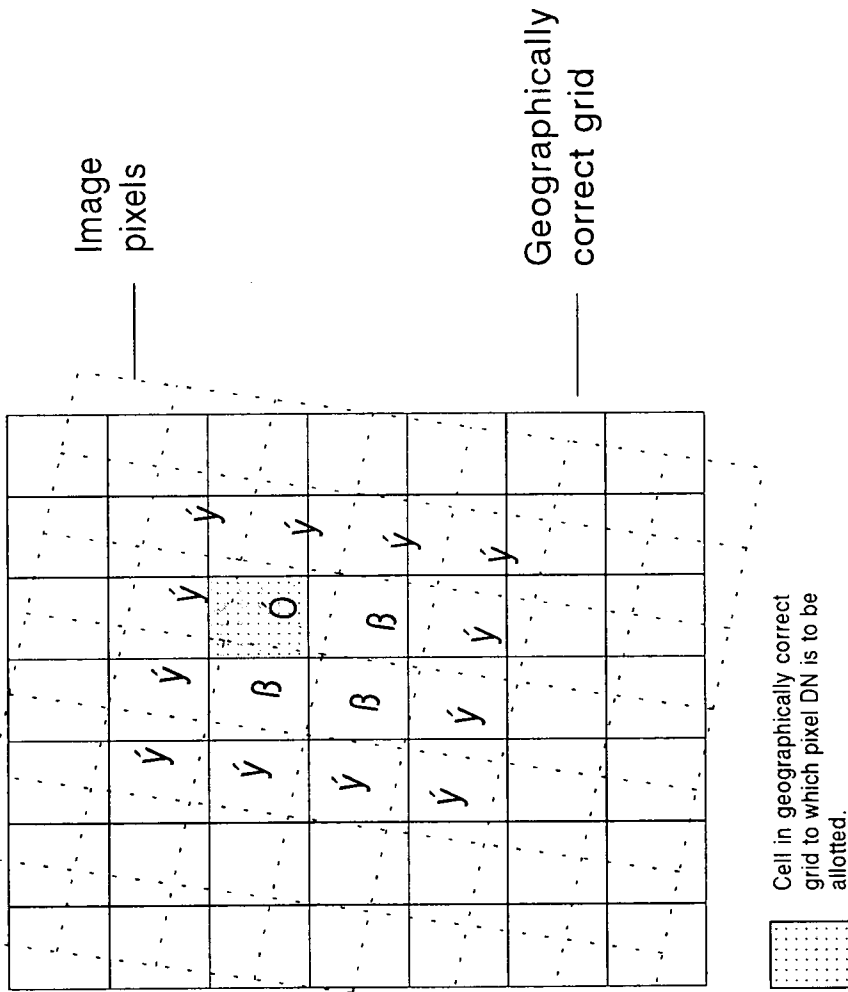
The problems encountered in overlaying classifications produced by different operators using different GCPs led to a different approach being taken for the second classification strategy. This approach was first to register the classified Landsat 5 TM images used in the present study to a "master" image (the 7/9/91 Landsat 5 TM image) using a series of GCPs. This is possible with relatively small resampling errors to sub-pixel accuracy, since the geometry of the scenes are very similar (N.E.R.C., 1983). The registered classifications were then geometrically corrected using the same GCPs that were used to correct the master image to the geometrically correct grid. This proved to give a much more satisfactory method of producing accurate overlays and considerably reduced the potential for error between operators.

The next problem with regard to the geometric correction of an image is how to estimate the values of pixels in the corrected image, based on information in the uncorrected image. The simplest strategy from a computational perspective is the Nearest Neighbour approach which simply assigns each corrected pixel the value from the nearest uncorrected pixel. This method has the advantages of being relatively simple to use and preserves the original pixel values of the uncorrected scene (Campbell, 1987). This method was used to

register the series of classifications to the "master" image. The disadvantage of this method is that it results in noticeable positional errors which can be especially severe in easily recognisable linear features, such as the sea embankment, where the realignment of pixels is obvious.

The method adopted to register the "master" image and its dependents (the classifications that were registered to it) to the geometrically correct coverage imported from *pcArc/Info* was Cubic Convolution (Fig 5.9). This is the most widely used method of resampling. Cubic convolution uses a weighted average of values within a neighbourhood of sixteen adjacent pixels. Images produced by this method are typically much more attractive than those produced by the Nearest neighbour approach, but it must be noted that the data sets are altered much more drastically when using the cubic convolution approach.

Geometric Correction



In the cubic convolution method of geometrically correcting an image each pixel in the Landsat 5 TM image is resampled onto the geometrically correct grid using the relationship defined by ground control points. The transfer is the evaluated weight of the nearest sixteen pixels to give a very smooth output.

Fig 5.9 Geometric correction by cubic convolution. (Curran, 1985).

MASKING

The third issue to be addressed is how to reduce the information in the data set so that only the areas of saltmarsh and tidal flats will be exported into the GIS. This is done by adding the classification to a coverage exported from pcArc/Info. The coverage contains a mask which removes all areas other than the saltmarsh and tidal flats. This mask is added to the classification using the Terra-Mar BIGRIBS program (Terra-Mar 4.0) and results in the creation of a two band image.

The two band image must then be imported into T-SPECTRA. The software is used to multiply the two bands together (the mask and the classified image). This has the effect of producing a single band image area containing only the intertidal vegetation and intertidal flat areas. This is performed through a fairly complex series of operations which are outlined below.

1. A suitable .IDF file must be created so that the two band image (classification and mask) can be accessed by T-Spectra.
2. Using T-Spectra the two bands, classification and mask, are multiplied together to create a new single band image file which contains only the classified saltmarsh and tidal flats areas.
3. The band multiplication results in the scaling of the values between 0 and 256, with unclassified pixels having a value of zero. As the conversion of the image to pcArc/Info coverage requires polygons having a coding other than zero a value of 2 must be added to all pixels (1 will not do as this will result in 256 being assigned a value of 0). This procedure is carried out using the Terra-Mar utility program DIRTYADD.
4. A 512 byte header using the copy/b command must then be added to create a new .IMG file that can be read by the Terra-Mar image processing system.

5. The header record must be edited in Terra-Mar MICROIMAGE to give the new image file the correct number of lines and pixels so that it can be read by the Terra-Mar image processing system.

This complex series of operations is bypassed when the image is exported to GRID. Masking can be done very quickly and easily in GRID simply by the application of the SETMASK command.

The final step is to use the export option in Terra-Mar to create a .LAN file. This puts the coverage into a form which can be imported by pcArc/Info.

Having imported the classified images into pcArc/Info the GRIDPOLY command is used to create a coverage from the classified, masked image. ARCEDIT is used to remove the boundary polygon and leave the area of interest as the coverage. This has to be CLEANED before dBase is used to update the .PAT file with the thematic information relating the classification class values to appropriate vegetation types. The coverage is then available for area calculations and interrogation using the MEASURE LENGTH and IDENTIFY commands in ARC/PLOT. These commands are used to generate the information in the counts of the Maximum Likelihood Classifications (chapters 6). In the case of the mixture model analysis the data are imported into GRID using the IMAGEGRID command. Processing is carried out using the COMBINE and RECLASS commands (chapter 7).

METHOD OF COMPARISON OF SURVEYS WITHIN THE GIS

In order to allow comparison with the work carried out by Sproxton the same methodology was used. This involved comparing the total saltmarsh areas and the aggregated zone classes. In all cases the classified images were first compared with the 1982/4 N.C.C. survey. Comparison was taken a stage further in the present study by using cross tabulation techniques. This calculated the % agreement between the surveys of the different classification techniques.

The brief overview of the work carried out by Sproxton in establishing the Wash Geographical Information system illustrates many of the advantages that can be reaped from combining satellite imagery into a coastal monitoring GIS. The information once in geometrically correct digital form can be easily manipulated to provide valuable and timely information concerning the dynamics of the intertidal zone. This chapter also illustrated many of the difficulties of integrating satellite sensor data into a commercial GIS such as pcArc/Info. As Curran states, "a GIS is a powerful technique for turning large volumes of spatial data into useable information... remote sensing is a powerful technique for the collection of multi-temporal data sets but there is a significant gap between data collection and utilisation."

GRID proves to be a much more satisfactory method of incorporating satellite sensor data into a GIS, being considerably quicker and more convenient, and avoids many of the complex operations needed to convert a classified satellite image into a pcArc/Info coverage. GRID is also a more accurate method of evaluating satellite surveys as there is no confining arc per polygon limit and thus avoids the application of spatial filters. It is also a relatively easy operation to convert existing pcArc/Info vector coverages into a GRID format. It is strongly recommended that future studies convert the satellite sensor data into a raster GRID format rather than a vector coverage format.

Campbell, J.B. 1987: **Introduction to Remote Sensing**. Guildford Press, London.

Curran, P.J. 1985: **Principles of Remote Sensing**. Longman, New York.

Davis, F.W. and Simonett, D.S. 1991: GIS and remote sensing. In Maguire, D.J., Goddchild, M.F. and Rhind, D. (eds): **Geographical Information Systems - Principles and Applications**. Longman Scientific and Technical, New York: 191-213.

Hill, M.I. 1988: **Saltmarsh Vegetation of the Wash. An Assessment of Change From 1971 to 1985**. N.C.C. Publications, Peterborough.

Jackson, M.J. 1992: Integrated geographical information systems. **International Journal of Remote Sensing**. vol. 13: 1343-1351.

Kestner, F.J.T. 1975: The loose-boundary regime of the Wash. **Geographical Journal**. vol. 141: 388-414.

National Environment Research Council, 1976: **The Wash Water Storage Scheme Feasibility Study. A Report on the Ecological Studies**. N.E.R.C. Publications Series C, No.15.

National Environment Research Council, 1983: **Thematic Mapper Data: Characteristics and Use**. Landsat-4, February 4, 1983. Reading, Berkshire.

Randerson, P.F. 1975: The saltmarshes of the Wash. **Wash Feasability Study Ecological Report**. Scientific study D (unpublished).

Shennan, I. and Sproxton, I. 1992(b): **Anglian Sea Defence Management Study - stage III**. Satellite data classification - Sub-Contract WV ACP 421. Unpublished work.

Terra-Mar Resource Information Service 1991: **Terra-Mar 4.0**. Mountain View, California, USA.

CHAPTER 6

MAXIMUM LIKELIHOOD CLASSIFIER

A basic problem in the analysis of remotely sensed data is to estimate the proportion of a given scene devoted to a particular land cover type. The usual approach to solving this type of problem is to design a classifier for identifying the land cover of interest. The scene is then classified and the proportion of pixels classified as the land cover of interest becomes the desired estimate (Lenninton and Sorensen, 1984). The accuracy of a classification is essentially dependent on the degree of spatial and spectral resolution that is required. In the context of the remote sensing of saltmarshes a high degree of accuracy can be obtained by using broadly defined classes such as Upper, Middle and Lower saltmarsh zones. The degree of accuracy deteriorates as new classes are introduced. The purpose for which the classification is to be used should dictate the number of classes chosen, providing a balance between the number of classes and the degree of accuracy.

The results of the classifications carried out in the present study were imported into the Wash GIS, using the techniques described in the previous chapter and overlaid on the N.E.R.C. (N.E.R.C., 1976) and N.C.C. (Hill, 1988) surveys. As was mentioned in the preceding chapter although these two surveys are broadly similar they used different classification schemes. For the purpose of the present study these surveys were aggregated into the four broad zones used by Sproxton mentioned in the previous chapter: **Upper Marsh** (*Agropyron*, *Upper marsh grass*, *Puccinellia* and *Spergularia*), **Middle Marsh** (*Puccinellia*, *Puccinellia* and *Halimione* and *Halimione*), **Lower Marsh** (Transitional Lower marsh, *Aster*, *Salicornia* and *Aster*) and **Pioneer Marsh** (*Salicornia*, *Spartina*, *Salicornia* and *Spartina*, *Salicornia* and *Suaeda* and *Suaeda maritima*). The maximum likelihood satellite classifications used eight classes: *Agropyron*, Uppermarsh grass, *Puccinellia*, *Puccinellia* East (the inclusion of this class was in recognition of the fact that the distinctive stands of *Puccinellia* on the East shore marshes, at Wolferton and Wooton, were spectrally separable from the more mixed *Puccinellia* communities elsewhere on the Wash Estuary (chapter 3)), *Puccinellia* and *Halimione*, *Halimione*, Lower marsh and Pioneer zone. In the Wash GIS

these classes were again aggregated to give the four broad vegetation zones mentioned above. The aggregations allowed comparisons to be made between the image classifications and the N.E.R.C. and N.C.C. surveys.

The first classification strategy examined was the Maximum Likelihood Classifier (MLC). The method was chosen as it is the most accurate and commonly used of the established supervised classification techniques such as the minimum distance to means classifier and the parallelepiped classifier. The MLC is also relatively easy to use. This would be an important factor in an operational mode where the user may be a non-specialist. Supervised classifications have the advantage of making use of the experiences and local knowledge of the operator. Again this may be advantageous in an operational mode where the user may be an environmental manager with good local knowledge of the area that is to be classified.

In the present study the MLC classification was carried out by two independent operators in an attempt to establish the objectivity of the processing methods. Consistency between operators would be essential in an operational mode. The first operator had the benefit of local knowledge and fieldwork in the study area, the second operator lacked such experience. There would be little point in producing classifications that could not be objectively generated. Similarly for the purpose of monitoring intertidal vegetation over a temporal scale it would be important that processing methods were held constant. The use of the two operators would also help to establish the level of experience that an operator would need to have in order to generate a satisfactory classification.

MULTISPECTRAL CLASSIFICATION

For each pixel in a Landsat 5 TM image, the spectral brightness is recorded for seven different wavelength bands. For vegetation studies band 6 is commonly excluded. A pixel may be characterised by its spectral signature, which is determined by the relative reflectance in the different wavelength bands. In practice the operator starts by extracting training areas from the scene which represent different landcover classes. Multispectral classification is a process that analyses the spectral signatures of the training areas. The spectral characteristics

of pixels from the whole dataset are subsequently calculated and assigned to categories based on similarity with the spectral characteristics of the training areas (Curran, 1985).

Multispectral classification is illustrated diagrammatically in Fig 6.1 (adapted from Sabins, 1987). The reflectance, in TM bands 3, 4, and 5, of hypothetical saltmarsh training areas are plotted on a three dimensional graph, producing clusters or ellipsoids that represent different spectral classes. For the sake of simplicity the cluster diagram is shown with only three axes. The MLC used in the present study uses a separate axis for each of the six TM bands. The surfaces of the ellipsoids form decision boundaries which are used to determine decision rules for the classification of each pixel in the whole data set (Sabins, 1987). The computer calculates the spectral values for each pixel in a whole image and determines its position in the classification space. Should the pixel fall within one of the clusters, it is classified accordingly. The MLC operates by calculating the mean vector, variance and correlation for each training set in the data. The mean vector is arrived at by calculating the mean DN of all six TM bands in each training set. This information allows the spread of all pixels in the dataset, around each mean vector in spectral space, to be described using a probability function which equates to the minimum mahalanobis distance. Pixels from the whole data set are assigned to the class with which they have the highest probability of membership (Curran, 1985; James, 1985).

TRAINING AREA SELECTION

The selection of accurate and pure training data is often essential to the accuracy of the overall classification. In the case of saltmarshes it is desirable to locate areas which are dominated by different saltmarsh species. Accurate information about the distribution of the different saltmarsh species, especially when included in monitoring studies, may provide the coastal manager with valuable information such as the rates of saltmarsh advance and retreat, and the rate of saltmarsh recovery after reclamation.

Operator 1 identified three training areas for each of the ground cover types from areas of known saltmarsh communities identified by field survey. The spectral signatures for those training areas large enough to permit the calculation of statistics by the Terra-Mar

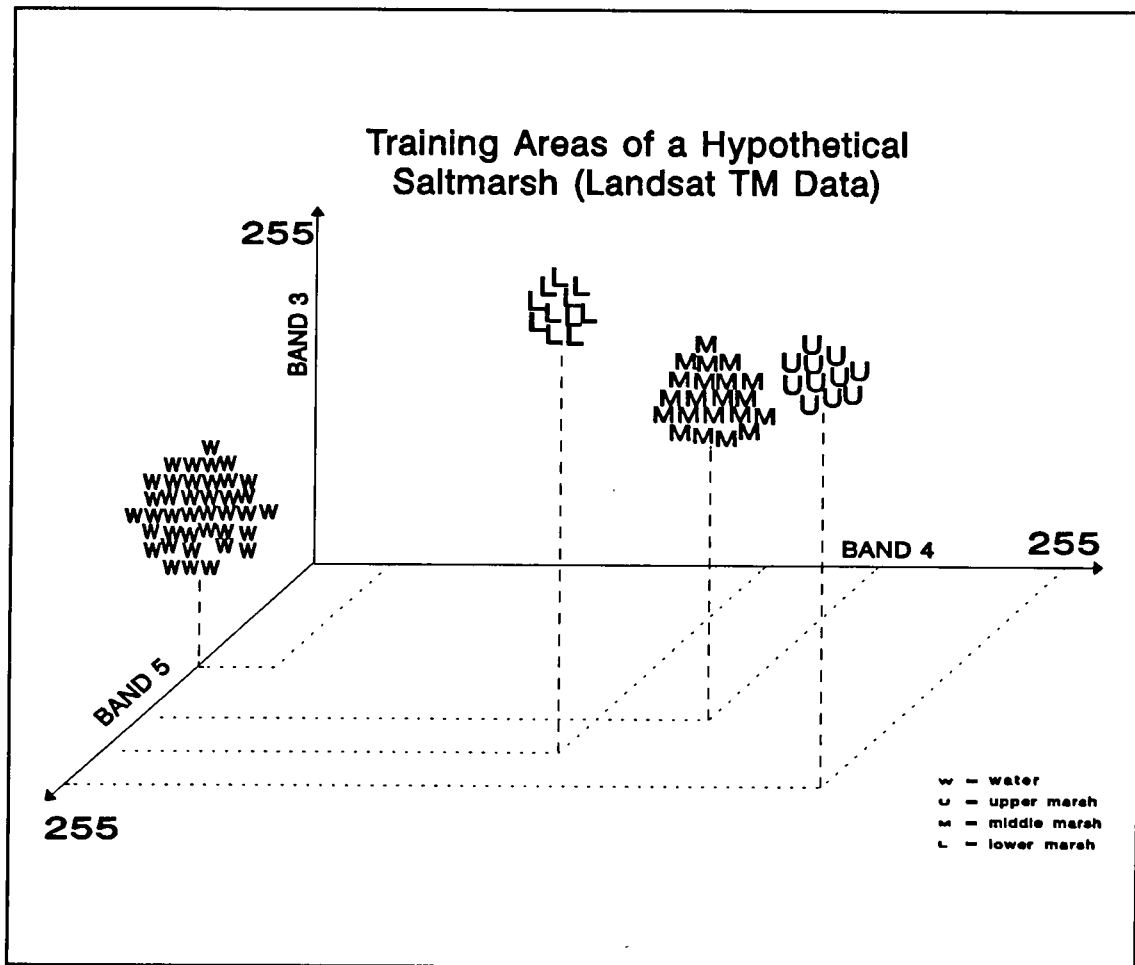
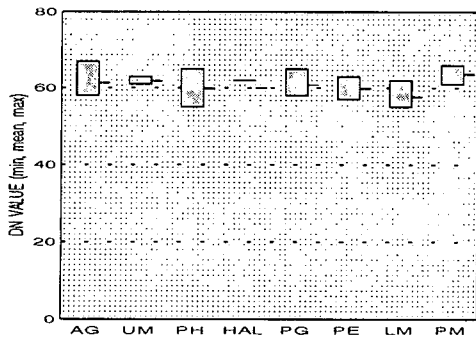


Fig.6.1 Three-dimensional cluster diagram of training sets used in a classification.

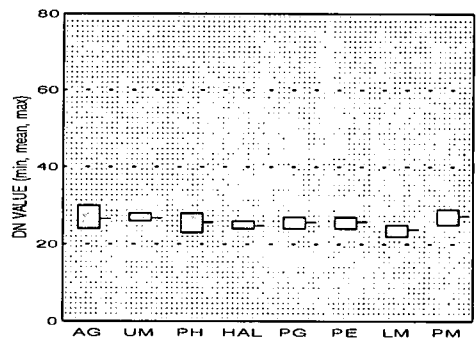
image processing software were compared for internal homogeneity by studying the histograms for each class in each band. The degree of spectral separation between species classes may be established by looking at the spectral responses in each band (Fig. 6.2 and chapter 3). The statistics extracted from the training areas form the basic input into the MLC. As was expected from the analysis of the spectral characteristics of the training areas documented in chapter three, there is great similarity between the classes in the visible TM bands, 1, 2, and 3, and the greatest potential for discrimination is seen in the near infrared TM bands, 4 and 5 (Fig.6.2).

September 1991 Training Sets

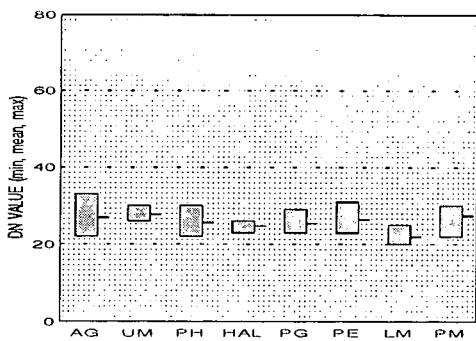
TM Band 1



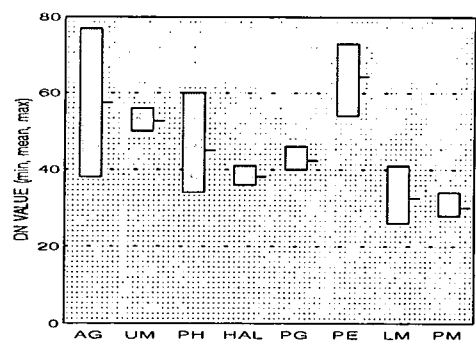
TM Band 2



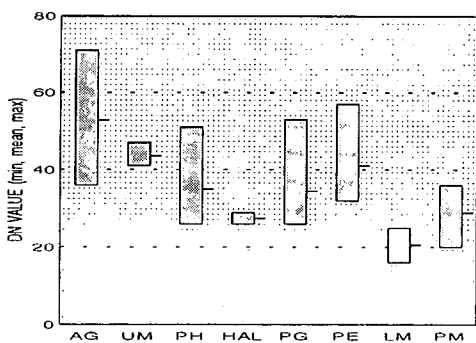
TM Band 3



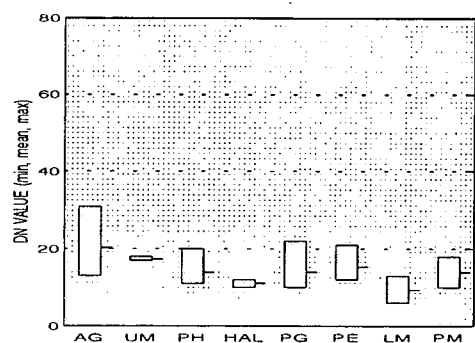
TM Band 4



TM Band 5



TM Band 7



AG	Agropyron	PG	Puccinellia
UM	Upper Marsh	PE	Puccinellia East
PH	Puccinellia and Halimione	LM	Lower Marsh
HAL	Halimione	PM	Pioneer Marsh

Fig. 6.2 High-Low Graphs Summarising the Spectral Characteristics of the 1991 Training Sets.

Using these methods operator 1 established a set of training areas consisting of the eight classes: *Agropyron*; Upper marsh grass; *Puccinellia* and *Halimione*; *Puccinellia*; *Halimione*; *Puccinellia* East; Lower marsh; and Pioneer zone. Operator 2 had no experience of fieldwork in the area and therefore relied purely on the 1984 N.C.C. survey maps in order to establish a set of training areas. The training areas were then identified on the satellite image using the Terra-Mar EXTRACT POLYGONS AND STATISTICS function (Terra-Mar 4.0) (Fig.6.3) and mean spectral characteristics were calculated for each training area in each of the six TM bands used (Fig.6.2).

The classification of the May 1984 and September 1991 Landsat 5 TM images followed the same procedure and used approximately the same training areas. The training areas for the 1991 and 1984 Landsat 5 TM images varied slightly in their position due to seasonal changes and other changes in the position of some of the vegetation classes. Similarly the spectral response of the training areas changed between the images due to seasonal influences (chapters 2 and 3). Differences in radiometric, atmospheric and illumination conditions had already been corrected by the application of the radiometric rectification techniques (chapter 4).

Ideally the selection of training areas should be based on fieldwork carried out simultaneously with the remote sensing of the area. This is often logistically impractical. The greater the time lapse between the remote sensing of the area and groundwork, the greater the potential there is for the introduction of errors into the classification as the nature and composition of the surface may change as a result of phenology and senescence. Similarly tidal conditions may change between the two measurements and this may have a significant effect on spectral responses (Donoghue and Zong, 1992).



Fig. 6.3 Location of training areas on the September 1991 Landsat5 TM image (operator 2). (red = TM4, green = TM3, blue = TM2).

There proved to be considerable difficulty in relating the training areas, identified on the N.C.C. maps, to the remotely sensed images. The relatively coarse spatial resolution of Landsat TM data (30 m) makes this problem even more troublesome. The identification of the small training areas, often only the size of five or six pixels, on the Landsat TM images proved to be difficult. This problem is especially relevant in the context of saltmarshes where plant communities form complex mosaics. As a result training areas containing pure stands of *Halimione*, *Puccinellia* and Upper marsh grass proved to be very difficult to distinguish on the satellite images. Training area definition was also problematical at the seaward margin of the saltmarsh where Lower marsh and Pioneer species grow in relatively narrow strips. Although in these areas potentially suitable stands of vegetation could be identified on the image they were too small for calculation of statistics by the Terra-Mar image processing software (Terra-Mar 4.0, 1991).

The problem of identifying suitable training sets on the satellite image is confused by the spectral similarity of many of the saltmarsh classes (chapter 3 and Fig.6.2). Whereas the broad zones of the saltmarsh (Upper, Middle and Lower marsh) can be identified relatively easily, the same cannot be said for the finer classes within these broad zones. This is most clearly illustrated by the Middle marsh zone. *Puccinellia* East (PE) is spectrally distinct but there is likely to be confusion when trying to separate *Halimione* (HAL) , *Puccinellia* (PG) and *Puccinellia/Halimione* (PH) (Fig 6.2). A similar problem may be seen in the Upper Marsh zone when trying to distinguish between the Upper Marsh grass and *Agropyron*. The similar spectral characteristics of many of the classes makes selection of suitable training areas difficult. Even in broadly defined vegetation classes it proved very difficult to separate the Lower Marsh zone from the Pioneer zone, and the Pioneer zone from the intertidal flats due to spectral similarity. This proved to be a problem in both of the images. In the May 1984 image, vegetation in the pioneer zone, predominantly *Salicornia*, has not yet developed sufficiently. The vegetation spectral signature in this image is masked by mud and the Pioneer zone is classed accordingly. In the September 1991 image the Pioneer zone class has a similar signature to that of algal blooms on the intertidal mudflats and results in much of the intertidal flat being classified wrongly as Pioneer marsh. This is clearly illustrated in Figs 6.5 and 6.6. The areas of light and dark green represent areas of Lower and Pioneer marsh. Confusion with the spectral signature of algae is marked by the presence of green areas far

out on the tidal flats.

Having selected the training areas the MLC was applied to the 1984 and 1991 Landsat 5 images (Fig 6.4-6.6). Figure 6.4 is an extract of the unclassified TM data (red = TM4, green = TM3, blue = TM2) and Fig. 6.5 is the corresponding extract after the MLC had been applied. Fig.6.6 illustrates the Terra-Mar output after operator 1 had applied the MLC to the September 1991 Landsat 5 TM image. The data has been considerably simplified to produce a thematic map with red representing *Agropyron*, blue Middle marsh, orange representing areas of pure *Halimione*, purple *Puccinellia* East and the two shades of green the Lower marsh and Pioneer zone. The areas of agricultural land classed as *Agropyron*, due to spectral similarity and the actual presence of marsh grasses along drainage ditches, are removed by the masking techniques described in chapter 5.

RESULTS OF THE MAXIMUM LIKELIHOOD CLASSIFICATION

The results of the classifications were imported into the WASH GIS using the procedures discussed in chapter 5 (Figs. 6.7, 6.8). Three different methods were used for analysing the results of the classifications. At the macro scale the total saltmarsh areas for the whole of the Wash Estuary were calculated and compared (Table 6.8). This was done by removing the internal boundaries of the saltmarsh classes using the OVERLAY module in pcArc/Info. This was designed to evaluate the MLC's accuracy in defining the total saltmarsh area. At the meso scale the areas of the different saltmarsh zones were calculated and compared (Upper marsh, Middle marsh, Lower marsh and Pioneer zone) (Table 6.8). This was done in order to evaluate the MLC's ability to map the different vegetation communities within the saltmarsh. At the micro scale cross tabulation of coverages was carried out to assess the MLC's ability in correctly locating different vegetation communities within the saltmarsh. Cross tabulation was performed using the OVERLAY and TABLE modules within pcArc/Info. This process involves the overlaying of two coverages and identifies areas of matching cover classes. The results of the cross tabulations are displayed in Tables 6.1-6.7. A summary of the findings are presented in Table 6.8 and Fig. 6.12.

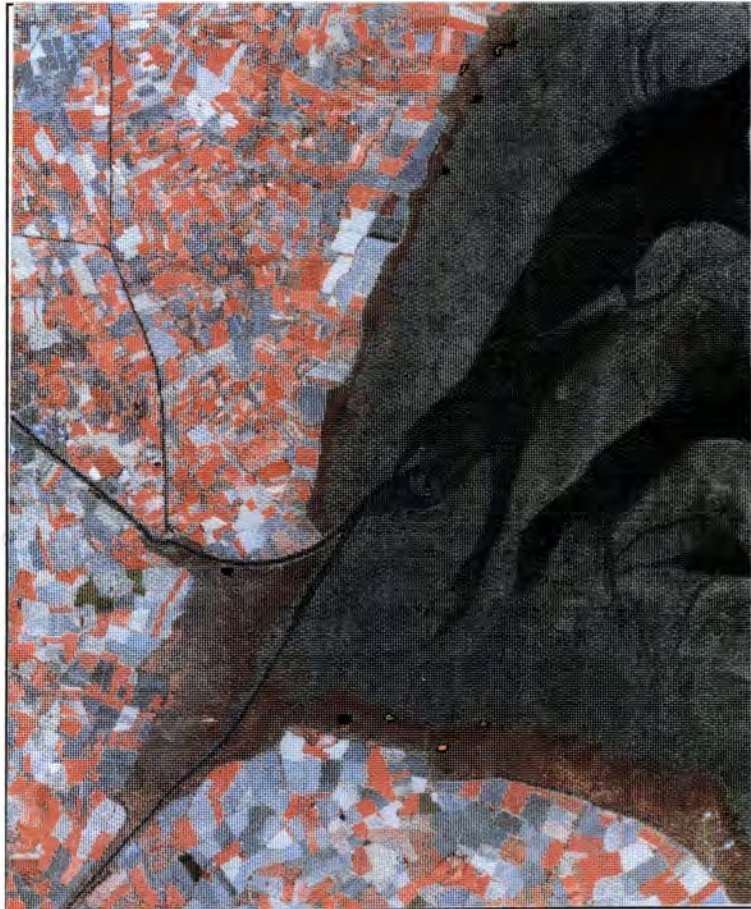


Fig. 6.4 Extracted area of the September Landsat 5 TM image of the Wash Estuary (operator 1 training sets illustrated).

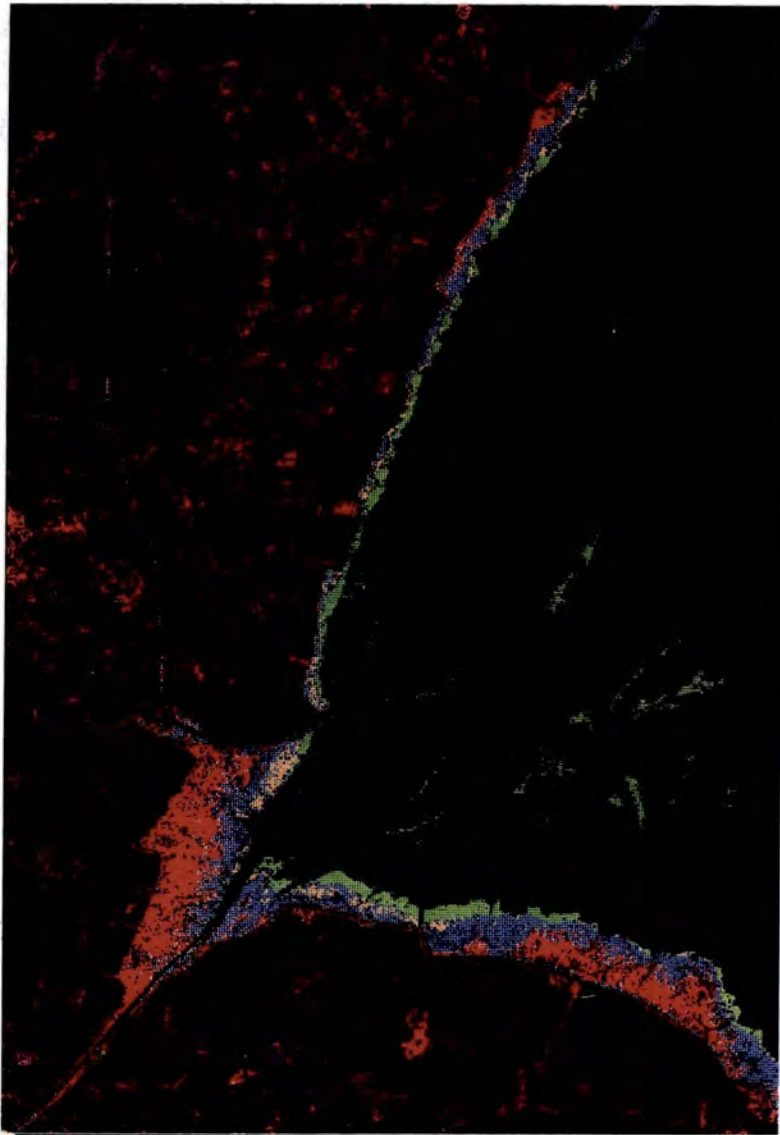


Fig. 6.5 Application of the Maximum Likelihood Classifier to an extract of the September Landsat 5 TM image of the Wash Estuary (operator 1 training sets used).

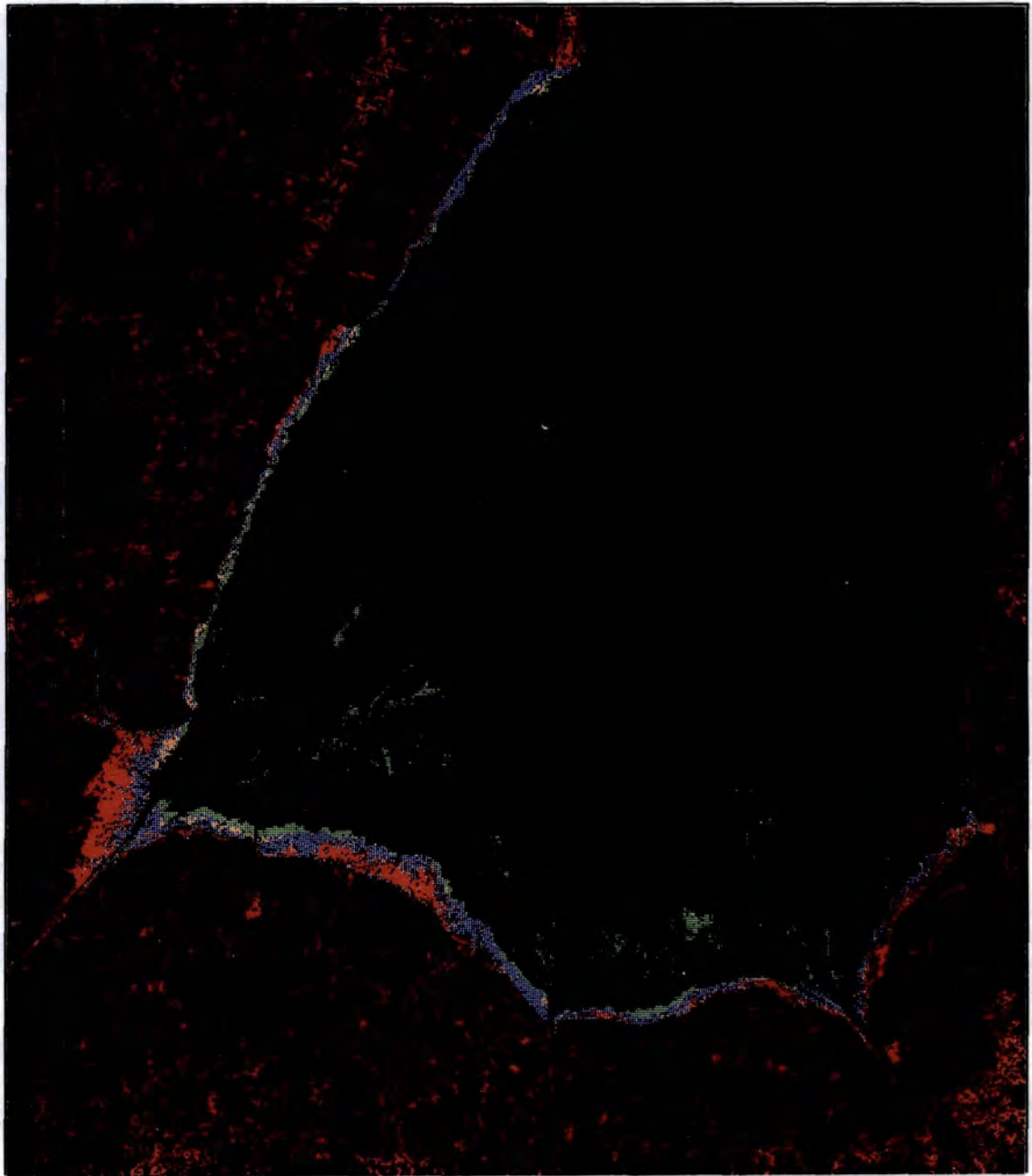
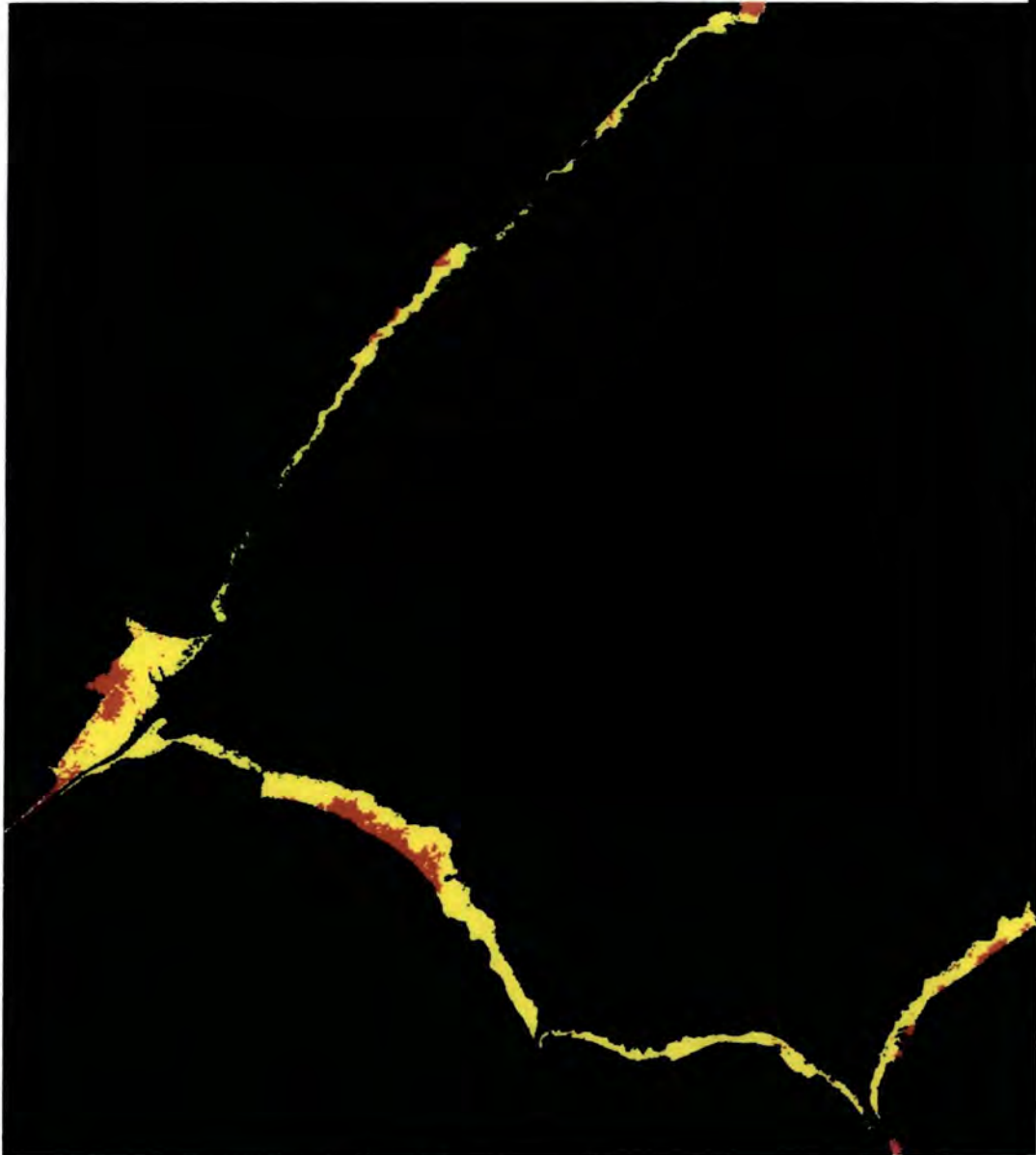


Fig. 6.6 The result of operator 1 applying the Maximum Likelihood Classifier to the September 1991 Landsat5 TM image.

Fig. 6.7 GENENERALISED VEGETATION COVER

OF THE WASH ESTUARY

Maximum Likelihood Classification of 14/5/84 Landsat5 TM Image



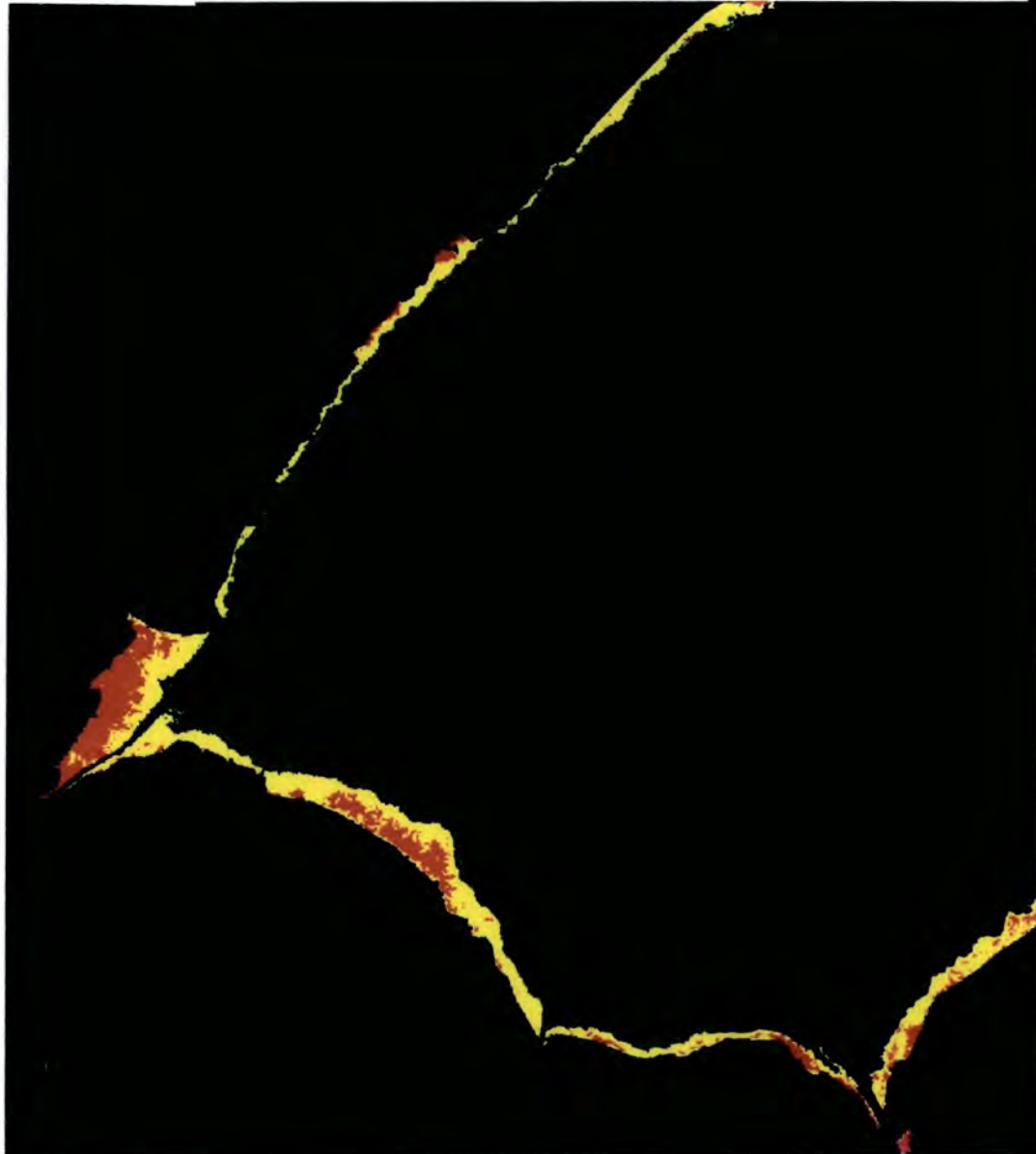
-  Upper Marsh
-  Middle Marsh
-  Lower and Pioneer Marsh

Fig. 6.8 GENENERALISED VEGETATION COVER

OF THE WASH ESTUARY

Maximum Likelihood Classification of 7/9/91 Landsat TM Image

scale 1 : 236,000



-  Upper Marsh
-  Middle Marsh
-  Lower and Pioneer Marsh

Table 6.1 Areas in hectares. Cross tabulation of the 1982/4 N.C.C. survey with the 1984 MLC - Operator 1.

1984 N.C.C.		MLC Classification of the May 1984 Landsat 5 TM Image - Operator 1						
Zone	Upper marsh	Middle marsh	Lower marsh	Others	Total Area	% Agreement		
Upper marsh	351.00	261.40	1.34	134.88	748.62	46.9		
Middle marsh	153.60	1827.52	128.52	256.51	2366.15	77.0		
Lower marsh	0.00	308.71	108.96	390.08	807.75	13.5		
Other	33.82	135.93	27.12	39.57	236.44	16.7		
Total area	538.42	2533.56	265.94	821.04	4158.96			

Table 6.2 Areas in hectares. Cross tabulation of the 1982/4 N.C.C. survey with the 1984 MLC - Operator 2.

1984 N.C.C.		MLC Classification of the May 1984 Landsat 5 TM Image - Operator 2						
Zones	Upper marsh	Middle marsh	Lower marsh	Others	Total Area	% Agreement		
Upper marsh	338.18	308.19	0.11	102.16	748.64	45.2		
Middle marsh	117.69	1772.69	91.42	384.35	2366.15	74.9		
Lower marsh	0.14	200.94	60.82	545.76	807.66	7.5		
Other	32.86	143.83	9.96	25.34	211.99	11.9		
Total area	488.87	2425.65	162.31	1057.61	4134.44			

Table 6.3. Areas in hectares. Cross tabulation of the 1982/4 N.C.C. survey with the 1991 MLC - Operator 1.

1984 N.C.C. Zones	MLC Classification Of the September 1991 Landsat 5 TM Image - Operator 1					Total Area	% Agreement
	Upper marsh	Middle marsh	Lower marsh	Others	Total Area		
Upper marsh	509.97	123.61	1.20	106.27	741.05	68.8	
Middle marsh	520.95	1556.64	65.02	211.05	2353.66	66.1	
Lower marsh	20.11	369.99	271.92	99.94	761.96	35.6	
Other	45.52	279.08	171.59	23.29	519.48	4.5	
Total area	1096.55	2329.32	509.73	440.55	4376.15		

Table 6.4. Areas in hectares. Cross tabulation of the 1982/4 N.C.C. survey with the 1991 MLC - Operator 2.

1984 N.C.C. Zones	MLC Classification of the September 1991 Landsat 5 TM Image - Operator 2					Total Area	% Agreement
	Upper marsh	Middle marsh	Lower marsh	Others	Total Area		
Upper marsh	495.31	166.88	0.0	86.50	748.69	66.2	
Middle marsh	503.32	1563.01	112.61	187.15	2366.09	66.1	
Lower marsh	13.99	306.96	313.88	172.91	807.73	38.9	
Other	63.75	274.08	131.11	23.78	492.72	4.8	
Total area	1076.37	2310.93	557.60	407.34	4352.24		

Table 6.5 Areas in hectares. Cross tabulation of Operator 1 1984 MLC and Operator 2 1984 MLC.

Operator 2		Operator 1					
Zones	Upper marsh	Middle marsh	Lower marsh	Others	Total Area	% Agreement	
Upper marsh	370.71	143.28	0.09	28.17	542.25	68.4	
Middle marsh	35.28	2040.57	57.87	402.39	2536.11	80.5	
Lower marsh	0.27	84.60	92.07	91.08	268.02	34.3	
Other	84.87	263.44	12.24	18.36	278.91	6.6	
Total area	491.13	2431.89	162.27	540.00	3625.29		

Table 6.6 Areas in hectares. Cross tabulation of Operator 1 1991 MLC and Operator 2 1991 MLC.

Operator 1		Operator 2					
Zones	Upper marsh	Middle marsh	Lower marsh	Others	Total Area	% Agreement	
Upper marsh	847.17	215.82	0.0	39.60	1102.59	76.8	
Middle marsh	114.48	1934.28	156.69	126.18	2331.63	82.9	
Lower marsh	1.17	48.42	379.71	80.46	509.76	74.5	
Other	83.79	118.98	12.15	5.13	220.05	2.3	
Total area	1046.61	2317.50	548.55	251.37	4164.03		

Table 6.7 Areas in hectares. Cross tabulation of the 1984 and 1991 MLCs - operator 1.

1991 Zones	1984 Classification				
	Upper marsh	Middle marsh	Lower marsh	New	
Upper marsh	415.26	587.34	8.01	91.98	
Middle marsh	78.30	1758.60	137.79	356.94	
Lower marsh	0.09	75.24	93.42	341.01	
Pioneer zone	0.00	0.54	1.17	114.30	
Mismatch	45.09	101.52	24.57		

Table 6.8 Areas (in hectares) of the saltmarsh zones

Zones	N.E.R.C. 1971/4	N.C.C. 1982/4	Imagery 1984		Imagery 1991	
			Operator 1	Operator 2	Operator 1	Operator 2
Upper marsh	625.53	748.67	542.25	490.86	1102.59	1062.00
Middle marsh	1913.33	2366.16	2536.11	2432.16	2332.49	2333.43
Lower marsh	818.93	432.44	268.02	162.27	509.76	557.82
Pioneer zone	178.5	375.28			116.01	
Total area	3536.29	3922.55	3346.38	3085.29	4060.85	3953.25

COMPARISON BETWEEN THE 1982/4 N.C.C. SURVEY AND THE MLC CLASSIFICATIONS OF THE MAY 1984 LANDSAT 5 TM IMAGE (Table 6.1, 6.2, Fig. 6.9)

Comparing the maximum likelihood classified images with the digitised cover of the 1982/4 survey provides the best means of evaluating the accuracy of the classification technique. It would perhaps be expected that the classified Landsat 5 TM May image of the Wash Estuary would provide the best results as this is closest to the N.C.C. survey date. The total area of the saltmarsh classified (Table 6.8) by operator 1 for this image is 14.7% less than the 1982/4 N.C.C. survey. The difference for operator 2 was 21.3%. If the Pioneer zone is not included the discrepancies are much smaller with only 5.6% for operator 1 and 13% for operator 2. Both the operators could not identify a Pioneer zone training area for the May 1984 image. This is best explained by the phenological characteristics of *Salicornia* which dominates the Pioneer zone of the Wash Estuary saltmarshes. When the image was taken, May 14 1984, the *Salicornia* had not yet fully matured. The spectral signal of the Pioneer zone of this image is therefore dominated by the substrate and cannot be separated from the intertidal flats using the MLC. The meso scale comparisons reinforce this point. The difference in areas classified as Lower marsh (a zone which is also contains much *Salicornia*) are 39% for operator 1 and 62% for operator 2. Much closer agreement occurred for the classification of the Middle and Upper marsh zones. The discrepancies for operator 1 were 28% for the Upper marsh zone and only 7% for the Middle marsh zone. For operator 2 there was a 35% discrepancy for the Upper marsh zone but less than 3% for the Middle marsh zone.

These findings are also reflected at the micro level of comparison (Table 6.1 and Table 6.2). Poor matches occur for the Lower marsh zone with operator 1 achieving only 13.5% agreement and operator 2 24.8%. The figures for the Upper marsh are 46.9% agreement for operator 1 and 45.2% for operator 2. The best matches were found in the Middle marsh zone classification with operator 1 achieving 77% agreement and operator 2 74.9%.



Fig. 6.9 COMPARISON OF THE 1982/4 N.C.C. Survey

AND THE 1984 MAXIMUM LIKELIHOOD CLASSIFICATION (OPERATOR 1)

MLC survey based on 14/5/84 Landsat5 TM image



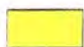


-  Saltmarsh areas mapped in both surveys
-  Saltmarsh mapped by the MLC survey but not by the N.C.C.
-  Saltmarsh mapped by The N.C.C. survey but not by the MLC

Fig. 6.9 illustrates the findings of this comparison. The green areas represent the areas classified as saltmarsh by the N.C.C. survey but not by the maximum likelihood classification. The green area forms a narrow band of Lower/Pioneer marsh fronting nearly all of the Wash Estuary saltmarshes and is especially noticeable at Leverton, Butterwick and Freiston. This helps to confirm the view that at this stage of the growing season the MLC is unable to identify large areas of the Lower marsh and Pioneer zone. The areas of red, such as those at Terrington and Wolferton, locate possible areas of expansion between the date of the N.C.C. survey, which commenced in 1982, and the date of the May 1984 image.

COMPARISON BETWEEN THE 1982/4 N.C.C. SURVEY AND THE MLC CLASSIFICATIONS OF THE SEPTEMBER 1991 LANDSAT 5 TM IMAGE (Tables 6.3, 6.4, Fig. 6.10)

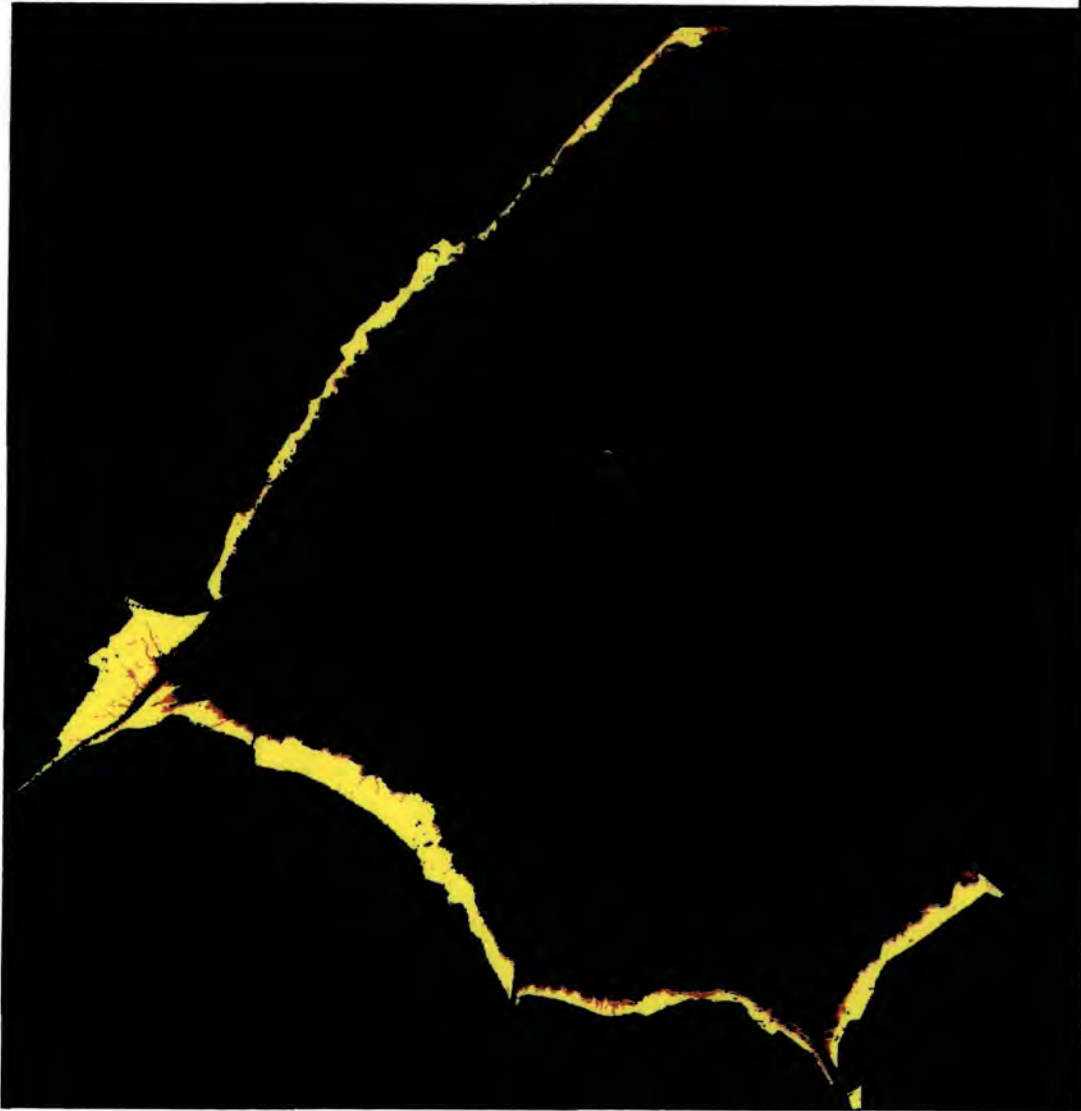
Comparing the total marsh areas of the 1991 classifications with the 1982/4 N.C.C. surveys reveals a discrepancy of 3.5% for operator 1 and less than 1% for operator two. This image was taken late in the growing season which means the Pioneer zone is more developed than in the May 1984 image and is therefore more easily identified by the MLC. This is reflected in the micro level comparisons where much higher agreement figures were reached for the Lower marsh zone than the figures from the classification of the May 1984 Landsat 5 TM image. 48.5% agreement was recorded for operator 1 and 38.9% for operator 2. The fact that at this stage of the growing season the MLC was able to identify the Pioneer zone more effectively is illustrated in Fig. 6.10. The broad green band of Fig. 6.9 has been replaced by a red band, marking areas of possible saltmarsh expansion notably at Wolferton, Terrington and the mouth of the Welland, and saltmarsh recovery on the shore of Freiston and Wainfleet. This is perhaps a more accurate map of expansion than Fig. 6.11 as seasonal effects are minimized. There remained areas of Pioneer marsh classified in the 1982/4 N.C.C. survey but not picked up in either of the MLC classifications. These areas are represented by the green areas of Fig. 6.10 and correspond with the Pioneer zone of Wrangle, Leverton and Friskney. Areas of Pioneer marsh recolonising the borrow pit were also not picked up by the MLCs indicating that even late on in the growing season the classifier has problems in accurately locating the Pioneer marsh.

Fig. 6.10 COMPARISON OF THE 1982/4 N.C.C. Survey

AND THE 1991 MAXIMUM LIKELIHOOD CLASSIFICATION (OPERATOR 1)

MLC survey based on 7/9/91 Landsat5 TM image

scale 1 : 236,000






-  Saltmarsh areas mapped in both surveys
-  Saltmarsh mapped by the MLC survey but not by the N.C.C.
-  Saltmarsh mapped by The N.C.C. survey but not by the MLC




Fig. 6.11 COMPARISON OF THE 1991 MAXIMUM LIKELIHOOD CLASSIFICATION

AND THE 1984 MAXIMUM LIKELIHOOD CLASSIFICATION (OPERATOR 1)

MLC surveys based on 14/5/84 & 7/9/91 Landsat5 TM images

scale 1 : 236,000



-  Saltmarsh areas mapped in both surveys
-  Saltmarsh mapped by the 1991 MLC survey but not by the 1984 MLC Survey
-  Saltmarsh mapped by The 1984 MLC survey but not by the 1991 MLC Survey

COMPARISON BETWEEN THE 1984 MLC CLASSIFICATION AND THE 1991 MLC CLASSIFICATION (Table 6.7, Fig. 6.11)

Considerable differences could be expected between these two coverages as there is a considerable time lapse and hence a period when vegetational change may have occurred in the Wash Estuary. Overlaying the 1991 classification (operator 1) onto the 1984 classification (operator 1) (Table 6.8) indicates that total marsh area excluding Pioneer zone has increased by 618.75 hectares. Looking more closely at the changes among saltmarsh zones (Table 6.7) suggests that 678.3 hectares of the 1984 Upper marsh became Middle marsh in 1991. Furthermore, the Middle marsh gained 137.79 hectares from the Lower marsh and 255.42 hectares from new development (Tables 6.7 and 6.8). The Lower marsh clearly shifted seaward and gained 316.44 ha of new development. In short, the Upper marshes have expanded considerably (Tables 6.7, 6.8 and Fig. 6.11), associated with the seaward shifting of the Middle and Lower marshes even if seasonal effects are taken into account. This area of seaward expansion is clearly identifiable by the red band in Fig. 6.11. Considerable saltmarsh expansion is in evidence at Wainfleet, Freiston, Terrington and the mouth of the Welland. This continues a trend seen between the two surveys carried out in the 1970s and 1980s (Hill 1988).

COMPARISON OF THE TWO INDEPENDENT CLASSIFICATIONS (Table 6.5, 6.6)

At the broadest level of comparison, total marsh area, the results of the 1984 classifications from the two independent operators show a 7.8% difference in total saltmarsh area (Table 6.8). Results of the 1991 classifications are even closer with only a 2.7% difference in total saltmarsh area. If the Pioneer zone is excluded (operator two was unable to define a Pioneer zone training set) there is only 0.2% difference in the saltmarsh area.

At the meso scale of comparison, comparing the areas for the different saltmarsh zones in Table 6.8, it appears that the areas defined as Upper and Middle saltmarsh communities are very similar. In the 1991 classifications there is only a 3.7% difference in the area of Upper marsh and only a 0.04% difference in the area of Middle marsh. The corresponding figures for the 1984 classifications are 9.5% for the Upper marsh and 4% for

the Middle marsh. In both the dates there are much bigger differences in the areas classified as Lower marsh. The figure for the 1991 classifications is 8.6% and the figure for the 1984 classifications is 39.4%. The Pioneer zones were not compared as operator 2 was unable to define a Pioneer zone training area.

Cross tabulation of the 1984 classifications (Table 6.5) reveals that there is a reasonable match for the locations of areas of Upper and Middle marsh zones, the agreement figures being 68.4% and 80.5% respectively. This was a pattern that was matched in the 1991 classifications (Table 6.6) with the agreement figure for the Upper marsh calculated as 76.8% and that for the Middle marsh 80.5%. The agreement of the Lower marsh zone was 74.5% for the 1991 classifications but only 34.3% for the 1984 image. The great contrast in these figures is probably best explained by the fact that the delimitation of the Lower and Pioneer marsh in the 1984 image, being relatively early on in the growing season, is much harder to define than in the September 1991 image, late on in the growing season, when the Lower marsh and Pioneer zones are more easily located on the image.

The results are remarkably good and the differences between the classifications are most likely explained by differences in training area selection. The first operator had the benefit of fieldwork in the area and was able to establish eight different classes whereas the second operator could only establish six (no Upper marsh grass or Pioneer zone class). These results are very encouraging as it would suggest the methods used can provide a degree of consistency between operators. In an operational mode only one set of training areas would be used. It is feasible that these small areas could be resurveyed at the same date as future satellite surveys. The use of a standard set of training areas would reduce the potential for error between operators.

CONCLUSIONS FROM THE MAXIMUM LIKELIHOOD CLASSIFICATIONS

The macro scale comparisons generally revealed that the MLC is very accurate in determining the total area of intertidal vegetation in the Wash Estuary (Fig. 6.12). This could perhaps have been expected due to the very different spectral characteristics of vegetation and other surfaces at visible and near infrared wavelengths (chapter 2 and chapter 3). The small discrepancies that do occur in the total saltmarsh areas are nearly always accounted for by different estimations of the Lower marsh and Pioneer zone. This was borne out by the findings of the meso scale comparisons. It is this relatively small, but nevertheless important, saltmarsh community that the MLC has greatest problems in classifying (Fig. 6.12). This fact is discussed further in the final section of the chapter. Due to the fact that the area is relatively small, differences in area estimation of this community have little impact on the total saltmarsh area estimation. In all the classifications much better and concurring area estimates were achieved for the Upper and Middle marsh communities than for the Lower marsh and Pioneer communities.

The micro scale comparisons revealed the objective nature of the classification strategy used. Differences between the MLC classifications of the two independent operators and the 1982/4 N.C.C were only to be expected as the methods of classification were very different and the dates of the Landsat 5 TM images differed from the air photographs used in the 1984 N.C.C. survey. This was again most clearly illustrated by the differences in Pioneer zone classification. Indeed the timing of the 1984 image resulted in no training areas being established for the Pioneer zone (Fig. 6.12). More important was the agreement that occurred between the two independent operators as the methodology used in these cases was exactly the same. The macro and meso scale comparisons illustrated that there were only small differences in total area estimation and different saltmarsh community zone estimations, the exception to this being the estimation for the Lower marsh zone in the 1984 image. Cross tabulation for the micro level comparison revealed good agreement for the Upper marsh zone, generally over 70% and an even better 80% for the Middle marsh zone. In the 1991 MLC classifications good agreement also occurred for the Lower marsh zone. This agreement was not matched by the 1984 MLC classifications, again revealing the importance of the timing

WASH ESTUARY SALTMARSH SURVEYS

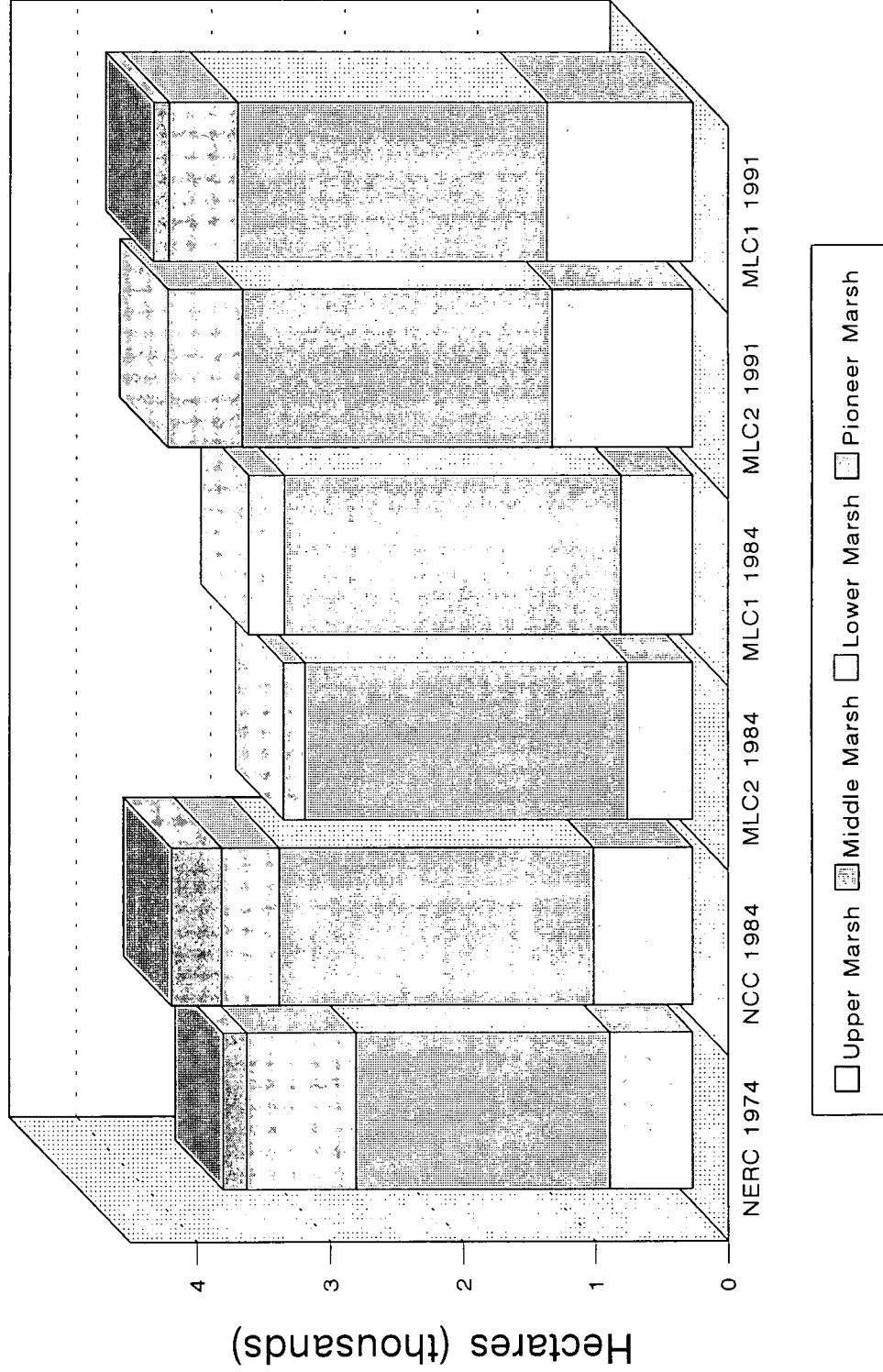


Fig. 6.12 Summary of the Maximum Likelihood Classifications

of the image in order to accurately classify the Lower marsh and Pioneer zones (Fig. 6.12). Considerably better results were achieved with the classification of the September 1991 image than with the May 1984 image. The results of the two independent operators are encouraging as they indicate there is a good degree of objectivity in the standardised methods used and this bodes well for using such classification strategies in an operational mode.

Perhaps the most useful comparison was the 1991 MLC classification with the 1984 classification as this illustrates the great potential for using classified Landsat 5 TM imagery for the monitoring of change in coastal vegetation. The basis of the comparisons were not ideal as the images were taken at different times of the year but still illustrate a continuing trend of expansion for the saltmarshes of the Wash Estuary as a whole (Figs. 6.10, Fig. 6.11, Fig. 6.12) and particularly for those saltmarshes fronting recent reclamations. Fig. 6.11 shows that even the marsh fronting the ambitious reclamations and over-deepened borrow pits on the Freiston Shore is beginning to recover. The MLC was able to clearly identify and quantify such areas, thus providing a potentially valuable tool for coastal managers. It is impossible to give exact figures for saltmarsh expansion as the images were taken at different times of the year and therefore it is very difficult to separate seasonal changes from actual saltmarsh expansion. The seasonal effects are clearly seen by comparing figures 6.7 and 6.8. Ideally comparisons should be made of images taken at similar times of the year if a more realistic estimate of expansion is to be gained. This is another consideration which should be borne in mind if the technique is to become operational.

The most disappointing aspect of the MLC classifications was its inability to accurately classify the Pioneer zone. This is often the area that coastal managers are most interested in as it is a very sensitive and early indicator of saltmarsh expansion and contraction.

PROBLEMS WITH THE MAXIMUM LIKELIHOOD CLASSIFIER

Traditional forms of classification, such as the MLC, have severe limitations. The classification technique is based on the membership concept of classical set theory. This states that a set has a precisely defined boundary and an element is either inside the set or outside it. In remote sensing a pixel often contains a mixture of surface classes. This is especially relevant when trying to establish training areas in a dataset. The problem, known as spectral mixing, is confounded by the large pixel size of Landsat 5 TM data (30 m) compared with the intricate mosaic of the saltmarsh. Any impurities or mixing in the training set data will contribute to the spectral response and will lead to a less accurate classification (Wang, 1990). This problem should be kept in mind when attempting to establish training data and in evaluating the results of the MLC.

The fact that different species of saltmarsh often exist in complex mosaics, especially in the Upper and Middle marsh regions, introduces another serious spectral mixing problem that will lead to a deterioration in the accuracy of a classification. The coarse spatial resolution of Landsat 5 TM data means that a pixel in the image may often contain more than one landcover class. In the Middle and Upper areas of the saltmarsh, with their patchwork of vegetation communities, this is a significant problem. In the Lower and Pioneer areas of the marsh the problem is dominated by the mixture of mud, water and vegetation. Conventional classification techniques assign a single label to each pixel. Clearly in certain areas of the saltmarsh, when using Landsat 5 TM data, such an approach is unsuitable. When each pixel can be associated with only one cover class the classification cannot properly represent the mixture and intermediate conditions which occur in most remotely sensed images. This is illustrated by the failure to accurately classify *Salicornia* in any of the satellite images. *Salicornia* occurs in conjunction with mud flats and as a result the spectral signature of a pixel containing *Salicornia* is often masked by the spectral component from the mud flat. This is especially true in winter and early on in the growing season when the vegetation has not had a chance to develop. This was illustrated in the classifications of the 1984 image where it proved impossible to accurately classify the Pioneer zone using the MLC. In such cases accurate classification can only be achieved if each Landsat TM pixel is assigned several classes, along with the proportion assigned to each class present in each pixel. Such

a method can be achieved through the construction of a mixture model (Quarmby *et al.*, 1992; Wang, 1990). This method is looked at in more depth in the chapter 7.

To improve the accuracy of the MLC it is possible to interactively weight each class (Strahler, 1980). This was not done in the present study but is a consideration which should be taken into account in subsequent studies if a more realistic picture of the saltmarsh is to be modelled. It is often appropriate to use such a technique when the training set does not adequately represent the proportion of the classes in the total scene. For example in the training sets *Agropyron* is probably over-represented at the expense of the Upper Marsh grass class. The Upper Marsh grass class could be weighted in the classification to redress this bias. This is similarly illustrated by the over-representation of the Lower marsh class at the expense of the Pioneer zone class. The application of a weighting factor would illustrate more clearly the mosaic nature of the saltmarsh.

The use of multi-temporal images may assist in separating the finer, spectrally similar classes within the broad saltmarsh zones. Many saltmarsh species are characterised by seasonal growth (chapter 3), (Hobbs and Shennan, 1986). This helps to explain why it proved so difficult to identify areas of *Salicornia* and *Spartina* in the May 1984 image as at this time of year a seasonal species such as *Salicornia* would be very difficult to identify. The spectral signature early on in the season is dominated by mud and as a result it is almost impossible to distinguish between the Pioneer zone and the intertidal mudflats. Further on in the season *Salicornia* is almost indistinguishable from the Middle marsh classes. By subtracting a classification taken early on in the season from one taken later on the extent of the Pioneer zone may be more accurately approximated. This has been borne out by ground based fieldwork (Hobbs and Shennan, 1986). The differences in seasonal growth of different saltmarsh species would suggest that the use of multi-temporal images as an input into a classification may well lead to greater discrimination between classes.

The results of the classifications carried out by the two independent operators are encouraging with a view to incorporating satellite surveys into operational coastal management programmes as consistency between operators would be absolutely essential in an operational mode. Once a good set of training areas have been established they can be

subsequently used in future classification and monitoring surveys. For each subsequent survey all that would be required would be to resurvey the training areas. For the small training areas it becomes more practical and economically feasible to carry out the ground survey at the same time as the area is being remotely sensed. If areas of expansion are to be accurately mapped, comparison of images taken at similar times of the growing season should be compared. It has also been noted that there are several techniques which could be built into the classification strategy to improve the overall accuracy. Multi-temporal imagery and class weighting probably have the greatest potential. These improvements do not overcome the problems of spectral mixing and results in the need for evaluating the possibilities of using a mixture model for surveying intertidal vegetation.

Curran, P.J. 1985: **Principles of Remote Sensing**. Longman: New York

Donoghue, D.N.M., and Zong, Y. 1992: **Coastal Sediment Mapping in the Tees Estuary**. Department of Geography, University of Durham. Unpublished document.

Hill, M.I. 1988: **Saltmarsh Vegetation of the Wash. An Assessment of Change From 1971 to 1985**. N.C.C. Publications, Peterborough.

Hobbs, A.J. and Shennan, I. 1986: Remote sensing of saltmarsh reclamation in the Wash, England. **Journal of Coastal Research**. vol. 2: 181-198.

James, M. 1985: **Classification Algorithms**. Collins, London.

Janssen L.L.F. and Middlekoop 1992: Knowledge based crop classification of a Landsat TM image. **International Journal of Remote Sensing**. vol. 13: 2827-2837.

Lenninton, R.K. and Sorensen, C.T. 1984: A mixture model approach for estimating crop areas from Landsat data. **Remote Sensing of Environment**. vol. 14: 197-206.

National Environment Research Council, 1976: **The Wash Water Storage Scheme Feasibility Study**. A Report on the Ecological Studies. N.E.R.C. Publications Series C, no. 15.

Quarmby, N.A., Townshend, J.R.G., Settle, J.J. and White, K.H. 1992: Linear mixture modelling applied to A.V.H.R.R. data for crop area estimation. **International Journal of Remote Sensing**. vol. 13: 415-425.

Sabins, F. 1987: **Remote Sensing Principles and Interpretation**. 2nd Edition, W.H. Freeman and Company, New York.

Strahler, A.H. 1980: The use of prior probabilities in maximum likelihood classification of remotely sensed data. **Remote Sensing of Environment**. vol. 10: 135-163

Wang, F. 1990: Improving remote sensing image analysis through fuzzy information representation. **Photogrammetric Engineering and Remote Sensing**, vol. 56: 1163-1168.

CHAPTER 7

MIXTURE MODELLING

The results of the maximum likelihood classifier in the preceding chapter highlighted the problem of spectral mixing. The radiance recorded by a satellite sensor integrates the radiation from the field of view of the sensor (Shimabukuro and Smith, 1991; Holben and Shimabukuro, 1993). In the case of saltmarshes, with the relatively coarse spatial resolution of Landsat 5 TM data (30 m) compared with the mosaic nature of the surface, it is almost inconceivable that only one kind of surface material will be contained in a single pixel (Figs. 5.3 and 5.4). It is far more likely that an individual pixel will contain a mixture of surface classes including several vegetation species, detrital material, mud, water and shadow. All of these substances have a spectrally distinct signal but these individual signals will be integrated to give a single reflectance signal for the Landsat 5 TM pixel. It is more realistic to talk of "mixels" rather than pixels. The reflectance of any pixel is the result of the mixing of the spectral signatures from several different surface covers. Mixture modelling is potentially a much more accurate and powerful analysis technique than conventional multivariate classification strategies such as the maximum likelihood classifier. The approach aims to decompose sub-pixel spectral mixtures. Unmixing analysis has been used in the analysis of data gathered by multispectral broad band sensors for a variety of applications which include mineral mapping (Millington *et al.*, 1989; Adams *et al.*, 1986) and vegetational surveys (Quarmby *et al.*, 1992; Cross *et al.*, 1991; Lenninton *et al.*, 1984). The principal disadvantages of the technique are that it is computationally intensive, both in terms of time taken for the model to run and also in terms of the large volumes of data in the output compared with other more traditional classifications such as the MLC. Similarly, as a result of the large volume of data, the output is difficult to represent in an understandable hard copy format. Its application is restricted by the number of spectral bands in the data and the identification of endmembers.

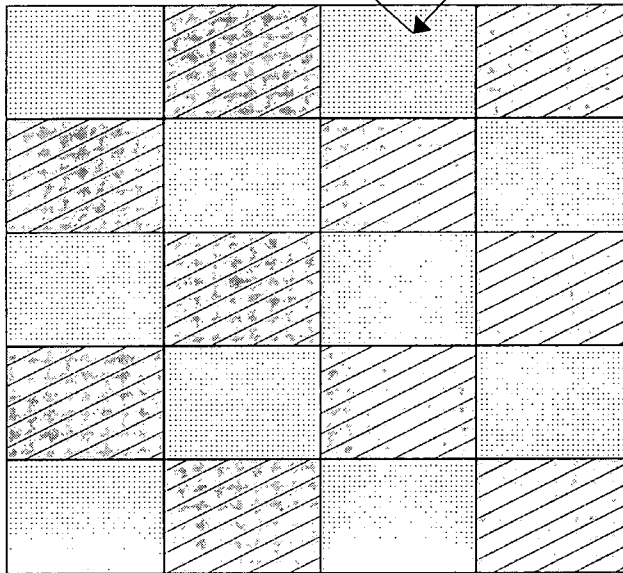
The problem of mixels in remote sensing has been recognised since the 1970s (Horwitz *et al.*, 1971; Detchmendy and Pace, 1972). The use of traditional multivariate

classification techniques, such as the maximum likelihood classification used in the preceding chapter, produce poor results where the remotely sensed data has a coarse spatial resolution compared with the surface features being imaged. This was most clearly seen in the maximum likelihood classifier's failure to adequately classify the Pioneer zone. Each pixel in the Pioneer zone contains a mixture of vegetation (predominantly *Salicornia*) mud and water. The maximum likelihood classification cannot cope with such mixtures and tries to force the pixel into a single class such as vegetation, mud or water. The aim of mixture modelling is to decompose each "mixel" into its respective components or endmembers. Endmembers are defined in the present study as "the response that would be received in the absence of noise by a pixel containing nothing but the component of interest" (Settle and Drake, 1993) and correspond with different surface types. The model produces a set of images describing the proportional cover of each endmember within an individual pixel. A grey scale is most often used to represent the proportions within a pixel.

Spectral mixing of different surface components can be linear or non-linear. Linear mixing occurs if electromagnetic radiation interacts with only one surface cover type during its journey from the sun to the sensor. A number of factors may determine whether mixing occurs in a linear or non-linear manner. The way in which surface components are distributed within a single pixel is important. If surface components are distributed in large discrete areas, each smaller than the spatial resolution of the sensor, then spectral mixing will tend to be linear. This is explained by the fact that electromagnetic radiation may only interact with more than one surface component at the boundaries of each discrete area. This is referred to as "checkerboard mixing" (Singer and McCord, 1979) (Fig. 7.1). If different surface components are mixed intimately together within a pixel then mixing will be non-linear. The close proximity of particles of different composition enables incoming electromagnetic radiation to interact with more than one surface component resulting in non-linear mixing (Fig. 7.1).

Spectral Mixing

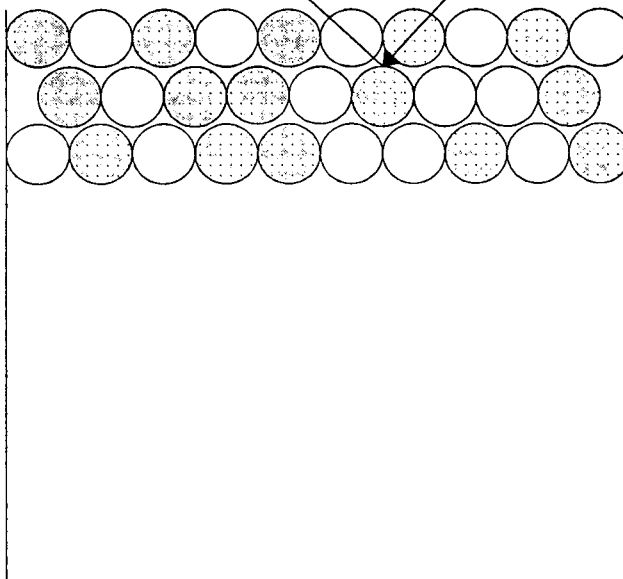
Path of reflected photon Path of incoming photon



Landsat5 TM Pixel

1. Linear mixing or "checkerboard" mixing. An individual photon generally interacts with only one surface component within the pixel.

Path of reflected photon Path of incoming photon



Landsat 5 TM Pixel

2. Non-linear mixing or intimate mixing. In this case an individual photon interacts with more than one surface component within the pixel.

Fig. 7.1 Linear and Non-Linear Mixing

The type of mixing between vegetation and mineral components varies depending on the type and condition of the vegetation. Plants in arid environments have been demonstrated to mix linearly with mineral components (Adams and Adams, 1984). Adams suggested that the thick waxy cuticles typical of desert vegetation prevented light passing through the leaf and interacting with other surface covers. However, Roberts (1991) suggested that mixing between green vegetation and soils may be non-linear. The non-linear mixing resulting from the transmission and scattering of near infrared light by green vegetation. This would have a significant effect on the present study as the mixture model used assumes linear mixing. Non-linear mixture modelling cannot be performed using simple linear combinations of endmember spectra (Hapke, 1981). Mixture modelling is a much simpler problem where surface materials are considered to mix linearly. Each spectrum in the image is regarded as a simple linear combination of the specific endmembers selected.

The selection and identification of the number of endmembers in an image is the key to success of a linear mixture model. In order to solve mixing equations the operator must establish the number of surface components or endmembers that are involved. Two different approaches have generally been used to define endmembers in a mixture model: the use of a library of mineral reflectance spectra (Adams *et al.*, 1986); the use of training spectra extracted from the image data itself. As no library spectra exist for vegetation (the complexity of such a task is referred to in chapters two and three) the second approach was adopted in this study. The use of image endmembers has the advantage of bypassing a number of complex atmospheric and radiometric correction techniques that must be carried out in order to allow the direct comparison of laboratory spectra with satellite sensor data (Settle and Drake, 1993).

If image endmembers are employed then the number of endmembers and their location in the image must be identified if the mixing equations are to be solved. A common approach to this problem is to reduce the dataset to its intrinsic dimensionality by the application of a Principal Component Analysis (PCA) (Smith *et al.*, 1985). The number of endmembers is taken to be one more than the number of dimensions required to explain the variance of the data (Gillespie *et al.*, 1990; Settle and Drake, 1993). Examination of the feature space of those components which contain information reveals the location of the

purest pixels in the image representing each endmember. The use of image endmember spectra may cause irregularities in the derived proportion maps if the endmembers themselves are mixtures of two or more components. In this case the proportion estimates will be relative proportion estimates. This is likely to be the case in the present study as there may be no pure endmembers within the Landsat 5 TM scenes. For example a saltmarsh vegetation canopy endmember is likely to include not only a vegetation spectral signature but also that of shadow and detrital material.

LINEAR MIXTURE MODELLING

The feature space of two hypothetical PCs are represented in Fig 7.2. Points E1 and E2 are the locations of two spectrally distinct endmembers. In the absence of noise, any pixel composed of a mixture of the two endmembers would lie directly on a line between the two points (Settle and Drake, 1993). With linear mixing a pixel whose spectral signature is composed of 50% endmember E1 and 50% of E2 should lie halfway between the two endmembers. Atmospheric and radiometric effects introduce a noise component into the data so the observed pixel values form a scatter cloud around the mixing line. Mixing planes may clearly be identified in the Wash Estuary data by looking at the scatterplots in Fig. 7.6 and 7.20. The "water" and "intertidal" mixing planes form lines very similar to those illustrated in Fig. 7.2.

Every pixel scattered around the mixing plane in Euclidean space is assigned a proportion estimate of endmember components by the linear mixture model algorithm. This is achieved by minimizing the scatter. This would imply that a pixel a1 (Fig. 7.2) would be assigned a proportion estimate according to its location on the mixing line. This is normally performed using a least squares fit of the scattered data points to the mixing line. In a fully constrained mixture model the scatter of points around the mixing line is confined by the area bounded by endmembers E1 and E2. In an unconstrained mixture model the scatter area may extend beyond the endmembers and results in pixels, such as a2 (Fig. 7.2), being assigned an estimate which is greater than 100% (Shimabukuro and Smith, 1991). Estimates of proportions greater than 100% indicate a poor choice of image endmembers. The mixture model used in the present study is a fully constrained model.

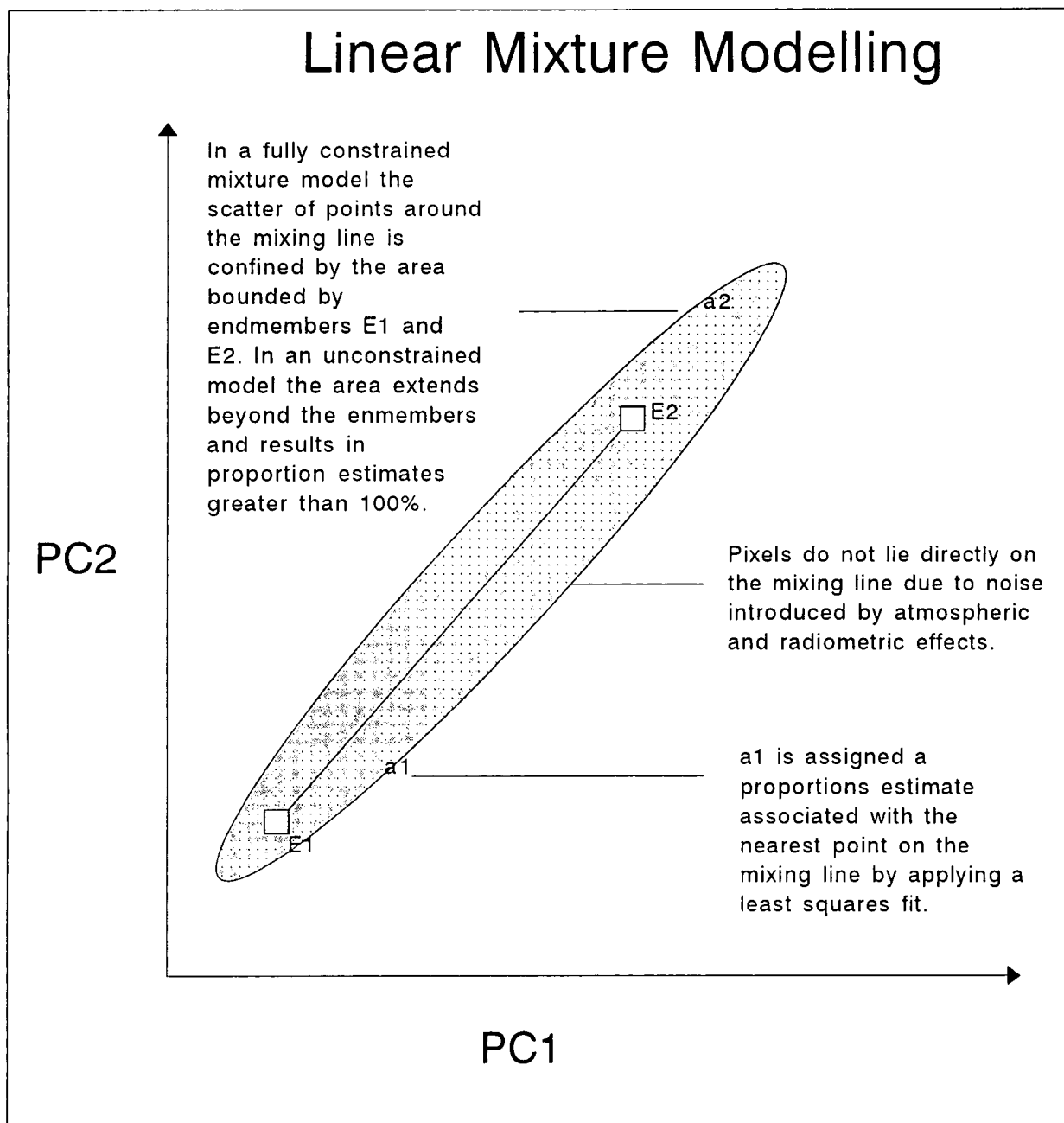


Fig. 7.2 Euclidean space of Principal Components 1 and 2 illustrating the scatter of pixels around a single mixing plane (E1-E2). This is comparable to the water and tidal flat mixing lines in Fig 7.6.

In the present study a linear relation is assumed to represent the spectral mixture of surface components within an individual pixel. The spectral response of each pixel in any band is considered to be a linear combination of the spectral responses of the endmembers which are assumed to be in the mixture. This implies each pixel, which can take any value within the grey scale, contains information about the proportion and spectral response of each surface component within the ground resolution cell (Shimabukuro and Smith, 1991). It is possible to model each pixel spectrum of the Landsat 5 TM images as a linear combination of a finite set of components (equation from Shimabukuro and Smith, 1991):

$$r_i = \sum_{j=1}^n (a_{ij}x_j) + e_i$$

- r_i mean spectral reflectance for the i th TM band of a pixel containing one more spectral components.
- a_{ij} spectral reflectance of the j th component in the pixel for the i th TM band.
- x_j proportion value of the j th component in the pixel.
- e_i error term for the i th TM band.
- n number of endmembers in the model.
- j 1,2,..n (endmembers assumed for the model).
- i 1,2,3,4,5,7 (TM sensor bands)

In the fully constrained mixture model used in the present study a linear constraint is added so that the sum of the proportions for any pixel must add to unity. As long as the number of components (n) is less than the number of TM bands the system of linear equations is over determined and may be solved through the adoption of a number of mathematical techniques. The method used by the mixture model in the present study solves the equations by means of the least squares approach (Shimabukuro and Smith, 1991). This method estimates the proportion of each component in a pixel by minimising the sum of the squares of the errors. The fully constrained mixture model means that the proportion values must be non-negative and they must also add to unity.

APPLICATION OF THE MIXTURE MODEL TO LANDSAT 5 TM DATA OF THE WASH ESTUARY

ENDMEMBER SELECTION

In order to apply a mixture model to a data set it is essential to identify and locate the number of endmembers in an image. This allows the solving of the linear mixing equations. If library spectra are not available the most common method of doing this is through the application of principal component analysis (PCA) in order to reduce the data to its intrinsic dimensionality (Smith *et al.*, 1985). The application of PCA to the entire Wash Estuary and the surrounding area provided no useful information concerning the number and location of intertidal endmembers. The dataset is "swamped" by the mass of pixels corresponding to the surrounding agricultural land and deep water pixels from the North Sea (Fig. 7.3). Small extract images were therefore produced that only contained intertidal vegetation, intertidal mud and sand flats and water in an attempt to give the PCA a more limited range in which to locate intertidal endmembers (Fig. 7.5-7.8).

The number of endmembers in an image is taken to be one more than the number of dimensions required to explain the variance of the data. Fig 7.4 indicates that nearly all of the data in the 1991 Landsat 5 TM extract is explained in the first four dimensions. This would indicate that there are five endmembers present in this section of the intertidal zone. This is very fortunate as the solving of equations in a mixture model demands that there is one more spectral band than there are endmembers so that the equation set becomes overdefined and can therefore be solved. In the present study six Landsat 5 TM bands (1,2,3,4,5,7) were used.

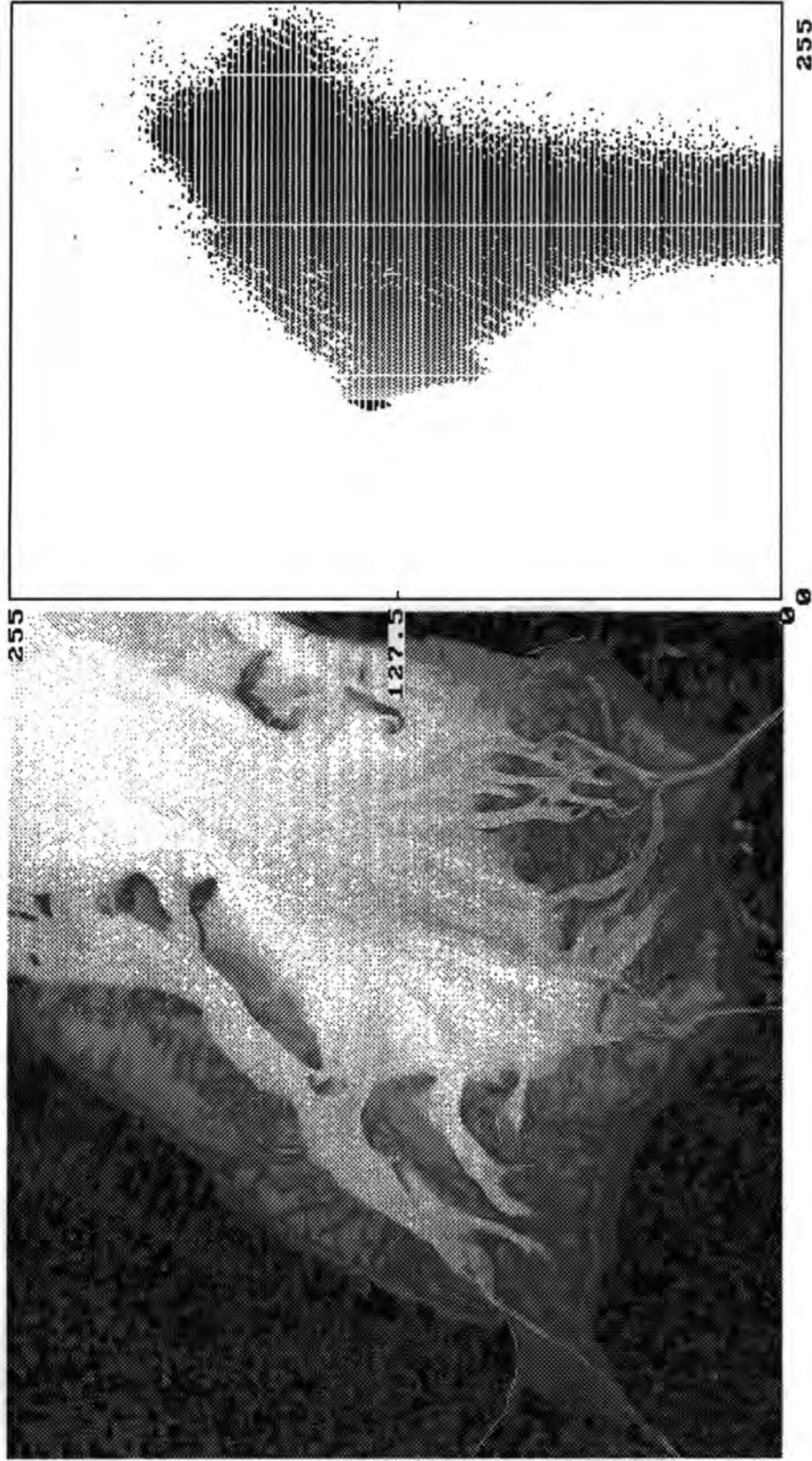


Fig 7.3 Scatter plot of the entire Wash Estuary (PC1 against PC2). Data concerning the intertidal endmembers is swamped.

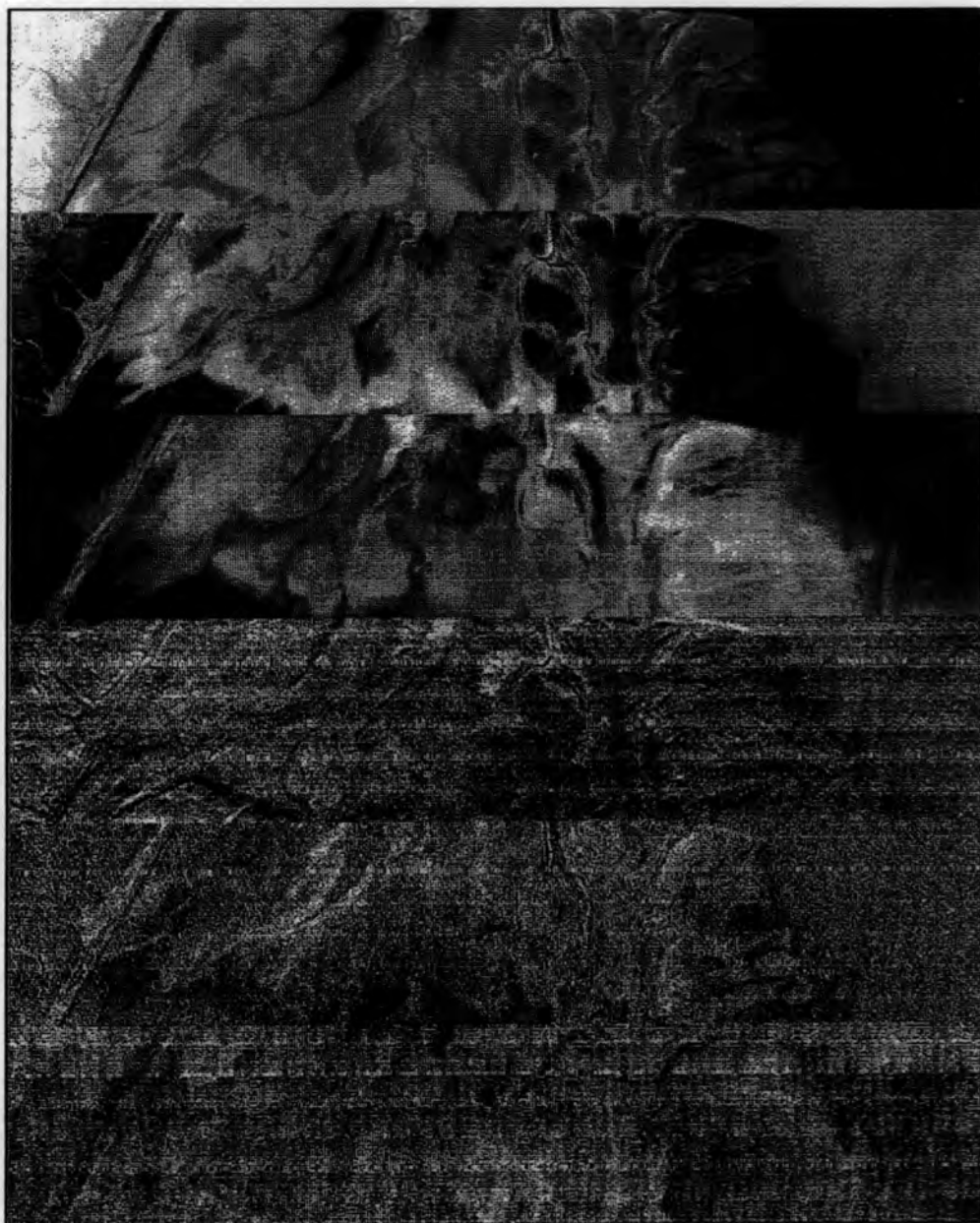


Fig. 7.4 Principal Component Analysis of a small extract of the intertidal zone of the Wash Estuary (Landsat5 TM 7/9/91). Six components are illustrated starting with PC1 at the top and PC6 at the bottom.



Fig. 7.5 Friedman and Turkey Projection Pursuit Algorithm

In order to ensure that Principal Component Analysis provided the best method of reducing the data to its intrinsic dimensionality Friedman and Turkey's projection pursuit algorithm (Friedman and Turkey, 1974) was applied to the extracted data to find the optimal planar projection. Fig 7.5 shows that the best method of reducing the intrinsic dimensionality of the data is indeed the application of PCA.

A major concern about applying standard linear mixture models to the intertidal zone has been the fact that mixing may be non-linear. If this were so it would be inappropriate to use a least squares model as this would involve modelling non-linear relations with a linear model. In order to identify the type of mixing present in the intertidal zone the principal component data was imported into T-Spectra. A scatterplot was generated of PC1 against PC2 for Extract 1 (Fig 7.6). Spectra were then identified systematically on the mixing lines using the T-Spectra ENQUIRE function (Figs. 7.7a, 7.8a, 7.9a). This gave the line and sample location of the pixel in the original image. These pixels were then located in the Landsat 5 TM image and their spectra plotted (Figs. 7.7b, 7.8b, 7.9b).

The graphs are highly encouraging as they indicate that the predominant form of mixing in the intertidal zone is linear. Endmembers were identified by locating pixels from the extremes of the mixing planes (Fig. 7.10). This was also done for PC1 against PC3 (Figs. 7.11a, 7.11b) and PC2 against PC3 (Figs. 7.12a, 7.12b) and the results compared. The endmembers proved to be very similar with a water (blue), saltmarsh (green), Pioneer zone (red) and two intertidal endmembers (purple and yellow) identified in all of the plots (Figs. 7.11b, 7.12b).

The same analysis was carried out on the 1984 Landsat 5 TM image. In this case no Pioneer zone endmember could be located (Fig. 7.13). This can be attributed to the effects of phenology. The image was taken early in the growing season when the vegetation in the Pioneer zone had not developed sufficiently to add a significant spectral signature to pixels covering this area.

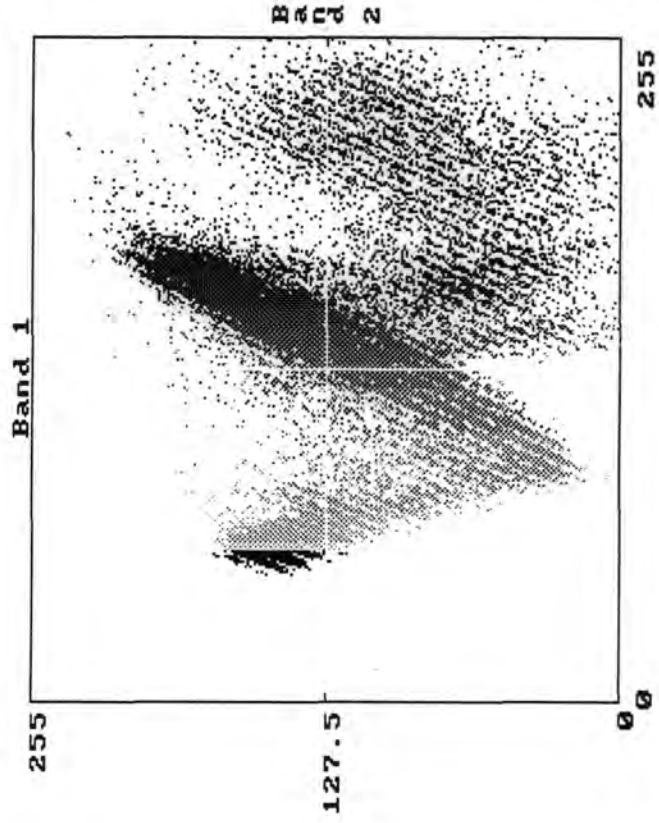
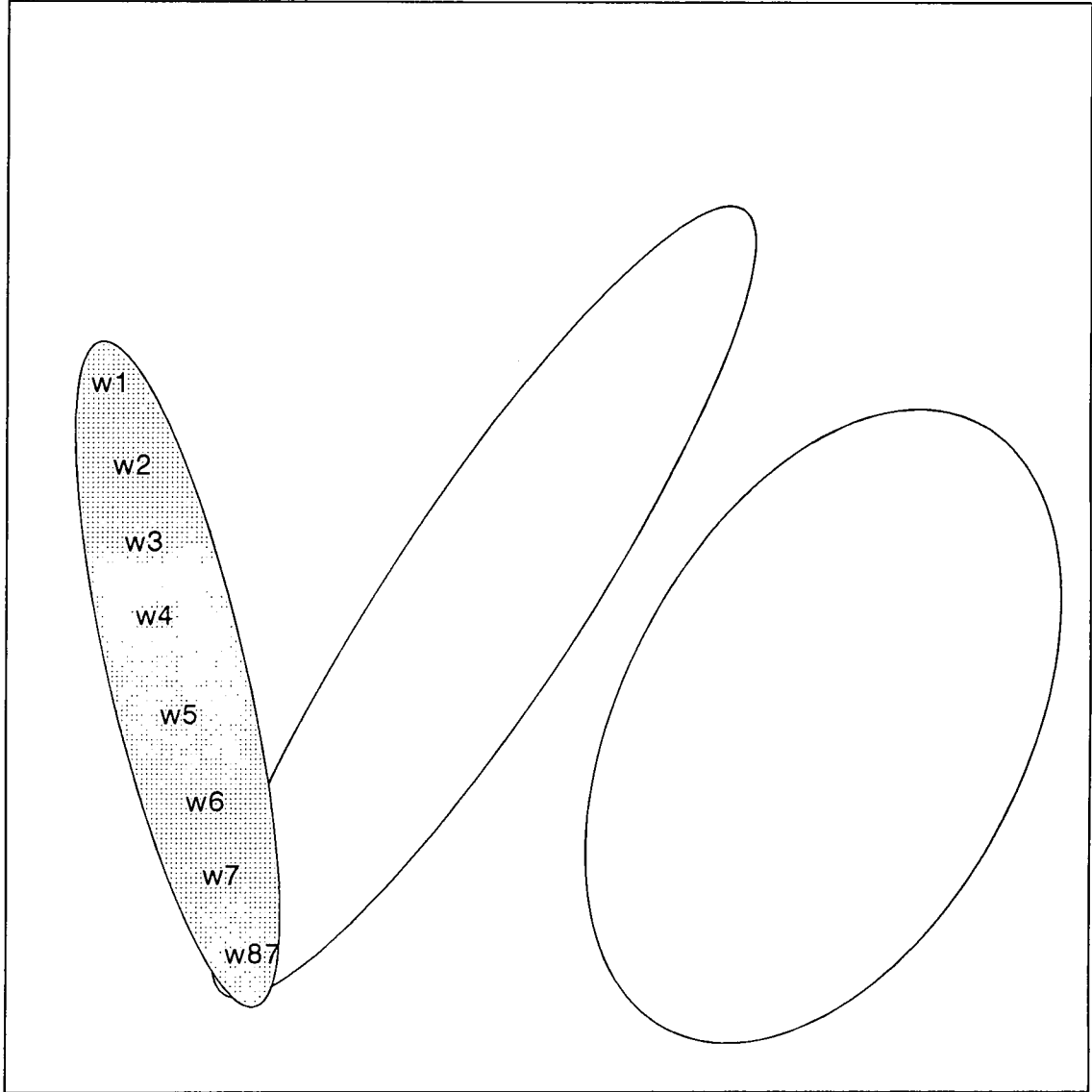


Fig 7.6 Principal Component Analysis of Extract 1. Scatterplot of PC1 against PC2.

PC 2

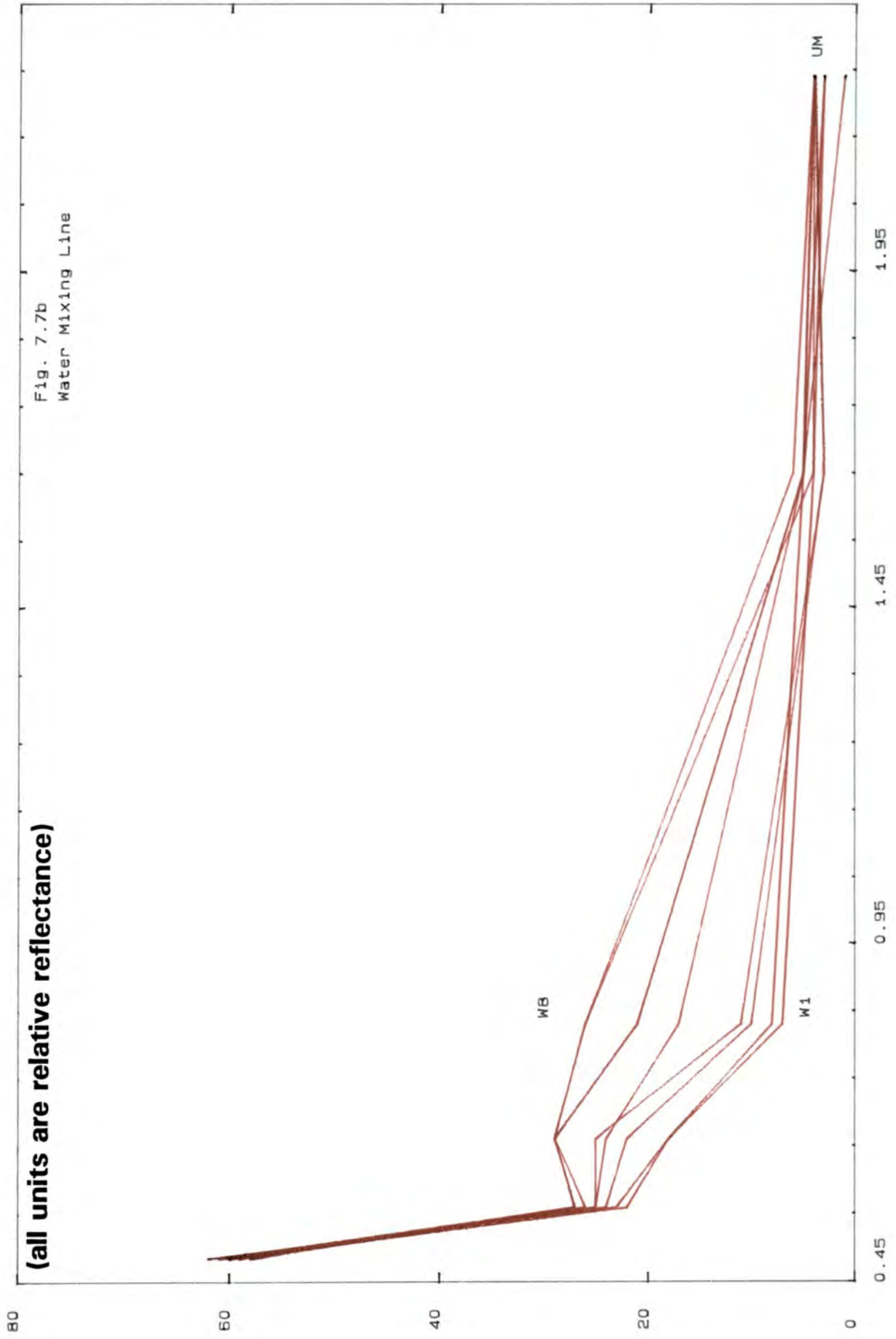


PC 1

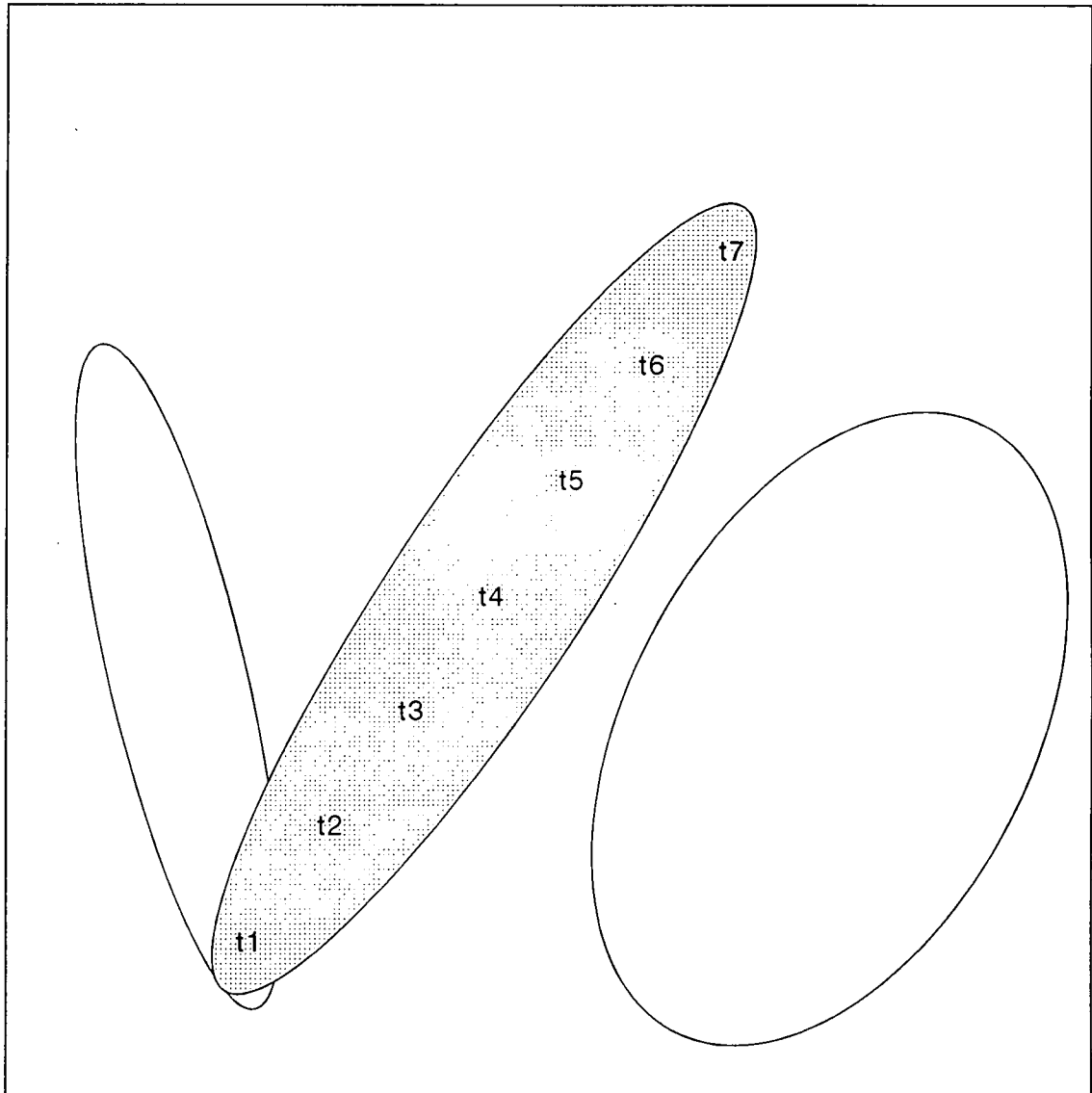
Fig 7.7a Location in feature space of the spectra taken from the water/sediment mixing line. The spectra are illustrated overleaf

(all units are relative reflectance)

Fig. 7.7b
Water Mixing Line



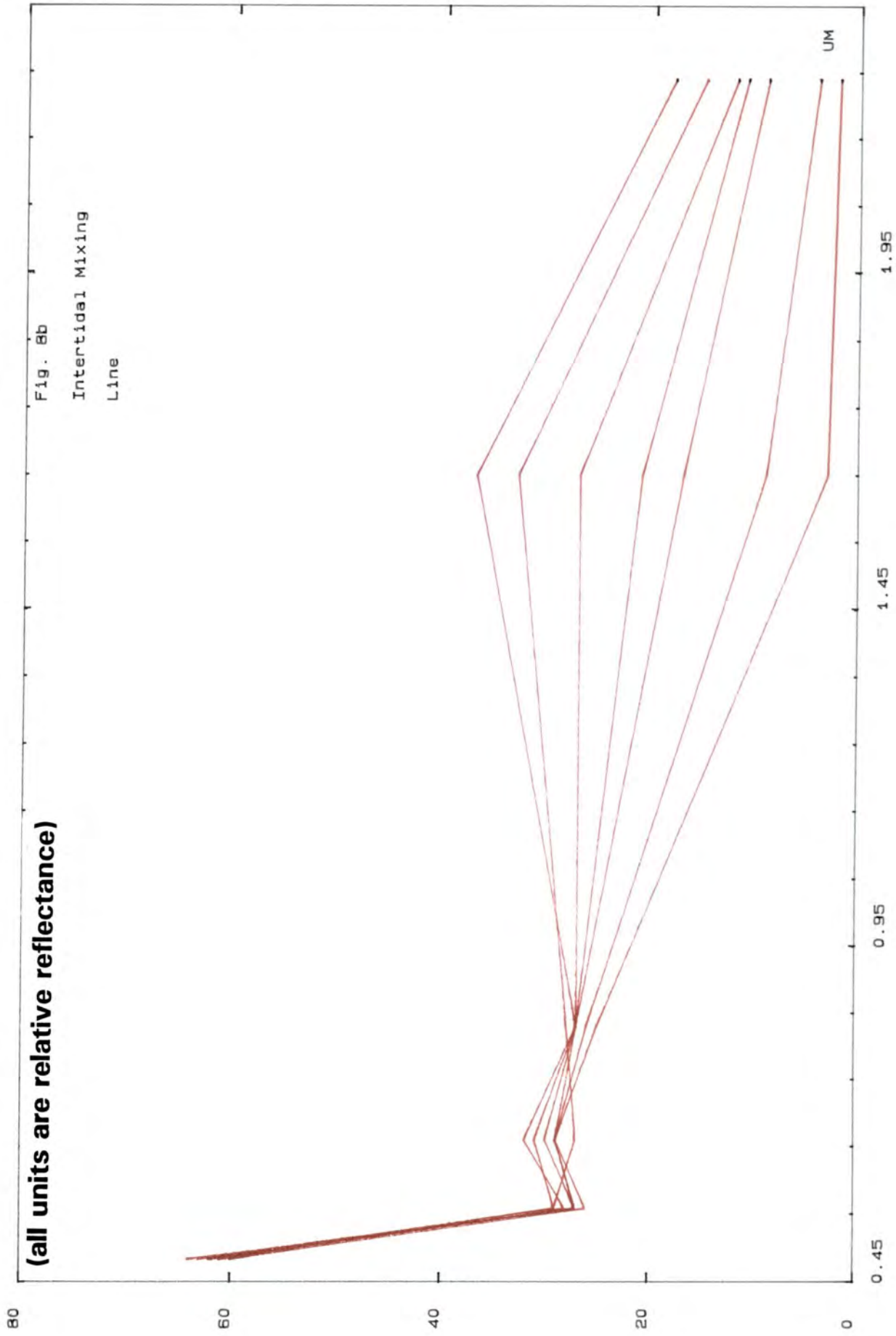
PC 2



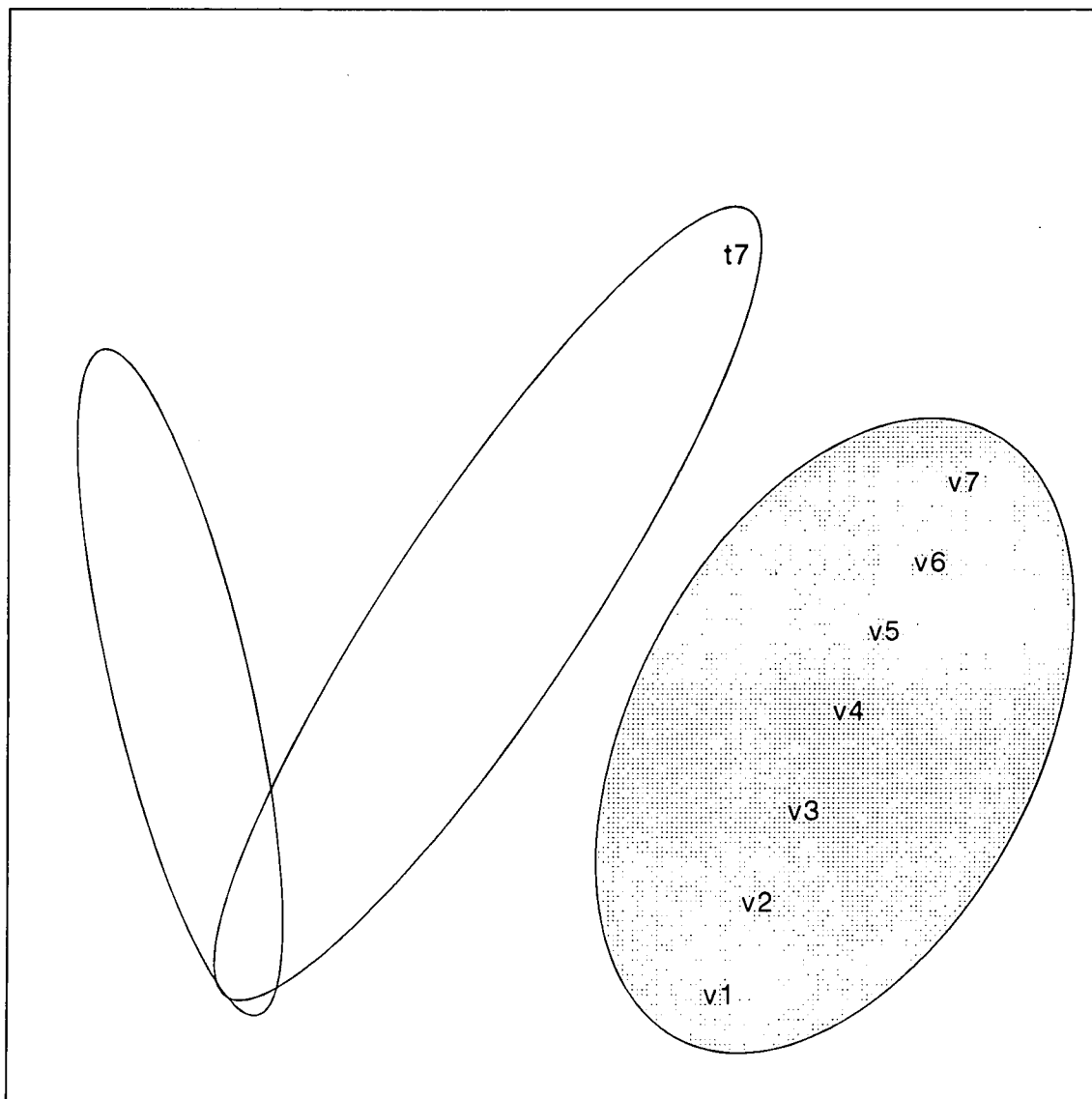
PC 1

Fig 7.8a Location in feature space of the spectra taken from the intertidal mixing line. The spectra are illustrated overleaf.

(all units are relative reflectance)



PC 2



PC 1

Fig 7.9a Location in feature space of the spectra taken from the vegetation mixing line. The spectra are illustrated overleaf.

(all units are relative reflectance)

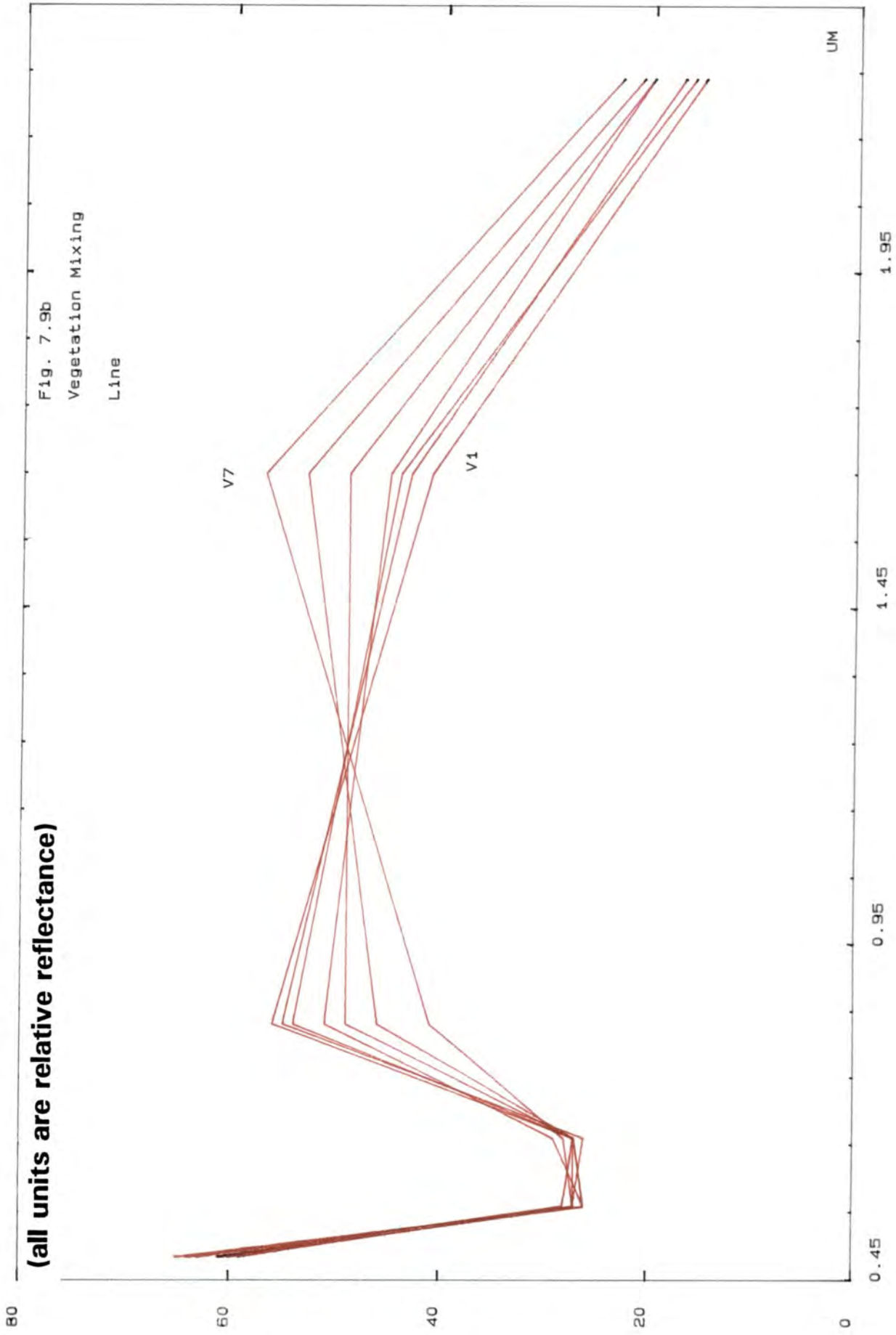
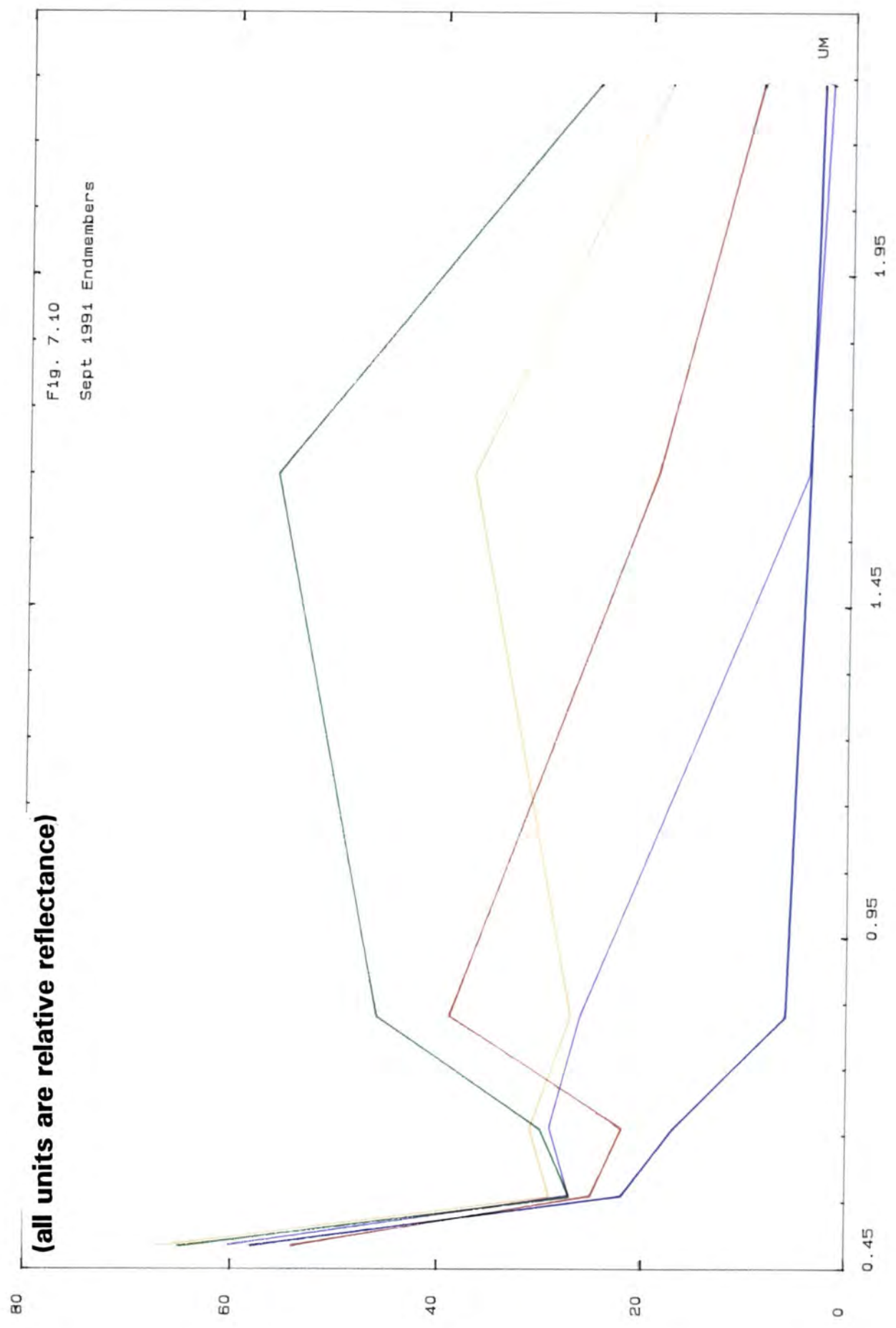


Fig. 7.9b
Vegetation Mixing
Line

(all units are relative reflectance)

Fig. 7.10
Sept 1991 Endmembers



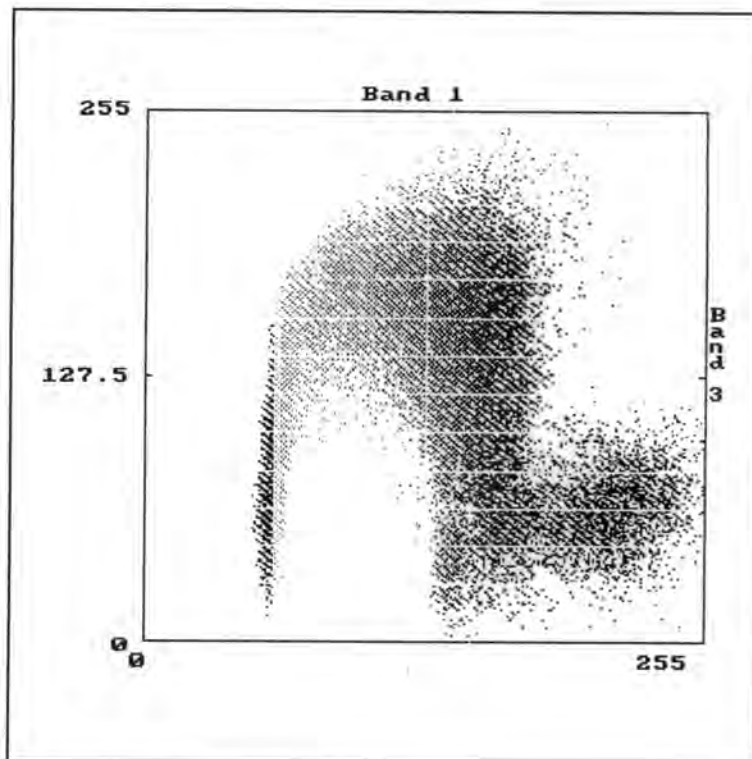


Fig 7.11a Extract 1, PC1 against PC3.

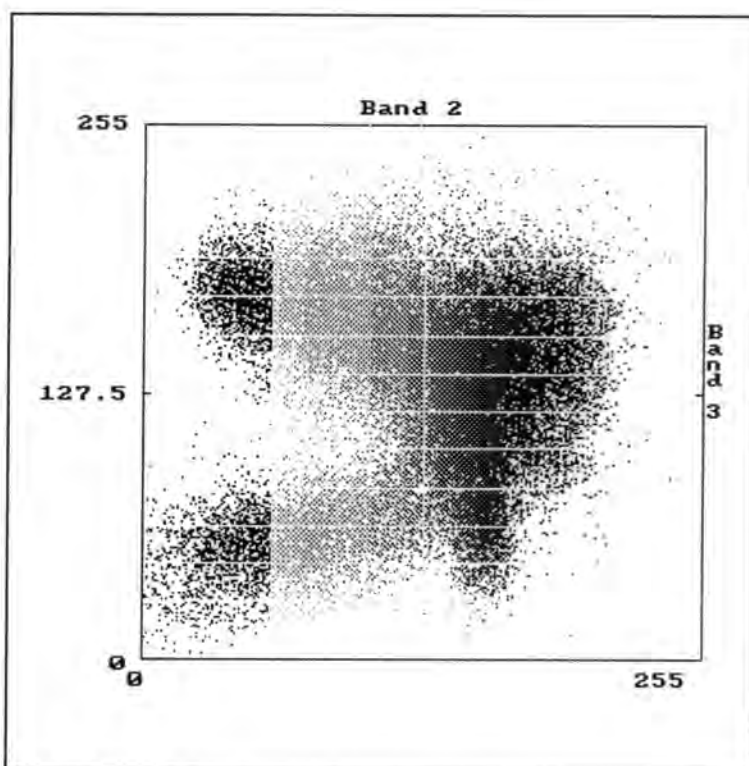
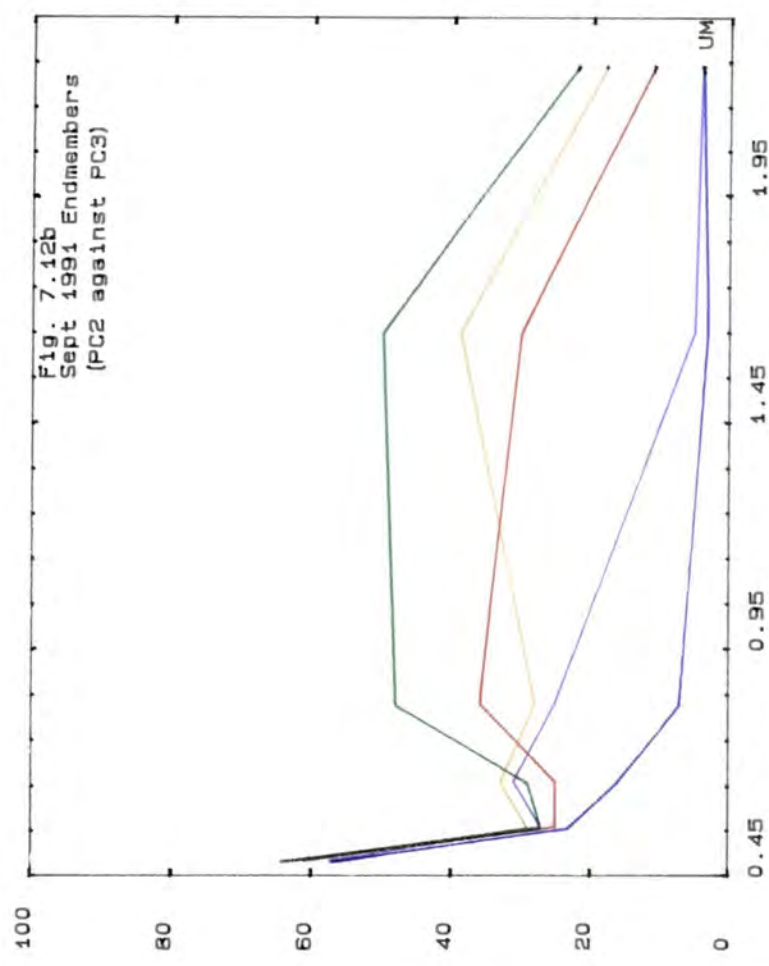
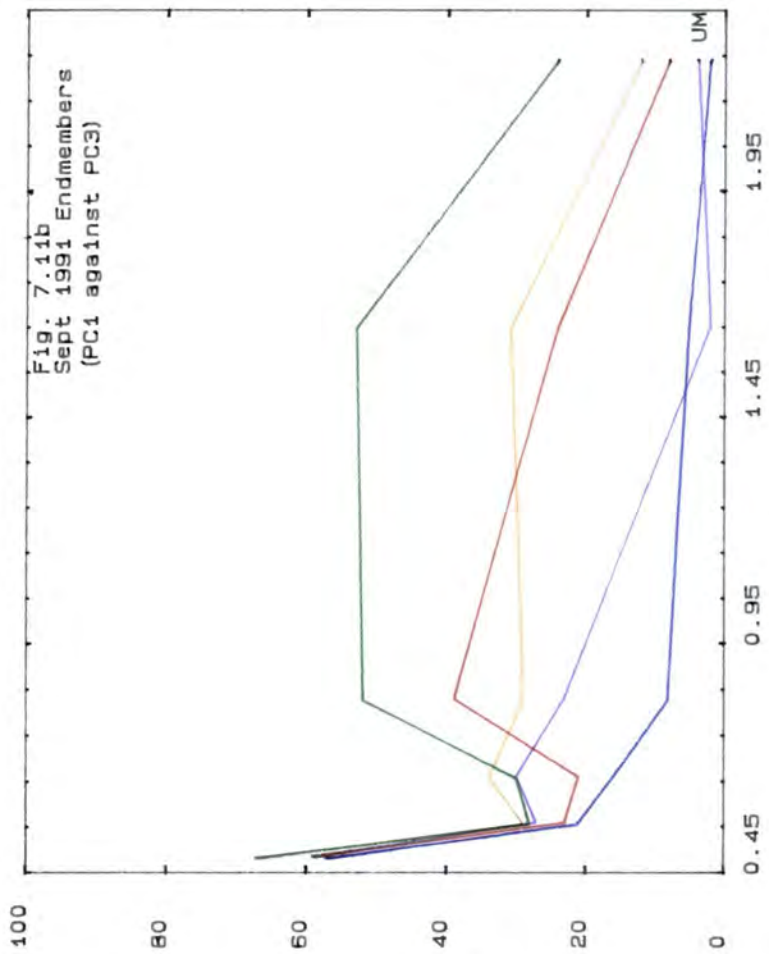


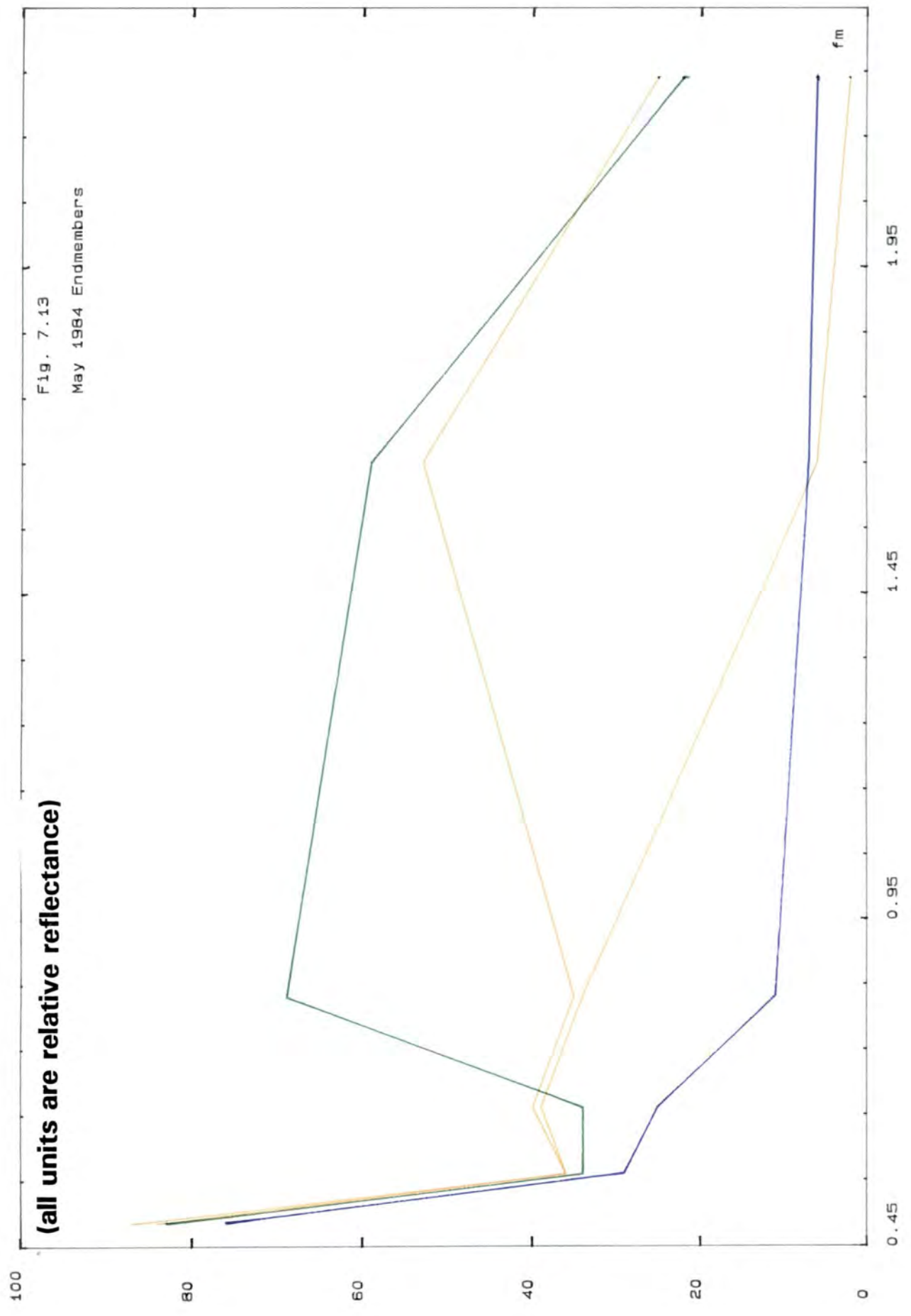
Fig 7.12a Extract 1, PC2 against PC3.



(all units are relative reflectance)

(all units are relative reflectance)

Fig. 7.13
May 1984 Endmembers



To ensure that the endmembers identified in the extracted image of the Wash Estuary held true for other areas of the Estuary an additional two extracts were taken (Figs. 7.14, 7.15) and the respective scatterplots and endmembers compared (Figs. 7.16, 7.17, 7.18, 7.19). The figures are very encouraging as the shape of the scatterplots are all very similar to each other. Fig. 7.20 summarises the mixing planes of the intertidal zone.

The Mixtool model (developed by Alan Mazer of J.P.L.) demands that all end member spectra be in Spectral Analysis Manager format (SPAM). SPAM data is in 512 continuous bands ranging from 0.456-2.5 μm . This presents a considerable problem for Landsat 5 TM data which only contains six bands ranging from 0.45-2.35 μm . A further problem is that the TM bands are discrete. A C-program written by Dr D. Donoghue (Department of Geography, University of Durham) rescaled the Landsat 5 TM spectra into a SPAM format which could be read by the mixture model. Figures 7.21-7.24 illustrates the spectral endmembers in a TM format and in the rescaled SPAM format. The mixture model is so computationally intensive that even on a Sun Workstation only small data sets could be used. As a result the 1984 and 1991 Landsat 5 TM images of the Wash Estuary were split up into manageable sizes using the Terra-Mar BIGRIBS program (Terra-Mar 4.0). The Mixtool model was then applied to the data sets. The resulting proportion maps were rejoined using the Terra-Mar MOSAIC program to produce mixture model proportion maps for the whole of the Wash estuary. In order to remove all areas other than the intertidal vegetation and sand and mudflats a mask was applied to the data (chapter 5). Finally the data was scaled between 0 and 100 so the mixtures could be read as percentages. The resulting scaled proportion maps are illustrated in Figs. 7.25-7.29.

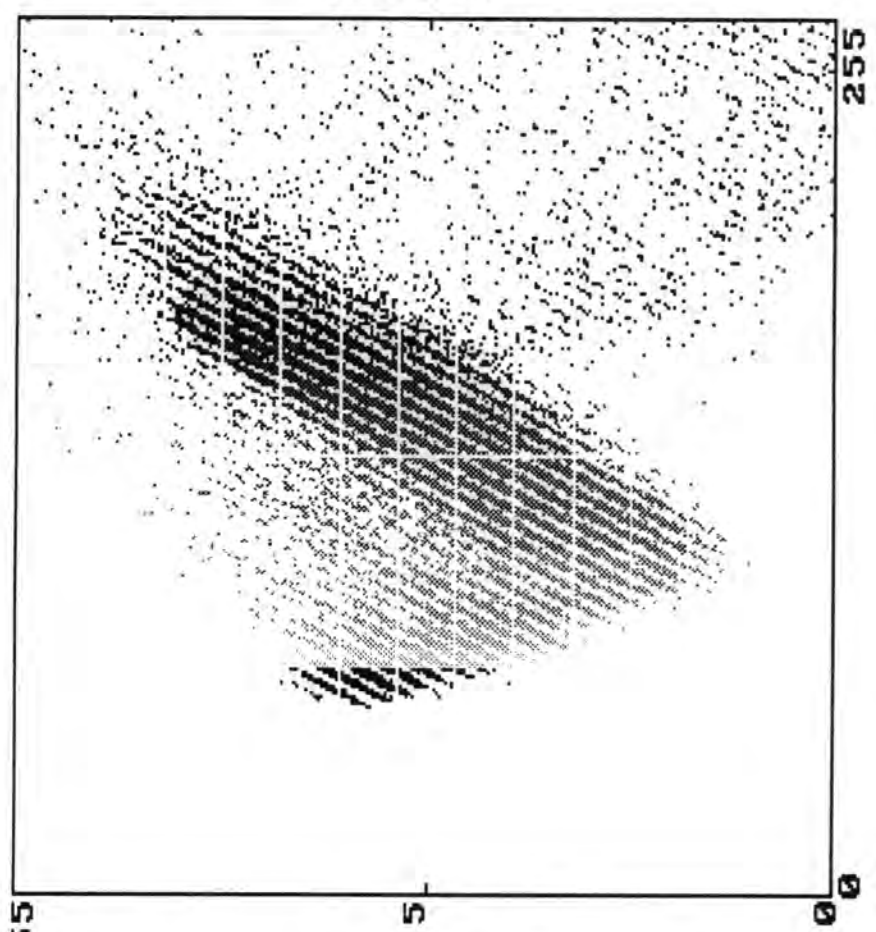
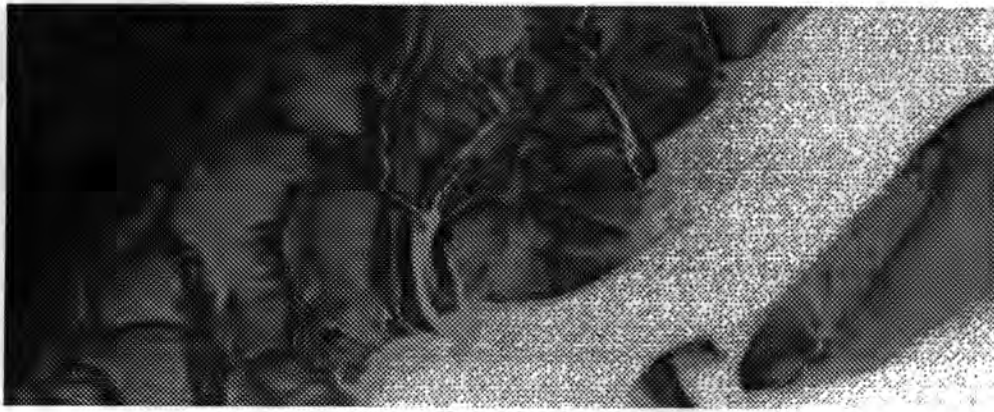


Fig 7.14 Principal Component Analysis of Extract 2.



Band 1

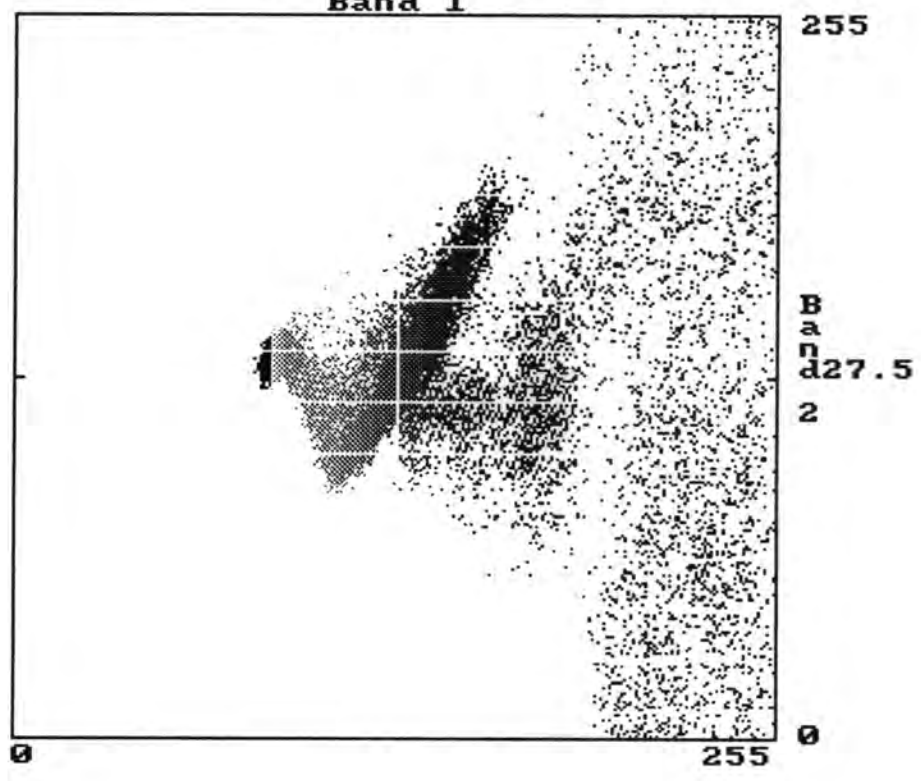
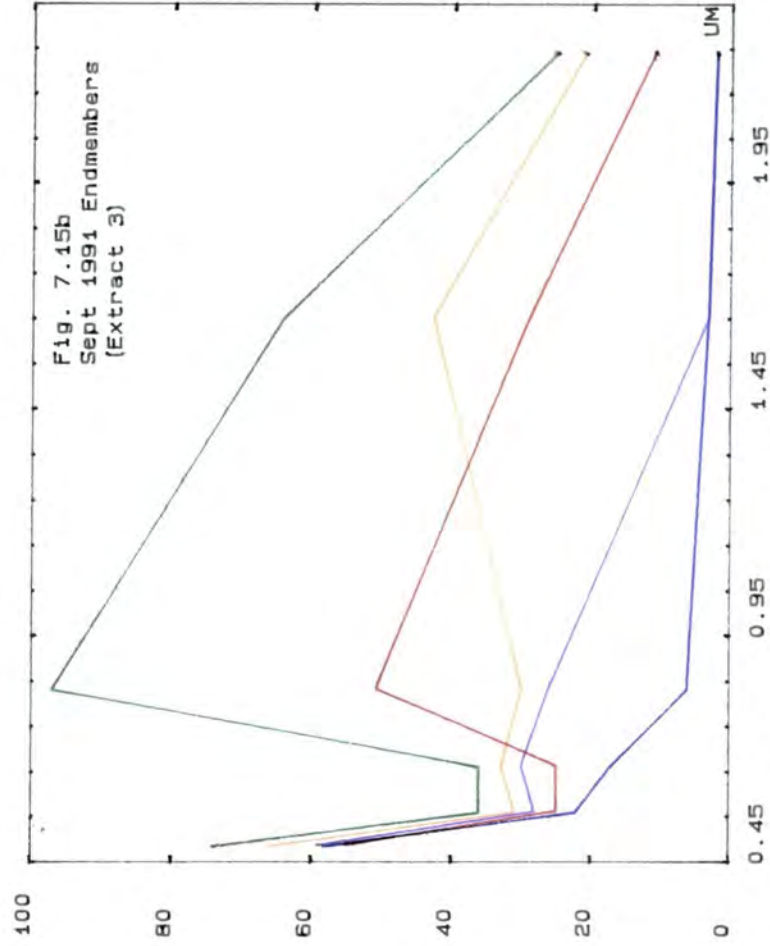
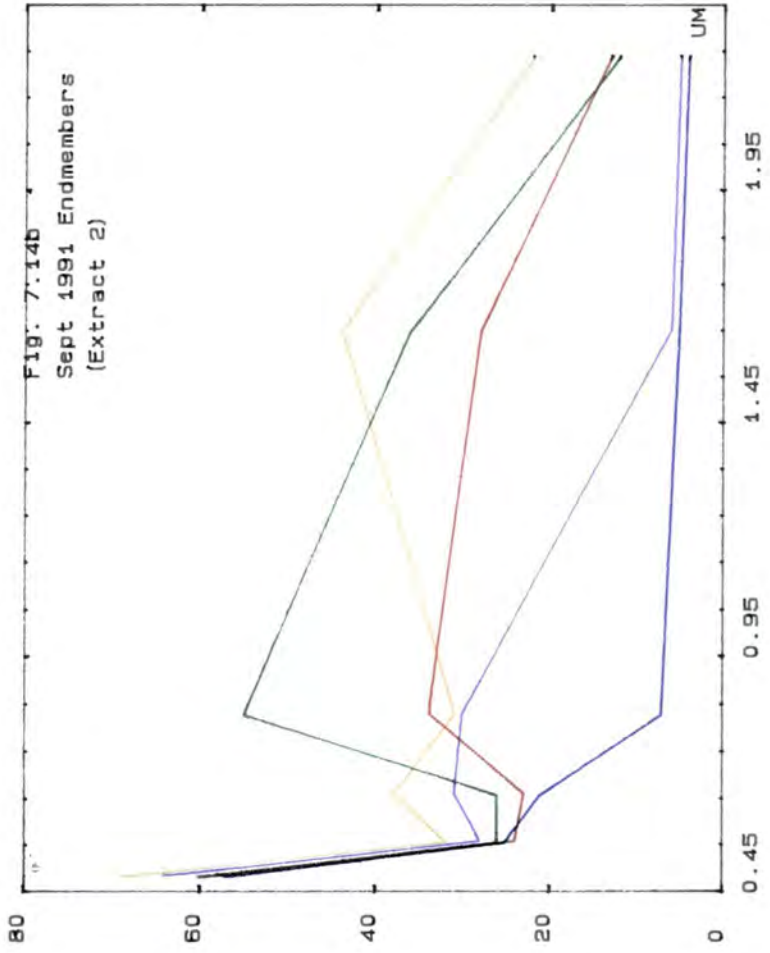


Fig 7.15 Principal Component Analysis of Extract 3.



(all units are relative reflectance)

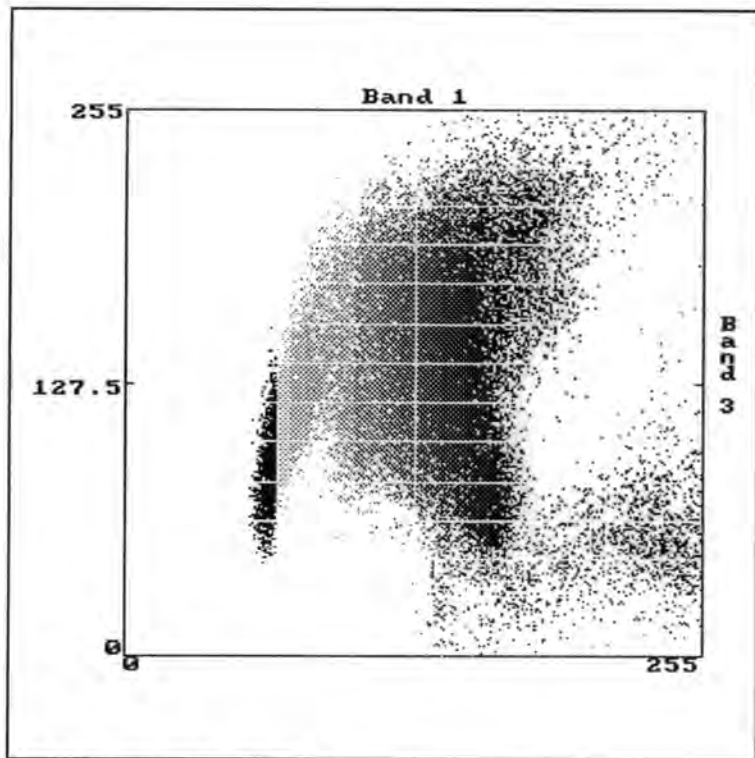


Fig 7.16 Extract 2, PC1 against PC3.

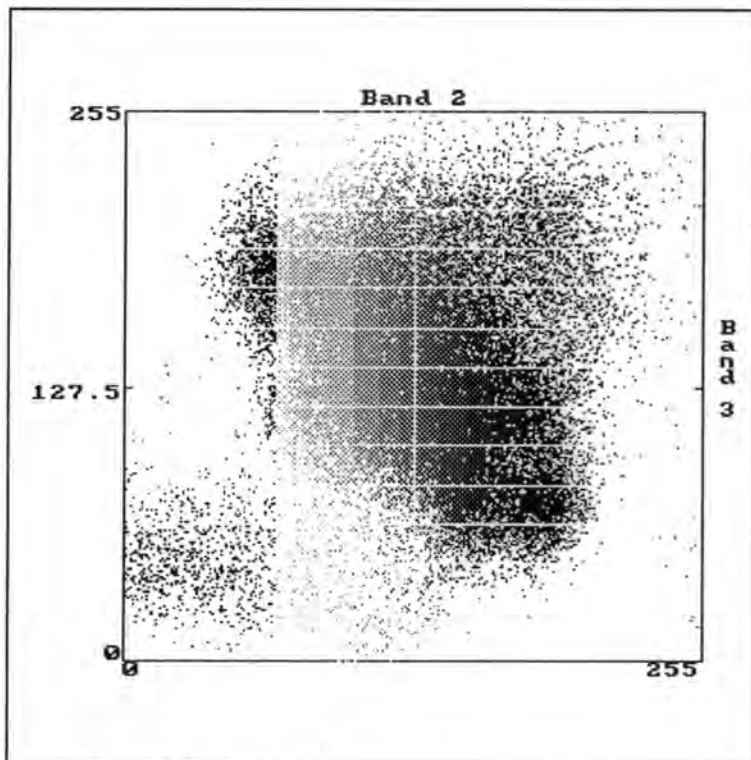


Fig 7.17 Extract 2, PC2 against PC3.

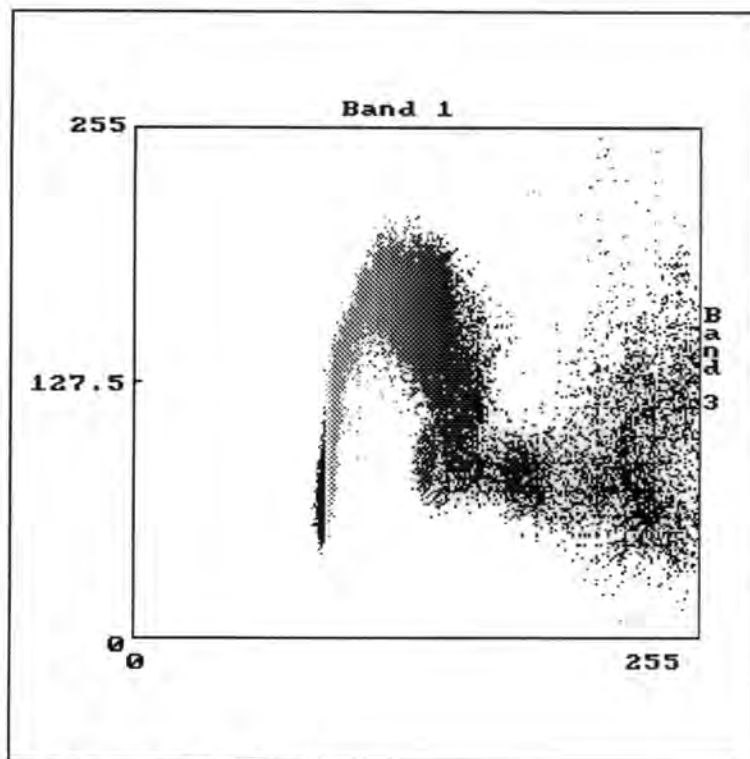


Fig 7.18 Extract3, PC1 against PC3.

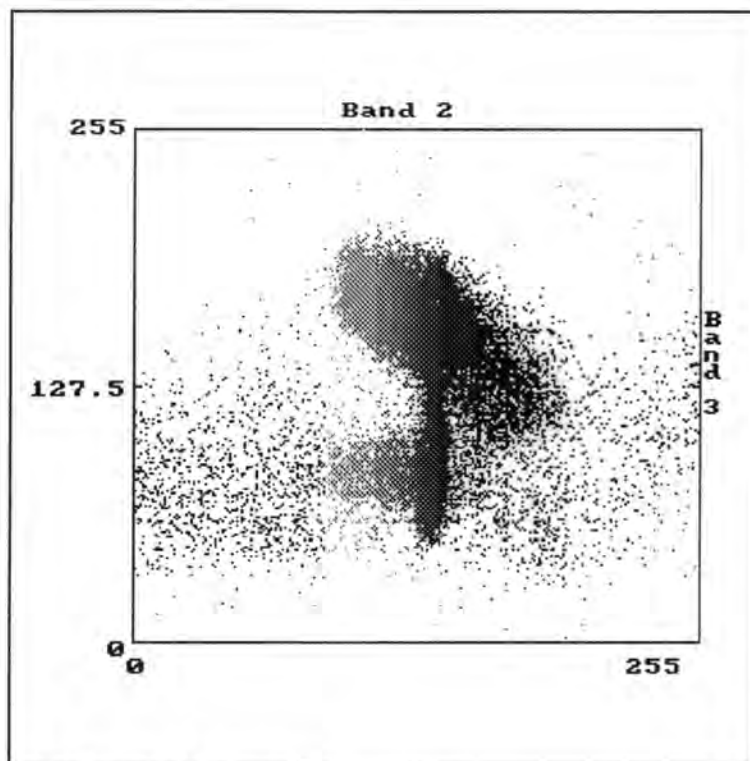


Fig 7.19 Extract 3, PC2 against PC3.

Generalised Linear Spectral Mixing Within the Intertidal Zone

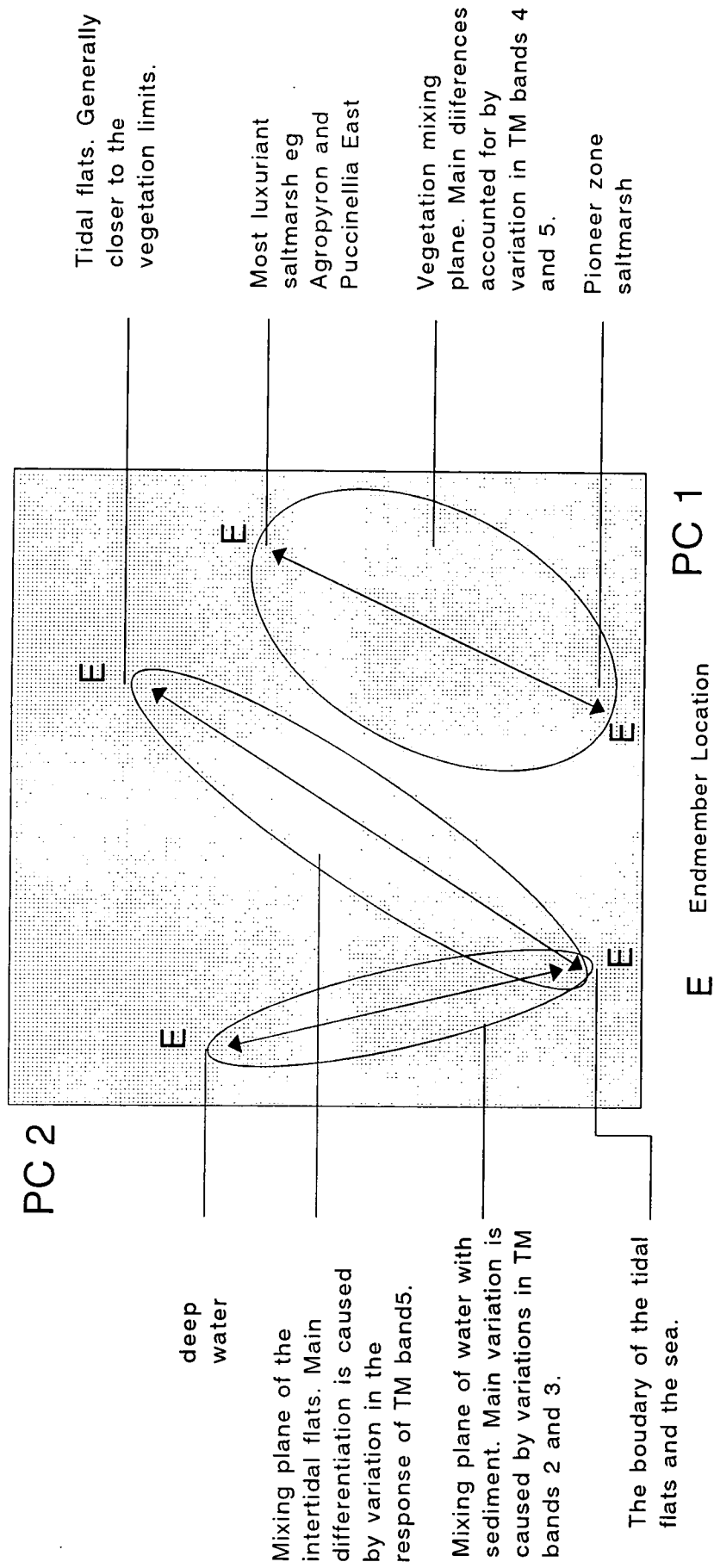
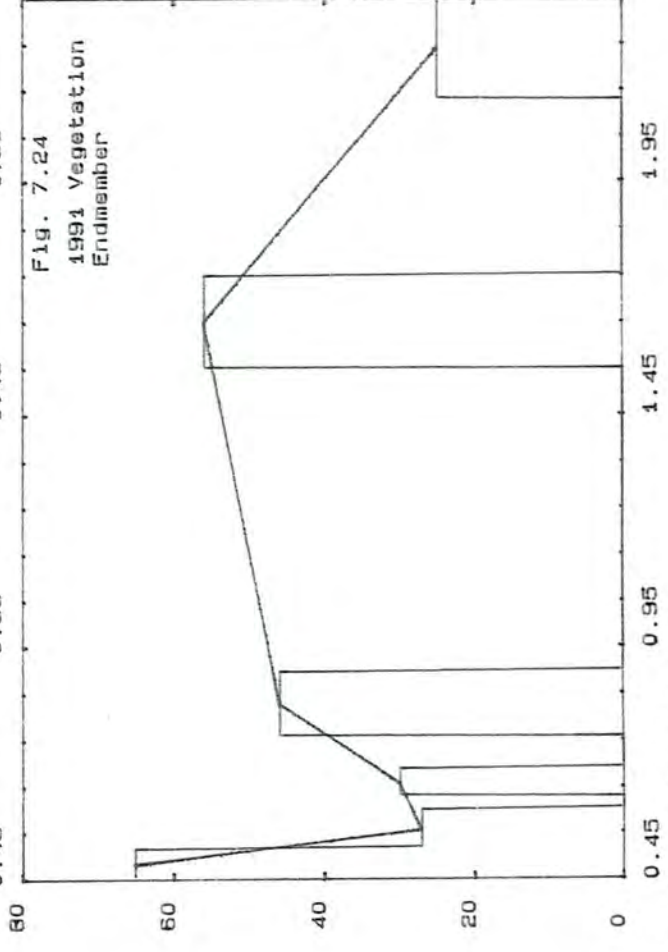
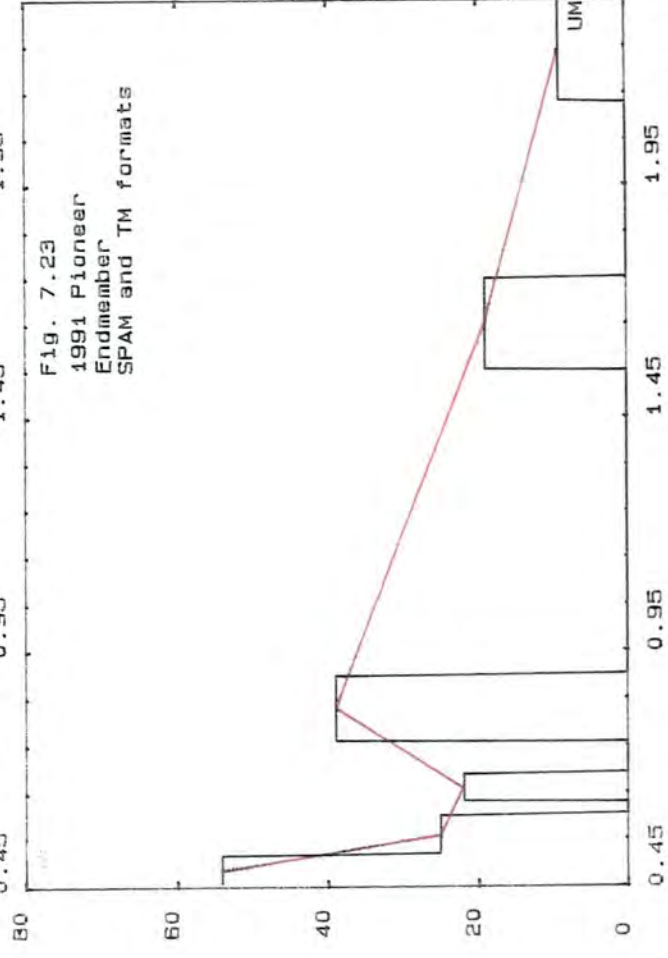
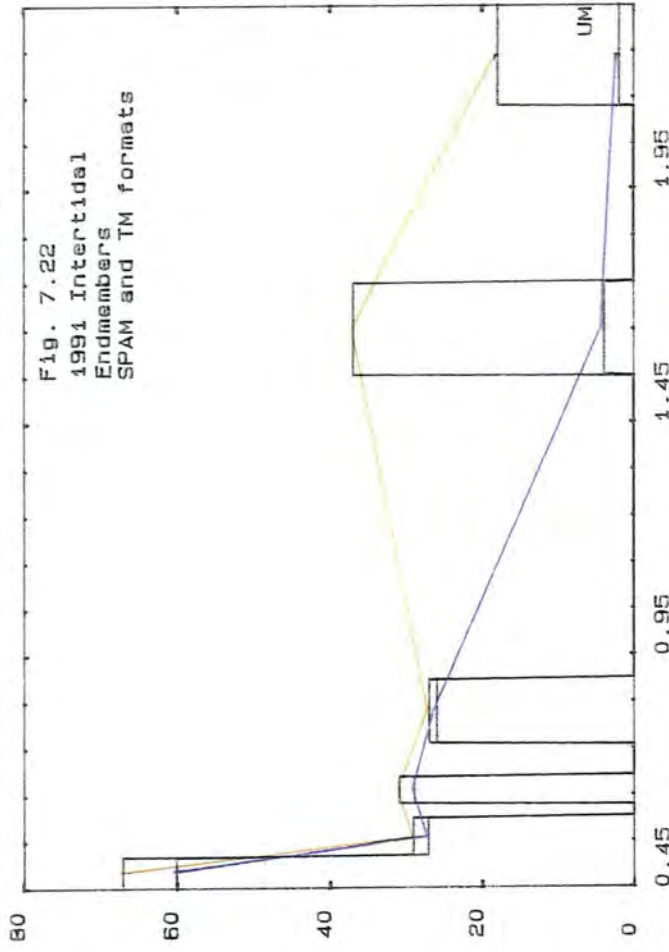
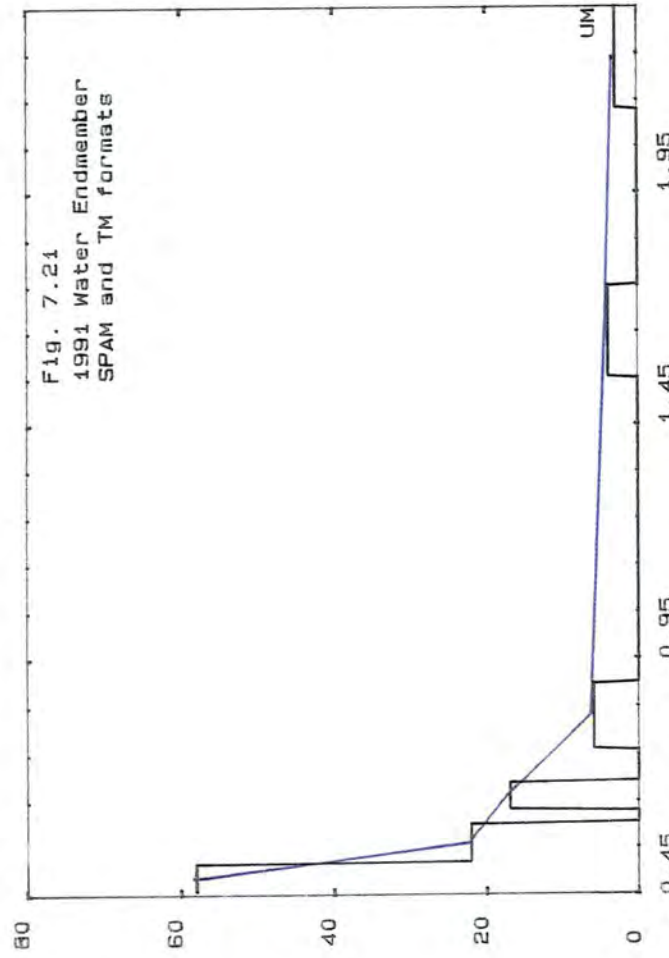


Fig. 7.20



(all units are relative reflectance)



Fig. 7.25 September 1991 Proportion Map of the Water Endmember



Fig. 7.26 September 1991 Proportion Map of the First Intertidal Sand/Mudflat Endmember

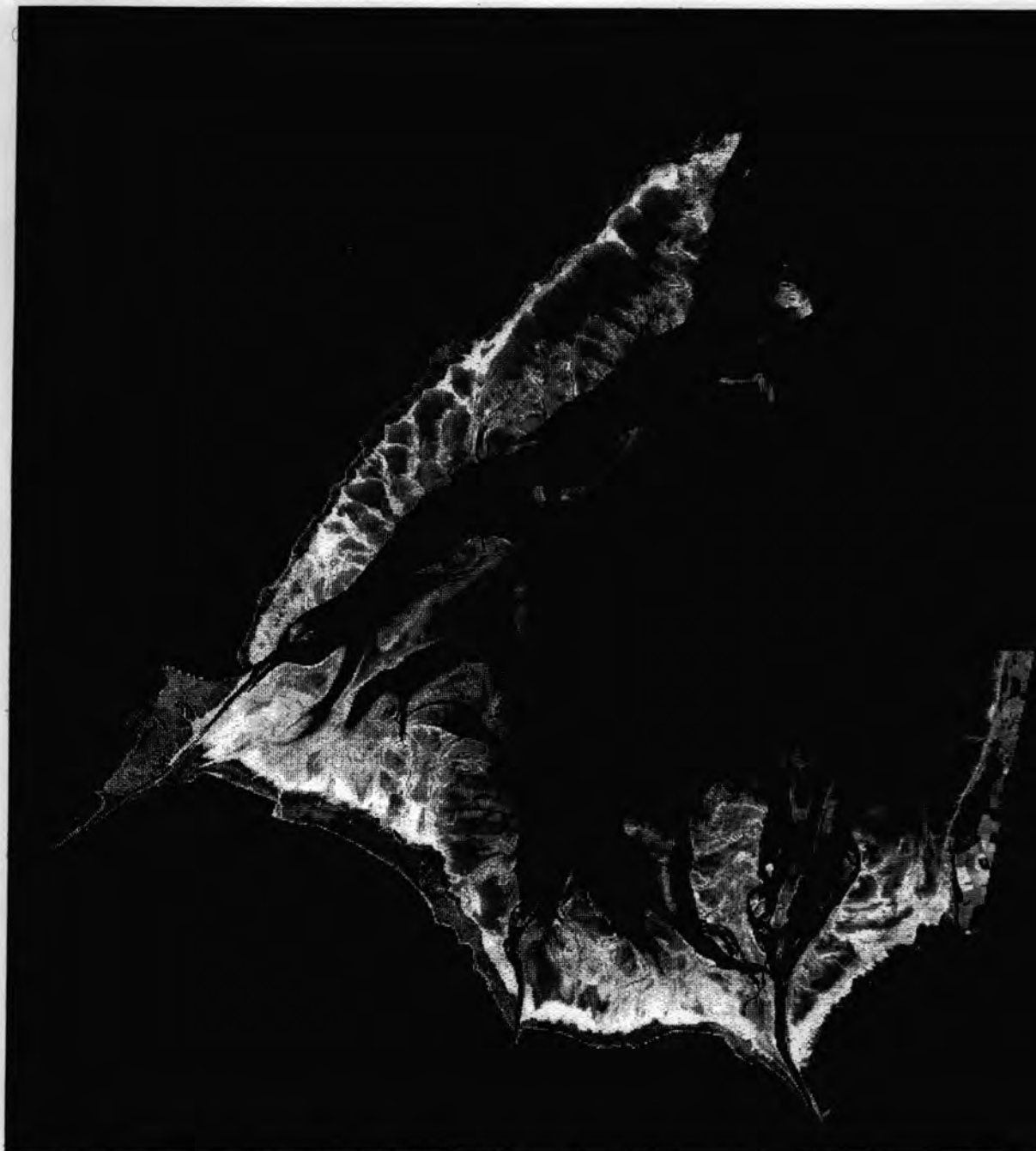


Fig. 7.27 September 1991 Proportion Map of the Second Intertidal Sand/Mudflat Endmember

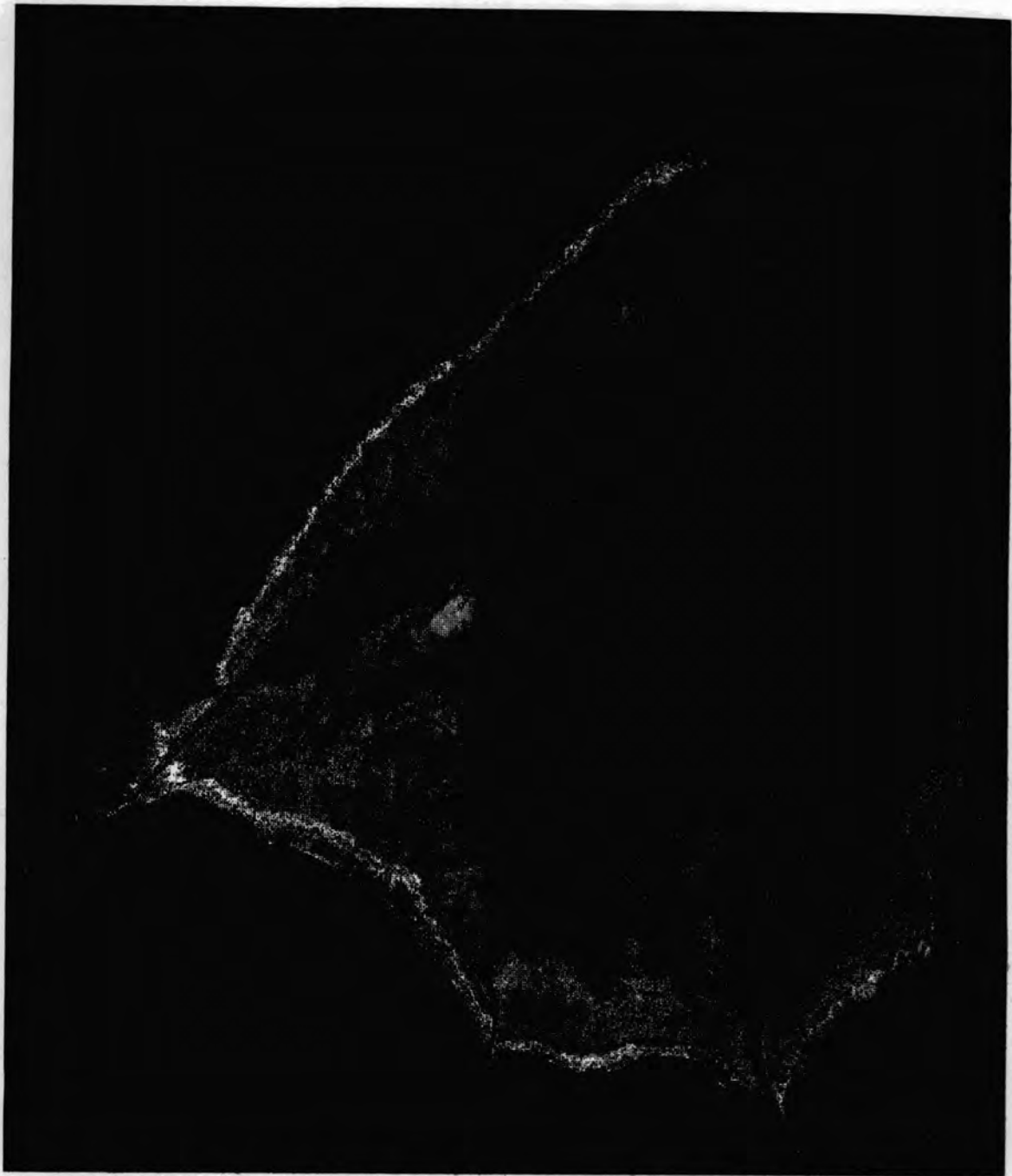


Fig. 7.28 September 1991 Proportion Map of the Pioneer Endmember

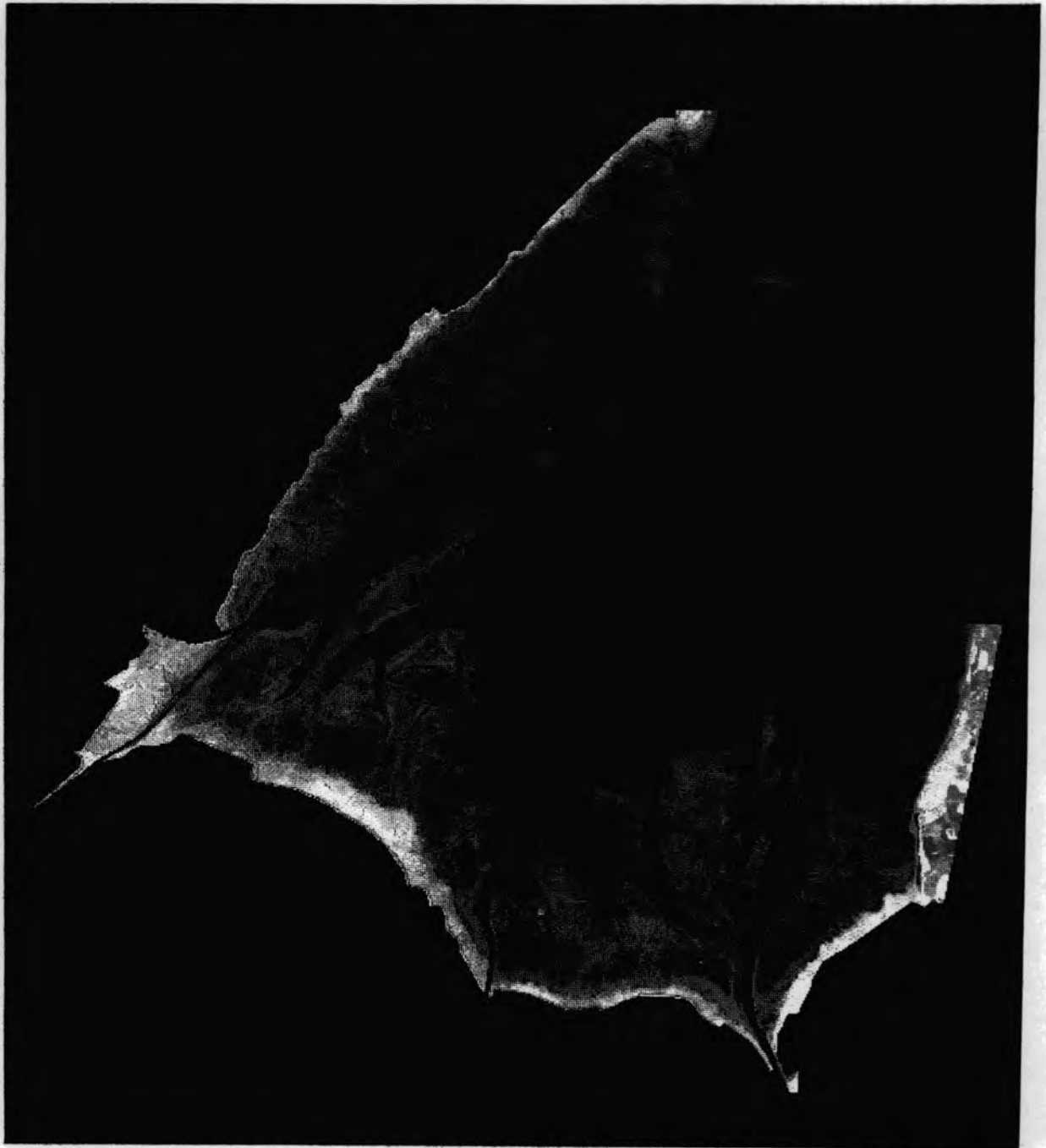


Fig. 7.29 September 1991 Proportion Map of the Saltmarsh Vegetation Endmember

Fig. 7.30 % SALT MARSH VEGETATION COVER OF THE WASH ESTUARY

Proportion image from 14/5/84 Landsat 5 TM image

scale 1 : 236,000

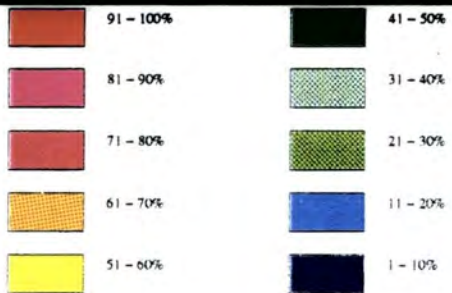
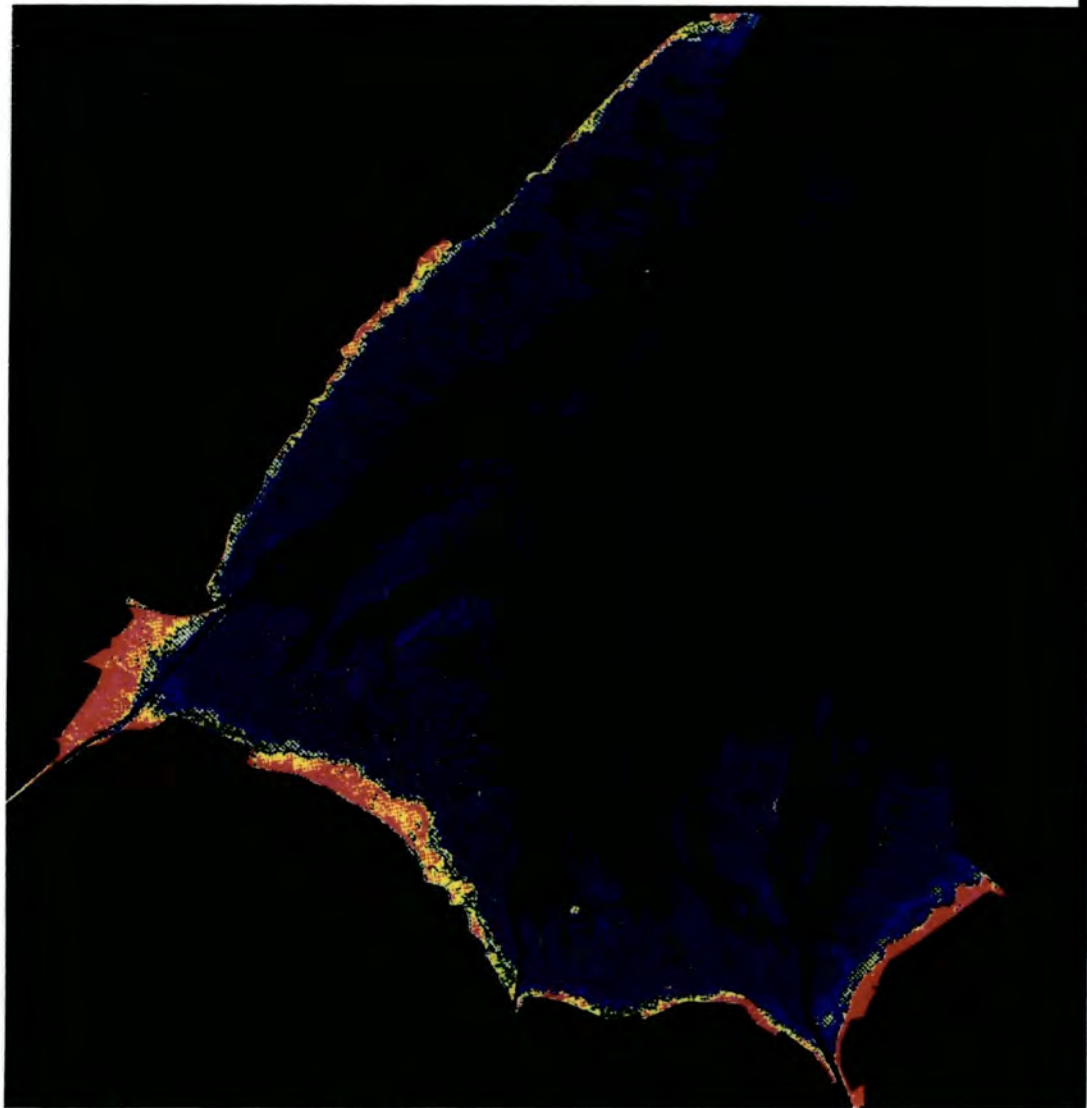
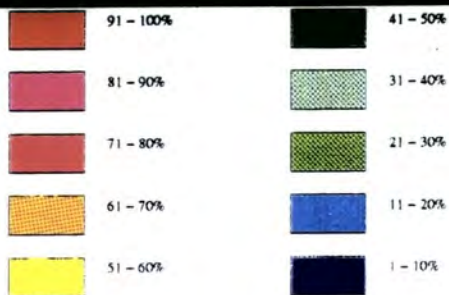
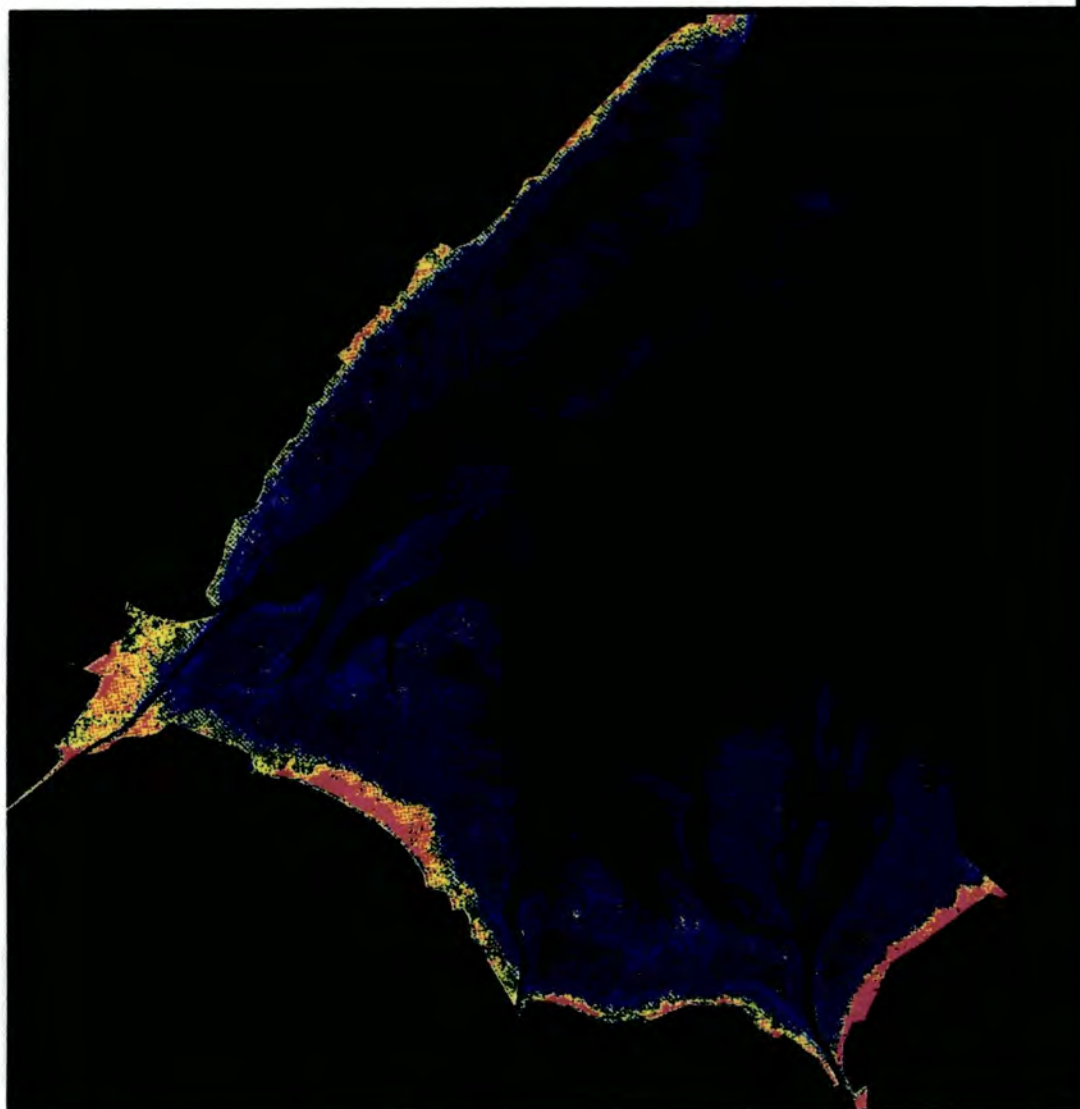


Fig. 7.31 % SALT MARSH VEGETATION COVER OF THE WASH ESTUARY

Proportion Image from 7/9/91 Landsat 5 TM Image

scale 1 : 236,000



The mixture model proportion maps were imported into the GRID module of Arc/Info running on a Sun Workstation. As this project was concerned with the mapping of intertidal vegetation only the vegetation endmember proportion maps were examined in detail. It should be noted that much information concerning the nature of the whole intertidal area is contained in the other proportion maps. A criticism commonly levelled at mixture model proportion maps is that they are very difficult to interpret visually, especially if a grey scale is used to represent the different proportions within each pixel. The data was therefore aggregated and a rainbow colour scheme adopted (Table 7.1, Figs. 7.30, 7.31) to produce a density sliced image which is much easier to assess visually.

% Vegetation Cover	1984 Mixture Model (ha)	1991 Mixture Model (ha)
91-100	720	13.95
81-90	347.31	528.48
71-80	458.91	464.31
61-70	504.99	644.49
51-60	553.14	770.31
41-50	553.95	731.25
31-40	426.42	623.97
21-30	344.52	502.38
11-20	1073.07	1628.73
1-10	13466.97	14011.74
TOTAL	18449.28	19919.61

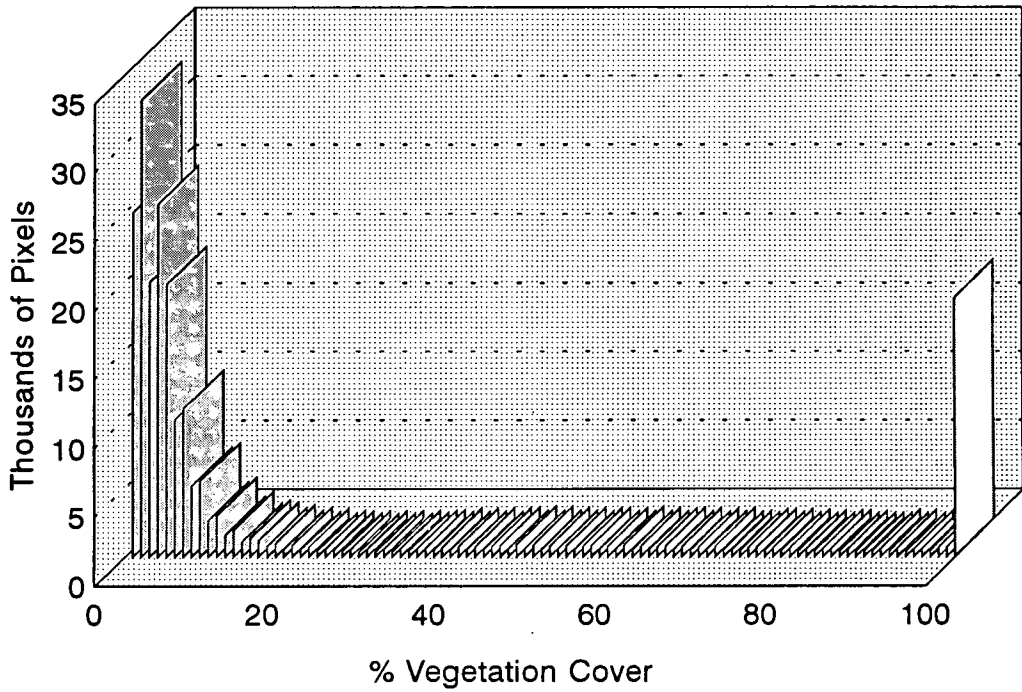
Table 7.1 Mixture Model estimates of % vegetation cover in May 1984 and September 1991 Landsat 5 TM images of the Wash (area in hectares)

The figures in Table 7.1 and the resulting maps (Figs. 7.30, 7.31) are not directly comparable as different endmembers were used in each of the mixture models. In the 1984 mixture model the saltmarsh vegetation endmember came from an area of *Puccinellia maritima* (corresponding to the *Puccinellia* East class in the MLC classifications) whereas in the 1991 mixture model the saltmarsh vegetation endmember came from an area of *Agropyron* (corresponding to the *Agropyron*/Upper marsh class in the MLC classifications). The most likely explanation for the differences in endmembers is the effects of phenology. The 1984 image was taken in May when much of the *Puccinellia*, especially on the S.E. coast of the Wash Estuary appears to be the most active saltmarsh vegetation and proves to

have the strongest "vegetation" signal in the Principal Components Analysis. In the September 1991 image *Agropyron* has the strongest vegetation signal and is found at the extremity of the vegetation mixing plain in the Principal Components Analysis. Seasonal changes in the form of a vegetation spectra may have a significant effect upon endmember selection.

It must also be noted that the mixture model used in the present study is a fully constrained mixture model, the effects of which are illustrated by the % vegetation cover histograms (Fig. 7.32). Cover corresponds to the spectral contribution of the vegetation endmember in the spectral signature of an individual pixel. The shape of the histograms are broadly comparable apart from the sharp rise at the 100% mark in the 1984 histogram. The shape of the histogram of the 1984 image suggests that the endmember selection has been poor. Any pixel that had a vegetation component greater than 100% (comparable with a2 in Fig. 7.2) is simply assigned a value of 100% by the constrained mixture model, hence the marked rise at 100% cover indicating poor endmember selection. As only extracts of the intertidal zone were used to identify endmembers it is quite possible that a stronger vegetation signal was missed. This is indicated by the large number of pixels assigned values of 100% vegetation cover. The histogram from the 1991 image indicates a much better selection of vegetation endmember as the data is drawn completely along the vegetation mixing plain. The histograms also illustrate that a density slice form of representation is the most appropriate method of displaying the proportion maps rather than any attempt to link individual proportions with particular plant species. The changes are much more gradual than are suggested by images produced from maximum likelihood classification which establishes abrupt boundaries. The mixture model is able to approximate the mosaic nature of the saltmarsh more accurately than the maximum likelihood classifier. Comparisons with the MLC classifications are discussed in the concluding chapter.

Vegetation Cover Histogram (Proportion Map From Landsat5 TM 14/5/84)



Vegetation Cover Histogram (Proportion Map From Landsat5 TM 7/9/91)

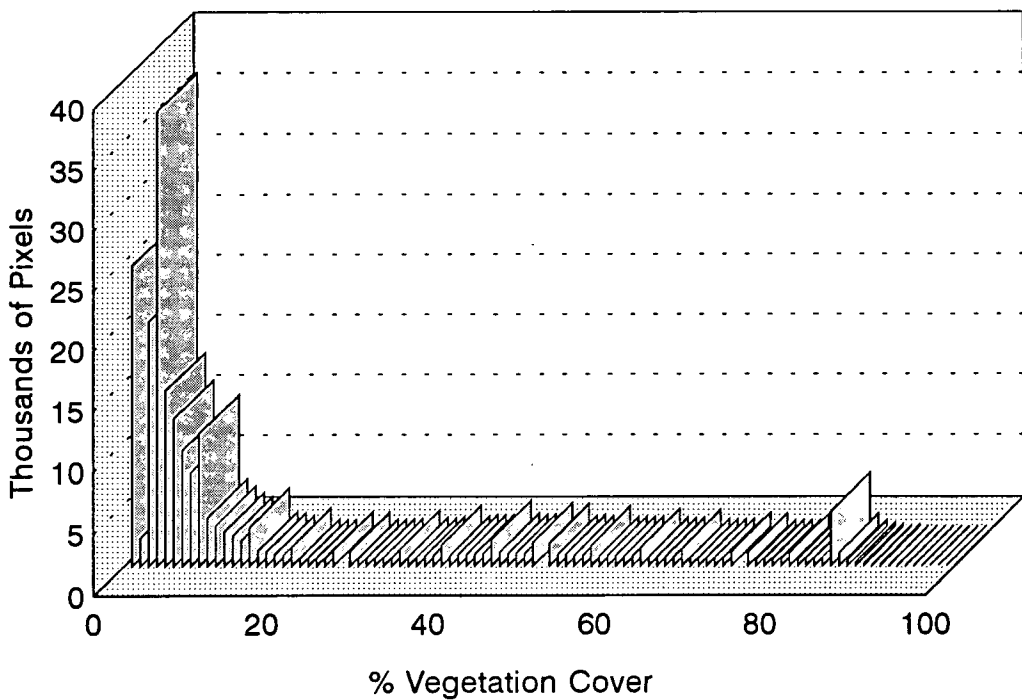


Fig. 7.32 Histograms of the data contained in the Vegetation proportion maps of the 1984 and 1991 Landsat5 TM images.

In order to allow comparison between the two images the data were aggregated further. Both histograms indicate a cut off point between the saltmarsh and the large area of intertidal mud and sand flats at the 20% vegetation cover mark. This was used to discriminate saltmarsh from the rest of the intertidal area. The saltmarsh area was divided into two sub-zones (Upper/Middle marsh > 40% vegetation cover; Lower/Pioneer marsh 20-40% vegetation cover). This second division was made on the basis of transects at Butterwick and Leverton saltmarshes carried out during March 1993 (Figs. 7.33-7.36). The corresponding zones of the 1982/4 N.C.C. survey were also aggregated to compare and evaluate the performance of the mixture model surveys.

TRANSECT COMPARISON

In order to establish and evaluate the relationship between the ground cover estimates of the mixture model and actual ground cover as observed in the field a preliminary study was carried out. This compared ground survey transect lines on Butterwick and Leverton saltmarshes with corresponding transects of mixture model images located using Terra-Mar software (Terra-Mar 4.0). The choice of saltmarshes meant that both an immature saltmarsh, Butterwick, and a mature marsh, Leverton, were studied. This provided a good mix of saltmarsh cover conditions.

The comparison was by no means ideal as the fieldwork was carried out during late March 1993 whereas the mixture model data came from the processing of the September 1991 Landsat 5 TM image. The transect study involved walking down the saltmarsh on a compass bearing, stopping every ten metres to give an estimate of vegetation cover in a ten metre square. The ground data was aggregated to correspond with the size of the satellite pixels. The identification of the individual transects proved difficult to locate on the mixture model data even though grid and compass references were gained from the ground transects. To overcome this problem the comparison was made with not just one line of pixels in the image but also with the adjacent pixel lines. Table 7.2 reports the correlation analysis carried out between the aggregated ground data and the pixel transects. Also included are the adjacent pixels (pixel 1, pixel 2) and the pixel means, minimums and maximums. The results of the analysis are displayed graphically in figures 7.33-7.36.

TABLE 7.2 TRANSECTS FROM BUTTERWICK SALT MARSH

	Ground Data	Pixel 1	Pixel 2	Pixel 3	Pixel Mean	Pixel Minimum	Pixel Maximum
Ground Data	1.0000						
Pixel 1	0.7333	1.0000					
Pixel 2	0.8237	0.8337	1.0000				
Pixel 3	0.7543	0.8287	0.8648	1.0000			
Pixel Mean	0.8145	0.9337	0.9525	0.9512	1.0000		
Pixel Min	0.8084	0.8635	0.9180	0.9682	0.9695	1.0000	
Pixel Max	0.8251	0.9573	0.9348	0.9040	0.9844	0.9208	1.0000

TRANSECTS FROM LEVERTON SALT MARSH

	Ground Data	Pixel 1	Pixel 2	Pixel 3	Pixel Mean	Pixel Minimum	Pixel Maximum
Ground Data	1.0000						
Pixel 1	0.3232	1.0000					
Pixel 2	0.4988	0.8678	1.0000				
Pixel 3	0.5014	0.7604	0.8587	1.0000			
Pixel Mean	0.4736	0.9251	0.9679	0.9304	1.0000		
Pixel Min	0.4983	0.8285	0.9498	0.9606	0.9728	1.0000	
Pixel Max	0.3801	0.9789	0.9133	0.8207	0.9572	0.8578	1.0000

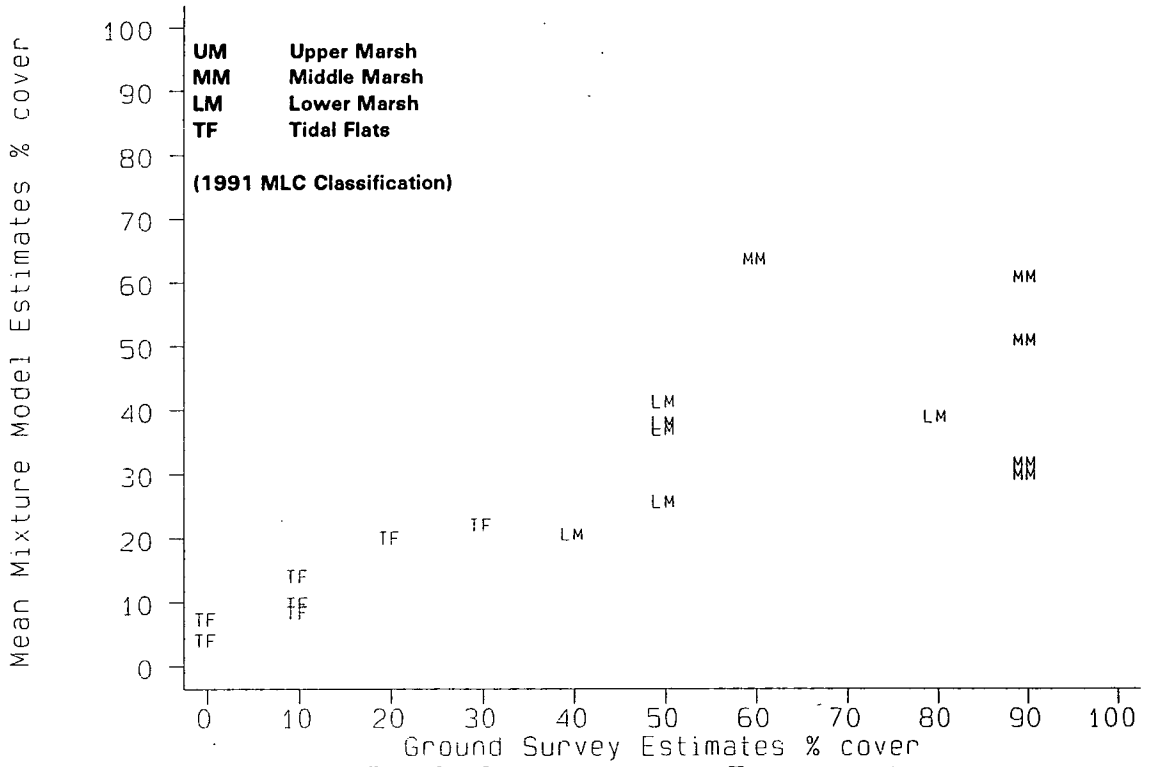


Fig. 7.33 Butterwick Transect

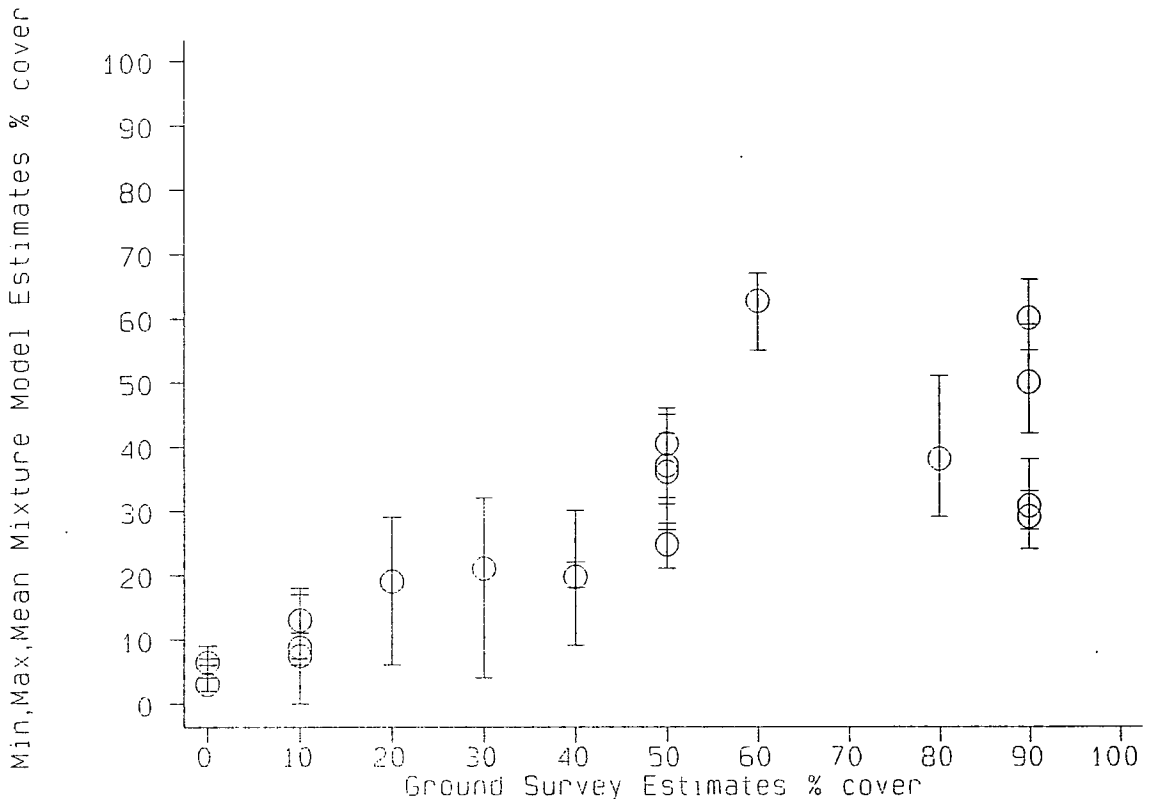


Fig. 7.34 Butterwick Transect

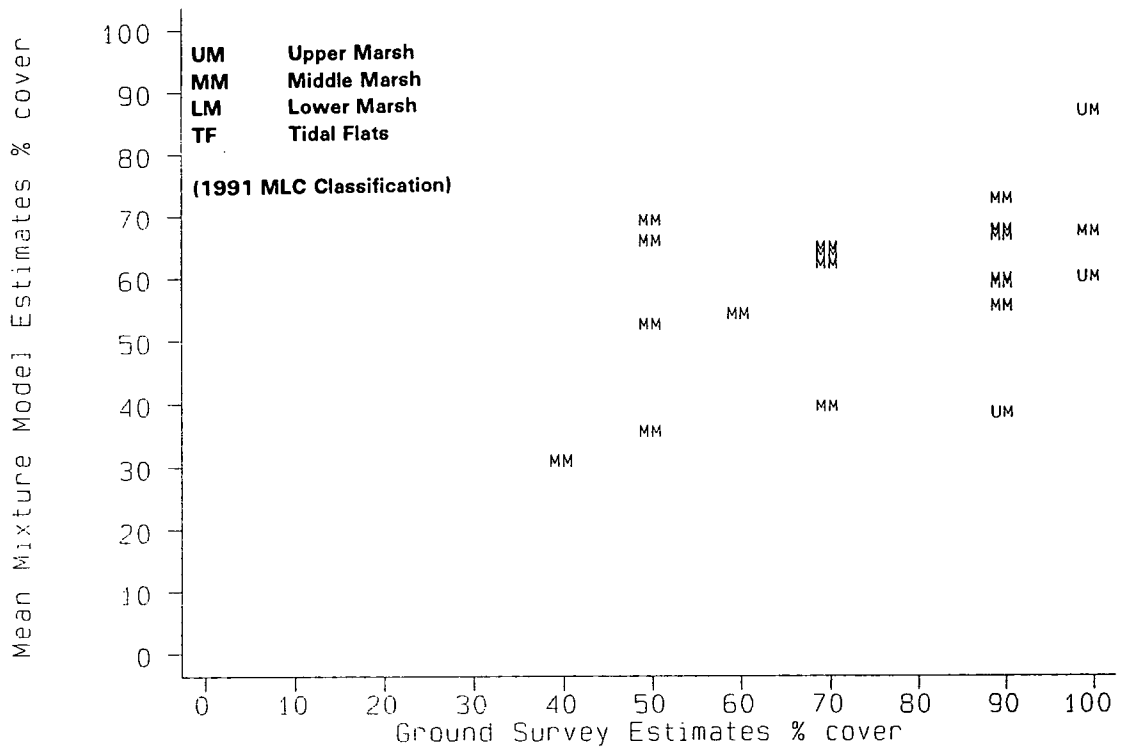


Fig. 7.35 Leverton Transect

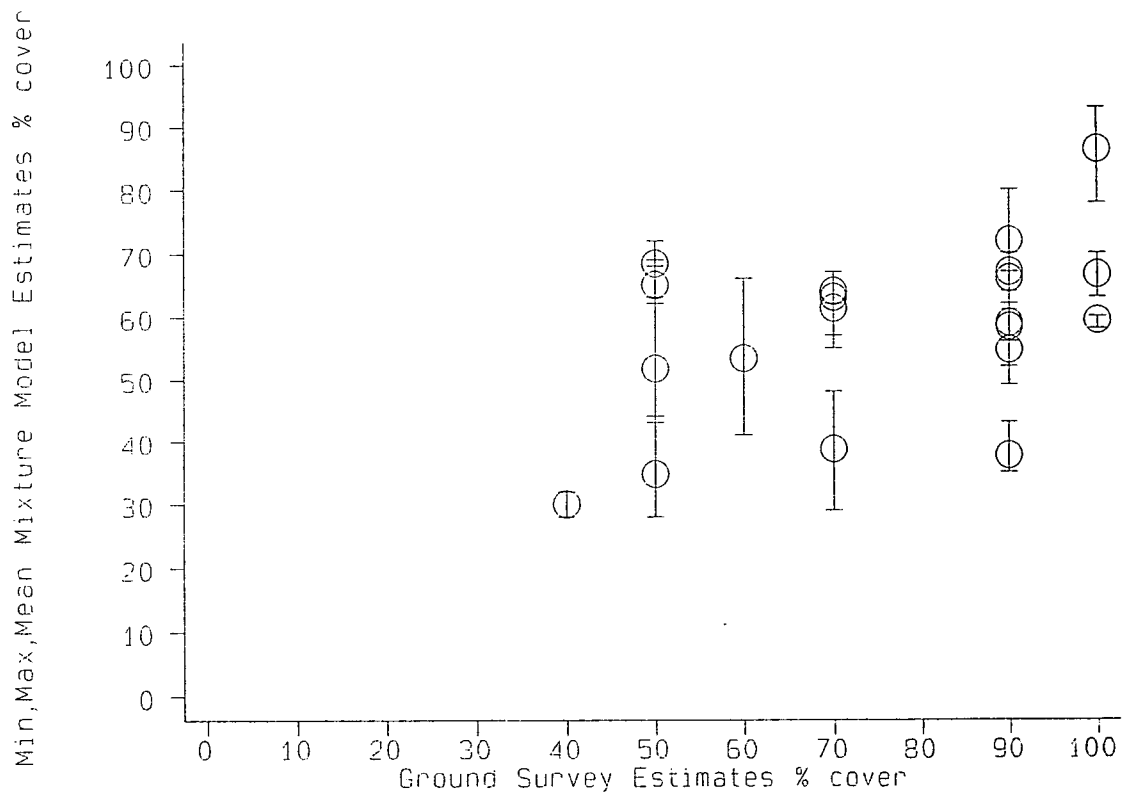


Fig. 7.36 Leverton Transect

The ground coverage estimates of the mixture model show a good level of correlation with the ground survey estimates at Butterwick marsh. The correlation figure is over 0.7 and is above 0.81 for the Pixel mean and Pixel 2. Figures 7.33 and 7.34 illustrates this relationship graphically. Fig. 7.33 illustrates the plot of the pixel means against the ground survey estimates. The lettering represents how the pixels were classified in the maximum likelihood classification (operator 1) of the 1991 Landsat 5 image. This illustrates a general trend of decreasing vegetation cover from the Middle marsh towards the intertidal flats. This is also seen in the vegetation cover maps of the whole Wash Estuary (Figs. 7.30, 7.31). The minimum and maximums of the three pixels along the mixture model transect form the ends of the high-low lines with the mean values marked by circles (Fig. 7.34). There is a good linear relationship between the two survey methods (correlation figure of 0.81) although the mixture model consistently underestimated the saltmarsh cover in the upper regions of the saltmarsh. Better agreement was achieved further down the saltmarsh at coverage levels of less than 60%. The large spread of estimates of the High-low lines reflects the mosaic nature of the saltmarsh where % cover can change very quickly, even within the distance of a pixel.

The results of the correlation of the mixture model data with the ground survey estimates of Leverton saltmarsh are less encouraging. The highest correlation value was only just over 0.5. Figures 7.35 and 7.36 illustrates that although a general linear relationship can still be identified it is much less defined than in the Butterwick graphs. Figure 7.35 illustrates that vegetation cover decreases from the Upper to the Middle marsh. Figure 7.36 again illustrates that the mixture model consistently underestimated the cover of the saltmarsh in the upper regions of the saltmarsh compared with the ground survey estimates. In the limited time available for fieldwork the transect was only carried out to a distance of 600 m. At this point on Leverton the saltmarsh is still dominated by Middle marsh species. This is the area where there are the largest discrepancies with the mixture model survey. The spread within the high-low lines again emphasises the mosaic nature of the saltmarsh.

The poor relationship between the Upper/Middle marsh does not necessarily mean that the mixture model is a poor estimator of ground cover. Surface cover is very difficult to assess on the ground and the differences in the angle that the saltmarsh is being observed at in the different survey methods may account for much of the error. General trends can be

observed between saltmarsh class and vegetation cover. Further work needs to be carried out to establish regression relationships between ground cover and the estimates of the mixture model if the model is to be used in an operational mode.

RESULTS OF THE MIXTURE MODEL ANALYSIS

Comparison was carried out at three levels: at the macro scale involving total saltmarsh area estimation; at the meso scale using the two broad sub-zones within the saltmarsh; at the micro-level the GRID COMBINE command was used to cross tabulate different surveys to establish the degree of agreement. Cross tabulation was carried out on the two broad zones and on the saltmarsh as a whole. The results of these comparisons are reported in Tables 7.3 - 7.9 and in Figs. 7.37 - 7.40.

ZONE	1982/4 N.C.C. Survey	1984 Mix Model	1991 Mix Model
Upper/Middle Marsh	3114.83	3095.10	3090.87
Lower/Pioneer	807.72	746.91	1023.39
Total	3922.55	3842.01	4114.26

Table 7.3 Summary of mixture model and 1984 N.C.C. saltmarsh surveys (area in hectares)

N.C.C. 1982/4	1984 Mixture Model				
Zone	Upper/Middle Marsh	Lower/Pioneer Marsh	Other	Total Area	% Agreement
Upper/Middle Marsh	2666.16	326.52	60.66	3053.34	87.3
Lower/Pioneer Marsh	172.89	197.10	421.92	791.91	24.9
Other	256.05	223.29	4427.46	4906.80	90.2
Total Area	3095.10	746.91	4910.04	8752.05	

Table 7.4 Cross tabulation of the 1984 mixture model and the 1982/4 N.C.C Survey (area in hectares)

N.C.C. 1982/4	1991 Mixture Model				
Zone	Upper/Middle Marsh	Lower/Pioneer Marsh	Other	Total Area	% Agreement
Upper/Middle Marsh	2544.75	442.44	62.28	3049.47	83.4
Lower/Pioneer Marsh	245.97	292.14	237.15	775.26	37.68
Other	300.15	288.81	4338.36	4927.32	88.0
Total Area	3090.87	1023.39	4637.79	8752.05	

Table 7.5 Cross tabulation of the 1991 mixture model and the 1982/4 N.C.C Survey (area in hectares)

1984 Mixture Model	1991 Mixture Model				
Zone	Upper/Middle Marsh	Lower/Pioneer Marsh	Other	Total Area	% Agreement
Upper/Middle Marsh	2641.59	381.96	65.34	3088.89	85.5
Lower/Pioneer Marsh	297.27	262.71	178.29	738.27	35.6
Other	158.22	387.36	4379.31	4924.89	88.9
Total Area	3097.08	1032.03	4622.94	8752.05	

Table 7.6 Cross tabulation of the 1984 mixture model with the 1991 mixture model (area in hectares)

N.C.C. 1982/4	1984 Mixture Model			
	Zones	Saltmarsh	Other	Total Area
Saltmarsh	3362.67	482.58	3845.25	87.4
Other	479.34	49194.00	49673.34	99.0
Total Area	3842.01	49676.58	53518.59	

Table 7.7 Cross tabulation of the 1984 mixture model total saltmarsh estimate with the N.C.C. 1982/4 survey total saltmarsh estimate (area in hectares)

N.C.C. 1982/4	1991 Mixture Model			
	Zones	Saltmarsh	Other	Total Area
Saltmarsh	3525.30	299.43	3824.73	92.17
Other	588.96	48204.00	48792.96	98.79
Total Area	4114.26	48503.43	52617.69	

Table 7.8 Cross tabulation of the 1991 mixture model total saltmarsh estimate with the N.C.C. 1982/4 survey total saltmarsh estimate (area in hectares)

1984 Mix Model	1991 Mixture Model			
	Zones	Saltmarsh	Other	Total Area
Saltmarsh	3583.53	258.48	3842.01	93.3
Other	530.73	4379.31	4910.04	89.19
Total Area	4114.26	4637.79	8752.05	

Table 7.9 Cross tabulation of the 1984 mixture model total saltmarsh estimate with the 1991 mixture model total saltmarsh estimate (area in hectares)

COMPARISON BETWEEN THE VEGETATION PROPORTION MAP OF THE MAY 1984 LANDSAT 5 TM IMAGE AND THE N.C.C. 1982/4 VEGETATION SURVEY (TABLES 7.4, 7.7. Fig. 7.37)

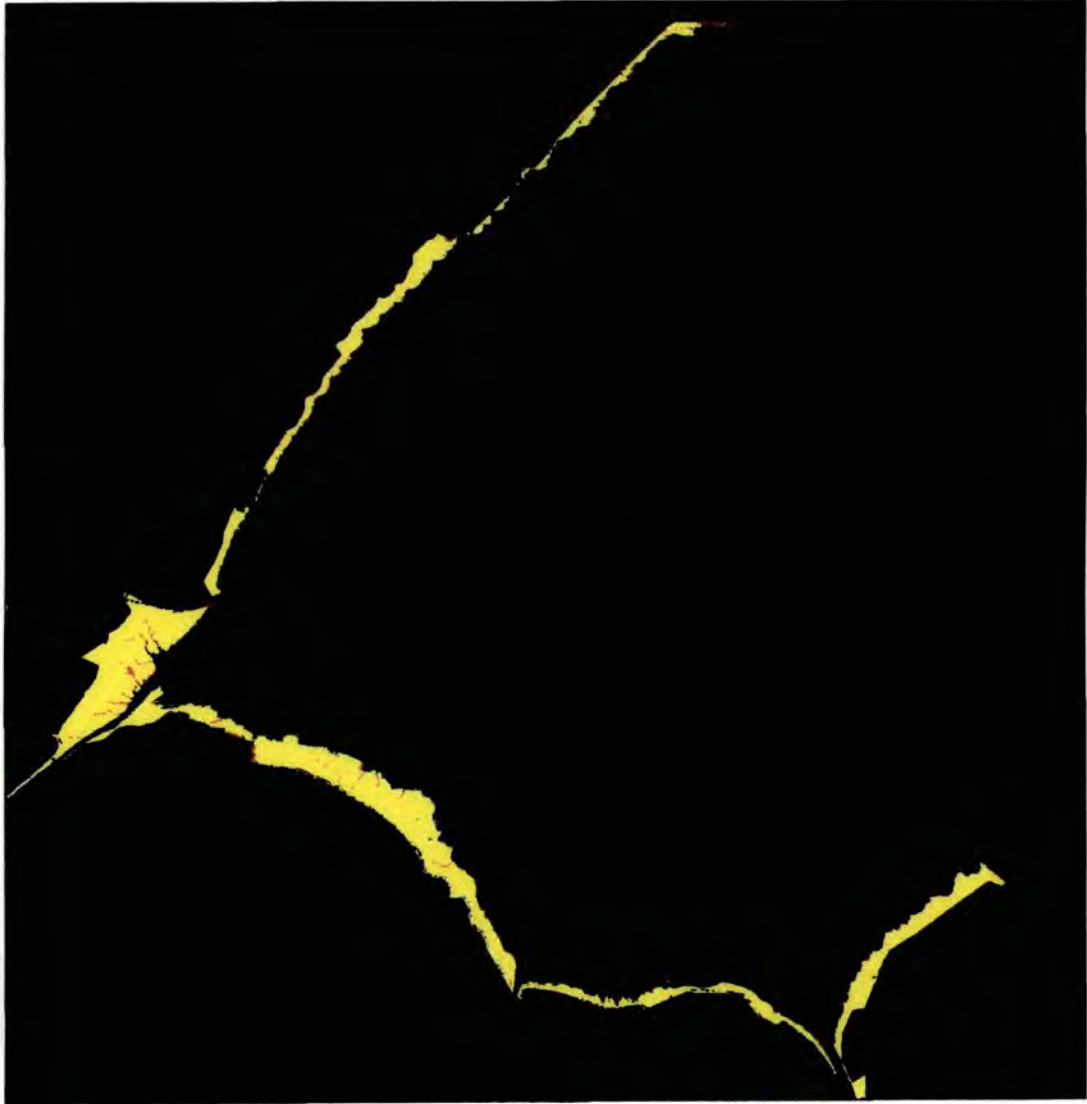
The comparison of the 1984 vegetation proportion map with the 1982/4 N.C.C. survey provides the best means of evaluating the accuracy of the mixture model mapping technique. It was hoped that the comparison would reveal a close correlation as the May 1984 Landsat 5 TM image is closest in time to the N.C.C. survey period. Table 7.4 indicates that there is less than a 3% difference in the total saltmarsh area mapped by the two different survey methods. Comparing the area estimates for the two broad saltmarsh zones reveals less than a 1% difference for the Upper/Middle marsh and a difference of 7.5% for the Lower/Pioneer marsh area. In both cases the N.C.C. survey estimated slightly larger areas. The micro-scale comparison was achieved by overlaying the two classifications. The result was an 85% agreement for the Upper/Middle marsh class but only a 25% agreement for the Lower/Pioneer marsh class. Considerable variability would be expected between the two surveys within the broad saltmarsh classes. Membership in the N.C.C. survey classes is dependent on the presence or absence of certain vegetation species whereas membership in a mixture model class is dependent on the spectral contribution of the vegetation endmember within the spectral signature of an individual pixel. This is illustrated by the 326 hectares of saltmarsh classified as Upper/Middle saltmarsh in the N.C.C. survey but as Lower/Pioneer saltmarsh in the mixture model. Similarly 172 hectares of Lower/Pioneer saltmarsh in N.C.C. survey were classified as Upper/Middle saltmarsh in the vegetation proportion map. The effects of such confusion are bound to have a greater effect on the Lower/Pioneer zone cross tabulation agreement figures due to the significantly smaller size of this zone.




An area of 422 hectares, classified as Lower/Pioneer saltmarsh in the N.C.C. survey, failed to be classified as saltmarsh by the mixture model. In all, over 480 hectares of saltmarsh failed to be classified as saltmarsh by the 1984 mixture model (Table 7.7). Fig. 7.37 illustrates the location of these areas and reveals that they are precisely the ones that it was hoped the mixture model would be able to identify - the extremities of the Lower marsh and Pioneer zone. This would indicate that this first attempt at using the mixture model to locate the Pioneer zone has been unsuccessful.

Fig. 7.37 COMPARISON OF THE 1982/4 N.C.C. SURVEY AND
THE 1984 VEGETATION PROPORTION MAP

Proportion Image From 14/5/84 Landsat 5 TM Image

scale 1 : 236,000



-  Saltmarsh areas mapped in both surveys
-  Saltmarsh mapped by the N.C.C. survey but not in the mixture model
-  Saltmarsh mapped by the mixture model but not by the N.C.C. survey

In order to improve the performance of the mixture model the tolerance of the Lower/Pioneer class could be increased to include areas with less than a 20% vegetation component within the spectral signature of an individual pixel. The problem with this is that as soon as the tolerance is lowered large areas of algae present on the intertidal mud and sand flats become incorporated into the saltmarsh class.

A second possibility is that, like the maximum likelihood classifier the mixture model classification is severely hampered by the effects of subtle differences in phenology. This is quite possible as the vegetation canopy is likely to be less well developed early on in the growing season and so the spectral component of the vegetation endmember within a pixel in the Pioneer zone is likely to be very small and cannot be used to distinguish the Pioneer zone from non vegetated areas of the intertidal zone. The 1991 mixture model was compared with the 1982/4 N.C.C. survey and the 1984 mixture model survey in order to establish whether the model performs any better late on in the growing season.

Areas of saltmarsh mapped by the mixture model but not in the N.C.C. survey tend to be small in area and confined to the back of the saltmarsh in the region of the borrow pit. One notable exception is the area fronting the Wolferton saltmarsh. It is probable that this area is not actually saltmarsh, as it was not classified as such in the N.C.C. survey, but is a very large and intense algal bloom and has been confused with Lower/Pioneer marsh in the mixture model.

COMPARISON BETWEEN THE VEGETATION PROPORTION MAP OF THE SEPTEMBER 1991 LANDSAT 5 TM IMAGE AND THE 1982/4 N.C.C. VEGETATION SURVEY (TABLES 7.5, 7.8, Fig. 7.38)

The macro-scale comparison indicates a 4.5% difference in total marsh area, the mixture model estimates an additional 191.7 hectares of saltmarsh. The Upper/Middle marsh zone decreased by 24 hectares, a decline of less than 1%, and the Lower/Pioneer zone expanded by 215 hectares, an increase of over 20%. The overlaying of the two broad saltmarsh zones indicates 83.4% agreement for the Upper/Middle zone (compared with 87.3% in 1984) and 37.7% agreement for the Lower/Pioneer class (compared with 24.9% in 1984). Once again there is considerable confusion amongst the classes with over 400 hectares of saltmarsh classified as Upper/Middle marsh in the N.C.C. survey being classified as Lower/Pioneer saltmarsh in the 1991 vegetation proportion map. This highlights the different criteria for membership of the classes in the different surveys and implies that such comparisons are of limited value. Of more importance is the overlay of the entire saltmarsh areas which revealed a 92% match between the two surveys. This compares with a match of 87% between the N.C.C. survey and the mixture model of the 1984 Landsat 5 TM image.

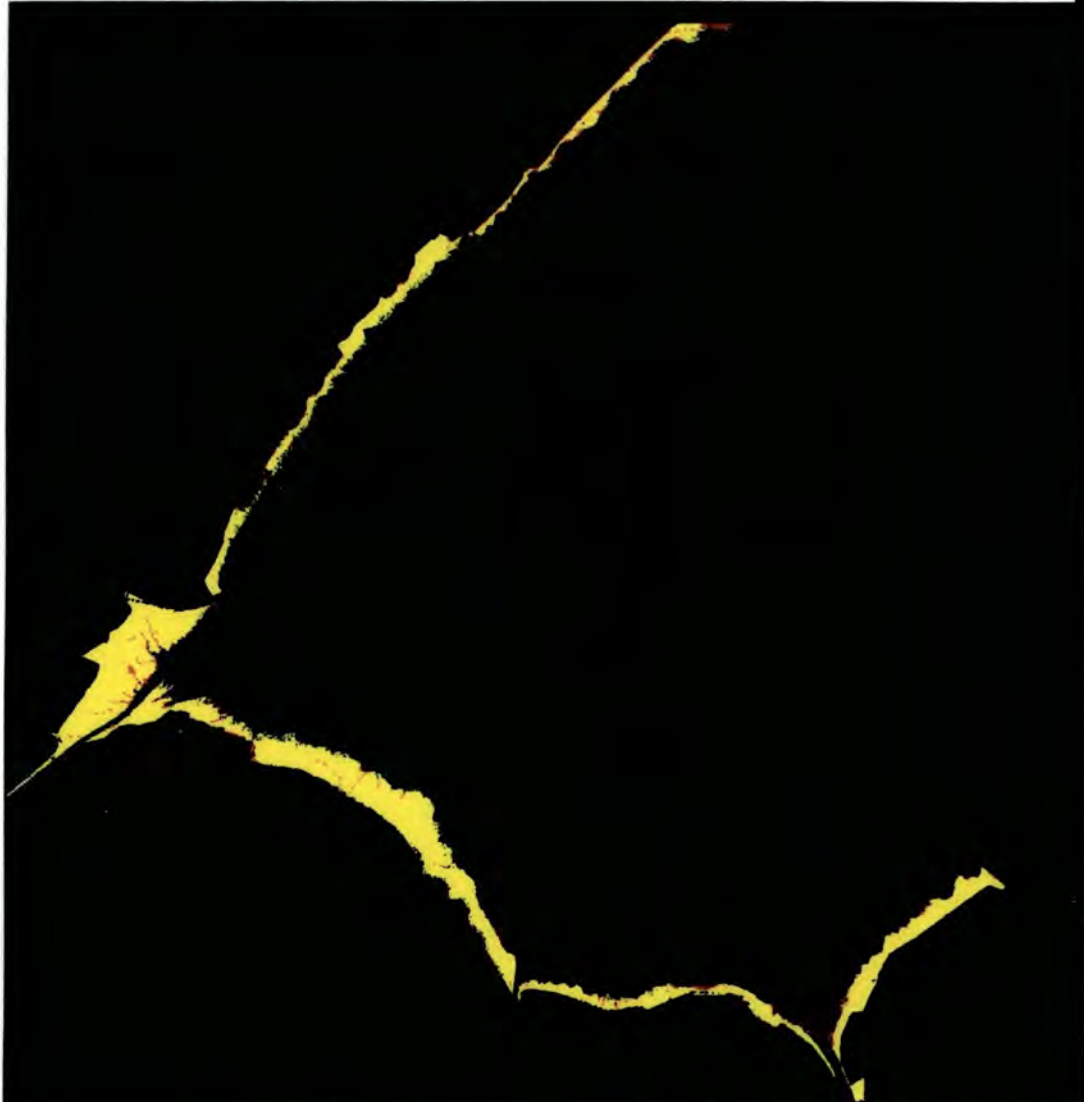
As with the 1984 mixture model a cause for concern is an area of nearly 300 hectares classified as saltmarsh in the N.C.C survey but not included in the 1991 proportion map (Table 7.8). This area once more proved to be the extremities of the Pioneer zone, notably along the fronts of Butterwick and Holbeach saltmarshes (Fig. 7.38). The 1991 mixture model is slightly better at identifying areas of Pioneer marsh than the mixture model of the 1984 image implying that phenology does have an effect on the performance of the mixture model. This is further highlighted by the comparison between the two mixture model surveys.




The areas mapped by the mixture model but not by the N.C.C. are likely to be areas of saltmarsh expansion between the two survey dates. The areas include the saltmarsh recovering from the effects of reclamation at Freiston and saltmarsh expansion at the front edges of Friskney and Wainfleet saltmarshes and at the mouth of the Great Ouse close to Terrington marsh.

Fig. 7.38 COMPARISON OF THE 1982/4 N.C.C. SURVEY AND
THE 1991 VEGETATION PROPORTION MAP

Proportion Image From 7/9/91 Landsat 5 TM Image

scale 1 : 236,000



-  Saltmarsh areas mapped in both surveys
-  Saltmarsh mapped by the N.C.C. survey but not in the mixture model
-  Saltmarsh mapped by the mixture model but not by the N.C.C. survey

COMPARISON BETWEEN THE VEGETATION PROPORTION MAP OF THE MAY 1984 LANDSAT 5 TM IMAGE AND THE VEGETATION PROPORTION MAP OF THE SEPTEMBER 1991 LANDSAT 5 TM IMAGE (TABLE 7.6, 7.9, Fig. 7.39)

The broadest level of comparison, that of total saltmarsh area, reveals a 6.6% difference in area, implying an expansion of 272.25 hectares between the two survey dates. The meso scale comparison suggests that the area of Upper/Middle marsh has actually contracted by 4 hectares and the Lower/Pioneer marsh has expanded by over 700 hectares (27% increase). The micro scale comparison reveals a 85.5% match for the Upper/Middle marsh class. A considerable amount of confusion is again present within the sub-zones defined by the two surveys. This is illustrated by the 382 hectares of saltmarsh classed as Upper/Middle marsh in the mixture map of the 1984 image being classed as Lower/Pioneer marsh in 1991 vegetation proportion map. Similarly nearly 300 hectares of saltmarsh classed as Upper/Middle marsh in the 1991 survey were classed as Lower/Pioneer marsh in the 1984 survey. This confirms the fact that the two broad zones of the different mixture models are not directly comparable as a result of the use of different vegetation endmembers in each of the surveys.

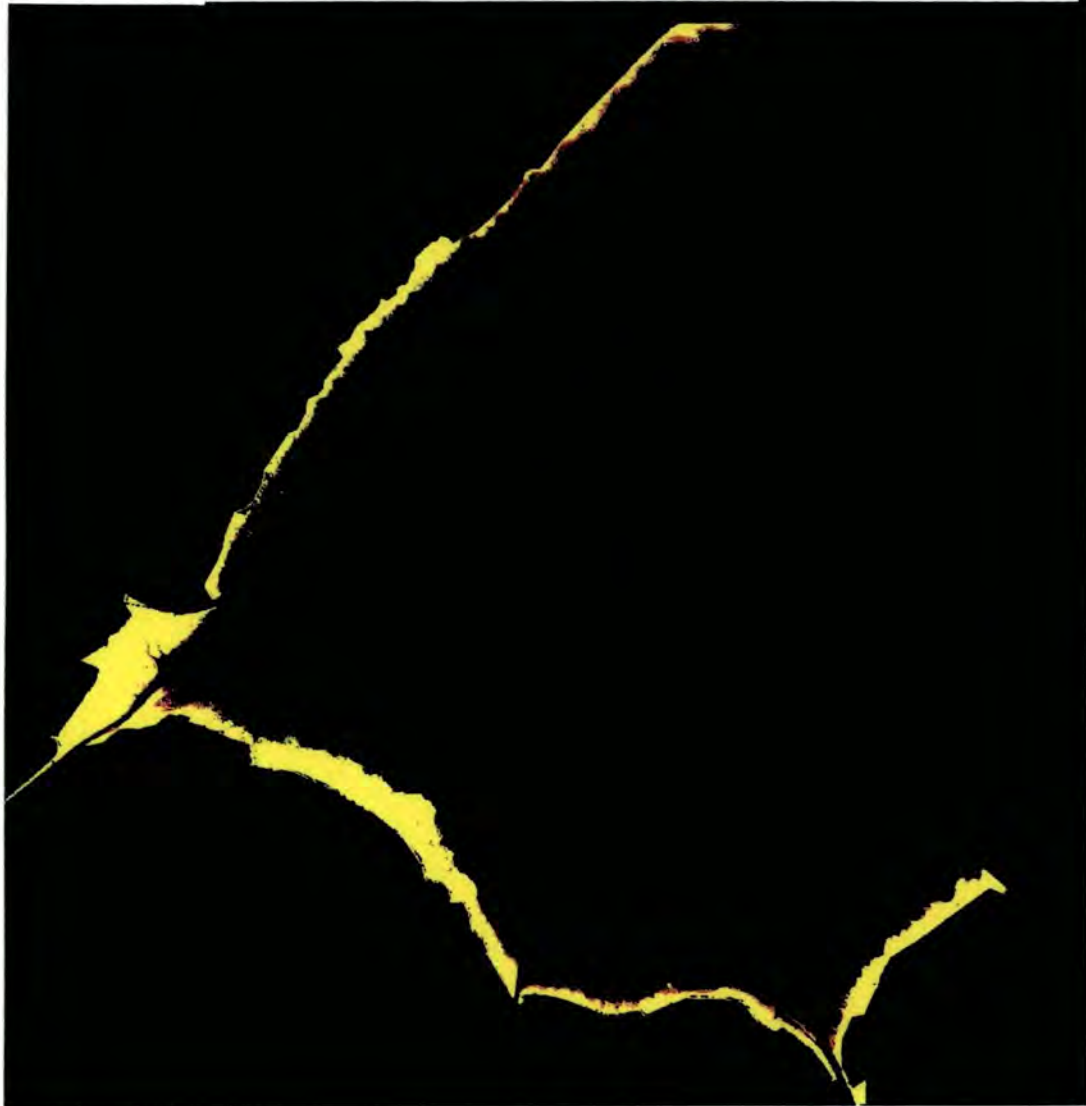
Cross tabulation of the Lower/Pioneer class reveals only a 35.5% match. This poor match may again be explained in part by confusion within the two broad saltmarsh classes. The Lower/Pioneer class involves a comparatively small area and therefore the inclusion of large areas of Middle marsh in the class, caused by artificial boundaries between Upper/Middle and Lower/Pioneer marsh, would have a large effect on the cross tabulation as revealed by the low agreement for the Lower/Pioneer zone. Of greater use is the cross tabulation of the saltmarsh area as a whole. The histograms reveal a consistent mark for separating the saltmarsh area from the rest of the intertidal zone. This cross tabulation reveals a 93% match. The main disagreement results from an area of over 500 hectares of saltmarsh classified in the 1991 vegetation proportion map that fail to be classified as saltmarsh in the 1984 vegetation proportion map. The thin green band at the edge of nearly all the saltmarsh in Fig 7.39 highlights this area and as expected corresponds with the Lower/Pioneer marsh zone. This area could not be detected in the 1984 image due to phenological effects and confirms the fact that the accuracy of the mixture model is affected by phenology.




Fig. 7.39 COMPARISON OF THE MAY 1984 VEGETATION PROPORTION MAP

AND THE SEPTEMBER 1991 VEGETATION PROPORTION MAP

Proportion Maps based on 14/5/84 & 7/9/91 Landsat 5 TM image(s)

scale 1 : 236,000



-  Saltmarsh areas mapped in both surveys
-  Saltmarsh mapped by the 1991 proportion map but not by the 1984 proportion map
-  Saltmarsh mapped by The 1984 proportion map but not by the 1991 proportion map

The effects of penology make it very difficult to identify areas of actual saltmarsh expansion as opposed to seasonal changes. Areas of expansion would appear to be present at the fronts of Terrington, Wainfleet, Wrangle And Freiston shores as well as at the mouth of the River Welland (Fig. 7.39). These cannot be confirmed as areas of saltmarsh expansion as there is no way of removing seasonal effects simply by comparing the two images. A more accurate map of expansion is gained through the comparison of the 1991 mixture model image and the 1982/4 N.C.C. survey. Also of interest are the areas of contraction illustrated in Fig. 7.39. These are generally small in area with the exception of the area fronting the Wolferton saltmarsh. The comparison of the 1984 vegetation proportion map with the N.C.C. survey suggested that this area corresponds to an intense algal bloom. Algal blooms are very dynamic and it is quite possible that such an intense feature may have disappeared by the time of the 1991 Landsat 5 TM image.

CONCLUSIONS FROM THE MIXTURE MODEL SURVEYS

The different classifications are summarised in Fig. 7.40. The meso and micro scale comparisons revealed much confusion among the classes defined by each of the surveys. This was to be expected as the criteria for membership in a class in the mixture model surveys and in the N.C.C. survey are very different. This may be illustrated by the example of heavily grazed areas of saltmarsh that tend to be confined to the Upper and Middle marsh zones. The presence of Upper marsh and Middle marsh plant species would result in these areas being classified as Upper/Middle marsh in the N.C.C. survey but the muddy surface of such areas, caused by the presence of grazing cattle, would result in such areas being classed as Lower/Pioneer marsh in the mixture model surveys. There is also considerable confusion between the classes of the two mixture models. This is expected as different saltmarsh vegetation endmembers were defined for each of the mixture models. The confusion between the definition of the classes in each of the surveys makes the use of the meso and micro scale comparisons questionable. Of greater significance are the macro scale comparisons and the %agreement resulting from the cross tabulation of the saltmarsh areas as a whole. Such comparisons avoid the confusion of sub-class definitions.

The comparison of the 1982/4 N.C.C. survey and the vegetation proportion map derived from the application of the mixture model to the May 1984 Landsat 5 TM image reveals a good overall match in estimating the area and extent of the intertidal saltmarsh. There is less than a 3% difference in total area and an 87% agreement produced by overlaying the two saltmarsh areas. The main differences were accounted for by the mixture model's failure to identify the extremities of the Lower and Pioneer saltmarsh. The effect of phenology on the mixture model was highlighted by the comparison of the N.C.C. survey with the 1991 mixture model and also by the comparison between the two mixture model surveys. Although the significance of the comparison between the N.C.C. survey and the mixture model of the 1991 image is slightly questionable as there is a seven year time lapse between the two surveys it does demonstrate the effects of seasonality on the mixture model and highlights areas of saltmarsh expansion. The 1991 mixture model mapped an area 4.5% larger than the 1982/4 N.C.C. survey and over 90% agreement was produced by overlaying the two saltmarsh areas. This level of agreement, with the comparison map (Fig. 7.39), illustrates that the 1991 mixture model is more effective than the 1984 mixture model in mapping the Lower and Pioneer zones of the saltmarsh. The comparison map also demonstrates that even late on in the growing season the mixture model still has difficulties in mapping the extremities of the Pioneer zone. The effects of phenology were further highlighted by the comparison of the vegetation proportion maps from the different images (Fig 7.39). The effects of phenology make it very difficult to identify areas of actual saltmarsh expansion rather than simply seasonal changes. In order to identify areas of change it is preferable to compare images taken at similar times of the year. This issue is discussed further in the closing chapter of the thesis.

PROBLEMS WITH THE MIXTURE MODEL

The use of a fully constrained model provided a number of problems in relation to the method of endmember selection used in the present study. Endmembers were selected from analysis of extracts of the intertidal zone, not from the analysis of the intertidal zone as a whole. This makes it likely that the "real" endmember, similar to E1 in Fig. 7.2, may not have been identified. This was demonstrated by the histograms in Fig.7.32. This could

be corrected by using an unconstrained mixture model or by the application of a mask to the intertidal zone assigning everything other than the intertidal area a no data value. The use of the mask would allow the application of a principal components analysis over the entire intertidal area and allow a more representative selection of endmembers.

A more serious problem associated with the method of endmember selection is that meaningful comparisons of mixture models applied to images of different dates at anything other than the macro scale is highly problematical. The main reason for this is that different endmembers were selected by the Principal Component Analysis of the two images. The problem again comes down to the dynamic nature of vegetation spectral signatures. Even after atmospheric and radiometric normalisation of images the same vegetation endmembers cannot be used for images of different dates as the spectral signature of a vegetation endmember constantly changes through the growing season. This means that image, rather than library endmembers, must be used for the purpose of applying a mixture model to saltmarsh vegetation. Comparisons between proportion maps derived from images taken from different dates become highly problematical. Considerable in-depth analysis needs to be carried out on the behaviour of vegetation spectra through the growing season to allow comparison at anything other than the broadest levels. The issue of vegetation spectrometry is addressed further in the concluding chapter.

Perhaps the most disappointing feature of the mixture model was its inability to identify the limits of the Pioneer zone. Phenology is an important factor in the performance of the mixture model but even late on in the growing season the mixture model proved unable to distinguish the extremities of the Pioneer zone from the intertidal sand and mudflats. There are several factors that may account for this poor performance and these must be addressed if the mixture model technique of mapping the intertidal zone is to be taken further.

The first of the problems is concerned with the scaling and aggregation techniques used in the present study. In order to mask out areas other than the intertidal zone the raw mixture model data was combined with a mask in T-Spectra. This program unfortunately re-scales the data between 0 and 255. The re-scaled data was then converted into % and

aggregated to provide the equivalent of a density sliced image. The analysis of raw un-aggregated mixture model data may provide a means of further discriminating the vegetation endmember component within a pixel. It does however remain questionable as to whether the mixture model could discriminate between Pioneer marsh and algal blooms on the intertidal flat. Analysis of the scaled data revealed that even when the tolerances of the saltmarsh class was widened to include pixels with 19 and 18% vegetation endmember contribution, significant areas of the intertidal mud and sandflats became included in the saltmarsh class. It may be that this is the limit of the capabilities of Landsat 5 TM data and that the Pioneer zone may only be discriminated from algae if data with greater spectral resolution are used. This may only be established through spectral analysis comparing the spectral signatures of algae and those of Pioneer marsh.

The mixture model proved to be accurate in defining the limits of the intertidal zone with the notable exception of the Pioneer zone. The use of the data from the mixture model is far from exhausted. This study concentrated only on the vegetation proportion maps. Considerable data is contained in the other proportion maps. For example an examination of Fig 7.25, the proportion map for the water endmember reveals a striking band (10 - 40% component of the spectral signature) that seems to correspond to the Pioneer zone. When this narrow band was isolated within GRID and combined with the saltmarsh map derived from the vegetation proportion map the resulting cross tabulation of the total saltmarsh area estimates with the 1982/4 N.C.C. survey led to an increased agreement of 94%, an improvement of 1.8%. When the same was done to the 1984 proportion maps the agreement rose to 90.4%, an improvement of 3%. The increase in agreement resulted from a greater area of the Pioneer zone being delimited. Some of the extremities still could not be identified but the overall performance was improved. The downside of this mapping technique is that areas of algae began to be included in the saltmarsh class.

A similar method of combination was carried out using the proportion map of the Pioneer endmember derived from the 1991 Landsat 5 TM image. In this case cross tabulation with the 1982/4 survey provided an overall match of greater than 95%. Only 118.5 hectares of saltmarsh mapped in the 1982/4 N.C.C. survey were not classified in the map resulting from the combination of the Pioneer endmember proportion map and the saltmarsh vegetation

endmember proportion map (Table 7.10). These were mainly accounted for by the extremities of the Pioneer zone on the Benington shore (Fig. 7.41). The use of the Pioneer endmember again had the side effect of including areas of algae on the intertidal flats being in the saltmarsh class, hence the large expansion figure of 846 hectares. The use of the other proportion maps demonstrates that the full potential of the mixture model data is far from being realised. The proportion maps related to the intertidal sediment endmembers contain much information that may be of considerable use in the mapping of intertidal sediments.

N.C.C. 1982/4	1991 Mixture Model			
Zones	Saltmarsh	Other	Total Area	% Agreement
Saltmarsh	3641.67	118.53	3760.20	96.8
Other	846.00	3608.57	4454.57	81.0
Total Area	4487.67	3727.10	8214.77	

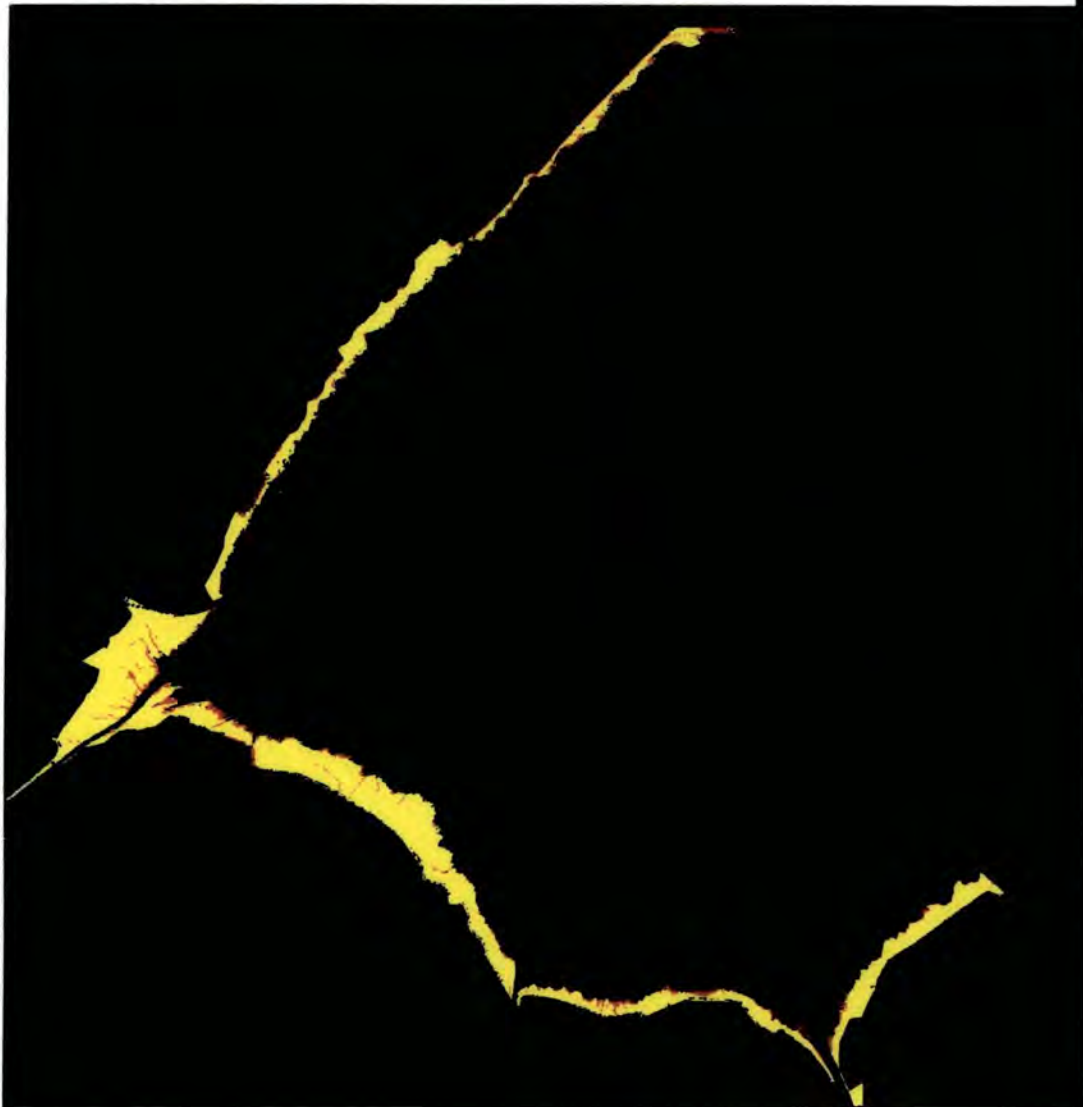
Table 7.10 Cross tabulation the total saltmarsh estimate of the N.C.C. 1982/4 survey and that of the map produced from the combination of the 1991 vegetation and pioneer proportion maps (Fig. 7.41)




The greatest concern with the mixture model technique is that a degree of non-linear spectral mixing may be taking place among the surfaces of the Pioneer zone. The inability of the mixture model to accurately locate the Pioneer zone makes this highly probable. This suspicion is enhanced by the water proportion map. The presence of large amounts of surface water and moisture is found throughout the saltmarsh. It however, only comes into the mixing equation in the Lower marsh and Pioneer zones as in the Upper and Middle marsh areas it is effectively masked by the presence of a well developed vegetation canopy. The canopy of the Lower and Pioneer marsh is by no means complete and so a more complex mixture equation has to be modelled involving the spectral signature of the water endmember and other surface components such as algae. The mixing nature of the spectral signature of water is a subject of considerable conjecture and the case for it mixing non-linearly is a strong one. The mixture models' difficulty in mapping the Pioneer zone adds supports to the argument that water mixes non-linearly. If this is the case then the application of a linear mixture model is bound to produce very poor results. Experimental work is required to establish the spectral mixing features of water.

Fig. 7.40 COMPARISON OF THE 1982/4 N.C.C. SURVEY AND
THE COMBINED 1991 VEGETATION & PIONEER PROPORTION MAPS

Proportion Images From 7/9/91 Landsat 5 TM Image

scale 1 : 236,000



-  Saltmarsh areas mapped in both surveys
-  Saltmarsh mapped by the N.C.C. survey but not in the mixture model
-  Saltmarsh mapped by the mixture model but not by the N.C.C. survey

WASH ESTUARY SALTMARSH SURVEYS

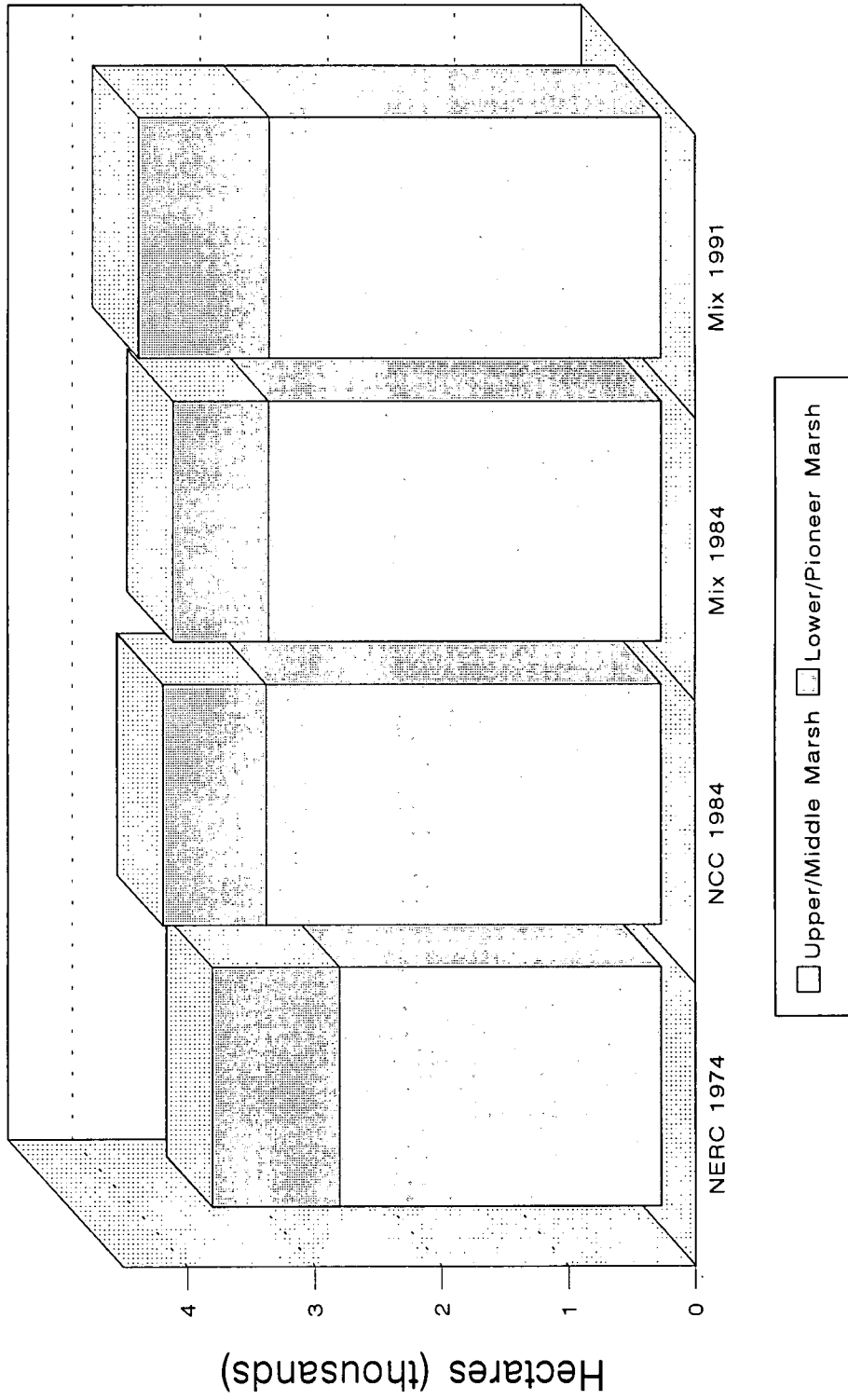


Fig. 7.41

Mixture modelling of the intertidal zone is highly problematical and really requires a number of models for the different components of the intertidal zone: the Upper and Middle marsh; the Pioneer zone; and the intertidal flats. It is perhaps surprising that the mixture model was successful in mapping and discriminating over 90% of the intertidal saltmarsh. The plots produced by the Principal Components indicate that mixture modelling has considerable potential in mapping and classifying intertidal sediments as the mixing plane is very clearly defined (Figs. 7.6, 7.14a, 7.15a) unlike that of vegetated surfaces. Although the preliminary spectral analysis of the vegetation spectral cloud in the Principal Component plots suggests a linear relationship, the analysis only looked at mixing along one plane. It is highly probable that there are a number of mixing planes within this cloud, which may or may not be linear in their nature. For example, it is highly unlikely that the spectral signal of algae can be modelled by a linear relationship as photons are likely to interact with more than one surface component thus adding considerable complexity to the mixing problem. The application of data with increased spectral resolution may be able to discriminate other endmembers within the vegetation cloud. This is not possible with the six TM bands used in the present study. The final chapter of the thesis compares the results of the two classification strategies and identifies their relative merits and drawbacks.

Adams, J.B. and Adams, J.D., 1984: Geologic mapping using Landsat MSS and TM images: removing vegetation by modelling spectral mixtures. **Proceedings of the Third Thematic Conference on Remote Sensing for Experimental Geology**. Colorado Springs, Colorado, (Michigan: ERIM): 615-622.

Adams, J.B., Smith, M.O., and Johnson, P.E., 1986: Spectral mixture modelling: a new analysis of rock and soil types at the Viking Lander I site. **Journal of Geophysical Research**. vol. 91: 8098-8112.

Adams, J.B., Smith, M.O., Johnson, P.E. 1985: Spectral mixture modelling: A new analysis of rock and soli types at the Viking Lander I site. **Journal of Geophysical Research**. vol. 7: 8098-8112.

Cross, A.M., Settle, J.J., Drake, N.A. and Paivinen, R.T.M. 1991: Sub-pixel measurement of tropical forest cover using A.V.H.R.R. data. **International Journal of Remote Sensing**. vol. 12: 1119-1129.

Detchmendy, D.M and Pace, W.H. 1972: A model for spectral signature variability for mixtures. in Shahrokhi, I.F.(ed) **Remote Sensing of Earth Resources**. University Tennessee Press. vol. 1: 596-620.

Friedman, J.H. and Turkey, J.W. 1974: A projection pursuit algorithm for exploratory data analysis. **I.E.E.E. Transactions on Computers**. vol. 2: 881-889.

Gillespie, A.R., Smith, M.O., Adams, J.B., Willis, S.C., Fischer, A.F. and Sabol, D.E. 1990: Interpretation of residual images: spectral mixture analysis of AVIRIS images. Owens Valley, California, **Proceedings of the Airborne Science Workshop: AVIRIS, JPL, Pasadena, C.A., (JPL Publication 90-54): 243-270.**

- Hapke, B. 1981: Bidirectional reflectance spectroscopy. **Journal of Geophysical Research**. vol 86: 3039-3054.
- Holben, B.N. and Shimabukuro, Y.E. 1993: Linear mixing model applied to coarse spatial resolution data from multispectral satellite sensors. **International Journal of Remote Sensing**. vol. 14: 2231-2240.
- Horwitz, H.M., Nalepka, R.F., Hyde, P.D., and Morgenstern, J.P. 1971: **Estimating The Proportions of Objects Within a Single Resolution Element of a Multispectral Scanner**. University of Michigan, Ann Arbor, Michigan, NASA Contract NAS-9-9784.
- Lenninton, R.K., Sorensen, C.T. and Heydorn, R.P. 1984: A mixture model approach for estimating crop areas from Landsat data. **Remote Sensing of Environment**. vol. 14: 197-206.
- Millington, A.C., Drake, Townshend, J.R.G, Quarmby, N.A. 1989: Settle, J.J. and Reading, A.J. : Monitoring salt playa dynamics using thematic mapper data. **I.E.E.E. Transactions on Geoscience and Remote Sensing**. vol. 27: 754-761.
- Quarmby, N.A., Townshend, J.R.G., Settle, J.J. and White, K.H. 1992: Linear mixture modelling applied to A.V.H.R.R. data for crop area estimation. **International Journal of Remote Sensing**. vol. 13: 415-425.
- Roberts, D.A. 1991: Leaf spectral types, residuals and canopy shade in an AVIRIS image. **Proceedings of the 3rd AVIRIS Workshop**. Pasadena, May 20: 43-50.
- Settle, J.J., Drake, N.A. 1993: Linear mixing and the estimation of ground cover proportions. **International Journal of Remote Sensing**. vol. 14: 1159-1177.
- Singer, R.B. and McCord, T.B. 1979: Large scale mixing of dark and bright surface materials and implications for analysis of spectral reflectance. **Proceedings of the 10th Lunar Planetary Science Conference**: 3557-3561.
- Shimabukuro, Y.E. and Smith, A.S. 1991: The least-squares mixing models to generate fraction images derived from remote sensing multispectral data. **I.E.E.E. Transactions on Geoscience and Remote Sensing**. vol. 29: 16-20.
- Smith, M.O., Johnson, P.E., and Adams, J.B. 1985: Quantitative determination of mineral types and abundances from reflectance spectra using principal component analysis. **Journal of Geophysical Research**. vol. 90: 792-804.

CHAPTER 8

DISCUSSION AND CONCLUSIONS

In order to evaluate the strengths and weaknesses of the different classification strategies the surveys were compared with each other. A summary of all the surveys incorporated into the Wash GIS is presented in Table 8.1. Areal comparisons were carried out at the macro and meso scales. The Upper and Middle marsh zones of the MLC classification were aggregated to allow comparison with the mixture model surveys. Cross tabulation was carried out on the broad zones and on the total saltmarsh areas. The results of the cross tabulation of the two classification strategies are presented in Tables 8.2-8.9.

ZONE	1971/4 NERC Survey	1982/4 NCC Survey	1984 MLC Operator 1	1984 MLC Operator 2	1984 Mix Model	1991 MLC Operator 1	1991 MLC Operator 2	1991 Mix Model
Upper/ Middle Marsh	2538.86	3114.83	3078.36	2923.02	3095.10	3435.08	3395.43	3090.87
Lower/P ioneer	997.43	807.72	268.02	162.27	746.91	725.77	557.82	1023.39
Total	3536.29	3922.55	3346.38	3085.29	3842.01	4160.85	3953.25	4114.26

Table 8.1 Wash Estuary Surveys. Areas in hectares.

1984 Mix Model	MLC 1984 Operator 1				
Zone	Upper/Middle Marsh	Lower/Pioneer Marsh	Other	Total Area	% Agreement
Upper/Middle Marsh	2567.70	92.25	319.23	2979.18	86.2
Lower/Pioneer Marsh	321.66	126.09	271.17	718.92	17.5
Other	108.63	44.73	4282.47	4435.83	96.5
Total Area	2997.99	263.07	4872.87	8133.93	

Table 8.2 Cross tabulation of the 1984 mixture model with the 1984 MLC (operator 1). Areas in hectares.

1984 Mix Model	MLC 1984 Operator 2				
Zone	Upper/Middle Marsh	Lower/Pioneer Marsh	Other	Total Area	% Agreement
Upper/Middle Marsh	2410.74	79.92	604.44	3095.10	77.9
Lower/Pioneer Marsh	304.20	92.60	350.10	746.90	12.4
Other	16.20	3.51	4890.33	4910.04	99.6
Total Area	2731.14	176.03	5844.87	8752.04	

Table 8.3 Cross Tabulation of the 1984 Mixture model with the 1984 MLC (operator 2). Areas in hectares.

1991 Mix Model	MLC 1991 Operator 1				
Zone	Upper/Middle Marsh	Lower/Pioneer Marsh	Other	Total Area	% Agreement
Upper/Middle Marsh	2402.37	187.20	461.43	3051.00	78.7
Lower/Pioneer Marsh	387.54	239.13	393.66	1020.33	23.4
Other	220.32	171.70	4240.08	4632.10	91.5
Total Area	3010.23	598.03	5095.17	8703.43	

Table 8.4 Cross tabulation of the 1991 mixture model with the 1991 MLC (operator 1). Areas in hectares.

1991 Mix Model	MLC 1991 Operator 2				
Zone	Upper/Middle Marsh	Lower/Pioneer Marsh	Other	Total Area	% Agreement
Upper/Middle Marsh	2771.55	66.24	253.08	3090.87	89.7
Lower/Pioneer Marsh	522.00	261.45	239.94	1023.39	25.5
Other	119.70	324.54	4193.55	4637.79	90.4
Total Area	3413.25	652.23	4686.57	8752.05	

Table 8.5 Cross tabulation of the 1991 mixture model with the 1991 MLC(operator 2). Areas in hectares.

1984 Mix Model	1984 MLC Operator 1			
Zones	Saltmarsh	Other	Total Area	% Agreement
Saltmarsh	3107.70	590.40	3698.10	84.0
Other	153.36	4372.47	4525.83	96.6
Total Area	3261.06	4962.87	8223.93	

Table 8.6 Cross tabulation of the 1984 mixture model with the 1984 MLC (operator 1). Areas in hectares.

1984 Mix Model	1984 MLC Operator 2			
Zones	Saltmarsh	Other	Total Area	% Agreement
Saltmarsh	2887.47	954.54	3842.01	75.1
Other	19.71	4890.33	4910.04	99.6
Total Area	2907.18	5844.87	8752.05	

Table 8.7 Cross tabulation of the 1984 mixture model with the 1984 MLC (operator 2). Areas in hectares.

1991 Mix Model	1991 MLC Operator 1			
Zones	Saltmarsh	Other	Total Area	% Agreement
Saltmarsh	3216.24	855.09	4071.33	78.9
Other	392.04	4240.08	4632.12	91.5
Total Area	3608.28	5095.17	8703.45	

Table 8.8 Cross tabulation of the 1991 mixture model with the 1991 MLC (operator 1). Areas in hectares.

1991 Mix Model	1991 MLC Operator 2			
Zones	Saltmarsh	Other	Total Area	% Agreement
Saltmarsh	3621.24	493.02	4114.26	88.0
Other	444.24	4193.55	4637.79	90.4
Total Area	4065.48	4686.57	8752.05	

Table 8.9 Cross tabulation of the 1991 mixture model with the 1991 MLC (operator 2). Areas in hectares.

COMPARISON BETWEEN THE VEGETATION PROPORTION MAP OF THE MAY 1984 LANDSAT 5 TM IMAGE AND THE MLC CLASSIFICATIONS OF THE MAY 1984 LANDSAT 5 TM IMAGE (Tables 8.2, 8.3, 8.6, 8.7, Fig. 8.1)

The comparison of the two classification strategies is useful as it emphasises the different criteria used in each classification strategy. This highlights the merits and disadvantages of each technique. At the broadest level of comparison, that of total saltmarsh area, the mixture model survey estimated a considerably larger area of saltmarsh. The mixture model survey estimated 495 hectares (14%) of saltmarsh more than the MLC classification of operator 1 and 757 hectares (20%) more than operator 2. In both cases the differences were accounted for by large differences in area estimates of the Lower and Pioneer marsh. This is explained by the poor performance of the MLC in classifying the Lower and Pioneer areas of saltmarsh during the early part of the growing season (chapter 6).

The comparison of the broad saltmarsh zones reveals that there is less than a 10% difference between the Upper/Middle marsh areas estimated by the different survey techniques. The estimates for the Lower/Pioneer class show a difference of 479 hectares (65%) between the mixture model and the MLC (operator 1), and a difference of 585 hectares (75%) with operator 2. In both case the mixture model estimated the larger area.

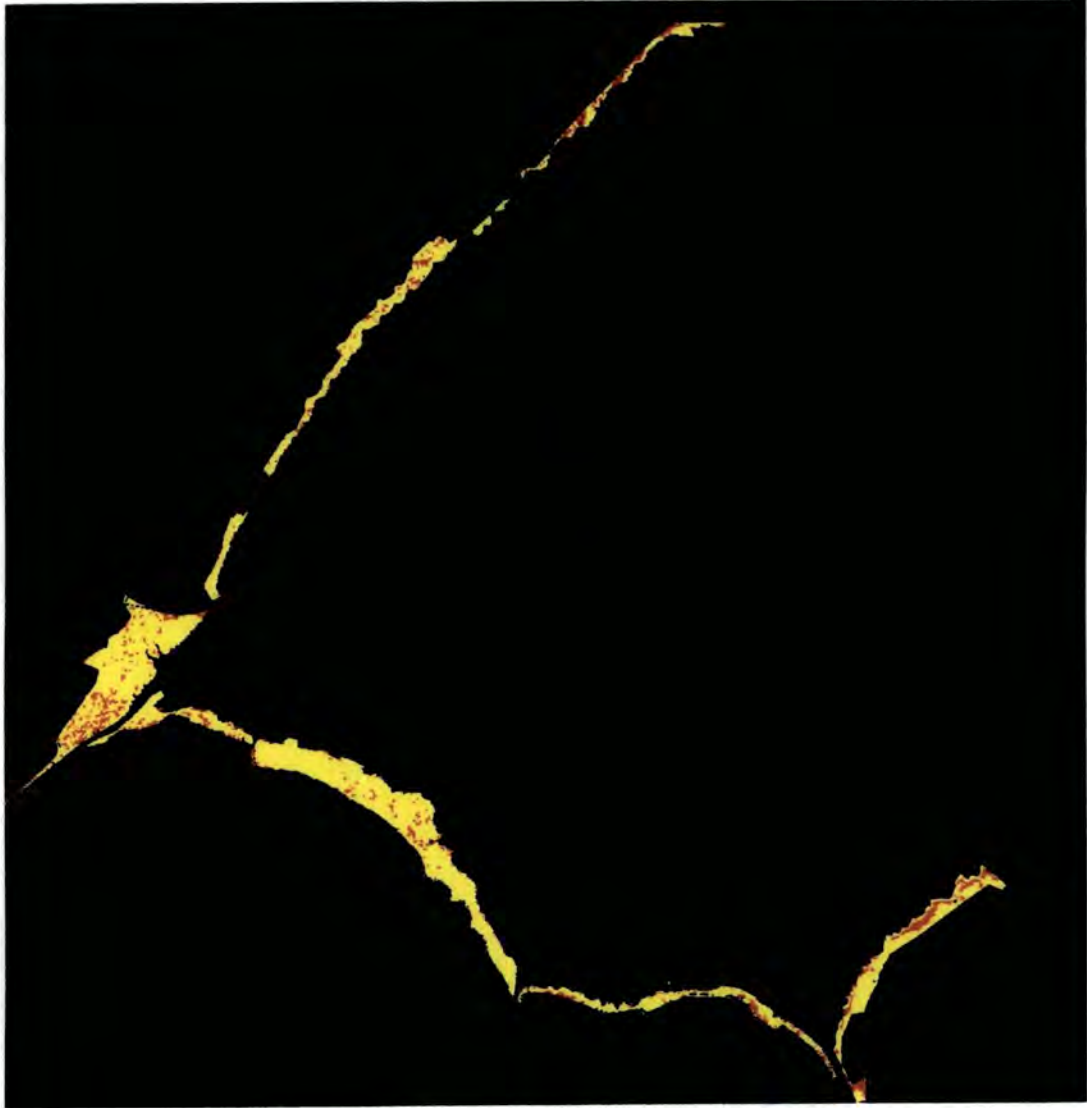
Cross tabulation between the 1984 mixture model and the 1984 MLC classifications reveals greater than 75% agreement for the Upper/Middle marsh class. This compares with only a 17.5% agreement for the Lower/Pioneer zone (operator 1, and 12.4% operator 2). Examination of Table 7.2 reveals that the large discrepancy in the Lower/Pioneer comparison figure results from 271 hectares of saltmarsh classified as Lower/Pioneer marsh in the mixture model failing to be classified as saltmarsh in the MLC classification (operator 1). In the comparison with the classification of operator 2 this figure is 350 hectares. There are also over 319 hectares of saltmarsh classified as Upper/Middle marsh in the mixture model that are not classified as saltmarsh in the MLC classification (operator 1). There is considerable confusion between the classes of the different surveys. This is illustrated by the 321 hectares of saltmarsh classified as Lower/Pioneer marsh by the mixture model but as




Fig. 8.1 COMPARISON OF THE 1984 MIXTURE MODEL SURVEY

AND THE 1984 MAXIMUM LIKELIHOOD CLASSIFICATION (OPERATOR 2)

Surveys based on 14/5/84 Landsat5 TM image

scale 1 : 236,000



-  Saltmarsh areas mapped in both surveys
-  Saltmarsh mapped by the mixture model but not by the MLC
-  Saltmarsh mapped by the MLC but not by the mixture model

Upper/Middle marsh by the MLC (operator 1). Membership in the MLC classifications is dependent on the similarity of the spectral signature of a pixel with the spectral signature of the training areas. In the mixture model, class is dependent on the spectral contribution of the vegetation endmember within the spectral signature of a pixel.

Cross tabulation of the entire saltmarsh area results in agreement of 84% for the MLC of operator 1 (Table 8.6) and 75% for the MLC of operator 2 (Table 8.7). The differences are caused by large areas of saltmarsh not being identified by the MLC due to the effects of phenology. This is highlighted by Fig. 8.1. The red identifies areas of saltmarsh located by the mixture model but not by the unfiltered MLC. Areas of Lower and Pioneer marsh not identified by the MLC are most notable on the Wainfleet shore, Benington, Terrington and Wolferton saltmarshes. There are also considerable areas of Upper/Middle saltmarsh not identified by the MLC. Good illustrations of this may be seen at Leverton, Frampton and Kirton saltmarshes. There are virtually no areas classified as saltmarsh by the MLCs but not by the mixture model. The mixture model appears to be less affected by phenology during the early stages of the growing season than the MLC. During the early part of the growing season the mixture model is a more effective survey technique for establishing the extent of the saltmarsh. Whether this holds true for the rest of the growing season is revealed by the comparison of the mixture model of the September 1991 Landsat 5 TM image and the corresponding maximum likelihood classifications.

COMPARISON BETWEEN THE 1991 MAXIMUM LIKELIHOOD SURVEYS AND THE 1991 MIXTURE MODEL SURVEY (Tables 8.5, 8.6, 8.8, 8.9, Fig. 8.2)

There is a very good correlation between the total saltmarsh area estimates of the two different survey methods. The 1991 mixture model estimated an area of saltmarsh only 1% smaller than the estimate from the MLC of operator 1 and an area 4.1% larger than that of operator 2. There is considerable confusion within the estimates of the two broad zones of saltmarsh. The MLC classification (operator 1) estimated 344 hectares of Upper/Middle marsh more than the mixture model but 298 hectares less of Lower/Pioneer marsh. Similarly the MLC of operator 2 estimated 305 hectares of Upper/Middle marsh more than the 1991 mixture model but 465 hectares less of Lower/Pioneer marsh. This is most likely explained

by confusion between the definition of the classes. The confusion is confirmed by the micro-level comparisons. The agreement for the saltmarsh zones of the maximum likelihood classifications (operator 1) are 79% for the Upper/Middle marsh and only 23% for the Lower/Pioneer marsh. The differences are in part caused by the confusion between the classes with over 380 hectares classified as Lower/Pioneer marsh by the mixture model survey being classified as Upper/Middle marsh in the MLC of operator 1. This confusion was even more evident in the comparison with the MLC classification of operator 2. Table 8.5 illustrates that 500 hectares of saltmarsh classified as Lower/Pioneer marsh by the mixture model were classified as Upper/Middle marsh by the MLC.

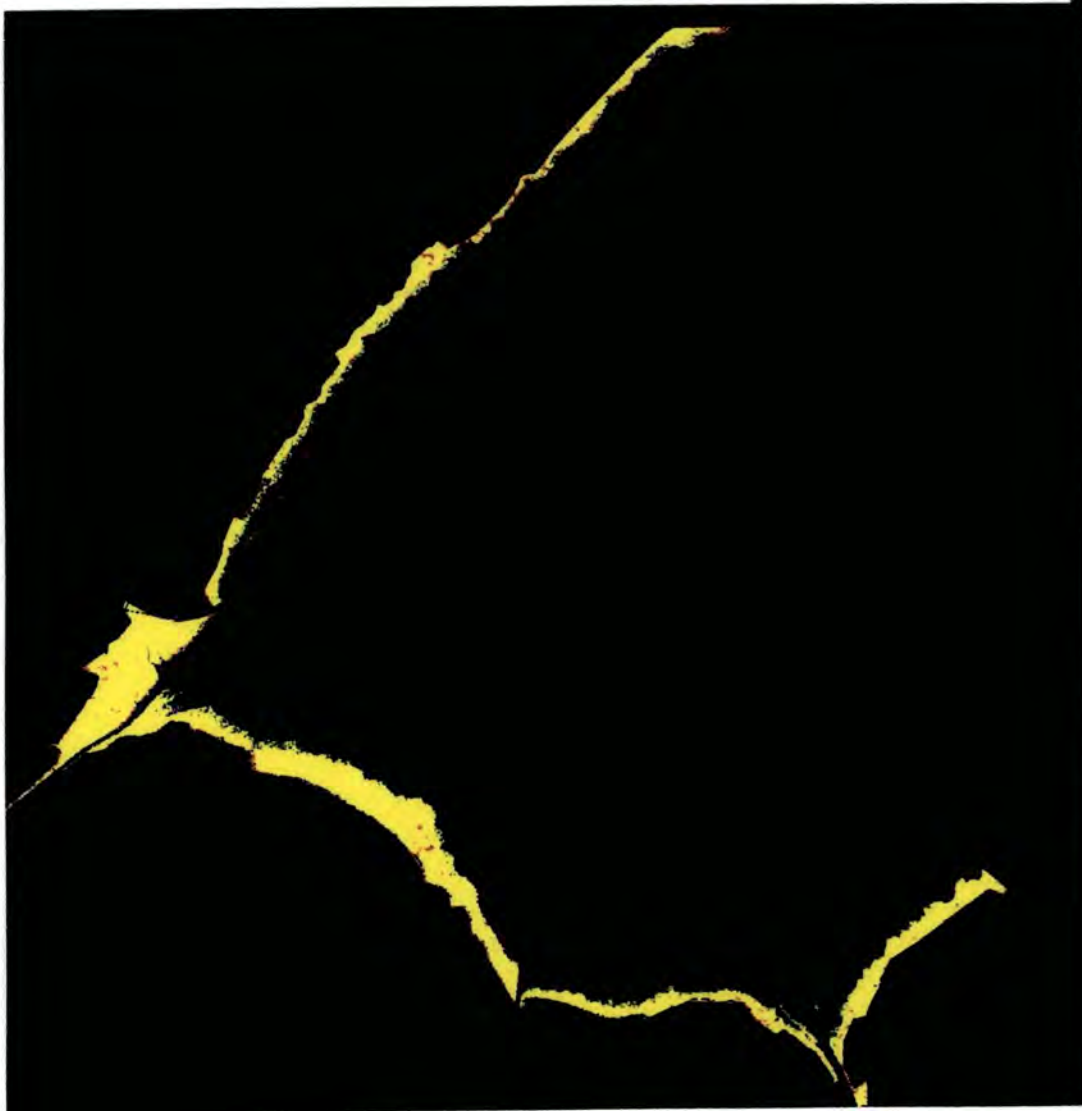
Of greater interest is the cross tabulation of the total saltmarsh areas. The agreement between the MLC of operator 1 and the mixture model is 79%. Table 8.8 reveals that there are considerable areas of saltmarsh picked up by only one of the surveys. 855 hectares of saltmarsh classified by the mixture model were not classified by the MLC (operator 1) but there are also 392 hectares of saltmarsh classified by the MLC but not by the mixture model. Fig. 8.2 identifies these respective areas. The areas in green represent the areas mapped by the MLC (operator 1) but not by the mixture model survey. These generally correspond with a thin band of Lower/Pioneer marsh along almost all of the seaward edges of the Wash Estuary saltmarshes and are especially noticeable at Leverton, Butterwick, Holbeach, Terrington and at the mouth of the Welland. The area in red represents saltmarsh classified by the mixture model but not by the MLC (operator 1). In general these correspond with development at the back of the saltmarsh in the area of the borrow pits. These areas are mapped as Pioneer saltmarsh by the mixture model but are not identified by the MLC classifications. A good example of this is the development at the back of the Freiston shore where the saltmarsh is only just beginning to recover from the most recent reclamations. There are also considerable areas of saltmarsh on the shores of Wainfleet and Friskney that were classified by the mixture model but not by the MLC. The Pioneer zone at Kirton and Frampton was similarly identified by the mixture model but not by MLC classifications.

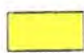


Fig. 8.2 COMPARISON OF THE 1991 MIXTURE MODEL SURVEY

AND THE 1991 MAXIMUM LIKELIHOOD CLASSIFICATION (OPERATOR 1)

Surveys based on 7/9/91 Landsat5 TM image

scale 1 : 236,000



-  Saltmarsh areas mapped in both surveys
-  Saltmarsh mapped by the mixture model but not by the MLC
-  Saltmarsh mapped by the MLC but not by the mixture model

CONCLUSIONS FROM THE COMPARISON OF THE TWO SURVEY METHODS

The macro level comparisons revealed good agreement for the surveys resulting from the processing of the September 1991 Landsat 5 TM image but much poorer agreement for the surveys resulting from the processing of the May 1984 image (Fig. 8.3). The poor levels of agreement for the 1984 surveys occurred due to the problems that the maximum likelihood classifications had in identifying areas of Lower and Pioneer marsh. These were revealed both through the cross tabulations and the resulting map (Fig 8.1).

The poor ability of the MLC in identifying areas of Lower and Pioneer marsh proved to be a seasonal problem as the comparisons of the 1991 surveys revealed that the maximum likelihood method of classification was more successful in identifying the Pioneer zone (Fig. 8.2). Although the MLC was more successful at this stage in the growing season in identifying the Pioneer zone there were still considerable areas of saltmarsh that the mixture model classified as saltmarsh that were not identified by the MLC. This is most likely attributable to the different criteria for membership in the classes of the two survey methods. This resulted in confusion and poor agreement figures for the broad zone cross tabulations and especially for the Lower/Pioneer zone. Figures of over 75% agreement resulted from the cross tabulation of the entire saltmarsh areas. The disagreements in the surveys illustrate that each of the classification strategies has its own particular merits. Two different types of information are given by the classifications. The MLC reveals information about the vegetation species whereas the mixture model reveals information about the vegetation cover. The most accurate classification strategy should therefore include both techniques.

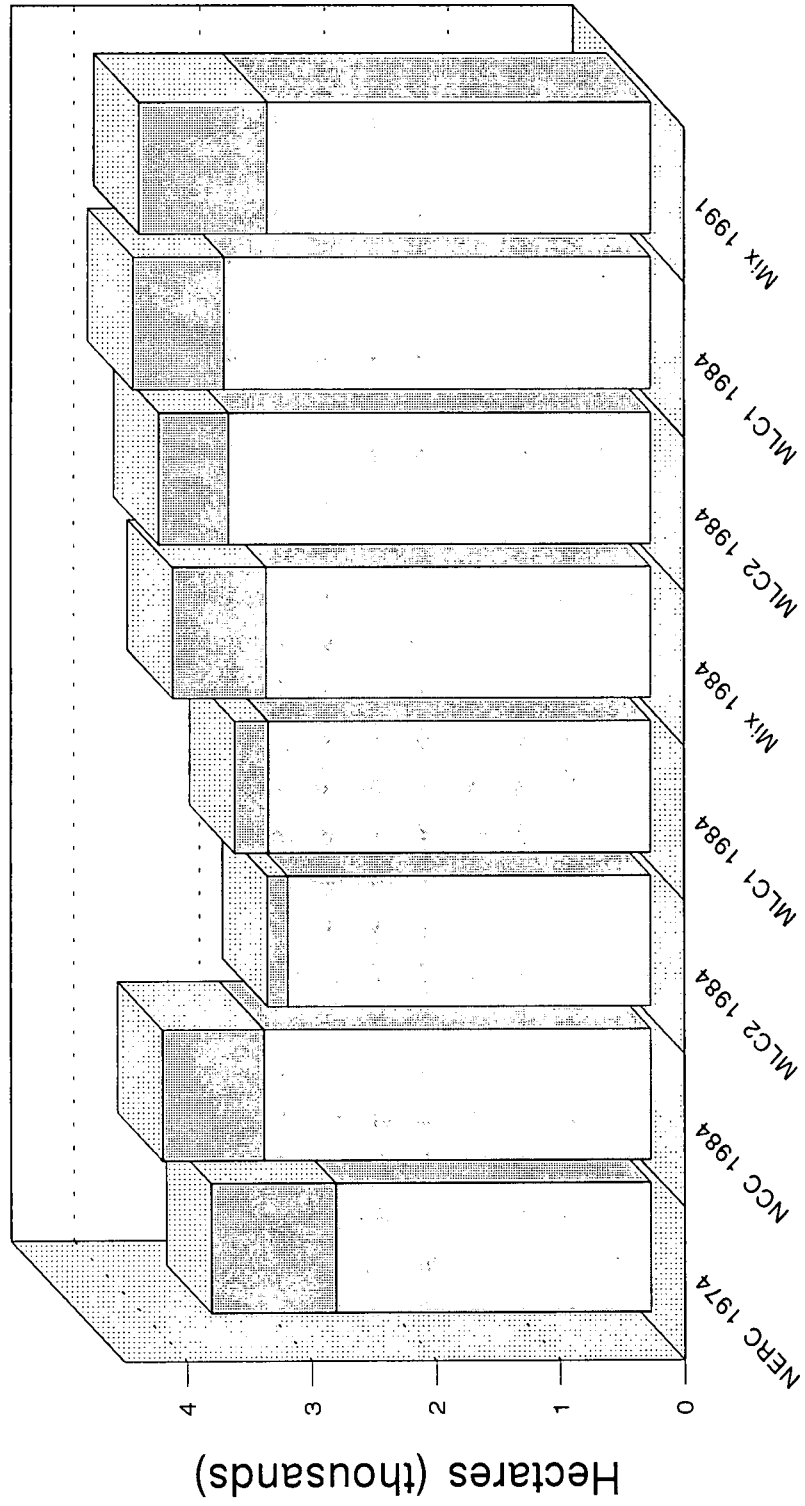
CONCLUSIONS FROM THE CLASSIFICATION STRATEGIES

Table 8.10 and Fig. 8.3 summarises the information gained from comparing the different classification surveys with the 1982/4 N.C.C. survey. The examination of the two classification strategies revealed that the extent of saltmarsh vegetation can be accurately estimated using Landsat 5 TM data.

Table 8.10 Summary of Wash Estuary Saltmarsh Surveys

Saltmarsh Area Estimate (Compared with that of the 1982/4 N.C.C. survey)					
	1984 MLC 2	1984 Mix	1991 MLC 1	1991 MLC 2	1991 Mix
% Difference compared with N.C.C. survey	-21.3	-2.0	+6.1	+0.8	+4.9
1984 MLC 1	-14.1				
Saltmarsh Zonal Area Estimates (Compared with those of the 1982/4 N.C.C. survey)					
	1984 MLC 2	1984 Mix	1991 MLC 1	1991 MLC 2	1991 Mix
Zones					
Upper/Middle marsh	-6.2	-0.6	+10.3	+9.0	-0.8
Lower/Pioneer marsh	-79.9	-7.5	-10.1	-30.9	+26.7
1984 MLC 1					
Matching Zonal Areas of Saltmarsh (Cross Tabulated with the 1982/4 N.C.C. survey)					
	1984 MLC 2	1984 Mix	1991 MLC 1	1991 MLC 2	1991 Mix
Zones					
Upper/Middle Marsh	81.4	87.3	87.6	87.6	83.4
Lower/Pioneer marsh	7.5	24.9	35.6	38.9	37.7
1982 MLC 1					
Total Saltmarsh Area Agreement (Cross Tabulated with the 1982/4 N.C.C. survey)					
	1984 MLC 2	1984 Mix	1991 MLC 1	1991 MLC 2	1991 Mix
% Agreement	70.7	87.4	89.2	90.1	92.2
1984 MLC 1					
80.1					

WASH ESTUARY SALTMARSH SURVEYS



□ Upper/Middle Marsh □ Lower/Pioneer Marsh

Fig. 8.3

The largest difference in area estimate came from the 1984 MLC classifications. Operator 1 estimated an area 14.1% less than the 1982/4 N.C.C. survey whilst the figure for operator 2 was 21.3%. The difference between all the other surveys and the 1982/4 N.C.C. was less than 7%. Cross tabulation of the broad zones revealed good agreement for the Upper/Middle marsh but much poorer agreement for the Lower/Pioneer marsh. The highest agreement reached for the Lower/Pioneer zone was only 38.9% (1991 MLC, operator 2). Cross tabulation of the entire saltmarsh areas estimated by the surveys and the 1982/4 N.C.C. revealed that no survey achieved less than 70% agreement. If the 1984 MLC classifications are not included none of the surveys achieved less than 87% agreement. 92% agreement was achieved by the 1991 mixture model.

The comparison of the maximum likelihood classifications with the 1984 N.C.C. survey illustrated that the Upper, Middle marsh zones could be located with a high degree of accuracy. Similarly late on in the growing season the Lower marsh could be delimited. All the classifications had considerable difficulty in surveying the Pioneer zone. Cross tabulation with the N.C.C. survey revealed poor levels of agreement. Indeed the highest level of agreement achieved was only 38.9%. The poor levels of agreement in part reflect not only the dynamism of this region of the saltmarsh but also the limitations of the classification strategies. Particularly poor results were achieved early on in the growing season with the mixture model performing marginally better. Early on in the growing season the spectral signature of the Pioneer zone vegetation is not strong enough to be separated from the spectral signal of the intertidal mud and sand flats. Late on in the growing season it is difficult to distinguish the spectral signal of the Pioneer zone from that of algae. In the Pioneer zone water and algae enter the mixing equation. It is likely that these components do not mix linearly. Mixture modelling has normally been applied to relatively simple mixing problems such as geological mapping in a desert environment (Millington *et al.*, 1989) or vegetation mapping of agriculture (Quarmby *et al.*, 1992). It is therefore surprising that the mixture model operated so well in the complex mixing environment of the intertidal zone. The spectral resolution of Landsat 5 TM data is not sufficient to separate the spectral signature of algae from that of sparse vegetation in the Pioneer zone. Detailed spectrometry will reveal if higher spectral resolution data can separate these components. Similarly the use of data with more spectral bands may allow more endmembers to be defined. Spectral

readings of saltmarsh vegetation taken throughout the growing season may also identify the point in the growing season when optimum species differentiation may be achieved. There also remain other classification strategies to be examined of which Neural Networking is an example.

In order to quantify accurately saltmarsh expansion and contraction it is important that images taken at similar times in the growing season are compared. This helps to account for the effects of season. At present this is often difficult to achieve as the return period of the Landsat 5 satellite is approximately 16 days and the presence of cloud often results in much data being unusable. The introduction of sensors, such as SPOT HRV, which are able to acquire images at different viewing angles and have "steering" capabilities considerably reduces the return period. This may have a considerable impact on the ability to monitor the environment from satellite altitudes.

Fig 8.3 illustrates a continuing trend of saltmarsh expansion. The Wash GIS is not only able to quantify this expansion but can pinpoint specific areas of expansion and contraction and estimate rates. Similarly the GIS can estimate and model rates of recovery after reclamation. The MLC classification reveals considerable information about the distribution of plant species within the saltmarsh and the rate of maturity. The mixture model gives added information about the vegetation cover. This may be valuable in monitoring the effects of grazing on a saltmarsh. Used in conjunction the classification strategies provide accurate, relatively inexpensive and quick method of surveying intertidal vegetation. The use of Arc/Info GRID provides a fast, accurate and manageable method of incorporating the information gained from the satellite imagery into the coastal monitoring GIS and avoids the complex series of operations needed to convert the classifications into coverages.

A considerable amount of work still needs to be done if the method is to be used in an operational mode. Subjectivity is present in the selection of training areas and endmembers. In an operational mode it is suggested that the same training areas should be used and only modified on subsequent surveys, not changed completely. The selection of endmembers is much more amenable to automatic selection. A C-Program could be written to extract pixels from the extremes of the mixing planes. Objectivity also remains in the

selection of GCPs for geometrically rectifying the classifications. The revised methodology outlined in chapter 5 reduces the potential for error in this operation. The possibility exists for producing a valuable tool for monitoring and managing the coastal environment.

Millington, A.C., Drake, Townshend, J.R.G, Quarmby, N.A. 1989: Settle, J.J. and Reading, A.J. : Monitoring salt playa dynamics using thematic mapper data. **I.E.E.E. Transactions on Geoscience and Remote Sensing**. vol. 27: 754-761.

Quarmby, N.A., Townshend, J.R.G., Settle, J.J. and White, K.H. 1992: Linear mixture modelling applied to A.V.H.R.R. data for crop area estimation. **International Journal of Remote Sensing**. vol. 13: 415-425.

REFERENCES

- Adams, J.B. and Adams, J.D. 1984: Geologic mapping using Landsat MSS and TM images: removing vegetation by modelling spectral mixtures. **Proceedings of the Third Thematic Conference on Remote Sensing for Experimental Geology**. Colorado Springs, Colorado, (Michigan: ERIM): 615-622.
- Adams, J.B., Smith, M.O., and Johnson, P.E. 1986: Spectral mixture modelling: a new analysis of rock and soil types at the Viking Lander I site. **Journal of Geophysical Research**. vol. 91: 8098-8112.
- Allen, J.R.L and Pye, K. 1992: Coastal saltmarshes: their nature and importance. In Allen, J.R.L. and Pye, K. (eds) **Saltmarshes. Morphodynamics, Conservation and Engineering Significance**. Cambridge University Press, Cambridge: 1-18.
- Banninger, C. 1990: Fluorescence Line Imager Measured "Red Edge" Shifts. **Proceedings In Imaging Spectroscopy of the Terrestrial Environment**. vol. 1298.
- Bartlett, D.S. and Klemas, V. 1979: Assessment of tidal wetland habitat and productivity. **Proceedings of the 13th Symposium on Remote Sensing of Environment**. Ann Arbor, Michigan: 1241-1260.
- Bartlett, D.S. and Klemas, V. 1980: Quantitative assessment of tidal wetlands using remote sensing. **Environmental Management**. vol. 4: 337-345.
- Bauer, M.E., Daughtry, C.S.T., Biehl, L.L., Kanemasu, E.T., and Hall, F.G. 1986: Field spectroscopy of agricultural crops. **Transactions on Geoscience and Remote Sensing**. vol. 24: 65-75.
- Brampton, A.H. 1992: Engineering significance of British saltmarshes. In Allen, J.R.L. and Pye, K. (eds) **Saltmarshes. Morphodynamics, Conservation and Engineering Significance**. Cambridge University Press, Cambridge: 115-122.
- Browder, J.A., Nelson May, L., Rosenthal, A., Gosselink, J.G. and Baumann, R.H. 1989: Modelling future trends in wetland loss and brown shrimp production in Louisiana using Thematic Mapper Imagery. **Remote Sensing of Environment**. vol. 28: 45-59.
- Budd, J.T.C. and Milton, E.J. 1982: Remote sensing of saltmarsh in the first four proposed thematic bands. **International Journal of Remote Sensing**. vol. 3: 147-161.
- Campbell, J.B. 1987: Remote Sensing Applications in the Plant Sciences. **Introduction to Remote Sensing**. Guildford Press, London: 366-403.

- Carter, V. and Schubert, J. 1973: Coastal wetlands analysis from ERTS MSS digital data and field spectral measurements. **Proceedings of the Ninth International Symposium on Remote Sensing of the Environment**. Ann Arbor Michigan, USA: 1241-1260.
- Collins, W. 1978: Remote Sensing of Crop Type and Maturity. **Photogrammetric Engineering and Remote Sensing**. vol. 44: 43-55.
- Crist, E.P. and R.C. Cicone 1984: A physically-based Transformation of Thematic Mapper Data - The TM Tassled Cap, I.E.E.E. **Transactions in Geoscience and Remote Sensing**. vol. 10:1127-1134.
- Cross, A.M., Settle, J.J., Drake, N.A. and Paivinen, R.T.M. 1991: Sub-pixel measurement of tropical forest cover using A.V.H.R.R. data. **International Journal of Remote Sensing**. vol. 12: 1119-1129.
- Curran, P.J. 1985: **Principles of Remote Sensing**. Longman, New York.
- Dalby, R. 1957: Problems of Land Reclamation, 5. **Saltmarsh in the Wash Agricultural Review**. vol. 2: 31-37.
- Dave, J.V. 1980: Effect of Atmospheric Conditions on Remote Sensing of Vegetation Parameters. **Remote Sensing of Environment**. vol. 10: 87-99.
- Davidson, N.C. 1991: **Estuaries , Wildlife and Man. A Summary of Nature Conservation and Estuaries in Great Britain**. Peterborough, Nature Conservancy Council.
- Davis, F.W. and Simonett, D.S. 1991: GIS and Remote Sensing. In Maguire, D.J., Goddchild, M.F. and Rhind, D. (eds) **Geographical Information systems - Principles and Applications**. Longman Scientific and Technical, New York: 191-213.
- Detchmendy, D.M and Pace, W.H. 1972: A model for spectral signature variability for mixtures. in Shahrokhi, I.F.(ed) **Remote Sensing of Earth Resources**. University Tennessee Press. vol. 1: 596-620.
- Donoghue, D.N.M. and Shennan, I. 1987: A preliminary assessment of Landsat TM imagery for mapping vegetation and sediment distribution in the Wash estuary. **International Journal of Remote Sensing**. vol. 8: 1101-1108.
- Donoghue, D.N.M., and Zong, Y. 1992: **Coastal Sediment Mapping in the Tees Estuary**. Department of Geography, University of Durham. Unpublished work.
- Doody, J.P. 1992: The conservation of British saltmarshes. In Allen, J.R.L. and Pye, K. (eds) **Saltmarshes. Morphodynamics, Conservation and Engineering Significance**. Cambridge University Press, Cambridge: 80-114.

- Drake, B.G. 1976: Seasonal Changes in Reflectance and Standing Crop Biomass in Three Salt Marsh Communities. **Plant Physiology**. vol. 58: 696-699.
- Friedman, J.H. and Turkey, J.W. 1974: A projection pursuit algorithm for exploratory data analysis. **I.E.E.E. Transactions on Computers**. vol. 23: 881-889.
- Gillespie, A.R., Smith, M.O., Adams, J.B., Willis, S.C., Fischer, A.F. and Sabol, D.E. 1990: Interpretation of residual images: spectral mixture analysis of AVIRIS images. Owens Valley, California, **Proceedings of the Airborne Science Workshop: AVIRIS, JPL, Pasadena, C.A.**, (JPL Publication 90-54): 243-270.
- Goetz, A.F.H. 1992: Imaging spectrometry for earth remote sensing. In Toselli, F. and Bodechtal, J. (eds) **Imaging Spectroscopy: Fundamentals and Prospective Applications**. Kluwer Academic Publishers, London: 1-20
- Goetz, A.F.H. 1984: High spectral resolution of the land. **Proceedings In the Society for Optical Engineering**. vol. 47.
- Gray, A.J. 1992: Saltmarsh plant ecology: zonation and succession revisited. In Allen, J.R.L. and Pye, K. (eds) **Saltmarshes. Morphodynamics, Conservation and Engineering Significance**. Cambridge University Press, Cambridge: 63-79.
- Gross, M.F., Klemas, V. and Levasseur, J.E. 1986: Remote sensing of *Spartina anglica* in Five French Salt Marshes. **International Journal of Remote Sensing**. vol. 7: 657-664.
- Gross, M.F., Klemas, V. and Levasseur, J.E. 1988: Remote sensing of saltmarsh vegetation in France. **International Journal of Remote Sensing**. vol. 9: 397-408.
- Hall, F.G., Strebel, D.E., Nickeson, J.E., and Goetz, J.D 1991: Radiometric Rectification: Toward a Common Radiometric Response Among Multidate, Multisensor Images. **Remote Sensing of Environment**. vol. 35: 11-27.
- Hapke, B. 1981: Bidirectional reflectance spectroscopy. **Journal of Geophysical Research**. vol. 86: 3039-3054.
- Hill. M.I. 1988: **Saltmarsh Vegetation of the Wash. An Assessment of Change From 1971 to 1985**. N.C.C. Publications, Peterborough.
- Hill, J. and Sturm, B. 1991: Radiometric Correction of Multitemporal Thematic Mapper Data For Use In Agricultural Land-cover Classification And Vegetation Monitoring. **International Journal Of Remote Sensing**. vol. 12: 1471-1491.
- Hobbs, A.J and Shennan, I. 1986: Remote sensing of saltmarsh reclamation in the Wash, England. **Journal of Coastal Research**. vol. 2: 181-198.

- Holben, B.N. and Shimabukuro, Y.E. 1993: Linear mixing model applied to coarse spatial resolution data from multispectral satellite sensors. **International Journal of Remote Sensing**. vol. 14: 2231-2240.
- Hong, J.K and Iisaka, J. 1982: Coastal environmental change analysis by Landsat MSS data. **Remote Sensing of Environment**. vol. 12: 107-116.
- Horler, D.N. 1983: Red Edge Measurements For Remote Sensing Plant Chlorophyll Content. **Space Research Symposium on Remote Sensing and Mineral Exploration**. Ottawa.
- Horwitz, H.M., Nalepka, R.F., Hyde, P.D., and Morgenstern, J.P. 1971: **Estimating The Proportions of Objects Within a Single Resolution Element of a Multispectral Scanner**. University of Michigan, Ann Arbor, Michigan, NASA Contract NAS-9-9784.
- Hubbard, J.C.E. and Grimes, B.H. 1974: Coastal vegetation surveys. In Barrett, E.C and Curtis L.F. (eds) **Environmental Remote Sensing**. Edward Arnold, London: 127-142.
- Jackson, M.J. 1992: Integrated geographical information systems. **International Journal of Remote Sensing**. vol. 13: 1343-1351.
- James, M. 1985. **Classification Algorithms**. Collins, London.
- Janssen, L.L.F and Middlekoop, H. 1992. Knowledge Based Crop Classification of a Landsat TM Image. **International Journal of Remote Sensing**. vol. 13: 2827-2837.
- Jordan, C.F. 1969: Derivation of Leaf Area Index From Quality of Light on the Forest Floor, **Ecology**. vol. 50: 663-666.
- Kauth, R.J. and G.S.Thomas 1976: The Tassled Cap - A Graphic Description of the Spectral Development Of Agricultural Crops as Seen by Landsat, **Proceedings of the Symposium Machine Processing of Remote Sensing Data**. LARS, Purdue.
- Kestner, F.J.T. 1975: The loose-boundary regime of the Wash. **Geographical Journal**. vol. 141: 388-414.
- Lenninton, R.K., and Sorensen, C.T. and Heydorn, R.P. 1984: A mixture model approach for estimating crop areas from Landsat data. **Remote Sensing of Environment**. vol. 14: 197-206.
- Millington, A.C., Drake, Townshend, J.R.G, Quarmby, N.A. 1989: Settle, J.J. and Reading, A.J. : Monitoring salt playa dynamics using thematic mapper data. **I.E.E.E. Transactions on Geoscience and Remote Sensing**. vol. 27: 754-761.
- National Environment Research Council, 1976: **The Wash Water Storage Scheme Feasibility Study. A Report on the Ecological Studies**. N.E.R.C. Publications Series C, No.15.

- National Environment Research Council, 1983: **Thematic Mapper Data: Characteristics and Use.** Landsat-4, February 4, 1983. Reading, Berkshire.
- National Rivers Authority, Anglian Region, 1992: **East Anglian Salt Marshes.** N.R.A. Publications, Peterborough.
- Pethick, J.S. 1981: Long Term Accretion Rates on Tidal Saltmarshes. **Journal of Sedimentary Petrology.** vol. 51: 571-577.
- Pye, K. 1992: Saltmarshes on the Barrier Coastline of North Norfolk, Eastern England. In Allen, J.R.L. and Pye, K. (eds) **Saltmarshes. Morphodynamics, Conservation and Engineering Significance.** Cambridge University Press, Cambridge: 148-178.
- Quarmby, N.A., Townshend, J.R.G., Settle, J.J. and White, K.H. 1992: Linear mixture modelling applied to A.V.H.R.R. data for crop area estimation. **International Journal of Remote Sensing.** vol. 13: 415-425.
- Quarmby, N.A., 1992: Towards Continental Scale Crop Estimation. **International Journal of Remote Sensing.** vol. 13: 981-989.
- Randerson, P.F. 1975: The saltmarshes of the Wash. **Wash Feasibility Study Ecological Report.** Scientific study D (unpublished).
- Richter, R. 1992: Atmospheric Correction of Imaging Spectrometer Data, in F.Toselli and J.Bodechtel (eds) **Imaging Spectroscopy: Fundamentals and Prospective Applications.** Kluwer Academic Publishers, London: 259-266.
- Roberts, D.A. 1991: Leaf spectral types, residuals and canopy shade in an AVIRIS image. **Proceedings of the 3rd AVIRIS Workshop.** Pasadena, May 20: 43-50.
- Rouse, J.W., Hass, R.H., Schell, J.A. and Deering, D.W. 1973: Monitoring vegetation systems in the great plains with ERTS. **Third ERTS Symposium.** NASA SP-351 I: 309-317.
- Sabins, F. 1987: **Remote Sensing Principles and Interpretation.** 2nd Edition, W.H. Freeman and Company New York.
- Settle, J.J., Drake, N.A. 1993: Linear mixing and the estimation of ground cover proportions. **International Journal of Remote Sensing.** vol. 14: 1159-1177.
- Shennan, I. 1989: Holocene Crustal Movements and Sea Level Changes in Great Britain. **Journal of Quaternary Science.** vol. 4: 77-89.
- Shennan, I.S and Sproxton, I. 1992(a): **Monitoring Coastal Environmental Change Using Satellite Imagery Within A Geographical Information System.** Unpublished work.

Shennan, I. and Sproxton, I. 1992(b): **Anglian Sea Defence Management Study - stage III. Satellite data classification - Sub-Contract WV ACP 421. Unpublished work.**

Shimabukuro, Y.E. and Smith, A.S. 1991: The least-squares mixing models to generate fraction images derived from remote sensing multispectral data. **I.E.E.E. Transactions on Geoscience and Remote Sensing.** vol. 29: 16-20.

Singer, R.B. and McCord, T.B. 1979: Large scale mixing of dark and bright surface materials and implications for analysis of spectral reflectance. **Proceedings of the 10th Lunar Planetary Science Conference:** 3557-3561.

Slater, P.N., Biggar, S.F., Jackson, R.D., Mao, Y., Moran, M.S., Palmer, J.M. and Yuan, B. 1987: Reflectance- and Radiance-Based Methods For The Inflight Calibration of Multispectral Sensors, **Remote Sensing of Environment.** vol. 22: 11-37.

Smith, M.O., Johnson, P.E., and Adams, J.B. 1985: Quantitative determination of mineral types and abundances from reflectance spectra using principal component analysis. **Journal of Geophysical Research.** vol. 90: 792-804.

Strahler, A.H., 1980: The use of prior probabilities in maximum likelihood classification of remotely sensed data. **Remote Sensing of Environment.** vol. 10: 135-163.

Sturm, B. 1992: Atmospheric and Radiometric corrections for imaging spectroscopy. In F.Toselli and J.Bodechtel **Imaging Spectroscopy: Fundamentals and Prospective Applications.** Kluwer Academic Publishers, London: 47-60.

Terra-Mar Resource Information Service 1991: **Terra-Mar 4.0.** Mountain View, California, USA.

T-Spectra, 1991: **User's Guide to T-Spectra Software.** Terra-Mar Resource Information Services, Inc. Mountain View, California.

Tucker, C.J. 1979: Red and Photographic Infrared Linear Combinations For Monitoring Vegetation, **Remote Sensing of Environment.** vol. 8: 127-150.

Tucker, C.J., Fung, I.Y., Keeling, C.D. and Gammon, R.H. 1986: Relationship Between Atmospheric CO₂ Variations and a Satellite Derived Vegetation Index. **Nature.** vol. 319: 195-199.

Ungar, S.G. and Collins, 1977: **Atlas of Selected Crop Spectra, Imperial Valley California.** NASA Institute for Space Studies, GSFC Tech, Mem., TM-9473, June 1977.

United States Geological Survey and National Oceanic and Atmospheric Administration, 1984: **Landsat 4 Data Users Handbook.**

Wang, F., 1990: Improving Remote Sensing Image Analysis Through Fuzzy Information Representation. **Photogrammetric Engineering and Remote Sensing**, vol. 56: 1163-1168.

Woolley, J.T. 1971: Reflectance and Transmittance of Light by Leaves. **Plant Physiology** vol. 47: 656-662.



APPENDIX I

/ THE RECTIFICATION TRANSFORMATION */*
/ D.C. Reid Thomas */*

```
#include <stdio.h>
#include <stdlib.h>
#define LENGTH 460          /*Change for the size of dataset*/
#define NAME_LENGTH 10     /*Maximum length of a filename*/

main()
{
FILE*fin,                  /*file pointers*/
*fout;

    register int    l,      /*register ints*/
                 s;

    int    mnd             /*Min value of the dark range*/
          mxd,            /*Max value of the dark range*/
          mnb,            /*Min value of the light range*/
          mxb,            /*Max value of the light range*/
          minb=255,       /*Min DN of untransformed image*/
          maxb=0,         /*Max DN of untransformed image*/
          minr=255,       /*Min DN of transformed image*/
          maxr=0,         /*Max DN of transformed image */
          nd=0,           /*No. pixels in dark control set*/
          nb=0;           /*No. pixels in bright control set*/

    float  bri=0,         /*Mean value of bright reference set*/
          dri=0,         /*Mean value of dark reference set*/
          td=0.0,        /*Sum of pixels in dark control set*/
          tb=0.0,        /*Sum of pixels in bright control set*/
          avd=0.0,       /*Mean value of the dark control set*/
          avb=0.0,       /*Mean value of the bright control set*/
          v=0.0,         /*Represents part of transform equation*/
          r=0.0,         /*Represents part of transform equation*/
          w=0.0,         /*Represents part of transform equation*/
          t=0.0,         /*The transformed data*/
          scale=0.0;     /*Scaling factor*/

    short int lines=0,    /*Size of the dataset*/
            samples=0;

    unsigned char  lin[LENGTH],
                  lout[LENGTH];

    char input_filename[NAME_LENGTH],      /*Input filename*/
          output_filename[NAME_LENGTH];    /*Output filename*/

    printf("\nEnter the name of the input file :> ");
    scanf("%s",&input_filename);          /*image file input*/

    printf("Enter the name of the output file :> ");
    scanf("%s",&output_filename);         /*image file output*/
```

```

if ((fin = fopen(input_filename,"rb")) == NULL) {
    printf("cannot open the file !!!\n");
    exit(1);
} /*end if*/ /*open unrectified image file*/

if ((fout = fopen(output_filename,"wb")) == NULL) {
    printf("cannot open the output file !!!\n");
    exit(1); /*open output file*/
} /*end if*/ /*check data can be accessed*/

printf("\nEnter no of samples :> ");
scanf("%d", &samples); /*image dimensions - pixels*/

printf("Enter no of lines :> ");
scanf("%d", &lines); /*image dimensions - lines*/

printf("\nEnter min value of the dark range :> ");
scanf("%d", &mnd); /*dark control set in the subject image*/

printf("Enter max value of the dark range :> ");
scanf("%d", &mxd);

printf("\nEnter min value of the bright range :> ");
scanf("%d", &mnb); /*bright control set in the subject image*/

printf("Enter max value of the bright range :> ");
scanf("%d", &mxb);

printf("\nEnter the mean of the dark reference set :> ");
scanf("%f", &dri); /*reference image control sets*/

printf("Enter the mean of the bright reference set :> ");
scanf("%f", &bri);

for(l=0; l<lines; l++) { /*reads through the input data set*/

    fread(lin, sizeof(char), LENGTH, fin);

    for(s=0; s<samples; s++) {
        if(lin[s] <= mxd && lin[s] >= mnd) { /*pixels that are in the dark control sets*/
            td = td + lin[s];
            nd++;
        } /*end if*/

        if(lin[s] <= mxb && lin[s] >= mnb) { /*pixels that are in the bright control sets*/
            tb = tb + lin[s];
            nb++;
        } /*end if*/

        minb = min(minb,lin[s]); /*finds min DN*/
        maxb = max(maxb,lin[s]); /*finds max DN*/
    } /*end for samples*/
} /*end for lines*/

printf("\n\nEnd of First Pass...\n");

avd = (float) td/nd; /*finds mean of the control sets in the subject image*/
avb = (float) tb/nb;

```



```
        fwrite(fout, sizeof(char), LENGTH, fout);           /*writes to output file*/
    } /*end for lines*/

fclose(fin);
fclose(fout);

} /*end main*/
```


APPENDIX II

/* VEGETATION PARAMETER ALGORITHM */
/* D.N.M. Donoghue */

```
#include <stdio.h>
#include <stdlib.h>
#include <alloc.h>
#include <io.h>

int    Fhead = 0,
       Bhead = 0,
       Lhead = 0,
       Btail = 0,
       Ltail = 0,
       Samps = -1,
       Lines = -1,
       Bands = -1;

char   img[80];

float  *waves;

int    handle = -1;

long   BSIZE = 0L,
       specno = 0L;

extern void readidf(FILE *fp);
extern int getchannel(float *spec, float target, int N);
extern long initNspecbuffer(char far **buffer);
extern getnextNspex(char huge *buffer, long N);
extern void quitnextNspecbuffer(char *buffer);

#define GETGREENSTART    getchannel(waves, 0.5, Bands) /* 51 */
#define GETGREENSTOP    getchannel(waves, 0.6, Bands) /* 100 */
#define GETREDSTOP      getchannel(waves, 0.7, Bands) /* 150 */
#define GETNIRSTOP      getchannel(waves, 0.8, Bands) /* 298 */
#define GETREDRHSSTOP   getchannel(waves, 1.0, Bands)

int cdecl main()
{
    register int    X;

    FILE   *in;

    char           idfin[80];

    unsigned char huge    *buffptr;
    unsigned char huge    *spec;

    char far       *buffaddr;

    long   N,
           spectrum = 0L,
           s = 0L,
           BSIZE1;
```

```

int    green_start,
       green_stop,
       red_stop,
       nir_stop,
       red_rhs_limit,
       green_wvl_at,
       edge_wvl_at,
       red_wvl_at,
       red_rhs_at,
       red_depth,
       red_width;

int    gp = _creat("GPEAK", 0),
       rp = _creat("RPOSN", 0),
       rd = _creat("RDEEP", 0),
       rw = _creat("RWIDE", 0),
       re = _creat("REDGE", 0);

float  green_max = 0.0,
       red_min = 1000.0;

double diff = 0.0,
       red_edge = 0.0;

printf("\33[2JGP %d, RP %d, RD %d, RW %d, RE %d", gp, rp, rd, rw, re);
getIDFin:
printf("\nName of IDF to process >> ");
scanf("%s", idfin);

if( (in = fopen(idfin, "r")) == NULL ) {

    printf("Cannot open %s", idfin);
    goto getIDFin;

} /* if in */
readidf(in);
fclose(in);

BSIZE1 = (long) Samps * Lines;
BSIZE = BSIZE1 + Bhead;

N = initNspecbuffer(&buffaddr);

buffptr = (unsigned char huge *) buffaddr;
/*
  get channel numbers for spectral ranges
*/
green_start = GETGREENSTART;
green_stop = GETGREENSTOP;
red_stop = GETREDSTOP;
nir_stop = GETNIRSTOP;
red_rhs_limit = GETREDRHSSTOP;

while( spectrum < BSIZE1 ) {

    if( spectrum + N > BSIZE1 )
        N = BSIZE1 - spectrum;

    getnextNspex(buffptr, N);

```

```

spec = buffptr;
for(s=0L; s<N; s++ ) {
    green_max = 0;
    for(X=green_wvl_at=green_start; X<=green_stop; X++) {
        if( *(spec + X) > green_max) {
            green_max = *(spec + X);
            green_wvl_at = X;
        } /* if spec */
    } /* for green */
    red_edge = 0.0;
    for(X=edge_wvl_at=red_start; X<=nir_stop; X++) {
        diff = (double) ( *(spec + X + 1)
                          - *(spec + X) )
              / (waves[ X + 1 ] - waves[ X ] );
        if( red_edge < diff ) {
            red_edge = diff;
            edge_wvl_at = X;
        } /* if red_edge */
    } /* for X */
    red_min = 255;
    for(X=red_wvl_at=green_start; X<=red_stop; X++) {
        if( *(spec + X) < red_min) {
            red_min = *(spec + X);
            red_wvl_at = X;
        } /* if spec[X] */
    } /* for X */
    X = green_stop;
    do {
        red_rhs_at = X;
        X++;
    } while( *(spec + X) < green_max && X < red_rhs_limit);
} /* miss 0 at end */

red_depth = max( 0, green_max - red_min );
red_width = max( 0, red_rhs_at - green_wvl_at );

```

```

        _write(gp, &green_wvl_at, 1);      /* green peak */
        _write(rp, &red_wvl_at, 1);       /* red position */
        _write(rd, &red_depth, 1);       /* red depth */
        _write(rw, &red_width, 1);       /* red width */
        _write(re, &edge_wvl_at, 1);     /* red edge */

        spec += Bands;

    } /* for s */

    spectrum += N;

} /* while spectrum */

_close(handle);
_close(gp);
_close(rp);
_close(rd);
_close(rw);
_close(re);

quitnextNspecbuffer(buffaddr);

} /* end main */ #include <stdio.h>
#include <stdlib.h>
#include <alloc.h>
#include <io.h>

int    Fhead = 0,
       Bhead = 0,
       Lhead = 0,
       Btail = 0,
       Ltail = 0,
       Samps = -1,
       Lines = -1,
       Bands = -1;

char   img[80];
float  *waves;
int    handle = -1;
long   BSIZE = 0L,
       specno = 0L;

extern void readidf(FILE *fp);
extern int getchannel(float *spec, float target, int N);
extern long initNspecbuffer(char far **buffer);
extern getnextNspex(char huge *buffer, long N);
extern void quitnextNspecbuffer(char *buffer);

#define GETGREENSTART    getchannel(waves, 0.5, Bands) /* 51 */
#define GETGREENSTOP    getchannel(waves, 0.6, Bands) /* 100 */
#define GETREDSTOP      getchannel(waves, 0.7, Bands) /* 150 */
#define GETNIRSTOP     getchannel(waves, 0.8, Bands) /* 298 */
#define GETREDRHSSTOP   getchannel(waves, 1.0, Bands)

int cdecl main()
{
    register int    X;

```

```

FILE *in;

char idfin[80];

unsigned char huge *buffptr;
unsigned char huge *spec;

char far *buffaddr;

long N,
      spectrum = 0L,
      s = 0L,
      BSIZE1;

int green_start,
    green_stop,
    red_stop,
    nir_stop,
    red_rhs_limit,
    green_wvl_at,
    edge_wvl_at,
    red_wvl_at,
    red_rhs_at,
    red_depth,
    red_width;

int gp = _creat("GPEAK", 0),
    rp = _creat("RPOSN", 0),
    rd = _creat("RDEEP", 0),
    rw = _creat("RWIDE", 0),
    re = _creat("REDGE", 0);

float green_max = 0.0,
      red_min = 1000.0;

double diff = 0.0,
      red_edge = 0.0;

printf("\33[2JGP %d, RP %d, RD %d, RW %d, RE %d", gp, rp, rd, rw, re);
getIDFin:
printf("\nName of IDF to process >> ");
scanf("%s", idfin);

if( (in = fopen(idfin, "r")) == NULL ) {

    printf("Cannot open %s", idfin);
    goto getIDFin;

} /* if in */

readidf(in);

fclose(in);

BSIZE1 = (long) Samps * Lines;
BSIZE = BSIZE1 + Bhead;

N = initNspecbuffer(&buffaddr);

buffptr = (unsigned char huge *) buffaddr;

```

```

/*****
      Start of new veg code
*****/

/*
  get channel numbers for spectral ranges
*/
green_start = GETGREENSTART;
green_stop = GETGREENSTOP;
red_stop = GETREDSTOP;
nir_stop = GETNIRSTOP;
red_rhs_limit = GETREDRHSSTOP;

while( spectrum < BSIZE1 ) {

  if( spectrum + N > BSIZE1 )
    N = BSIZE1 - spectrum;

  getnextNspex(buffptr, N);

  spec = buffptr;

  for(s=0L; s<N; s++ ) {

    green_max = 0;

    for(X=green_wvl_at=green_start; X<=green_stop; X++) {

      if( *( spec + X ) > green_max ) {

        green_max = *( spec + X );
        green_wvl_at = X;

      } /* if spec */

    } /* for green */

    red_edge = 0.0;

    for(X=edge_wvl_at=red_stop; X<=nir_stop; X++) {

      diff = (double) ( *(spec + X + 1)
        - *(spec + X) )
        / (waves[ X + 1 ] - waves[ X ] );

      if( red_edge < diff ) {

        red_edge = diff;
        edge_wvl_at = X;

      } /* if red_edge */

    } /* for X */

    red_min = 255;
    for(X=red_wvl_at=green_stop; X<=red_stop; X++) {

      if( *(spec + X) < red_min ) {

        red_min = *(spec + X );

      }

    }

  }

}

```

```

        red_wvl_at = X;

        } /* if spec[X] */

    } /* for X */

    X = green_stop;

    do {

        red_rhs_at = X;
        X++;

    } while( *(spec + X) < green_max && X < red_rhs_limit);

                                                    /* miss 0 at end */

    red_depth = max( 0, green_max - red_min );
    red_width = max( 0, red_rhs_at - green_wvl_at);

    _write(gp, &green_wvl_at, 1);          /* green peak */
    _write(rp, &red_wvl_at, 1);           /* red position */
    _write(rd, &red_depth, 1);           /* red depth */
    _write(rw, &red_width, 1);          /* red width */
    _write(re, &edge_wvl_at, 1);        /* red edge */

    spec += Bands;

} /* for s */

spectrum += N;

} /* while spectrum */

_close(handle);
_close(gp);
_close(rp);
_close(rd);
_close(rw);
_close(re);

quitnextNspecbuffer(buffaddr);

} /* end main */

```

